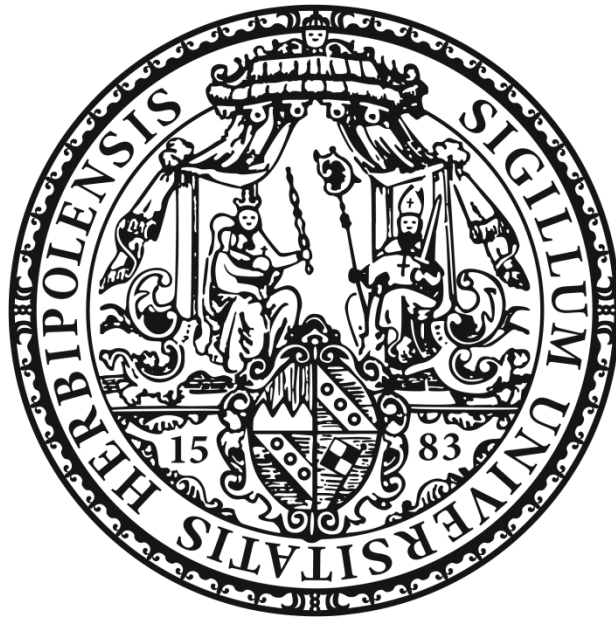


**Development and characterization of monoclonal antibodies to GDF-15 for
potential use in cancer therapy**

**Die Entwicklung und Charakterisierung monoklonaler Antikörper gegen
GDF-15 zur potenziellen Anwendung in der Krebstherapie**



Doctoral thesis for a doctoral degree
at the Graduate School of Life Sciences,
Julius-Maximilians-Universität Würzburg,
Section: Infection and Immunity

Submitted by
Markus Erich Junker
from
Ludwigshafen/Rhein, Germany

Würzburg 2015

Submitted on:.....

Office stamp

Members of the *Promotionskomitee*:

Chairperson: **Professor Dr. Caroline Kisker**

Primary Supervisor: **Professor Dr. Roland Benz** (Since 29th July 2015)

(From 3rd November 2008 - 20th July 2015 Professor Dr. Jörg Wischhusen)

Supervisor (Second): **Professor Dr. Roland Benz** (Until 29th July 2015)

Supervisor (Third): **Professor Dr. Thomas Hünig**

Date of Public Defence:.....

Date of Receipt of Certificates:.....

Table of contents

Table of contents	4
Zusammenfassung	8
Abstract	11
1 Introduction	13
1.1 Cancer.....	13
1.1.1 Development of Cancer.....	13
1.1.2 Tumor Progression and Metastasis	15
1.1.3 Elimination of Cancer Cells by the Immune System	16
1.1.3.1 Natural killer Cells	16
1.1.3.2 Cytotoxic T Lymphocytes	18
1.1.3.3 Leukocyte Recruitment	20
1.1.4 Immune Evasion.....	22
1.2 The TGF- β Superfamily	24
1.2.1 TGF- β	25
1.2.2 TGF- β and Cancer.....	26
1.2.3 GDF-15.....	27
1.2.3.1 GDF-15 - Structure and Biochemistry	28
1.2.3.2 Expression of GDF-15	30
1.2.3.3 GDF-15 and its Function.....	31
1.2.3.4 GDF-15 in Cancer	32
1.3 Treatment of Cancer with Targeted Therapy	34
1.3.1 Antibodies in the Clinic.....	35
1.3.2 Antibody Structure	36
1.3.3 Antibody Humanization	37
1.3.4 Mode of Actions of Antibodies	39
1.4 The Aim of the Thesis	40
2 Material and Methods.....	41
2.1 Material	41
2.1.1 Devices	41
2.1.2 Chemicals and reagents	42
2.1.3 Material for Immunohistochemistry.....	43
2.1.4 Material for protein biochemistry	44

2.1.5 Material for molecular biology	45
2.1.6 Kits and kit contents	46
2.1.7 Reagents, buffers for methods to generate monoclonal antibodies.....	47
2.1.8 Antibodies	48
2.1.9 Oligonucleotides.....	49
2.1.10 Cell lines.....	50
2.1.11 Plasmids	50
2.1.12 Reagents for FACS staining.....	51
2.1.13 Cytokines.....	51
2.1.14 Standard DNA and protein ladder	52
2.2 Methods	53
2.2.1 Immunohistochemical staining	53
2.2.2 Thawing of cells	54
2.2.3 Cryopreservation of cells	54
2.2.4 Isolation and preparation of human immune cells	54
2.2.4.1. Isolation of human peripheral lymphocytes from whole blood	55
2.2.5 Flow cytometry	56
2.2.6 Adherence Assay.....	57
2.2.7 Woundhealing assay.....	57
2.2.8 Determination of cell viability using the WST-1 assay	58
2.2.9 Protein biochemical methods	58
2.2.9.1 Preparation of cell lysates from human PBMCs, tumor cells and tissues.....	58
2.2.9.2 Determination of the total amount of protein by the Bradford method.....	59
2.2.9.3 Immunoblotting.....	59
2.2.10 Methods for gene expression analysis.....	61
2.2.10.1 Isolation of RNA from immune cells and HUVEC cells	61
2.2.10.2 Determination of RNA concentration	61
2.2.10.3 Synthesis of cDNA from isolated RNA	62
2.2.11 Polymerase Chain Reaction (PCR)	63
2.2.11.1 Isolation of genomic DNA from mouse ear punches.....	63
2.2.11.2 Mouse GDF-15 genotyping.....	63
2.2.11.3 DNA gel electrophoresis	64
2.2.11.4 Quantitative Realtime Polymerase Chain Reaction (qPCR)	64
2.2.12 DNA-Microarray (Affymetrix) on human PBMCs and HUVECs.....	66
2.2.13 Cloning	66
2.2.13.1 Ligation	66
2.2.13.2 Transformation in C2988 bacteria.....	67
2.2.13.3 Preparation of plasmids	68

2.2.13.4 Restriction digest of pJET1.2/blunt (Fermentas)	68
2.2.13.5 Colony polymerase chain reaction (colony PCR)	68
2.2.13.6 Vector Sequencing (Geneart)	69
2.2.14 Transfection of cells	70
2.2.15 Generation of monoclonal antibodies against GDF-15	70
2.2.15.1 Immunization of mice	70
2.2.15.2 Hybridoma fusion, selection and expansion	70
2.2.15.3 Screening for GDF-15 positive clones	71
2.2.15.4 Cloning/Subcloning for monoclonal antibodies.....	71
2.2.15.5 Production of mABs in CELLline Bioreactors / Antibody Expression	72
2.2.16 Purification of mABs using Proteus A columns	73
2.2.17 Isotyping of GDF-15 positive monoclonal antibodies	74
2.2.18 Epitope mapping	75
2.2.18.1 Linear epitope mapping (pepperprint GmbH).....	75
2.2.18.2 Epitope mapping of 3-dimensional epitopes (epitope excision)	76
2.2.19 kD-values-determination of antibodies	76
2.2.20 CDR Cloning of B1-23 heavy and light chains using degenerate primers (mouse IgG2a).....	76
2.2.21 Chimerization of B1-23.....	77
2.2.22 Humanization of B1-23	77
2.2.23 Animal Experiments.....	78
2.2.23.1 Glioma model.....	78
2.2.23.2 Melanoma Xenograft model.....	78
2.2.24 Statistics	79
3 Results	80
3.1 GDF-15 expression in solid tumors	80
3.1.1 GDF-15 is highly expressed in ovarian cancer	80
3.1.2 GDF-15 is overexpressed in brain tumors.....	81
3.2 The effects of GDF-15 <i>in vitro</i>	83
3.2.1 GDF-15 does not activate the canonical TGF- β signaling pathway in human PBMC	83
3.2.2 The effect of GDF-15 on the NKG2D receptor on NK cells and CD8 ⁺ T cells.....	85
3.2.3 GDF-15 reduces T-cell-adherence on endothelial cells	86
3.2.4 Microarray Analysis – the influence of GDF-15 on PBMC and HUVEC cells	88
3.2.5 In vitro scratch assay	94
3.3 GDF-15 knock down leads to prolonged survival in mice bearing glioma	96
3.4 Generation and characterization of monoclonal anti-GDF-15 antibodies.....	98

3.4.1 Confirmation of GDF-15 knock-out animals by PCR	98
3.4.2 Immunization of GDF-15 knock out mice with human GDF-15 resulted in several GDF-15 Abs for further characterization and development.....	99
3.4.3 Antibody production of hybridoma clones.....	101
3.4.4 B1-23 detects GDF-15 under semi-native conditions on Western Blots	102
3.4.5 Isotyping of B1-23	103
3.4.6 Epitope mapping of B1-23	104
3.4.7 Sequence identification of the hypervariable regions of B1-23.....	106
3.4.8 Chimerization of B1-23.....	108
3.4.9 Humanization of B1-23 and characterization of the humanized variants	109
3.4.10 In vitro effects of the developed anti GDF-15 antibodies.....	114
3.4.11 Assessment of cytotoxic effects of B1-23.....	116
3.5 B1-23 prevents tumor associated cachexia in BalbC ^{nu/nu} mice	118
4 Discussion	120
4.1 GDF-15 expression and physiological relevance.....	121
4.2 GDF-15: Growth Factor and Ligand - without a yet known receptor?.....	123
4.3 GDF-15 and its function <i>in vivo</i>	126
4.4 Generation of GDF-15 antibodies and preclinical testing thereof	128
4.5 Therapeutic potential of B1-23 / H1L5	129
Conclusion.....	131
5 References	133
List of Figures	152
List of Tables.....	154
Supplements	156
List of Abbreviations.....	162
Affidavit/Eidesstattliche Erklärung.....	164
Danksagung.....	165
Curriculum Vitae.....	167

Zusammenfassung

Hintergrund

GDF-15 ist ein divergentes Mitglied der TGF- β Superfamilie, welches zuerst als „macrophage inhibitory cytokine-1“ (MIC-1) mit immunmodulatorischen Eigenschaften beschrieben wurde. GDF-15 ist ein lösliches Protein, das unter physiologischen Bedingungen hauptsächlich in der Plazenta exprimiert wird und welches im Serum von Schwangeren in erhöhten Konzentrationen nachgewiesen werden kann. Mit Ausnahme der Plazenta wird GDF-15 in verschiedenen gesunden Geweben gefunden, hier jedoch in deutlich niedrigeren Konzentrationen, und ist in vielen soliden Tumoren überexprimiert. GDF-15 werden sowohl bei gesunden, als auch bei kranken Menschen, unterschiedlichste Funktionen zugeschrieben. Zum einen ist GDF-15 für eine erfolgreiche Schwangerschaft notwendig. Niedrige GDF-15 Spiegel im Serum während der Schwangerschaft korrelieren mit dem Verlust des Fötus. Zum anderen korreliert die Überexpression von GDF-15, welche bei unterschiedlichen Malignitäten beobachtet werden kann, mit einer schlechten Prognose. Darüber hinaus verursacht das von Tumorzellen sezernierte GDF-15 das sogenannte „Anorexie-Kachexie Syndrom“ in Mäusen. Das Ziel meiner Arbeit war es, die immunmodulatorische Funktion von GDF-15 im Tumorkontext zu untersuchen, insbesondere durch eine Hemmung des Zielmoleküls *in vitro* und *in vivo*. Aus diesem Grund wurde der Schwerpunkt auf die Generierung und Charakterisierung monoklonaler, GDF-15 spezifischer, blockierender Antikörper gelegt. Diese wurden sowohl *in vitro* als auch *in vivo* getestet, was einen großen Teil dieser Arbeit darstellt.

Ergebnisse

Es konnte gezeigt werden, dass GDF-15 in humanen gynäkologischen Tumoren wie auch in Hirntumoren überexprimiert ist. Weiterhin ließ sich zeigen, dass GDF-15 Effektorzellen des Immunsystems *in vitro* moduliert. Dabei verursacht GDF-15 eine moderate Herunterregulation des aktivierenden Killing Rezeptors NKG2D auf NK und CD8⁺ T Zellen, welcher eine hohe Bedeutung für eine effektive anti-tumorale Immunantwort hat. Darüber hinaus konnten wir zeigen, dass GDF-15 die Adhäsion von CD4⁺ und CD8⁺ T Zellen auf Endothelzellen *in vitro* herabsetzt. Eine daraus resultierende Reduktion der trans-endothelialen Migration von Leukozyten in entzündetes Gewebe erklärt möglicherweise die niedrige T Zell Infiltration in GDF-15 exprimierenden Tumoren, welche *in vivo* beobachtet werden konnten. Mäuse, denen (auf shRNA basierende) GDF-15-defiziente Gliomzellen appliziert wurden, zeigten im Vergleich zur Kontrollgruppe, welche GDF-15-exprimierenden

Gliomzellen erhalten hatte, ein verlängertes Überleben, vermindertes Tumorwachstum und eine erhöhte Immunzellinfiltration in das Tumormikromillieu. GDF-15 ist ein lösliches Protein, das von mehr als 50 % aller soliden Tumore sezerniert wird und mit dem Grad der Malignität korreliert. Daher wurde postuliert, dass ein neutralisierender monoklonaler Antikörper gegen GDF-15 eine effektive neue Antikrebstherapie ermöglichen sollte. Solch ein Antikörper wurde entsprechend in GDF-15-defizienten Mäusen generiert. Unter verschiedenen Klonen wurde der Antikörper Klon B1-23 identifiziert, welcher sowohl im Western Blot als auch im ELISA anwendbar ist. Dieser Klon detektiert ein drei-dimensionales Epitop des muren GDF-15 Dimers mit hoher Affinität und Spezifität. Um den Antikörper für eine spätere Anwendung im Menschen humanisieren zu können, wurden die variablen Regionen des Klons B1-23 durch eine spezielle PCR Methode unter Verwendung degenerierter Primer und nachfolgender Klonierung in einen Sequenzierungsvektor identifiziert. Die hierdurch gewonnenen Sequenzen ermöglichten die Generierung von chimären und humanisierten Varianten von B1-23. Nach anschließender intensiver Charakterisierung konnte sowohl der ursprüngliche Maus-Antikörper B1-23 als auch der chimäre B1-23 Antikörper (ChimB1-23) und der humanisierte B1-23 Antikörper (H1L5) in einer Melanom Xenograft Studie *in vivo* getestet werden. Zwar ließ sich mit keinem der Antikörper eine signifikante Hemmung des Tumorwachstums beobachten. Als herausragendes Ergebnis zeigte sich allerdings, dass der durch GDF-15 induzierte Gewichtsverlust signifikant durch die Verabreichung der GDF-15 spezifischen Antikörper verhindert werden konnte, was die antagonisierende Funktionalität des entwickelten Immunglobulins bestätigte.

Schlussfolgerung

GDF-15 ist ein vielversprechendes Zielmolekül bei Krebserkrankungen, welches bei der Tumorprogression und Tumor-assoziiertes Kachexie beteiligt ist. Es konnte ein monoklonaler Anti-GDF-15 Antikörper generiert werden, welcher zum einen molekularbiologisch zum Einsatz kam (z.B. Western Blot, ELISA, etc.) und zum anderen als antagonisierender Antikörper sowohl *in vitro* als auch *in vivo* Anwendung fand. Auch wenn B1-23 scheinbar keine Tumorwachstumshemmung durch die Depletion von GDF-15 in T Zell defizienten athymischen Mäusen zeigte, konnte derselbe Antikörper wie auch die abgeleiteten Varianten (chimärisiert und humanisiert) eindrücklich die Tumor assoziierte Kachexie im UACC-257 Melanom Modell verhindern. Der ausgebliebene antitumorale Effekt in unserem Melanom Modell in Nacktmäusen lässt sich nur zum Teil durch eine fehlende sekundäre Immunkomponente, insbesondere das Fehlen zytotoxischer T Zellen, erklären, da es in einem

ähnlichen Xenograft Melanom Modell, welches in Auftragsforschung (CRO) durchgeführt wurde, zu einer Reduktion des Tumorwachstums durch die Applikation von B1-23 kam. Diese Ergebnisse lassen vermuten, dass T Zellen unerlässlich für eine effektive antitumorale Antwort sind, eine Annahme, die durch die Ergebnisse des syngenem Gliom Maus-Modells unterstützt wird, in welchem es durch das Ausschalten von Tumor produziertem GDF-15 zu einer erhöhten intratumoralen T Zell Infiltration und einem längeren Überleben kam. Zusammengenommen erlauben uns diese Daten den Schluss, dass eine tumorbedingte Kachexie durch den GDF-15-Antikörper B1-23 bekämpft werden kann. Allerdings sind direkte B1-23 vermittelte antitumorale Effekte eher in immunkompetenten Modellen mit T Zellen als in einem athymischen, T Zell defizienten Nacktmaus-Modell zu erwarten.

Abstract

Background

GDF-15 is a divergent member of the TGF- β superfamily, which was first described as macrophage inhibitory cytokine-1 (MIC-1), revealing an immune modulatory function. GDF-15 is a soluble protein which is, under physiological conditions, highly expressed in the placenta and found in elevated levels in blood sera of pregnant women. Apart from the placenta, GDF-15 is expressed in healthy tissue, albeit to a lower extent and overexpressed in many solid tumors. A variety of different functions are attributed to GDF-15 in healthy as well as diseased humans. On the one hand, GDF-15 is required for successful pregnancy and low GDF-15 serum levels during pregnancy correlate with fetal abortion. On the other hand, overexpression of GDF-15, which can be observed in several malignancies is correlated with a poor prognosis. Furthermore, tumor derived GDF-15 leads to cancer associated anorexia-cachexia syndrome in mice. The aim of my PhD thesis was to further investigate the role of GDF-15 as an immune modulatory factor in cancer, in particular, by inhibiting the target molecule *in vitro* and *in vivo*. Therefore, the main focus was placed on the generation and characterization of monoclonal GDF-15 specific blocking antibodies, which were tested *in vitro* and *in vivo*, which represents a substantial part of my work.

Results

Here, GDF-15 was shown to be highly expressed in human gynecological cancer and brain tumors. We could then demonstrate that GDF-15 modulates effector immune cells *in vitro*. GDF-15 mediated a slight downregulation of the activating NKG2D receptor on NK and CD8⁺ T cells, which is crucial for proper anti-tumoral immune responses. Furthermore, we could demonstrate that GDF-15 reduces the adhesion of CD4⁺ and CD8⁺ T cells on endothelial cells *in vitro*. A negatively affected trans-endothelial migration of leukocytes into inflamed tissue could explain the low T cell infiltration in GDF-15 expressing tumors, which were observed *in vivo*, where mice bearing (shRNA mediated) GDF-15 deficient glioma cells revealed enhanced immune cell infiltrates in the tumor microenvironment, compared with the GDF-15 expressing control group. Those animals further exhibited a decreased tumor growth and prolonged survival. GDF-15 is a soluble protein, secreted by more than 50 % of solid tumors and associated with grade of malignancy. Therefore a neutralizing monoclonal antibody to GDF-15 was assumed to be an auspicious therapeutically anti-cancer tool. Such an antibody was thus generated in GDF-15 knock out mice against human GDF-15. Amongst many clones, the GDF-15 antibody clone B1-23 was found to be applicable in Western Blot

as well as in ELISA techniques, detecting a three-dimensional epitope of the mature GDF-15 dimer with high affinity and specificity. To enable the humanization for a later administration in humans, the variable regions of antibody B1-23 were identified by a special PCR method using degenerate primers and cloned into a sequencing vector. The sequence obtained thereby enabled the generation of chimeric and humanized B1-23 variants. After further comprehensive characterization, the original mouse antibody B1-23 as well as the chimeric antibody (ChimB1-23) and the humanized B1-23 antibody (H1L5) were applied in a melanoma xenograft study *in vivo*. None of the antibodies could significantly inhibit tumor growth. However of utmost importance, body weight loss mediated by tumor derived GDF-15 could be significantly prevented upon administration of all three GDF-15 specific antibodies, which confirmed the antagonizing functionality of the immunoglobulin.

Conclusion

GDF-15 is a promising cancer target, involved in tumor progression and cancer related cachexia. A monoclonal GDF-15 antibody was generated, which served on one hand as a tool for molecular biological applications (Western Blot, ELISA, etc.) and on the other hand was applied as an antagonizing antibody *in vitro* and *in vivo*. Even though tumor growth inhibition by GDF-15 depletion in T cell deficient athymic mice failed using B1-23, the same antibody and derivatives thereof (chimeric and humanized) impressively prevented tumor associated cachexia in UACC-257 melanoma bearing nude mice. The missing anti-tumor effect in our own melanoma model in nude mice can only partially be explained by the missing secondary immunity, in particular cytotoxic T cells, in the athymic animals, since in a similar melanoma model, performed by an external company, a tumor reduction in immunocompromised animals was observed, when B1-23 was administered. These findings support the idea that T cells are substantial for an effective tumor immunity and are in line with the results of the syngeneic, T cell comprising, mouse glioma model, where silencing of tumor expressed GDF-15 led to an enhanced intratumoral T cell infiltration and a prolonged survival.

Taken together our data allow for the conclusion that tumor associated cachexia can be combatted with the GDF-15 antibody B1-23. Further, B1-23 might elicit direct anti-tumor effects in immune competent models, which contain T cells, rather than in an athymic, T cell deficient nude mouse model.

1 Introduction

1.1 Cancer

Cancer is a multifactorial disease, which is – since 2012 – the leading cause of morbidity and mortality worldwide (Benjamin Anderson, 2011). The international agency for research on cancer (IARC) reported about 14 million new cancer incidences and more than 8 million deaths in 2012. Amongst men, cancer of lung, prostate, colon, stomach, and liver was most frequently diagnosed in 2012, whereas the most frequent tumor types of women were breast, colon, lung, cervix, and stomach cancer. The IARC expects an increase in cancer incidences from 14 million in the year 2012 to 22 million in the next 20 years. Thus, there is an enormous medical and social need to develop new therapeutics in order to fight cancer. Due to the various types of cancer, drug development requires comprehensive knowledge about the individual malignancy to be treated. In this respect, the following questions must be addressed: How do individual cancers develop? Which genetic alterations occurred? Which tumor targets are expressed and could they serve as target structures for the development of a therapeutic drug?

1.1.1 Development of Cancer

Tumors can basically develop in any human tissues or organs. In principle, tumors are the result of a number of accumulating genetic mutations, which lead to the transformation of a normal cell into a malignant cell (see next section) (Finlay, 1993, Vogelstein and Kinzler, 1993, Lodish H, 2000). Such genomic alterations are triggered by (1) environmental factors, (2) endogenous factors as well as (3) inherited aberrations (Devereux et al., 1999, De Bont and van Larebeke, 2004).

Exogenous influences are for example ultraviolet light, carcinogenic chemicals or radiation. Ultraviolet light can cause DNA damage in melanocytes and keratinocytes of the human skin due to ‘non-repairable’ changes in the DNA (Luther et al., 2000, Hussein, 2005, Boniol et al., 2012, Elsamadicy et al., 2015). Chemicals, as for example carcinogens in tobacco smoke, can cause mutations or cell damage in the human lung (Hecht, 1999). Furthermore, ionizing radiation, as for example from radioactive substances (α, β, γ -radiation) and x-rays, can lead to genomic instability, thereby causing somatic changes followed by cellular transformation (Rothkamm and Löbrich, 2003, Hall and Brenner, 2008, Vogiannis and Nikolopoulos, 2014). In addition, oncoviruses can cause genetic aberrations. A common example is the development of cervical cancer induced by human papilloma virus (Burd, 2003).

However, genomic DNA mutations can also occur without environmental influence, as for instance sporadic mutations or inherited genomic mutations (Kastrinos and Syngal, 2011). Mistakes during cellular replication, e.g. errors in proof reading, can cause damage ranging from point mutations to chromosomal aberrations, with risk of ending in cancer (Bernstein et al., 2013). All of these factors leading to the transformation of normal cells into cancer cells have in common, that somatic mutations have occurred in the genome of the respective cell. Analysis of cancer cell genomes identified a variety of such somatic mutations ending inter alia in constitutively activated signaling pathways (Vogelstein and Kinzler, 2004). Depending on the genomic location, a somatic mutation can result in loss-of-function mutations, impairing tumor suppressor genes (e.g. PTEN, p53, RB) and in gain-of-function mutations affecting oncogenes (e.g. KRAS, BRAF, FES) (Vogelstein and Kinzler, 2004). As indicated by the name, tumor suppressors protect cells from uncontrolled mitotic divisions (Cooper, 2000) (figure 1-1). In contrast, mutated oncogenes typically affect components of signaling pathways such as growth factors and growth factor receptors. Thereby they constitutively activate pathways, which drive cells continuously into cellular divisions, ending in an uncontrolled tumor growth (Vogelstein and Kinzler, 2004). For example, Davies and Samuels reported, that 42 % of melanoma cells display activating mutations, structurally affecting the B-RAF protein, leading to constitutive MAP Kinase signaling pathway via RAF (Davies and Samuels, 2010). Interestingly, two-thirds of adult cancers develop because of random mutations, compared to one-third of cancers induced by environmental factors or inherited, an event that Tomasetti and Vogelstein simply termed “bad luck” (Tomasetti and Vogelstein, 2015).

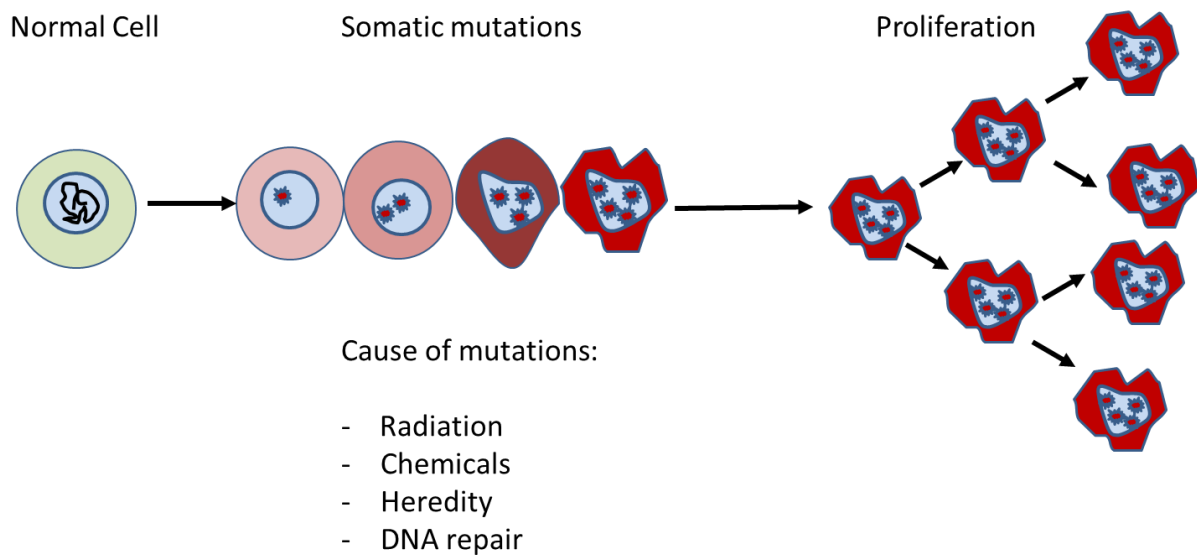


Figure 1-1 Development of tumor cells by somatic mutations

The illustration represents the sequence from normal cells towards tumor cells. Once a cell has acquired mutations, which might be introduced by either radiation, chemicals, failure of the cellular DNA repair system or even sporadic mutations, the transformed cell may proliferate in an uncontrolled manner, thereby promoting tumor growth (adapted from National Cancer Institute).

1.1.2 Tumor Progression and Metastasis

Many years decay, until cancer results in a clinically manifested disease (Fearon and Vogelstein, 1990). The reason is that –as mentioned in 1.1.1 - a series of mutations have to accumulate over a certain period of time in order to transform a pre-malignant cell into a tumor (Vogelstein and Kinzler, 1993). When either a suppressor gene or an oncogene mutation is acquired, transformed cells can be ‘forced’ to continuously proliferate, thereby either forming a benign neoplasia or a malignant tumor (Gatenby and Gillies, 2004). The difference between these two forms of tumors is the local restriction of benign tumor cells at the site of the origin organ or tissue, whereas malignant tumors do not remain at their site of origin (Alberts B., 2002). The latter ones are further characterized by high proliferation rates, invasive behavior, promoting angiogenesis as well as their ability to migrate and disseminate into the blood stream (Baba AI., 2007, Alberts B., 2002). Adorno and colleagues reported that mutations in the tumor suppressor gene p53 promote cellular migration and invasion (Adorno et al., 2009). Furthermore, mutations in the proto-oncogene KRAS are correlated with lung metastasis in colorectal cancers (Pereira et al., 2015). Once a tumor achieved such a fate,

cancer cells can subsequently form tumors remote of its primary site of development, frequently leading to failure of secondary organs (Alberts B., 2002). Such progressively growing tumors need to establish their own microenvironment, comprising of host stromal cells (e.g. fibroblasts), vasculature, lymphatic vessels and tumor cells (Descot and Oskarsson, 2013, Tarin, 2013). Interestingly, many immune cells are found in the microenvironment of solid tumors, which can be either beneficial or destructive for certain cancers and will be further discussed in the next sections (Shiao et al., 2011).

1.1.3 Elimination of Cancer Cells by the Immune System

One of its most important functions of the immune system is to prevent tumor formation at an early stage (Diefenbach and Raulet, 2002). Therefore, certain immune cell subsets play a crucial role in the eradication of transformed cells. In the human body, especially two types of immune cells are equipped in identifying and eliminating transformed cells and thus prevent the outgrowth of a tumor: the natural killer cells (NK cells) and cytotoxic T cells (CTLs) (Alderton and Bordon, 2012).

1.1.3.1 Natural killer Cells

Natural killer cells (NK cells) are part of the innate immunity. These immune cells are able to eradicate transformed cells such as virus infected cells or tumor cells independently of MHC-class I presented peptides (Cerwenka and Lanier, 2001, Waldhauer and Steinle, 2008) (further explained in 1.1.3.2). In order to discriminate between transformed cells and healthy cells, NK cells express two types of receptors: Inhibitory receptors and activating NK cell receptors (Ravetch and Lanier, 2000, Waldhauer and Steinle, 2008). Both receptor types can interact with ligands which are expressed on the surface of tumor cells, viral infected cells or host cells. Inhibitory receptors, comprising killer inhibitory receptors (KIR), immunoglobulin-like transcripts (ILT) and CD94/NKG2A, recognize MHC-I class molecules, which are highly expressed on most healthy cells and absent on several transformed cells (Alderson and Sondel, 2011, Pegram et al., 2011). Hence, NK cell activation can be described as “missing-self” recognition (Raulet and Vance, 2006). Activating receptors as for example NKG2D, DNAM-1, NKp46, NKp30 recognize their according ligand on tumor cells: NKG2D ligands are MIC-A, MIC-B, ULBP1-4 (Bahram et al., 1994, Cosman et al., 2001). DNAM-1 ligands are known as CD112 and CD155 (Pende et al., 2005). The NKp46 ligand activates its respective NKp46 receptor, whereas tumor cell expressed B7-H6 ligates the NKp30 receptor

(Lanier, 1998, Bottino C, 2005, Abul K. Abbas, 2007). Upon target cell ligation, NK cells integrate the inhibiting and activating signals, which can be elicited simultaneously, and decide to kill or not to kill the target cell, depending on whether NK cell activation exceeds inhibition. When an NK cell is finally activated through e.g. the NKG2D receptor, the cell releases perforin and granzymes, molecules stored in lytic granula (Smyth and Trapani, 2001). Perforin molecules assemble and form a pore in the target cell membrane, which allows granzymes to diffuse into the cell (Young et al., 1986, Browne et al., 1999). Subsequently, granzymes activate pathways in the target cell inducing apoptosis, thus leading to an early eradication of transformed cells (Chowdhury and Lieberman, 2008, van Domselaar et al., 2012). Another mechanism of target cell killing is FAS ligand mediated cytotoxicity (Screpanti et al., 2005). Tumors expressing FAS receptor undergo apoptosis upon ligation by either FAS-L or TRAIL (tumor necrosis factor related apoptosis inducing ligand) (Pahl and Cerwenka, Chua et al., 2004, Smyth et al., 2005). A further potent anti-tumor function of NK cells is the antibody dependent cellular cytotoxicity (ADCC), which is mediated via the Fc- γ -receptor (CD16) expressed on NK cells (Bakema and van Egmond, 2014). The Fc region of an antibody can trigger the activation of Fc- γ -receptors, when tumor cells are coated with an immunoglobulin (Nimmerjahn et al., 2015).

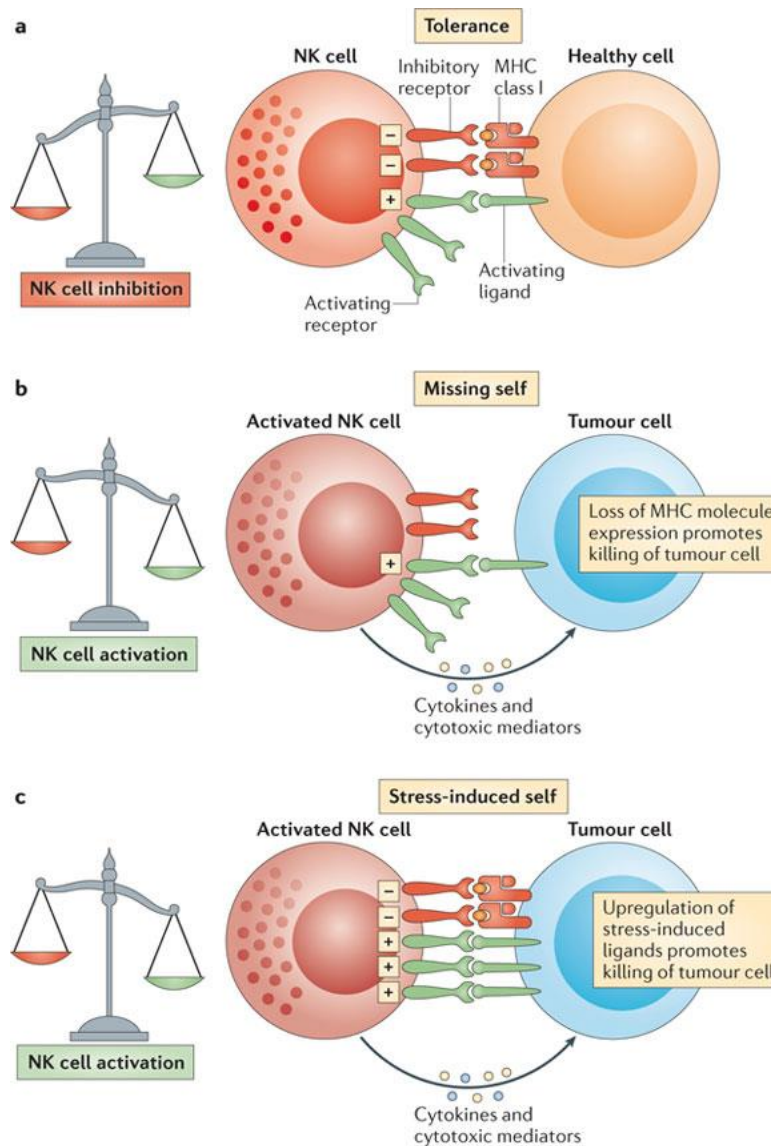


Figure 1-2 Tumor immunity of NK cells

Target cell killing is dependent on the expression and activation of NK cell receptors and target cell surface ligands. (a) tolerance towards a healthy cell is mediated by self-peptide presentation on MHC-I class molecules expressed on healthy cell, “activating” inhibitory receptors on NK cells ; (b) NK cells become activated when MHC-class I molecules are missing on a target cell; (c) NK cell is activated, when stress induced ligands like NKG2D ligands or DNAM-1 ligands are present on target cells, which in turn will be eliminated (adapted from Vivier et al., 2012, Nature Reviews Immunology,(Vivier et al., 2012) non-exclusive license received from NPG).

1.1.3.2 Cytotoxic T Lymphocytes

CD8⁺ T lymphocytes belong to the adaptive immune system. Unlike NK cells, CD8⁺ T cells need to be specifically activated to differentiate into cytotoxic T lymphocytes (CTLs; see figure 1-3). Each T cell has a unique T cell receptor (TCR) recognizing exclusively MHC-presented peptides, at least in healthy humans (Abul K. Abbas, 2007). Usually, T cells are able to differentiate between MHC presented self- and non-self-peptides (Abul K. Abbas,

2007). During early developmental stages in the thymus the TCR repertoire is established by a process called clonal deletion (Goldrath AW, 1999). This process eliminates T cells, which recognize self-peptides, and thus protects healthy tissue of the body from T cell attack, thereby avoiding later autoimmune diseases (Palmer, 2003). Such a mechanism leads to central immune tolerance (Abul K. Abbas, 2007, Coder et al., 2015). Genetic mutations, which lead to an altered amino acid sequence within the native protein upon a malignant transformation, predominantly occur after an individual's T cell repertoire has already developed. In general, those tumor antigens are recognized by T cells as non-self-antigens, thereby initiating an anti-tumor response (Coulie et al., 2014). Prior to cytotoxic T cell killing, the T cell requires an activation mediated by antigen presenting cells (APC), a process, which occurs predominantly in draining lymph nodes (Robinson et al., 1999). Here, dendritic cells (DCs) cross-present tumor associated peptides via direct ligation of the MHC-I presented cancer antigen with the TCR (Palucka and Banchereau, 2012) (figure 1-3). In addition to the MHC-I-peptide-TCR interaction, proper T cell activation further requires costimulation, which is for example mediated by CD86-CD28 interaction (Boise et al., 2010).

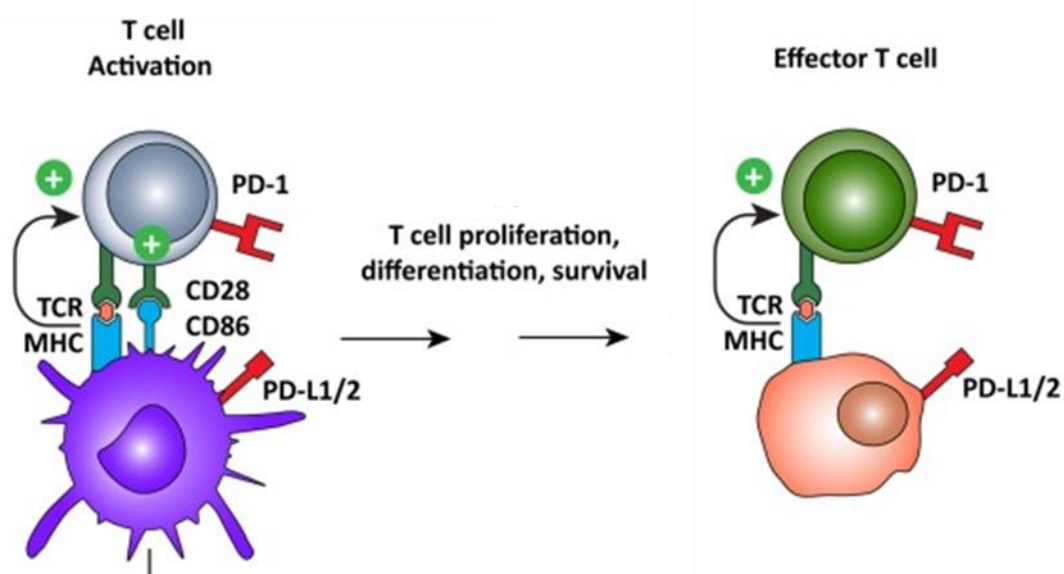


Figure 1-3 Activation of T cell by cross presentation of tumor antigens on APC

The graphic displays the activation of a naïve T cell (grey) by tumor antigen presenting dendritic cell (purple). The tumor associated antigen (orange)-MHC-class I complex binds the T cell receptor and initiates T cell activation and proliferation. In the second step, the activated T cell (green) recognizes tumor cells expressing the target cell (orange) and eliminates the target cell. (adapted and modified from Angela Vasaturo et al. Front Immunol.2013)(Vasaturo et al., 2013)

It has to be mentioned, that the process of T cell activation described here is rather simplified. Once the T cell has been activated, the CTL leaves the lymph nodes and enters the circulation to migrate towards the tumor site (Bellone and Calcinotto, 2013, Oelkrug and Ramage, 2014). Here, the activated T cell recognizes cancer cells presenting the respective antigen and T cell receptor activation is triggered, followed by either FasL mediated killing or the release of perforin and granzymes (Smyth and Trapani, 2001) (figure 1-4). The latter effector mechanism resembles that of NK cells (see 1.1.3.1). After degranulation, target cells are driven into apoptosis and die (Stinchcombe et al., 2001). The CTL is then released and capable to eradicate the next target cell (Janeway CA Jr, 2001).

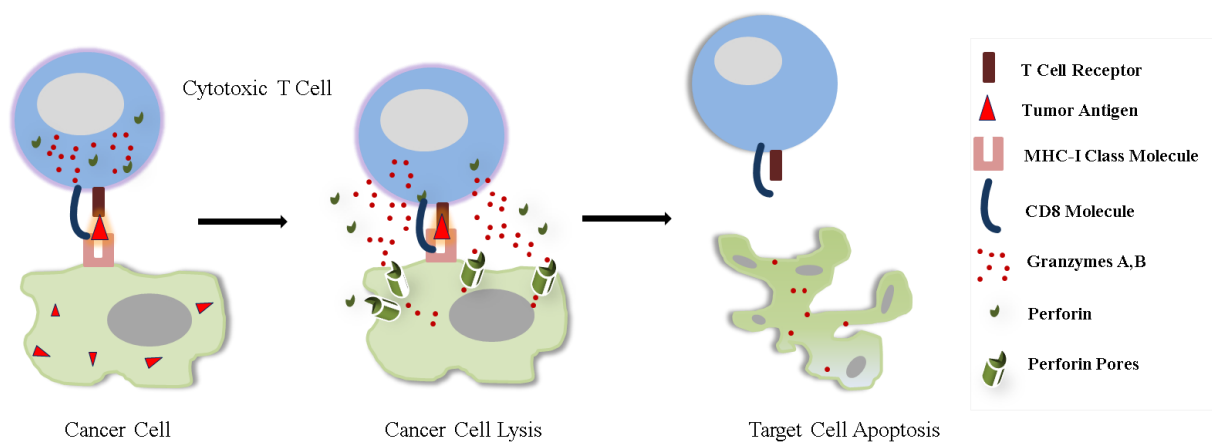


Figure 1-4 Cytotoxic T cell killing of a tumor cell presenting a specific peptide tumor antigen on MHC-class-I molecule

Schematic illustrates typical sequence of cytotoxic T cell killing: activated T cell recognizes tumor antigen presented on MHC-class I molecule expressed on the target cell. TCR-MHC-I interaction plus costimulation triggers the release of granzyme A and B as well as perforin from the T cell. Perforin enables the passage of granzymes into the tumor cell, which in turn induce apoptosis. After the target cell is lysed, the T cell leaves the destroyed target cell, capable to kill further cancer cells.

1.1.3.3 Leukocyte Recruitment

Cytotoxic effector functions of NK cells and T lymphocytes against tumor cells require direct cell-cell contact between the immune cell (effector cell) and the tumor cell (target cell) (Weigelin and Friedl, 2010). Thus, successful cytotoxic tumor cell killing requires the infiltration of immune cells into the tumor microenvironment in order to attain cell mediated cytotoxicity. Leukocyte recruitment is initiated upon the activation of CTLs in the lymph nodes (see 1.1.3.2). Once activated, cytotoxic T cells enter the circulation and navigate to the site of the primary tumor, following a chemokine gradient released from the tumor microenvironment (Newton et al., 2009). At tumor site, a process is initiated, which leads to the migration of CTLs from the blood vessel into the tumor tissue (Ley et al., 2007). This

process can be subdivided into three phases: Rolling of leukocytes (Phase I), adhesion (Phase II) and subsequent transmigration (Phase III) (figure 1-5). Rolling of leukocytes requires the expression of selectins on the surface of endothelial cells (Kunkel EJ, 2002). Selectins slow down leukocytes in the blood vessels by interacting with the selectin ligand on immune cells (Ley, Laudanna et al., 2007). Furthermore, expression of integrin-ligand is essential to subsequently force leukocytes to arrest on the endothelium (Abul K. Abbas, 2007). This cell-cell interaction is mediated by ligation to integrin on immune cells (Pindjakova and Griffin, 2011). Both cell surface molecules can be induced by pro-inflammatory cytokines such as TNF-alpha, a factor which is often found in the microenvironment of tumors (Burke-Gaffney and Hellewell, 1996). In a third step leukocytes transmigrate through the endothelial cells reaching the tumor and stromal tissue.

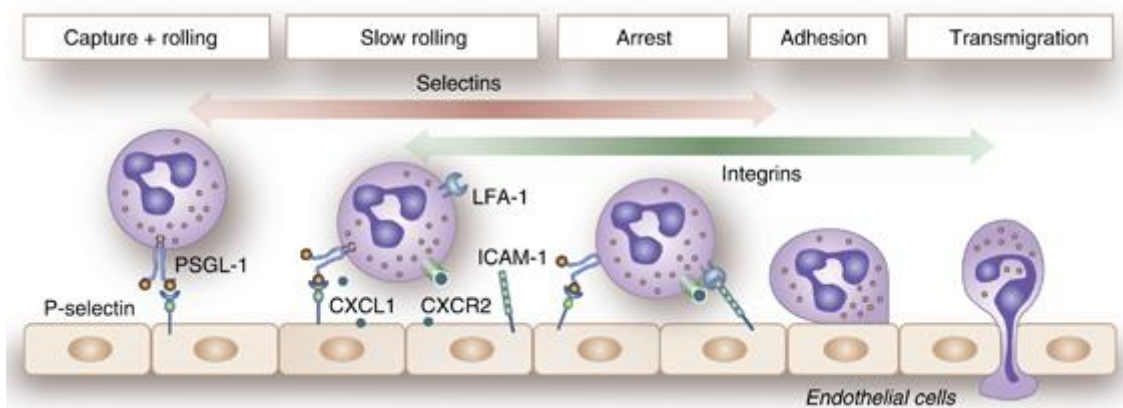


Figure 1-5 Rolling, adhesion and transmigration of leukocytes at the tumor site

The schematic illustrates the required steps of proper leukocyte recruitment to the site of inflammation (e.g. in certain tumor tissues), the rolling, the adhesion and transmigration through endothelial cells (adapted from Jana Pindjakova and Matthew D Griffin, *Kidney International*, non-exclusive license received from NPG)

Today, several publications demonstrate the importance of proper immune cell infiltration (Chew et al., 2012, Fridman et al., 2012) and report a positive correlation between cytotoxic T cell infiltrates in the tumor and a good prognosis for the patient (Dahlin et al., 2011, Tumeh et al., 2014). Therefore, mechanisms which enforce the infiltration of CTL into the tumor are promising approaches to improve tumor therapy.

1.1.4 Immune Evasion

Tumors are under permanent control of a body's immune system. This circumstance had been firstly described by Burnet 1957 as immune-surveillance (Burnet, 1957). Cancer cells or transformed cells are eliminated once immune cells are capable to carry out their killing function as effector cells (see section 1.1.3). However, successful malignant tumors develop "strategies" to escape the control of the immune system by different mechanisms (Kim et al., 2007, Prendergast, 2008).

One immune escape strategy of the tumor is to mask itself by cleaving tumor antigens from the cell surface, a mechanism termed shedding (Law, 1991). Thereby, the tumor cell releases tumor antigens into the circulation, which contribute to immune tolerance (Höchst and Diehl, 2012). Antigen binding without sufficient co-stimulation, as for example B7 – CD28 ligation, results in anergic T cells, which consequently tolerate the tumor cell (Guinan et al., 1994, Cuenca et al., 2003). Furthermore, tumor cells are capable to mediate the induction of regulatory T cells (T_{reg}) e.g. by TGF- β (Fu et al., 2004, Vignali et al., 2008). Regulatory T cells suppress the induction and proliferation of cytotoxic T cells, which in turn allows for enhanced outgrowth of a tumor (Lu and Finn, 2008). Furthermore, several tumors down regulate MHC-class-I molecules on their cell surface, thereby hiding tumor associated antigens from T cell recognition (Bubeník, 2003). However, NK cells are able to respond to low MHC-I class molecule expression on target cells (Waldhauer and Steinle, 2008). Tumors can bypass such NK cell recognition either by upregulating non-classical MHC molecules like HLA-G or by downregulating ligands of activating killing receptors, as for instance NKG2D or DNAM-1, on their cell surface (Rouas-Freiss et al., 2005, Waldhauer and Steinle, 2008). As described above proper effector-to-target-cell-contact is essential for an optimal anti-tumor response (Weigelin and Friedl, 2010). Several tumors express Fas ligand, which activates the Fas receptor expressed on T cells, thereby driving the CTL into cell death (Lu and Finn, 2008). A further immune escape mechanism of tumors is the expression and secretion of immunosuppressive factors, such as soluble HLA-G, IL-10 and TGF- β (Wittke et al., 1999, Rouas-Freiss, Moreau et al., 2005, Thomas and Massagué, 2005). As an example, most solid tumors overexpress TGF- β (Teicher, 2007, Wrzesinski et al., 2007). These soluble factors are secreted into the blood stream and suppress effector immune cell functions at a distant site of the tumor. This is a very effective escape mechanism, which turns NK cells and cytotoxic T lymphocytes into tolerogenic cells, before they could reach the target cell. TGF- β for instance leads to the downregulation of killing receptors on NK and CD8⁺ T cells (Crane et al., 2010). Interestingly, Thomas and Massagué could demonstrate, that the neutralization of TGF- β , by

use of soluble TGF- β type II receptors, restores the expression of perforin, granzyme A, granzyme B, and IFN γ in antigen-specific T cells *in vivo* (Thomas and Massagué, 2005). As a result, T cells regained their cytotoxic effector functions. A finding, which led to the conclusion, that tumor secreted soluble factors, especially those of the large TGF- β family, can act as inducers of immunological tolerance, and thus represent an ideal target structure for therapeutic drugs (e.g. blocking antibodies).

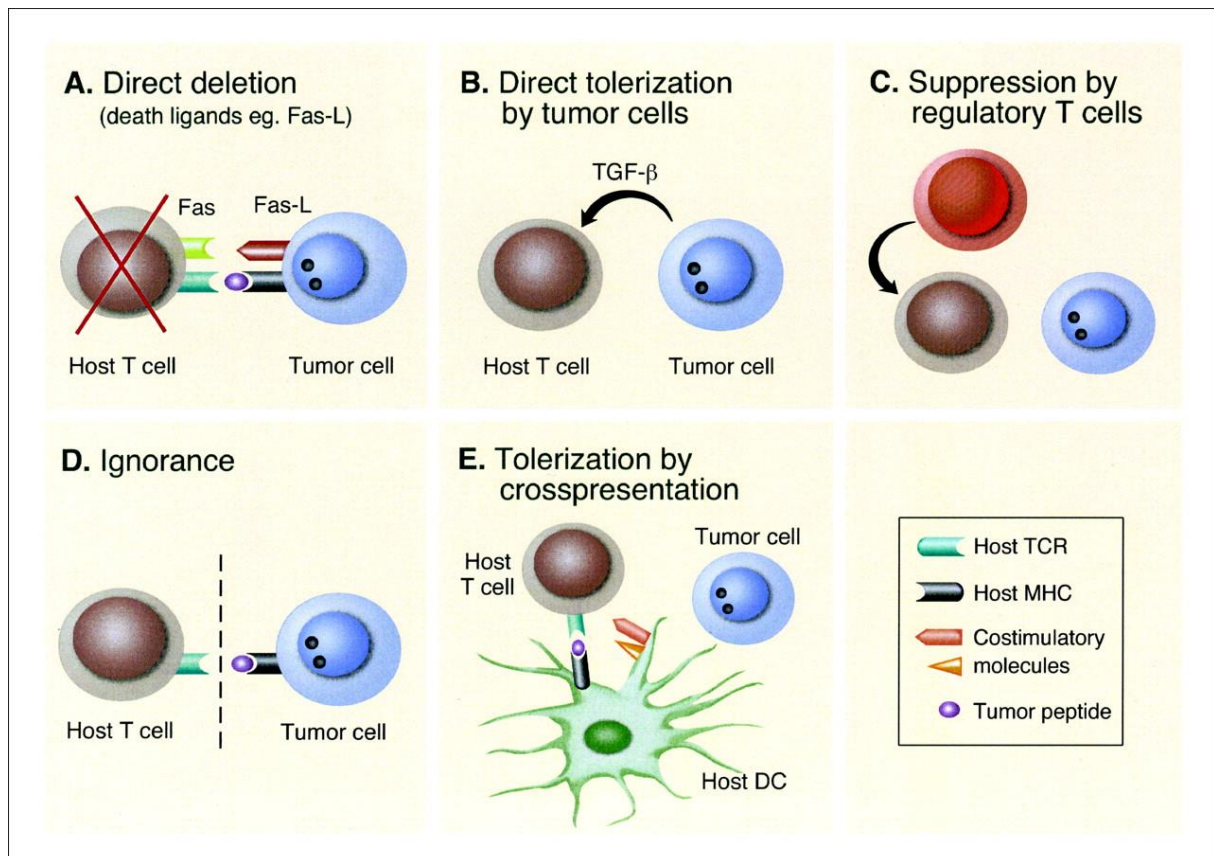


Figure 1-6 Mechanisms of tumor immune evasion

(A) Tumors can eliminate T cells by Fas-L mediated T cell killing, (B) Tolerization of effector T cells by secretion of immunosuppressive factors, (C) induction of regulatory T cells, subsequently repressing effector T cell functions, (D) insufficient immune cell infiltration, ignorance, (E) Tolerization via dendritic cell cross presentation (adapted from Markus Y. Mapara, and Megan Sykes JCO (Mapara and Sykes, 2004), non-exclusive license received from American Society of Clinical Oncology)

In my thesis I focused on the soluble and tumor produced target molecule **GDF-15**, which is structurally related to TGF- β and reported to be involved in immune tolerance, thus possibly contributing to tumor immune escape.

1.2 The TGF- β Superfamily

The TGF- β superfamily comprises about 33 members known so far (figure 1-7). Proteins of this family regulate cellular functions including cellular growth, differentiation, adhesion, migration and apoptosis and are structurally related to each other (Santibanez et al., 2011). Typically, members of that family are dimeric proteins, which are synthesized and secreted as homodimeric precursor proteins (Kingsley, 1994). After processing of the precursor molecules, the mature proteins display a typical seven cysteine knot, a characteristic structure, which is conserved throughout the entire TGF- β superfamily (Kingsley, 1994, Weiss and Attisano, 2013).

This family of sequence- and structurally related molecules can be further subdivided into four major groups (Santibanez, Quintanilla et al., 2011) (figure 1-7). The TGF- β group, consisting of TGF- β 1,-2,-3, Activin/Inhibins, Mullerian IS (MIS) and the bone morphogenic proteins (BMPs). Most of these family members function as ligands, thereby inducing cellular responses (Wakefield and Hill, 2013). These ligand receptor interactions are mediated by heteromeric receptor complexes, comprising type I and type II serine/threonine receptors (Weiss and Attisano, 2013). In humans, type I and type II receptors are subdivided into seven receptors and five receptors, respectively (Weiss and Attisano, 2013).

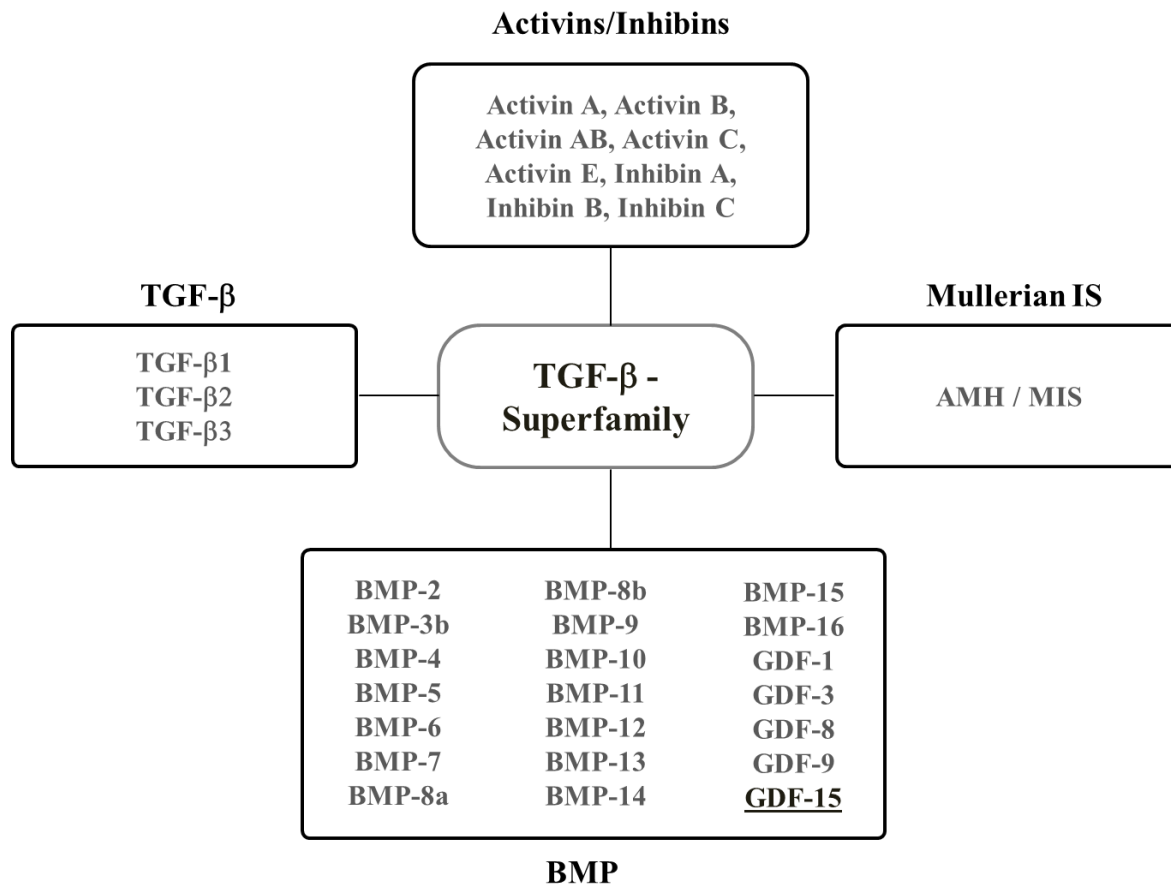


Figure 1-7 The TGF-β superfamily, major groups and members (adapted from Santibanez et al., Clinical Science, 2011)

GDF-15, among further growth and differentiation factors, belongs to the group of bone morphogenic proteins (BMP). The TGF-β superfamily further comprises the TGF-β group, the activins/inhibins group and the Mullerian IS group.

1.2.1 TGF-β

The transforming growth factor-β (TGF-β) is a highly immunosuppressive cytokine in humans which and is involved in malignant cancer progression (Wahl et al., 1988, Massague, 2008). There are three known isoforms denoted TGF-β 1, TGF-β 2, TGF-β 3. Even though TGF-β and its family members elicit different cellular responses, the signaling pathway was described as a linear path from activation of TGF-β receptor II, followed by recruitment of TGF-β receptor I and activation of SMAD proteins (Derynck and Zhang, 2003) (figure 1-8). The heterogeneous receptor ligand assembly causes a trans-phosphorylation of the cytoplasmic domains of the TGF-β-R-I by TGF-β-R-II and followed by the phosphorylation of R-SMAD protein (Derynck and Zhang, 2003). SMAD2 and SMAD3 proteins are phosphorylated once the canonical TGF-β pathway is activated. The SMAD phosphorylation

leads to the trimeric complex formation with Smad4, which then translocates into the nucleus and initiates transcription of target genes (Derynck and Zhang, 2003).

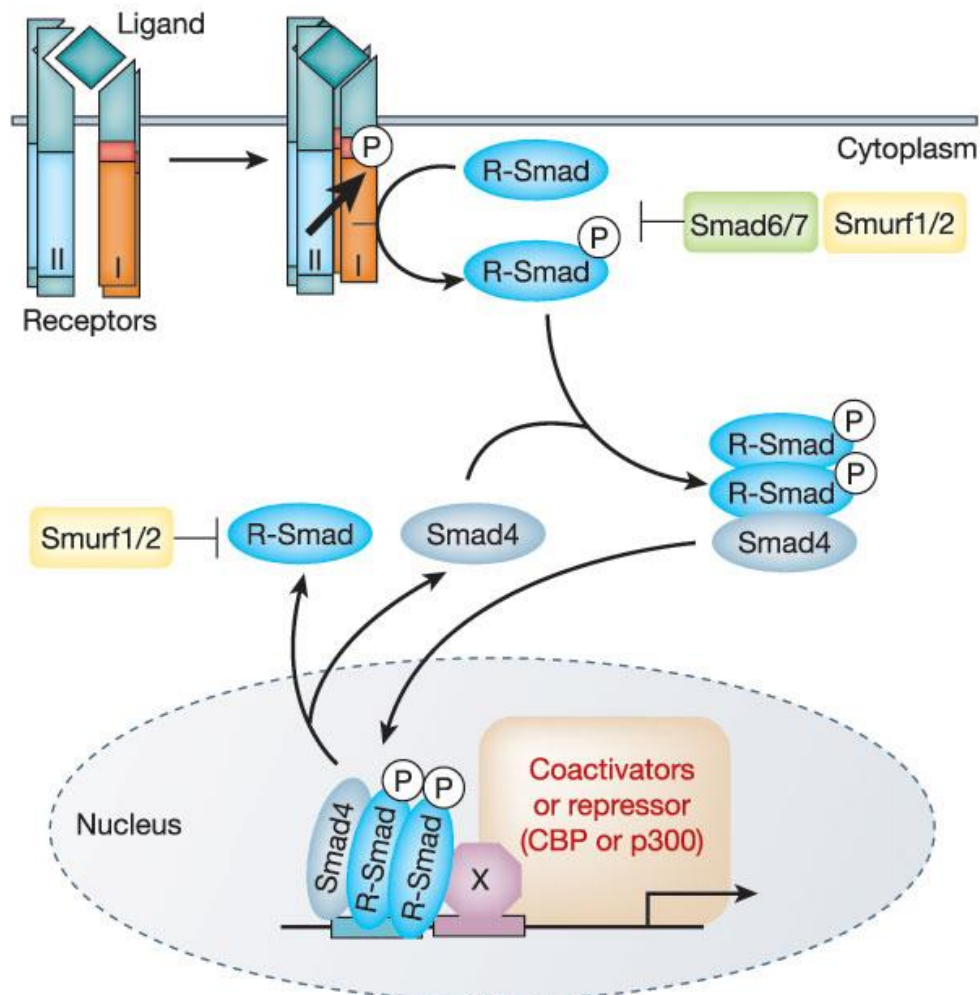


Figure 1-8 TGF-β signaling pathway and its components

This schematic depicts the canonical TGF beta signaling pathway. Upon ligand receptor complex formation R-Smad are phosphorylated and complex with Smad4. The heterotrimeric complex functions as transcription factor after nuclear translocation, resulting in either activation or repression of target genes (Image source: Rik Derynck and Ying E. Zhang, Nature, October 2003; non-exclusive license received from NPG)

1.2.2 TGF-β and Cancer

TGF-β is one of the most cited molecules in a cancer context. The protein has been excessively investigated by tumor immunologists, such as Joan Massagué, who was able to elucidate the role of TGF-β at certain stages of cancer development (Massague, 2008). TGF-β was described as a tumor suppressive factor in the pre malignant state of cancer development. A fact, which is contradictory to later cancer stages, where TGF-β promotes the outgrowth of

tumors (Massague, 2008). As one reason for the “switch” from anti- towards pro-tumorigenic function is the inactivation of components of the TGF- β signaling pathway, as for example the TGF- β receptors (Biswas et al., 2007, Massague, 2008). A further mechanism to bypass tumor suppression by TGF- β is the selective decapitation of the tumor suppressive arm of the TGF- β signaling pathway (Massague, 2008). Such a malfunction of the TGF- β signaling pathway consequently leads to tumorigenesis. Once this stage has reached, TGF- β contributes to tumor growth and invasion, helps the tumor to escape the immune system and promotes metastasis (Massague, 2008).

With regard to tumor immune escape, TGF- β was reported to diminish the expression of NKG2D receptors on both NK cell and CD8⁺ T cells, thereby affecting tumor-immune response (Friese et al., 2004). Importantly, Friese and colleagues could demonstrate that the NKG2D downregulation could be prevented, when the TGF- β synthesis has been silenced, which further indicates that inhibition of this immunosuppressive factor might “reactivate” the immune system, opening a very attractive target mechanism to therapeutically overcome immune escape mechanisms (Arteaga, 2006). Here, soluble and secreted immunosuppressive proteins like TGF- β and family members thereof offer valuable target structures for neutralization, for example with antibody.

1.2.3 GDF-15

The growth and differentiation factor 15 (GDF-15, also known as MIC-1, NAG-1, PTGF- β , PDF and PLAB) was first described 1997 by Bootcov and colleagues as a divergent member of the TGF- β superfamily (Bootcov et al., 1997). At that time the function of GDF-15 had been reported as macrophage inhibitory cytokine, consequently named MIC-1. The group showed that MIC-1 inhibits the production of TNF- α by macrophages upon lipopolysaccharide stimulation, indicating that MIC-1/GDF-15 acts as an autocrine regulatory molecule in macrophages (Bootcov, Bauskin et al., 1997). The fact that GDF-15 received so many synonyms underlines its various biological involvements in physiological and pathological processes (Mimeault and Batra, 2010). However, until today, the biological function of GDF-15 regarding its mechanism of action is still not fully unravelled. The missing puzzle for understanding the broad spectrum of GDF-15 mediated effects – reported in the literature- might be the GDF-15 receptor, which is still unknown.

1.2.3.1 GDF-15 - Structure and Biochemistry

Like TGF- β 1, the human GDF-15 gene is located on chromosome 19 (region p13.1-123.2), consisting of a nucleotide length of 2746 bps. Similar to other members of the TGF- β superfamily, GDF-15 protein sequence comprises a signal peptide encoding 29 amino acids (AA), a pro-peptide (167 AA) and a mature-peptide (112 AA) (Bootcov, Bauskin et al., 1997) (figure 1-9). GDF-15 is translated into a monomeric full length precursor protein of 308 amino acids, which dimerizes via a disulfide bond, located within the mature region, into a full length protein in the endoplasmic reticulum (Bauskin et al., 2000). This precursor protein is either rapidly secreted - a process occurring in the trans Golgi network - or further processed by proteolytic cleavage via a furin-like protease at position 196, resulting in N-terminal monomeric pro-peptides and homodimeric C-terminal mature protein (Bauskin et al., 2010) (figure 1-10). Because of these alternate secretory pathways, described by Bauskin and colleagues, supernatants of GDF-15 expressing cells contain various forms of GDF-15, including the pro-peptide and mature GDF-15 dimer (figure 1-10 a, b) as well as the dimerized full length precursor protein (Bauskin, Jiang et al., 2010).

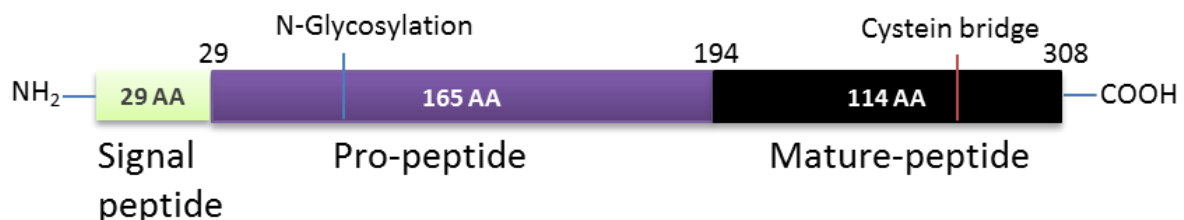


Figure 1-9: Full length GDF-15 protein

The GDF-15 protein comprises a signal peptide of 29 amino acid length, followed by a pro-peptide sequence with 165 amino acids and the mature GDF-15 peptide sequence of 114 amino acids. The pro-peptide contains an N-glycosylation site at amino acid position 70.

Bauskin and colleagues could show that the proform of GDF-15 is capable to bind extracellular structures and thereby building up stromal stores of GDF-15 including the uncleaved mature GDF-15 dimer (Bauskin et al., 2006, Bauskin, Jiang et al., 2010).

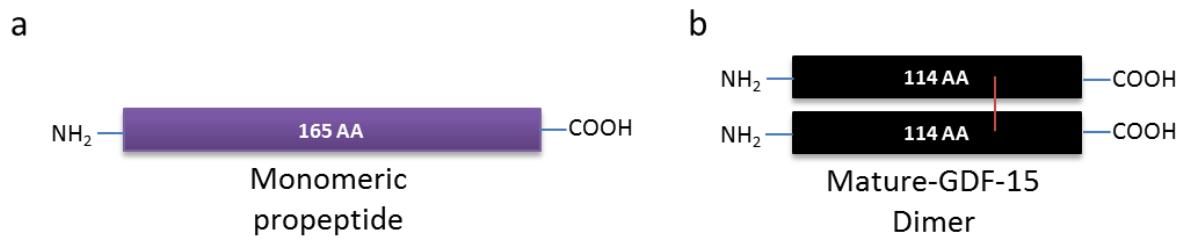


Figure 1-10 Processed forms of GDF-15 protein

The full length protein of GDF-15 is cleaved by a furin like convertase into the monomeric proforms of GDF-15 (a) and the mature dimer (b). The mature GDF-15 monomer dimerizes into a 25kDa GDF-15 dimer.

The diversity of GDF-15 and its various forms, which can be found in supernatants of tumor cells, is depicted in figure 1-11.

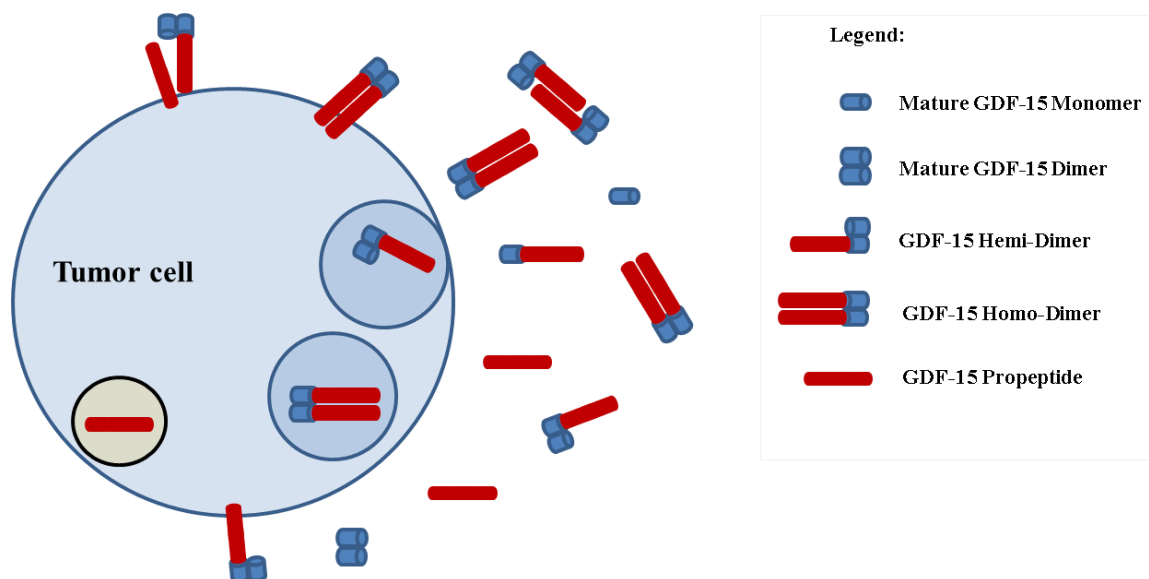


Figure 1-11 Schematic of GDF-15 forms expressed by tumor cells

In tumor cell supernatants the following forms are predominantly detected: the mature GDF-15 dimer, the propeptide containing GDF-15 hemi dimer, the full length homo dimeric GDF-15 form as well as the singular propeptide. It has to be mentioned that the mature monomer is seen to a far lesser extent in supernatants than all other forms. Possibly the mature monomer appears due to a disintegration of the GDF-15 dimer during a Western Blot procedure.

1.2.3.2 Expression of GDF-15

Under physiological conditions GDF-15 is mainly expressed in high levels in the placenta, which explains its synonyms “placental bone morphogenic protein” or “placental TGF- β ” (pBMP / PLAB; PTGF- β) (Hromas et al., 1997). By implication, high GDF-15 serum levels can be detected in pregnant woman (Moore et al., 2000, Tong et al., 2004). Compared to the high expression in the human placenta, GDF-15 can be found to lower extent in the liver, the kidney, the prostate, the lung and gastrointestinal tract (Mimeault and Batra, 2010). Further, Strelau and colleagues reported that GDF-15 is expressed in the central as well as peripheral nervous system in humans (Strelau et al., 2000). In mice, GDF-15 is reported to be expressed in and secreted by Schwann cells (Strelau et al., 2009).

Under pathological conditions the GDF-15 expression profile changes dramatically. GDF-15 protein level immediately increases in patients suffering from a myocardial ischemia (Kempf et al., 2011). Furthermore, GDF-15 serum levels are elevated when nonsteroidal anti-inflammatory drugs (NSAIDs) are consumed, the reason why GDF-15 is found in the literature as nonsteroidal anti-inflammatory drug-activated gene-1 (NAG-1) (Baek et al., 2001).

Last but not least, GDF-15 is found to be overexpressed in a variety of different cancers (table 1). The relevance of the GDF-15 expression in oncological indications will be described in detail in section 1.2.3.4.

Solid Cancer	Hematologic Cancer
Breast Cancer (Kim et al., 2008)	Multiple Myeloma (Corre et al., 2012)
Prostate (Brown et al., 2009)	
Ovarian Carcinoma (Staff et al., 2010, Staff et al., 2011)	
Colorectal Carcinoma (Baek et al., 2009) (Brown et al., 2003)	
Gastric Cancer (Lee et al., 2003)	
Oesophageal adenocarcinoma (Fisher et al., 2015)	
Oral squamous cell carcinoma (Zhang et al., 2009)	
Melanoma (Boyle et al., 2009, Huh et al., 2010)	
Pancreatic Cancer (Koopmann et al., 2004)	
Glioblastoma (Roth et al., 2010)	

Table 1: List of cancer types associated with elevated GDF-15 expression

1.2.3.3 GDF-15 and its Function

A variety of different functions have been reported for GDF-15 in the last two decades. Initially the protein revealed an inhibitory effect on macrophages (see 1.2.2), thereby suppressing the inflammation through the inhibition of macrophage activation (Bootcov, Bauskin et al., 1997).

GDF-15 plays an important role during pregnancy. When GDF-15 serum levels were below a certain amount in the early course of pregnancy, spontaneous abortion and preeclampsia was observed in retrospective analysis (Tong, Marjono et al., 2004). One might speculate that GDF-15 has an inhibiting effect on the immune system, which goes along with the suppressive effect of GDF-15 on human macrophages (Bootcov, Bauskin et al., 1997).

Strelau and colleagues identified GDF-15 as a trophic and neuroprotective factor in the central nervous system in midbrain dopaminergic rat neurons (Strelau, Sullivan et al., 2000). Herein, GDF-15 was reported to normalize motor behavior and exerts a protective effect on dopaminergic neurons. Furthermore, GDF-15 was reported to promote survival of lesioned dopaminergic neurons (Strelau et al., 2003).

Kempf and colleagues attributed GDF-15 a cardio protective function after a heart attack, permitting proper infarct healing (Kempf, Zarbock et al., 2011). The group demonstrated that, after a myocardial infarction, GDF-15 is rapidly released into circulation and lowers the adhesion of peripheral polymorphonuclear leukocytes (PMNs) in mice on the endothelium. As a result, leukocyte infiltration into the surrounding of the affected myocardium is reduced. The scientists concluded that GDF-15 functions as a protective factor, which prevents the heart from cardiac rupture due to massively infiltrating lymphocytes into the ischemic tissue (Kempf, Zarbock et al., 2011).

Recently, GDF-15 was additionally reported as a nuclear factor, modulating the transcriptional regulation of the Smad pathway (Min et al., 2015). The group around Min proposed that cytoplasmic GDF-15 is imported into the nucleus and interrupts the DNA-binding capacity of Smad proteins, thereby repressing Smad signaling. However, this finding is somewhat contradictory to the activation of the TGF- β -receptor in hypothalamic neurons mediated by GDF-15 (Johnen et al., 2007).

1.2.3.4 GDF-15 in Cancer

As described in 1.2.3.2 GDF-15 is overexpressed in many solid cancers. Hence, the question arises, why tumors upregulate GDF-15 expression and which advantage do they have?

Even though many publications allocate GDF-15 to certain malignancies, one has to differentiate between a plain correlation and a functional relevance.

A lot of opposing effects of GDF-15 are reported in the context of cancer, reviewed in detail by Mimeault and Batra (Mimeault and Batra, 2010). Several publications link GDF-15 with pro-apoptotic effects on cancer cells (Baek, Kim et al., 2001, Kadara et al., 2006). Others associate GDF-15 with pro-tumorigenic effects (Mimeault and Batra, 2010).

Regarding the pro-apoptotic and anti-tumorigenic effects, GDF-15 was shown to mediate cell morphological changes, thereby leading to apoptosis in prostate cancer cell lines *in vitro* (Liu et al., 2003). However, the effect of apoptosis was speculated to be a secondary effect, owed to the detachment of cells. Overexpression of GDF-15 in colorectal cancer cells led to an increase in cell death and revealed a reduction in colony formation on soft agar plates, which led to the authors conclusion that GDF-15 is a tumor inhibiting molecule (Baek, Kim et al., 2001). Kadara and colleagues could demonstrate that GDF-15 expression is induced in lung cancer cells as a response of treatment with apoptosis-inducing agents (e.g. retinoid related molecule RRM) (Kadara, Schroeder et al., 2006). However, the authors could also show that silencing GDF-15 did not affect the RRM induced apoptosis, concluding that GDF-15 is expendable (Kadara, Schroeder et al., 2006).

Despite the reports on anti-tumorigenic effects of GDF-15, there is accumulating evidence that GDF-15 exerts pro-tumorigenic effects and rather negatively influences cancer patients than to benefit. Apart from GDF-15's reported contribution to "all-cause mortality", its overexpression in cancer correlates with poor prognosis in colon carcinoma, endometrial cancer and oral squamous cell carcinoma (Boyle, Pedley et al., 2009, Zhang, Yang et al., 2009, Wiklund et al., 2010, Staff, Trovik et al., 2011). For example, Brown and co-worker demonstrated in a study, which included a large number of colorectal carcinoma patients, that elevated GDF-15 serum level at the time of diagnosis were associated with decreased overall survival (Brown, Ward et al., 2003). Staff and colleagues showed that high GDF-15 plasma levels correlate with poor prognosis in women suffering from endometrial cancer (Staff, Trovik et al., 2011). Similarly, Zhang et al could demonstrate a correlation between GDF-15 expression on RNA level and the grade of malignancy in oral squamous cell carcinoma (Zhang, Yang et al., 2009).

Elevated MIC-1/GDF-15 serum levels were reported to be frequently observed during the progression of a variety of aggressive cancers (Mimeault and Batra, 2010). In a glioma mouse model published by our group, GDF-15 contributed to tumor growth and immune escape (Roth, Junker et al., 2010). Downregulation of murine GDF-15 resulted in prolonged survival of glioma bearing mice, which might be explained by enhanced immune cell infiltration into the tumor microenvironment (Roth, Junker et al., 2010). Shnaper and colleagues reported that GDF-15 protein levels measured in cerebrospinal fluid correlates with poor prognosis in glioma patients (Shnaper et al., 2009).

Interestingly, Husaini and colleagues reported that GDF-15 has a growth inhibitory effect on prostate cancer cells *in vivo* but increases metastasis in mice (Husaini et al., 2012). Surprisingly, a recent publication assigned GDF-15 pro-tumorigenic potential during early development of prostate carcinoma, while anti-tumorigenic effects are assumed once prostate carcinoma has established (Rybicki et al., 2015).

Further evidence for its tumor promoting function was given by Lee and colleagues who demonstrated that GDF-15 takes part in the malignant progression of gastric cancer cells (Lee, Yang et al., 2003). Herein, migration assays were applied to show the GDF-15 mediated invasiveness of cancer cells upon activation of the MAPK signaling pathway (Lee, Yang et al., 2003).

Boyle et al could show that GDF-15 protein expression was elevated in more than 65% of 53 human melanoma cell lines, when compared to the expression of melanocytes (Boyle, Pedley et al., 2009). The group further observed strong GDF-15 expression in metastatic melanoma tissue, whereas GDF-15 expression in biopsies of primary melanoma was low. Furthermore, downregulation of GDF-15 in melanoma cells significantly lowered tumorigenicity (Boyle, Pedley et al., 2009). Moreover, Huh and co-workers could show that GDF-15 was able to promote angiogenesis in melanoma, leading to the conclusion, that GDF-15 stimulates the development of blood vessels in tumors, thereby increasing melanoma outgrowth (Huh, Chung et al., 2010).

Regarding its dual function, GDF-15 may act similarly to what Massagué has elucidated for TGF- β (Massague, 2008): in a pre-malignant cancer stage GDF-15 may act anti-tumorigenic, whereas tumor-promoting effects occur, once a progressive tumor stage has reached (Eling et al., 2006). Mimeault and Batra even state that GDF-15 “...*displays anti-tumoral activities in the early stages of cancer development*”, while it “...*rather promotes the invasion and metastases of cancer cells at distant tissues in the late stages of cancer.*” (Mimeault and Batra, 2010).

Summarizing the literature available so far, there is an obvious majority of reports assigning tumor promoting effects of GDF-15, thus turning this cytokine in a very attractive therapeutic cancer target, which could be neutralized and functionally inhibited.

Interestingly, GDF-15 does not only exert direct effects on the tumors. There is increasing evidence that GDF-15 systemically influences patient's health conditions by contributing to tumor associated "cancer anorexia-cachexia syndrome" (Johnen, Lin et al., 2007). Johnen and colleagues could impressively elucidate a biological function of GDF-15 in this context. They demonstrated, that tumor cell derived human GDF-15 causes anorexia by signalling on hypothalamic neurons in the central nervous system, thereby leading to tumor associated cachexia in a mouse model bearing human prostate cancer cells (Johnen, Lin et al., 2007). The protein is secreted by tumor cells into the blood stream, which could be shown by high GDF-15 serum levels in the mice, which in turn correlated with the loss of appetite and decreased body weight (Johnen, Lin et al., 2007). Using GDF-15 specific antibodies, this pro-cachectic effect could be completely rescued. A fact, that offers a new chance for cancer therapy, which is highly attractive when having in mind that more than 20% of cancer patients die due to cachexia (Warren, 1932, Tisdale, 2002). Furthermore, Tisdale reported that up to 50% of cancer patients suffer from cachexia and – referring to Dewys and colleagues- cancer-associated loss of weight is coherent with shortened survival of the cancer patient (Dewys et al., 1980, Tisdale, 2009). Referring to Inui, "*progressive wasting is one of the most important factors leading to early death in cancer patients*" (Inui, 1999).

Taken together, GDF-15 is a versatile molecule overexpressed in many cancers and predominantly correlated with worse outcome for cancer patients. Thus, the scientific community has recognized GDF-15 as a cancer target, worth to develop therapeutics against (Boyle, Pedley et al., 2009, Huh, Chung et al., 2010, Mimeault and Batra, 2010).

1.3 Treatment of Cancer with Targeted Therapy

Today, cancer treatment comprises a variety of methods and technologies such as surgical resection, radiation therapy, chemotherapy, hormonal therapy, as well as targeted- and immunotherapy (Sudhakar, 2009). Targeted cancer therapy comprises drugs, which specifically bind and interfere with molecular targets, thereby inhibiting cancer growth and

spread (Blay et al., 2005) . According to Oldham, “*pioneers in monoclonal antibody research believed that a new era of cancer therapy had begun*” in the early eighties, shortly after the first proof of principle with a monoclonal antibody could be demonstrated in humans (Nadler et al., 1980, Oldham and Dillman, 2008). At that time, targeted therapy came more and more in focus.

1.3.1 Antibodies in the Clinic

The importance of monoclonal antibodies as therapeutic agent for cancer treatment becomes more evident, when looking at the list of FDA approved cancer antibodies (Scott et al., 2012) (table 1). Far more antibodies are currently tested in clinical trials (Nelson et al., 2010). The advantages of monoclonal antibodies (biologicals) become clear, when looking at the variety of potential immunoglobulin derivatives, which can be engineered and thus “customized” for its optimal effector function (e.g. antibody fragments, Fc engineered antibodies, toxin-conjugated antibodies, etc.) (Chames et al., 2009).

International non proprietary name	Trade name	Target; Format	Indication first approved or reviewed	First EU approval year	First US approval year
Dinutuximab	Unituxin	GD2; Chimeric IgG1	Neuroblastoma	EC decision pending	2015
Nivolumab	Opdivo	PD1; Human IgG4	Melanoma, non-small cell lung cancer	EC decision pending	2014
Blinatumomab	Blincyto	CD19, CD3; Murine bispecific tandem scFv	Acute lymphoblastic leukemia	In review	2014
Pembrolizumab	Keytruda	PD1; Humanized IgG4	Melanoma	EC decision pending	2014
Ramucirumab	Cyramza	VEGFR2; Human IgG1	Gastric cancer	2014	2014
Obinutuzumab	Gazyva	CD20; Humanized IgG1; Glycoengineered	Chronic lymphocytic leukemia	2014	2013
Ado-trastuzumab emtansine	Kadcyla	HER2; humanized IgG1; immunoconjugate	Breast cancer	2013	2013
Pertuzumab	Perjeta	HER2; humanized IgG1	Breast Cancer	2013	2012
Brentuximab vedotin	Adcetris	CD30; Chimeric IgG1; immunoconjugate	Hodgkin lymphoma	2012	2011
Ipilimumab	Yervoy	CTLA-4; Human IgG1	Metastatic melanoma	2011	2011
Ofatumumab	Arzerra	CD20; Human IgG1	Chronic lymphocytic leukemia	2010	2009

Catumaxomab	Removab	EPCAM/CD3;Rat/mouse bispecific mAb	Malignant ascites	2009	NA
Panitumumab	Vectibix	EGFR; Human IgG2	Colorectal cancer	2007	2006
Bevacizumab	Avastin	VEGF; Humanized IgG1	Colorectal cancer	2005	2004
Cetuximab	Erbix	EGFR; Chimeric IgG1	Colorectal cancer	2004	2004
Tositumomab-I131	Bexxar	CD20; Murine IgG2a	Non-Hodgkin lymphoma	NA	2003#
Ibritumomab tiuxetan	Zevalin	CD20; Murine IgG1	Non-Hodgkin lymphoma	2004	2002
Gemtuzumab ozogamicin	Mylotarg	CD33; Humanized IgG4	Acute myeloid leukemia	NA	2000#
Trastuzumab	Herceptin	HER2; Humanized IgG1	Breast cancer	2000	1998
Rituximab	MabThera, Rituxan	CD20; Chimeric IgG1	Non-Hodgkin lymphoma	1998	1997

Table 2 List of FDA approved monoclonal antibodies used for treatment of oncological indications

#, Withdrawn or marketing discontinued for first approved indication

NA, not approved; Source: Janice M. Reichert, PhD, Reichert Biotechnology Consulting LLC; updated May 26, 2015; Use of that table was kindly permitted by Janice Reichert.

1.3.2 Antibody Structure

Antibodies are proteins, consisting of four polypeptide chains: Two heavy and two light chains (Janeway CA Jr, 2001). The heavy chain polypeptide has a molecular weight of ~50 kDa, whereas the light chain assesses 25 kDa (Janeway CA Jr, 2001). Antibodies are further subdivided in the variable and constant region. Within the variable region of each chain of an immunoglobulin (heavy and light) the complementarity determining regions (CDRs) are encoded (Al-Lazikani et al., 1997). Upon assembly of both light and heavy variable chains the functional antigen binding site (Fab; fragment of antigen binding) is formed (Abul K. Abbas, 2007). Since these variable regions define the specificity of an immunoglobulin towards its target antigen, its individual antigen binding sequences are also named hypervariable regions (Abul K. Abbas, 2007). The constant region is found in the heavy as well as in the light chain of an antibody. Depending on the immunoglobulin isotype, the heavy chain comprises three constant region Ig domains (IgA, IgD, IgG), or four Ig domains (IgM, IgE) (Janeway CA Jr, 2001). Typically antibodies contain an Fc part, which is part of the constant region of the heavy chain (Woof and Burton, 2004). This Fc part can interact with Fc γ -receptors on certain

immune cells (macrophages and NK cells), representing a further functional element of an antibody (Heyman, 1996, Bakema and van Egmond, 2014).

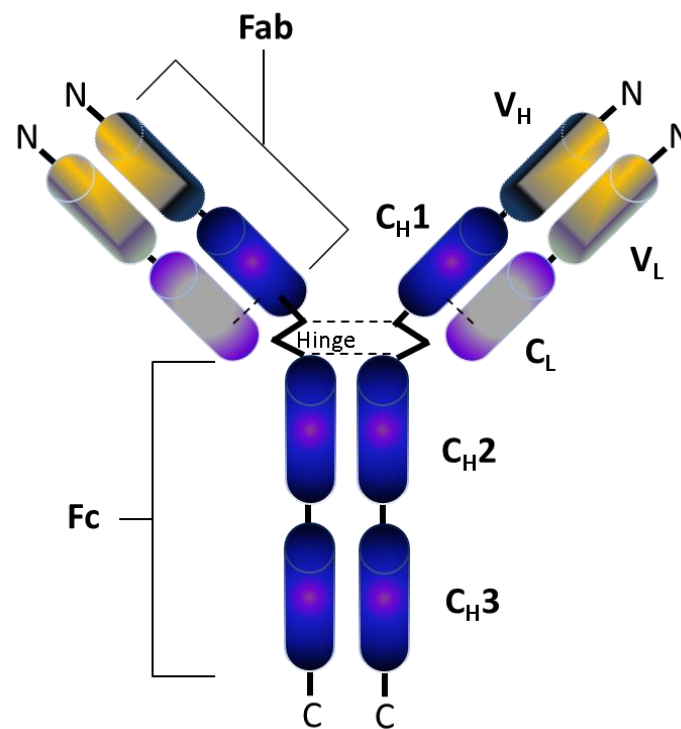


Figure 1-12 Schematic of an antibody structure

Immunoglobulin type IgG illustrates the typical structural and functional elements of antibodies. The heavy chain comprises three heavy chain constant regions (C_{H1} , C_{H2} , C_{H3} ; black/blue) and the heavy chain variable region (V_H ; gray/purple). The antigen binding site (Fab) is depicted in yellow. Fc part represents a region of the constant heavy chains. The Fc region of the antibody heavy chain is linked to the Fab site by the hinge region of the immunoglobulin.

1.3.3 Antibody Humanization

Mouse antibodies revealed an enormous disadvantage when clinically applied in humans (Nelson, Dhimolea et al., 2010). Since murine immunoglobulins are very immunogenic, the generation of human anti mouse antibodies (HAMAs) occurs even after single dose administration of mouse antibodies, which can either elicit immune responses in patients or decreases its therapeutic efficacy (Dillman et al., 1986, Dillman et al., 1994, Kuus-Reichel et al., 1994, Baert et al., 2003, Oldham and Dillman, 2008). To circumvent this problem, either chimeric, humanized or fully human antibodies are developed prior therapeutic administration

(Nelson, Dhimolea et al., 2010). In order to create chimeric antibodies from murine antibodies, typically the DNA sequence of the murine Fab region, which contains the antigen binding site, in particular the CDRs, is joined to the DNA sequence of the constant region coding a human immunoglobulin backbone (Morrison et al., 1984). Subsequent transfection of such chimeric DNA constructs into a suitable cellular system results in the expression of the designed immunoglobulin (Morrison, Johnson et al., 1984).

Humanized antibodies differ from chimeric ones, in that only the murine CDRs remain in the human immunoglobulin, which are - analogous to the above described method- genetically engineered, a procedure called CDR grafting (Kettleborough et al., 1991). Here, the murine framework regions (FR1-FR4) can be changed towards a more human sequence without loss of antigen binding, whereas the CDRs remain of murine origin (Harding et al., 2010) (figure 1-13). This minimizes the immunogenicity and results in a longer applicability of the drug, compared to fully murine antibodies, where a HAMA response is rapidly expected (Klee, 2000, An, 2008). The least immunogenic antibody form is a fully human antibody itself, which can be developed by either using transgenic mice containing the human immunoglobulin genes instead of the innate mouse Ig gene sequences or via phage display technology (An, 2008, Nelson, Dhimolea et al., 2010).

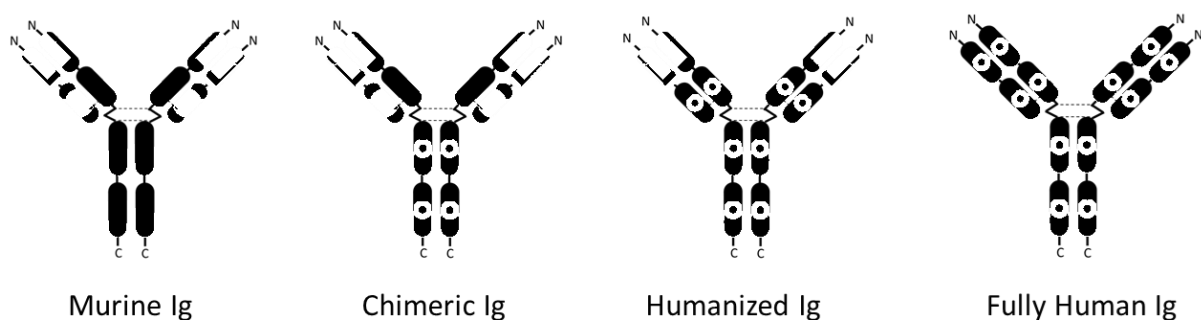


Figure 1-13 Different forms of clinically applied antibodies

Murine immunoglobulins: representing the most immunogenic type, when administered in patients. Chimeric antibody: containing the murine variable region of an antibody on a human Ig backbone. Humanized antibody: represents a human immunoglobulin with only murine CDRs. Fully human antibody: exceptionally human immunoglobulin sequences, resulting in lowest immunogenicity, when applied in human patients (e.g. Panitumumab, see table 2).

1.3.4 Mode of Actions of Antibodies

Antibodies elicit a variety of different effector mechanisms, which are used clinically to fight certain cancer (Weiner, 2007). One of these mechanisms include antibody dependent cellular cytotoxicity (ADCC) (Alderson and Sondel, 2011). Monoclonal antibodies bound to the cancer cell surface, enhance the recruitment of Fc- γ -receptor positive immune cells, thereby enabling a proper anti-tumor response (Weiner and Adams, 2000, Hudis, 2007). NK cells as well as macrophages recognize the Fc portion of an antibody via the Fc- γ -receptor, which leads to the activation of the immune cell, triggering an anti-tumor response (Janeway CA Jr, 2001). The FDA approved antibodies Rituximab (MabThera®) and Trastuzumab (Herceptin®) are examples for ADCC mediators. Rituximab targets the surface molecule CD20 on B cells, eradicating B cell lymphoma (Reff et al., 1994). Trastuzumab can be administered in patients with HER2 positive breast cancer (Hudis, 2007, Baselga, 2010). Beside further mechanisms of action described for Trastuzumab, ADCC serves as potent mechanism to eradicate cancer cells (Baselga, 2010, De et al., 2013).

Furthermore, antibodies are able to induce complement mediated cytotoxicity (Courtois et al., 2012). As an example Alemtuzumab, a FDA approved monoclonal antibody directed against CD52 expressed on B cell efficiently lyses lymphocytic leukemia B cells (B-CLL) by complement activation (Golay et al., 2004).

A further therapeutic approach is the use of antibody drug conjugates (ADC). Such antibodies can be linked to certain payloads, for example toxins, and lead to cell death once the antibody-toxin conjugate has been internalized by the target cell (Leal et al., 2014). As an example Trastuzumab-Emtansine (T-DM1), which represents the anti-HER2/NEU antibody Trastuzumab, conjugated with the toxic derivative of maytansine (DM1) (LoRusso et al., 2011).

Several antibodies can be clinically used to prevent signal transduction in cancer cells (e.g. targeting EGFR signaling by Cetuximab and Panitumumab), leading to tumor growth inhibition (Marcucci et al., 2013). Such interfering antibodies may target surface receptors, co-receptors but also the ligands thereof (Marcucci, Bellone et al., 2013).

Antibodies can also be used for neutralization of target molecules (Marcucci, Bellone et al., 2013). The most prominent example of this antibody class is Bevacicumab (Avastin®), which neutralizes VEGF and thus inhibits neovascularization of tumor tissue (Ferrara et al., 2004). In particular immunosuppressive molecules like TGF- β are optimal targets for an immunotherapy by “simply” antagonizing the soluble protein (Buijs et al., 2012). Although there is no FDA approved anti TGF- β antibody so far, several approaches to block the TGF- β

signaling are currently tested in clinical trials (Buijs, Stayrook et al., 2012). Until today, the results of a phase II clinical trial testing Fresolimumab (GC1008), a fully human monoclonal antibody, which targets and blocks all TGF- β isoforms 1, -2, -3 for the treatment of Relapsed malignant pleural mesothelioma, were not published yet, despite finalization of the study in 2010 (Buijs, Stayrook et al., 2012).

1.4 The Aim of the Thesis

GDF-15 seems to be a novel target for treating cancer. Development of a monoclonal antibody to GDF-15 seemed promising and was a relevant part of my PhD thesis. Based on the findings of our glioma model, in which silenced GDF-15 levels in tumor cells led to extended survival of animals, a systemic blocking of GDF-15 seemed to be a promising strategy to improve the outcome of tumor patients. Therefore, a monoclonal antibody which could block GDF-15 systemically, may act as an immunotherapeutic biological, reducing tumor growth, enhancing immune cell infiltration and improving cachexia syndrome at once. Accordingly, the goal of my thesis was to further characterize GDF-15 biology in the tumor context *in vitro*, to generate a highly specific blocking monoclonal antibody and to test that antibody after an extensive characterization in a xenograft mouse model.

The results of my work resulted in a substantial grant (“GO-Bio”) from the federal ministry of education and research (BMBF; grant no: FKZ031A148). This granted project intended the establishment of a spin-off biotech company focusing on immunotherapeutic drug research and development, a project which is still ongoing and not further mentioned here. However, this affects the freedom to describe several details of this thesis due to patent issues.

2 Material and Methods

2.1 Material

2.1.1 Devices

Devices	Manufacturer
ABI TaqMan 7500	Applied Biosystems, Life Technologies, Corporation, Carlsbad, California 92008, USA
Agarose gel electrophoresis apparatus	MupidexU, Eurogentec GmbH, Cologne, Germany
Autoclave	H P Labortechnik AG, 85764 Oberschleißheim, Germany
Balance	Sartorius AG, 37075 Goettingen, Germany
Centrifuges	5810 R, 5424 R Eppendorf, 22339 Hamburg, Germany Jouan C4i, Heraus Megafuge 16 Thermo Electron GmbH, 63303 Dreieich, Germany
CO ₂ Incubator	Thermo Electron GmbH, 63303 Dreieich, Germany
Digital camera	Canon, USA
ELISA-Reader Sunrise	TECAN, 74564 Crailsheim, German
Flow cytometer	FACS Calibur, Becton Dickinson, Franklin Lakes, NJ 07417, USA Attune®, Focusing Cytometer, Thermo Fisher Scientific
Freezers (-20°C, -86°C)	Liebherr, Germany ; Thermo Electron GmbH, 63303 Dreieich, Germany Philipp Kirsch GmbH. 77608 Offenburg, Germany

Heat block	Biometra GmbH, D-37079 Goettingen, Germany
Laminar flow hood	Heraeus, Hanau, Germany
Luminometer Orion II	Berthold Detection Systems, Germany
Microscope (inverted)	Leica, 35606 Solms, Germany
Photometer	Thermo Electron GmbH, 63303 Dreieich, Germany
Power-Supply	Thermo Electron GmbH, 63303 Dreieich, Germany
SDS gel electrophoresis system	Whatman, GE Healthcare, D-80807 Munich, Germany
UV lamp	Biometra GmbH, D-37079 Goettingen, Germany
Water bath	Julabo, 77960 Seelbach, Germany
Thermocycler	Biometra GmbH, D-37079 Goettingen, Germany

Table 3 Instruments and devices

2.1.2 Chemicals and reagents

The chemicals and reagents used for my thesis were obtained from Sigma-Aldrich (Taufkirchen), Roth (Karlsruhe), Applichem (Darmstadt), Merck (Darmstadt), Roche, Calbiochem (Darmstadt) and Peqlab.

2.1.3 Material for Immunohistochemistry

Item	Manufacturer/Provider
Paraffin embedded human ovarian cancer tissues (block)	Department of Obstetrics and Gynecology University Hospital of Wuerzburg, Germany
Paraffin embedded human glioblastoma tissue (block)	Dpt. Of. Pathology, Goethe-University Frankfurt, Germany
Xylol	Sigma-Aldrich, Taufkirchen, Germany
Ethanol	70%-100% (Sigma)
PBS 1x (Phosphate buffered saline)	PAA Laboratories, A-Pasching, Austria pH 7.4
Tissue mount DABCO	25 ml PBS, 0.625 ml DABCO 225 ml Glycerin
Haemalum solution (Mayer's haematoxylin)	Roth, Karlsruhe, Germany
VitroClud	Langenbrinck, Emmendingen, Germany
DAKO Pen	DAKO, Hamburg, Germany
Antibody Diluent	DAKO, Hamburg, Germany
Citric acid	500ml aqua dest., 10mM citric acid pH6
Dual Endogenous Enzyme Block	DAKO (K4065)
Labelled Polymer	DAKO (K4065)
Substrate buffer	pH7.5, containing hydrogen peroxide, DAKO (K4065)
DAB + Chromogen Solution	3,3'-diaminobenzidine chromogen solution DAKO (K4065)
Anti-mouse-HRP-antibody (Used when detection was performed without DAKO K4065-polymer)	Cell signaling (cat. # 7076)
Anti-rabbit-HRP-antibody (Used when detection was performed without DAKO K4065-polymer)	Cell signaling (cat. # 7074)

Table 4 Material and reagents for immunohistochemical staining

2.1.4 Material for protein biochemistry

Item	Composition
Electrophoresis Running buffer 10x	25 mM Tris, 193 mM Glycin, 0,5% SDS pH 8,8
Transfer buffer 1x	25 mM Tris, 192 mM Glycin, 20% Methanol
Lysis buffer	50 mM Tris-HCl, pH 8, 120 mM NaCl, 5mM EDTA, 0,5% NP-40, 2 µg /ml Aprotinin, 10µg /ml Leupeptin, 100 µg /ml PMSF, 50 mM NaF, 200 µM NaVO ₅
Lämmli-Loading buffer (modified from Lämmli UK., Nature 1970)	100 mM Tris(hydroxymethyl)aminomethane-HCl (pH6.8) 10% 2-β-Mercapto-ethanol 4% SDS 20% Glycerin 0.2% Bromophenol blue
TBS	10 mM Tris-HCl, 150 mM NaCl, pH 7,3
TBS-T	TBS, 0,05% Tween20
PBS (1x)	37 mM NaCl, 2,7 mM KCl, 80 mM Na ₂ HPO ₄ , 1,8 M KH ₂ PO ₄ , pH 7,4

Table 5 Buffers for SDS-PAGE

Buffer	Composition
Blocking buffer	5% skim milk powder in TBS-T
ECL solution A	50 mg Luminol in 200 ml 0,1 M Tris-HCl pH 6,8
ECL solution	1.1 mg/ml para-hydroxycoumaric acid in DMSO
TS-TM-BSA	10mM Tris-HCL 150mM NaCl 5% skim milk powder 0.1% Tween 20 2% BSA 0.1% NaN3
Stripping buffer	0,2 M Glycin, 0,5 M NaCl, pH 2,8
Neutralization buffer	1,5 M Tris Base pH 7.4

Table 6 Buffers used for Western Blotting

2.1.5 Material for molecular biology

Buffers and Reagents	Composition
LB Agar	10 g/l Bacto-Pepton 5 g/l yeast extract 10 g/l NaCl pH 7.0
LB medium (Luria Bertani)	10 g/l Bacto-Pepton 5 g/l yeast extract 10 g/l NaCl 7,5 g/l select Agar pH 7,0
Kanamycin	30 mg/ml in ddH2O diluted 1:1000 to final concentration
Ampicillin	50 mg/ml in ddH2O diluted 1:1000 to final concentration

Table 7 Reagents and chemicals for molecular biology

2.1.6 Kits and kit contents

Kit	Manufacturer
ADCC reporter Assay	Promega
iScript cDNA Synthesis Kit	Biorad (methods section)
ABsolute Blue QPCR SYBR Green low Rox mix	Thermo Fischer
E.Z.N.A tissue DNA kit	Omega Biotek
pJet Clone jet	Fermentas
Proteus A antibody purification	AbD Serotec

Table 8 Overview of kits

Kit	Manufacturer
7X Lysis Buffer*1	ZYMO RESEARCH „Zyppy™ Plasmid Miniprep Kit“
Neutralization	
Buffer*2 (Yellow)	
Endo-Wash Buffer	
Zyppy™ Wash Buffer (concentrate)	
Zyppy™ Elution Buffer	
Zymo-Spin™ Columns	
Collection Tubes	

Table 9: Components of plasmid isolation and purification kit (ZYPPY) for mini preparations

2.1.7 Reagents, buffers for methods to generate monoclonal antibodies

Buffers, reagents and media for hybridoma generation and antibody production CELLline bioreactor

Buffers and Reagents	Composition / Provider
Adjuvant-TiterMax® Gold	Sigma Aldrich (T2684)
Hanks Balanced Salt Solution	Sigma Aldrich
PEG	Roche (54457-10G-F)
HT Media Supplement (50x)	Sigma Aldrich (H0137)
HAT supplement (50x) in BSS	Biochrom AG (# F0483; Lot.# 0743S)
Ig stripped FCS	Roche (54457-10G-F)
Hybridoma Cloning Supplement	PAA

Table 10 Buffers and reagents for monoclonal antibody generation and production

Buffer formulation for antibody purification (Proteus A kit):

Buffers and Reagents	Composition
Binding buffer A (1.5 M Glycine / NaOH buffer, 3 M NaCl, pH 9.0)	112.6 g glycine (free base; 75.07 g/mol), 175.3 g NaCl (58.44 g/mol), 1.0 g NaN ₃ * Up to 1000 ml with ddH ₂ O, pH 9.0 (titrated with 5 M NaOH)
Elution Buffer B2 (0.2 M Glycine/ HCl buffer pH 2.5)	15.0 g glycine (free base 75.07 g/mol), 1.0 g NaN ₃ * to 1000 ml ddH ₂ O pH 2.5 (titrated with 5 M HCl)
Neutralization Buffer C (1 M Tris/HCl buffer pH 9.0)	103.72 g Tris base (121.1 g/mol), 22.72 g Tris hydrochloride (157.6 g/mol), 1.0 g NaN ₃ * Up to 1000 ml ddH ₂ O pH 9.0

Table 11 Buffers prepared for antibody purification with the proteus A kit. * NaN₃ was not added, when antibody was either used for *in vitro* experiments on primary cells, cell lines or for *in vivo* studies.

2.1.8 Antibodies

Antibody (Clone)	Dilution	Application	Manufacturer
B1-23	*	WB/ELISA/ <i>in vivo</i>	Result of thesis
ChimB1-23	*	WB/ELISA/ <i>in vivo</i>	Result of thesis
H1L5	*	WB/ELISA/ <i>in vivo</i>	Result of thesis
B12	*	ELISA/ <i>in vivo</i>	Result of thesis
Fab-(ChimB1-23)	*	WB/ELISA/ <i>in vivo</i>	Result of thesis
GDF-15 (HPA 011191)	1:100	IHC/WB	Sigma Aldrich
pSMAD2/3 (#8828)	1:1000	WB	Cell Signaling
total SMAD2/3 (#3102)	1:1000	WB	Cell Signaling
Human GAPDH (EPR1977Y)	1:1000	WB	Epitomics
Human β Actin (ab8226)	1:10000	WB	Abcam
Mouse IgG (H+L)-HRP (# 7076)	1:3000	WB	Cell Signaling
Rabbit IgG (H+L)-HRP (# 7074)	1:3000	WB	Cell Signaling
polyclonal anti-human-HRP	1:2000	WB	Dako
Human NKG2D-PE (BAT221)	1:100	FACS	MiltenyiBiotec
Human CD3-FITC (MEM-57)	1:50	FACS	Immunotools
Human CD3-PE (MEM-57)	1:100	FACS	ImmunoTools
Human CD4-FITC	1:100	FACS	Immunotools
Human CD8-PeCy5	1:100	FACS	eBiosciences
Human CD56- ACP (N901)	1:200	FACS	Beckman Coulter
IgG1 isotype PE (MOPC-21)	1:100	FACS	BioLegend

Table 12 Table of antibodies (* dilution depended on the application, see methods for applied concentrations)

2.1.9 Oligonucleotides

Gene	Application	Primer Sequence (5' to 3')
GDF-15 (mouse)	- / - primer (KO) PCR-1	CCC AGT CTT GTA GAC AGA GCA A
		TCG CCT TCT TGA CGA GTT CT
	+ / + primer (WT) PCR-1	ATG CGC ACC CAA GAG ACT
		GGC CAC CAG GTC ATC ATA AG
GDF-15 (mouse)	- / - primer (KO) PCR-2	GCA GAG AGG CTG AGG AAC TT
		GTT CTT GTT GGT CAA AGT AAA CGA
	+ / + primer (WT) PCR-2	TTG GGA AAA GGT TGG AGA GA
		GAT ACA GGT GGG GAC ACT CG
GAPDH	Realtime PCR	CCA TCT TCC AGG AGC GAG ATC C
		ATG GTG GTG AAG ACG CCA GTG
β -actin	Realtime PCR	TGT TTG AGA CCT TCA ACA CCC
		AGC ACT GTG TTG GCG TAC AG
18S	Realtime PCR	CGG CTA CCA CAT CCA AGG AA
		GCT GGA ATT ACC GCG GCT
pJET1.2	Sequencing	CGA CTC ACT ATA GGG AGA GCG GC
		AAG AAC ATC GAT TTT CCA TGG CAG

Table 13 List of primers used for genotyping of mice or for realtime PCR

2.1.10 Cell lines

Cell line / primary cells	Application (chapter)	Provider
UACC-257 (melanoma)	<i>In vitro</i> experiments (3.4) <i>In vivo</i> study: Cachexia (3.5)	NCI
CHO	Transient plasmid transfection / production of antibodies (3.4)	Dermatology
HEK-293T	Transient transfection/ expression of GDF-15 (3.4)	Department of Obstetrics and Gynecology Wuerzburg
P3-X63.Ag8 myeloma cell	Generation of hybridoma for antibody production (3.4)	Professor Dr. Thomas Hünig, Dpt. Immunobiology and Virology, University of Wuerzburg
HUVEC cells	<i>In vitro</i> experiments (3.2)	Millipore
MCF-7	<i>In vitro</i> experiments (3.2)	Department of Obstetrics and Gynecology Wuerzburg
PBMC	<i>In vitro</i> experiments (3.2)	Obtained from healthy blood donors or from the Department of Transfusion Medicine and Hemotherapy, University Hospital of Wuerzburg

Table 14 Cell lines and primary cells used *in vitro* and *in vivo*

2.1.11 Plasmids

Vector	Application	Provider
pcDNA3.1	Transient transfection / empty vector control	Invitrogen
pcDNA3.1-humanGDF-15 (full-length)	Transient transfection/ expression of human GDF-15	Prof. Unsicker, Heidelberg
pIRES2-eGFP	Transient and stable transfection/ empty vector control	Clontech
pIRES2-eGFP-GDF-15 (full-length)	Transient and stable transfection/ expression of human GDF-15	Prof. Samuel N. Breit, St Vincent's Hospital, Sydney
pJet1.2 (Fermentas)	Cloning vector/ sequencing	Fermentas
pEFh-variable-HC1-H1L5 (evitria)	Transient transfection/ expression of heavy chain	Evitria AG

	variable region of H1L5	
pEFh-variable-LC5-H1L5 (evitria)	Transient transfection/ expression of light chain variable region of H1L5	Evitria AG

Table 15 List of plasmids

2.1.12 Reagents for FACS staining

Reagent	Provider
FACS Clean Solution	Becton Dickinson
FACS Flow	Becton Dickinson
FACS Rinse	Becton Dickinson
FACS Buffer (PBS + 2% FCS)	PBS (Sigma Aldrich) FCS (Sigma Aldrich)
Beriglobin blocking solution	Novartis

Table 16 List of FACS staining reagents and buffers

2.1.13 Cytokines

Cytokine/Growth factor	Source/ Expression System	Manufacturer
Human GDF-15	Eukaryotic	R&D-Systems
Human GDF-15	Cell Culture	Peptrotech
Human GDF-15	SF9 cell derived	Professor Dr. Thomas Müller, University of Wuerzburg
Human GDF-15	E.Coli derived	Professor Dr. Thomas Müller, University of Wuerzburg
Human GDF-15	E.Coli derived	Pelobiotech
Human GDF-15	HEK-293 cell derived	Invigate
Human GDF-15	HEK-293 crude supernatant	Own preparation in this thesis
Human TGF- β -1	E.Coli derived	Peptrotech
Human TNF- α (300–1A)	E.Coli derived	Peptrotech

Table 17 Human cytokines

2.1.14 Standard DNA and protein ladder

As standard on DNA gels, the following DNA ladders were utilized:

TrackIt™ 1 Kb Plus DNA Ladder (Invitrogen)

TriDye™ 2-Log DNA Ladder (New England Biolabs)

As molecular-weight size marker on RNA gels, the RiboRuler High Range RNA Ladder (Thermo Fischer) was applied.

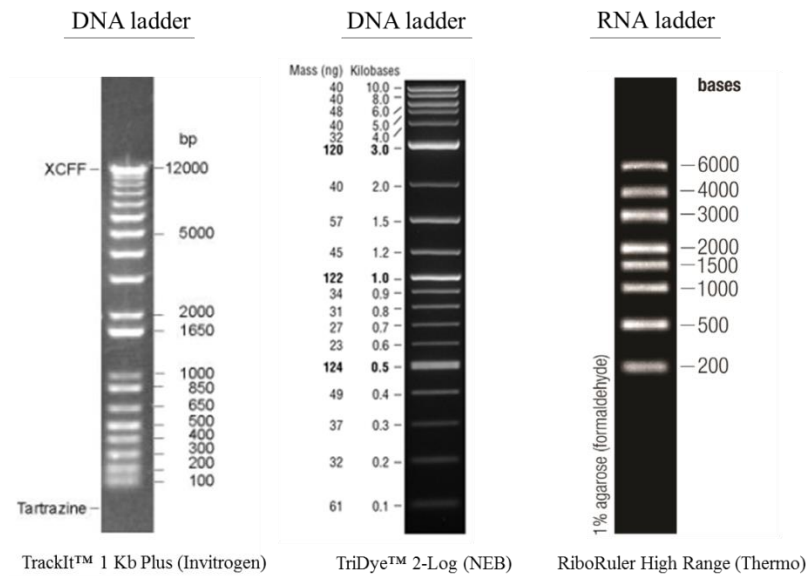


Figure 2-1 DNA and RNA ladders

To determine the molecular weight of proteins on Western Blots Spectra™ Multicolor Broad Range Protein Ladder (Thermo Fischer) was loaded on sodium dodecylsulfate polyacrylamide gels for separation.

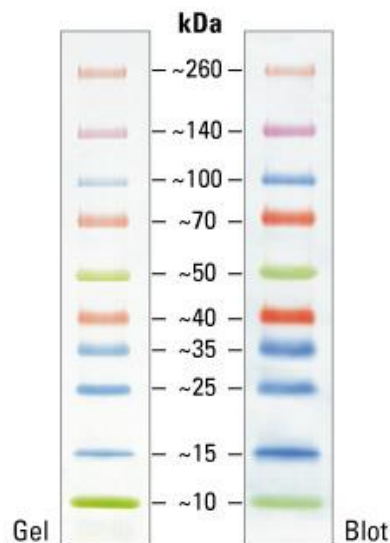


Figure 2-2 Protein ladder: Spectra™ Multicolor Broad Range Protein Ladder

2.2 Methods

2.2.1 Immunohistochemical staining

Immunohistochemical staining of GDF-15 in solid tumors was performed on paraffin embedded tissue from patients with ovarian cancer and glioblastoma multiforme as published previously (Kammerer et al., 2011, Kammerer et al., 2015). Paraffin blocked ovarian cancer tissue was obtained from the Department of Obstetrics and Gynecology at the University Hospital Wuerzburg. Paraffin embedded glioma tissue sections (placed on cover slips) were provided by Professor Dr. Mittelbronn, University of Frankfurt.

Sections of 2-4 μm were cut from cancer tissue blocks using a sliding microtome (Leica Histoslide SM200R instrument) and placed on cover slips (Superfrost, Langenbrinck). For simultaneous tissue processing, up to 16 cover slips were placed in one rack, enabling equal IHC-conditions and comparability. To remove paraffin from the tumor tissue, slides were placed in a 100% xylene bath twice for 10 minutes each. To attain access of antibodies to their target antigen, the tissue was rehydrated and antigen unmasking technique applied. Hereby, the slides were first rehydrated by stepwise washing in a series of decreasing ethanol concentration (diluted in distilled water; dH_2O): 100 % (2x) \rightarrow 90 % \rightarrow 80 % \rightarrow 70 %. Finally, slides were washed with dH_2O .

For antigen retrieval, slide holder was placed in a dish filled with citric buffer (10 mM citric acid, 500 ml dH_2O , pH 6.0) and microwaved at 600W/sec until boiling (10 min). After repeating the boiling step, slides were cooled for 20 minutes at room temperature in the retrieval solution and subsequently carefully washed with dH_2O . Tissue peroxidases, mainly present in erythrocytes, leading to unspecific background signals were inactivated by incubation of the sections in hydroxyl peroxide solution (90 ml methanol, 10 ml PBS + 30% v/v H_2O_2) for 10 min at RT. Tissue slides were then washed five times with dH_2O and incubated in PBS for five minutes. A lipophilic circle was drawn around the tissue section on the glass slides using a fatty pen (DAKO Pen). Possible unspecific binding sites due to Fc receptors on tissue samples were blocked for 15 minutes with an immunoglobulin blocking solution (Beriglobin, 1:50 dilution in PBS; Centeon, Marburg), before primary antibody incubation was performed adding 75 μl anti GDF-15 polyclonal rabbit antibodies (Sigma, HPA 011191, 1:100 in antibody diluent) on the tissue sections and incubating slides in humid chambers at 4°C overnight. Slides were washed five times in 1x PBS prior to incubation with the secondary HRP linked anti-rabbit antibodies diluted 1:100 in antibody diluent for 30 minutes at room temperature. After stringent washing, tissue samples were counterstained in hemalaune solution (Carl Roth) for one minute, washed twice with dH_2O

and subsequently repetitively washed using tap water for five minutes, to obtain the blue colour of nuclei. Tissues were then dehydrated following the reverse sequence of the above described ethanol concentration series, starting from 70% until 100% ethanol. Tissue samples were embedded in Vitroclud.

2.2.2 Thawing of cells

Frozen vials with cryoconserved cells were rapidly transferred (less than a minute) in from a liquid nitrogen tank (-196°C) to a water bath at 37°C. 1 ml of pre-warmed complete medium (RPMI-1640, 10% fetal calf serum, 5% penicillin/streptomycin, sodium pyruvate) was added to the cells, once they appeared to have thawed. Subsequently the resuspended cells were transferred into a 15 ml Falcon tube containing 10 ml complete RPMI-medium (prewarmed to 37°C). Cells were then centrifuged for 8 minutes at 1200 rpm. Supernatants were decanted and the resulting cell pellet was resuspended in 12 ml complete medium. Depending on the number of frozen cells in a cryopreservation vial, cells were seeded into a 25cm² or 75 cm² sterile cell culture flask and cultured at 37°C / 5% CO₂ in an incubator.

2.2.3 Cryopreservation of cells

For the generation of a working cell bank or long term storage of cell lines, cells were cryopreserved and deposited in a liquid nitrogen tank at -196°C. Therefore cell culture medium of adherent cells was aspirated and cells were washed with warm (37°C) PBS to remove medium and FCS. For the detachment of cells in flasks, 1 ml accutase (PAA, ready to use) was added per 75 cm² growth area and cells were placed in the incubator at 37°C for 5 minutes or until the cells peeled away from the bottom. The enzymatic reaction was then stopped by resuspending detached cells in 5 ml complete medium, followed by centrifugation at 1200 rpm for 5 minutes. 1 ml of cryomax II (PAA) was added to the cell pellet, immediately resuspended and transferred to a cryopreservation vial (Nunc). The cryo vial was then placed in a “slow freezing” device and put in -80°C overnight until storage in a liquid nitrogen tank.

2.2.4 Isolation and preparation of human immune cells

Peripheral human lymphocytes can be used *ex vivo* to investigate effects of growth factors, cytokines, proteins, chemicals, drugs and many more. These cells circulate in the periphery of the human blood circulation and can easily be withdrawn for the isolation thereof.

2.2.4.1. Isolation of human peripheral lymphocytes from whole blood

Human PBMC were isolated from peripheral blood from healthy donors by density gradient centrifugation. Therefore, 15ml of Ficoll medium was added to 50 ml Falcon tubes under sterile conditions. 5% of the anti-coagulant ACD-A (citrate dextrose solution) (v/v) was added to 50 ml whole blood and further diluted (1.4 fold) in warm PBS. The diluted blood was gently pipetted on the prepared Ficoll medium. The PBMC were then separated from the rest of the blood cells by centrifugation at 600 rpm for 30 minutes (acceleration and breaks were kept on lowest level) in a swing out bucket. To remove the platelets, 2.5 ml of supernatant was carefully removed from the surface. Tubes were centrifuged for another 30 minutes at 1400 rpm. The “buffy coat”, comprising the PBMC at the interphase between the Ficoll layer and the medium was aspirated (~ 5 ml) and washed twice with PBS. The washing steps were performed at 1800 rpm to completely remove residual Ficoll medium, which has toxic effects on cells. PBMC were resuspended in complete RPMI-medium and placed in the incubator for at least two hours before starting the *in vitro* experiments. In order to obtain peripheral blood lymphocytes (PBL), defined as cells derived from the lymphoid lineage, monocytes/myeloid cells were depleted. Therefore the PBMC were placed in a cell culture dish at 37°C for one hour. During that time, most of the monocytes have settled down and remained on the bottom. Cells in suspension were carefully aspirated, representing the human PBL. Unless noted otherwise, experiments were performed with final PBMC concentrations of 2.5 Mio/ml.

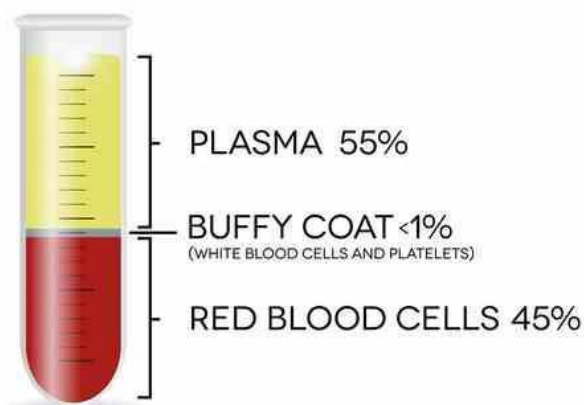


Figure 2-3 Schematic of human blood cells after centrifugation in density gradient

PBMC are located in the interphase between plasma and red blood cells. White blood cells are visible as a so called buffy coat on top of the opaque Ficoll medium (not shown in this illustration) (Author: Richard Tsai, Thermo Scientific)

2.2.5 Flow cytometry

Flow cytometry allows to phenotype primary cells or cell lines according to their characteristic surface antigens. A further advantage of this method is the ability to quantify cell surface proteins like receptors after various treatment conditions. Apart from immune cell surface staining, which is described in the following section, flow cytometry has also been performed for MCF-7 tumor cells after transfection with eGFP containing plasmids. In that case, the method was used to differentiate between GFP-positive and GFP-negative populations of tumor cells. Antibody staining could be omitted. Between 10^5 and 10^6 cells were taken up in 200 μ l FACS buffer and measured for fluorescence emission in the blue laser (488 nm) channel 1, using the Attune FACS instrument (unless otherwise noted).

NKG2D receptor surface staining using flow cytometry analysis:

For cell surface staining of human lymphocytes from healthy donors, PBMC or PBL were either treated with TGF- β (2 ng/ml and 5 ng/ml), or with increasing concentrations of recombinant GDF-15 (1 ng/ml, 4 ng/ml, 10 ng/ml, 20 ng/ml, 40 ng/ml, 80 ng/ml and 160 ng/ml) respectively, or left untreated for 24 hours. SD208, a TGF- β receptor tyrosine kinase I inhibitor, was added as a control. SD208 mediates the inhibition of TGF- β pathway and thus revealed the autocrine TGF- β signaling when compared to the untreated control. After the treatment, PBMC were washed with PBS. Cells were then transferred to FACS tubes and blocked with Beriglobin (1% in PBS) for 30 minutes at 4°C. Beriglobin contains immunoglobulins, thus used to block Fc- γ receptors on immune cells (e.g. macrophages or NK cells). This could avoid unspecific binding of primary antibodies (Honig et al., 2005). After blocking, immune cells were transferred to FACS plates and centrifuged at 1800 rpm at 4°C. To quantify the NKG2D receptor surface expression on NK cells, PBL were stained for CD3⁻ CD56⁺ cells and NKG2D receptor for 30 minutes at 4°C in the dark. Unless otherwise noted, the dilution for fluorochrome conjugated primary antibodies was 1:100 in FACS buffer (1x PBS, 2% FCS). Anti-CD3-APC (1:50), anti-CD56-PeCy5, PE-conjugated anti-NKG2D receptor antibody were used for staining. Subsequently, cells were washed twice and the pellets were resuspended in 200 μ l of FACS buffer. Flow cytometric analysis was performed on a FACS Calibur instrument (Becton Dickinson).

Quantification of NKG2D surface receptor on CD8⁺ T cells was performed with the same samples as for the NK cell staining (see above). The only difference was, that staining for NKG2D receptor on CD8⁺ T cells was carried out with anti-CD8-PECy5 antibody instead of the anti-CD56-PeCy5 antibody.

Data were analyzed with the summit 4.3 FACS-software (Beckman Coulter). Specific fluorescence intensities (SFI) were calculated by the following formula:

$$\text{SFI (NKG2D)} = \frac{\text{Median (fluorescence intensity NKG2D-receptor-PE)}}{\text{Median (fluorescence intensity Isotype-PE)}}$$

2.2.6 Adherence Assay

To test the influence of GDF-15 on the adherence of human PBMC on endothelial cells, a leukocyte adhesion assay was performed (Kucik and Wu, 2005). Human umbilical vein endothelial cells (HUVEC) were seeded at a density of 1×10^5 cells per well into a 24 well cell culture dish and cultured in supplemented medium (EndoGRO™, SCCE001, Millipore) at 37° C and 5% CO₂. After 24 hours and the formation of a confluent monolayer, HUVEC were stimulated with 20 ng/ml of recombinant tumor necrosis factor alpha (TNF-α) for four hours, in order to induce LFA-1 surface expression. As a control, global adherence of leukocytes on endothelial cells was induced by pre-treatment of PBMC with 2.4 μg /ml phytohemagglutinin (PHA) for 20 minutes. Subsequently, 2×10^6 PBMC per ml were treated with 100 ng/ml recombinant GDF-15 for 4 hours or left untreated and were added to the HUVEC monolayer.

Lymphocytes were kept on HUVEC for 90 minutes at 37° C and 5% CO₂. Non-adherent lymphocytes were collected by aspiration of medium from the endothelial cells. After washing of the HUVEC monolayer with RPMI and PBS at 37° C, adherent lymphocytes were collected together with HUVEC by trypsination of the cell culture dishes. Both non-adherent and adherent cells were sedimented at 500 g for 5 min at 4° C and blocked for 45 minutes at 4° C after resuspension in PBS containing 1 % FCS. Cells were stained for macrophages (CD14⁺), T helper cells (CD4⁺) and cytotoxic T cells (CD8⁺) with fluorophor labeled antibodies. Immune cell subset distribution in samples of non-adherent and adherent fractions were quantitatively analyzed by flow cytometry (see 2.2.5).

2.2.7 Woundhealing assay

To investigate the migration of cancer cells under the influence of GDF-15, woundhealing assay was performed according to Liang and colleagues (Liang et al., 2007). Therefore, a monolayer of wild type- as well as GDF-15-transgenic breast cancer cell line MCF-7 was grown in 6 well plates at 37°C in 5% CO₂ (for transfection protocol, see section 2.2.12). A scratch has been introduced with a 100 μl pipet tip concentrically splitting the 6 well into two

halves. Thereby, the pipet tip was pulled starting from the top margin of the well bottom down to the lower side of the well. Subsequently, scratched and floating cells were removed by three times washing the 6 well plates with 37°C pre-warmed PBS, followed by adding 2 ml of RPMI 1640 containing 2 % FCS and 5 % penicillin/streptomycin. Cells were placed in the incubator at 37°C and 5% CO₂ for at least two hours prior starting the treatments.

Wound healing was monitored daily and four pictures of each well were taken with the use of a microscope compatible camera and the TS View Digital imaging software. The four according pictures were aligned using Adobe photoshop and subsequently loaded in the image J software, where the scratch area was measured.

2.2.8 Determination of cell viability using the WST-1 assay

The WST-1 assay (Roche) served as a cytotoxicity assay to determine the viability of lymphocytes in the presence or absence of GDF-15 antibodies or drug substances. The GDF-15 monoclonal antibody B1-23/ HL5, B12, Ipilimumab and Avastin were added to human lymphocytes at a concentration of 10 µg /ml and incubated at 37°C for 24 hours. Untreated lymphocytes served as a negative control. Dacarbazine and Paclitaxel (Taxomedac®, medac) served for an *in vitro* comparison with antibodies and small molecules in regard to the toxicity. DMSO (5% v/v) served as a positive control for cellular cytotoxicity. WST-1 substrate was added as 1:10 dilution following an incubation time of at least one hour up to four hours.

Once a turnover of the substrate was visible by eye (yellow colour), the absorbance was measured with the Sunrise Reader (Tecan) at a wavelength of 450 nm.

2.2.9 Protein biochemical methods

2.2.9.1 Preparation of cell lysates from human PBMCs, tumor cells and tissues

In order to investigate changes of intracellular proteins of human PBMC upon various stimuli, between 2 and 5 Mio human leukocytes were transferred from 24 well plates to 15 ml Falcon tubes. Then the lymphocytes were centrifuged at 1500 rpm for 8 minutes. The pellet was washed in PBS, spun down and the dry pellet thereof was resuspended in Lysisbuffer P (composition listed in Table 3) and put on ice for 20 minutes. The resulting lysate was spun down at maximum speed to separate the cytoplasmic proteins from cellular debris, cell membranes and proteins thereof. Apart from the cell numbers and the necessity to detach

adherent tumor cell lines, cell lysis was performed in the same manner as described for the human PBMCs. A part of the lysate was used for quantification of the protein content.

2.2.9.2 Determination of the total amount of protein by the Bradford method

To quantify the amount of intracellular protein of cell lysates or tissue lysates, the Roti®-Quant assay (Carl Roth) was performed according to the manufacturer instructions.

2.2.9.3 Immunoblotting

In order to separate proteins according to their mass, sodium-dodecyl-sulfate polyacrylamide gel electrophoresis (SDS-PAGE) was performed (Renart et al., 1979). For those Western Blots (WB) performed under denaturing and reducing conditions, laemmli-loading buffer was added to the protein lysates and put on a heat block at 90°C for 10 minutes. Laemmli buffer contains β -mercapto-ethanol, which reduces the disulfid bonds in proteins (Laemmli, 1970). The high temperature leads to the denaturation of the proteins. 10 μ g of protein lysate in laemmli was then loaded on the stacking gel, running at 0.2 mA in a Biorad SDS-PAGE device.

For detecting native proteins, so called semi native Western Blot was performed. This is inevitable, when an antibody can only detect the native protein and loses its binding capability, once the protein has changed its conformation. This was the case for the GDF-15 antibody B1-23, which was generated as a part of my thesis. Semi native SDS PAG was performed without denaturing and reducing conditions. Therefore loading buffer without β -mercaptoethanol was added to recombinant proteins or cell supernatants and loaded on SDS-PAG without heat denaturing. Unless noted otherwise, SDS PAGE was performed with the following polyacrylamide gels:

Stacking gel (5%):
dd H ₂ O 0.68 ml,
Acrylamid/Bisacrylamid (30%) 0.17 ml,
Tris-HCl 1 M (pH 6.8) 0.13 ml,
SDS (10%) 10 μ l,
APS (10%) 10 μ l,
TEMED 1 μ l

Separating gel (10%):
dd H ₂ O 1.9 ml,
Acrylamid/Bisacrylamid (30%) 1.7 ml,
Tris-HCl 1.5 M (pH 8.8) 1.3 ml ,
SDS (10%) 50 µl,
APS
(10%) 50 µl,
TEMED 1 µl

Table 18 Polyacrylamid gels for SDS PAG electrophoresis

Proteins, denatured or native, were transferred from the SDS gel to a nitrocellulose membrane using the Biorad semi dry Western Blot apparatus. After the transfer membranes were placed in dishes and blocked with TBST buffer, containing 5% (w/v) skimmed milk, for one hour. Then, the blocking solution was removed and primary antibody (diluted in blocking buffer) was added to the membranes and incubated on a shaker under constant agitation overnight at 4°C. To investigate the activation of the canonical TGF- β signaling pathway, pSmad2 antibody was used, whereas total Smad2, GAPDH and β -actin served as loading control antibodies. The mouse anti-GDF-15 antibody (B1-23, 1 μ g /ml, generated during my thesis), human-(Fc) anti-GDF-15 antibody (ChimB1-23, 1 μ g /ml, product of the thesis), the human anti-GDF-15 antibody (H1L5, 1 μ g /ml, product of the thesis) were used for the detection of recombinant human GDF-15 and UACC-257 melanoma cell expressed GDF-15 under semi native SDS-PAGE-conditions. The rabbit anti-pro-GDF-15 antibody (H011191, Sigma Atlas antibodies) was used to detect precursor-GDF-15 under denatured as well as semi native conditions.

After three washes with TBST, the following secondary HRP-coupled antibodies, diluted in blocking buffer, were added to the nitrocellulose membranes and placed on a shaker for two hours at room temperature: polyclonal anti-mouse-(H+L) antibodies, anti-rabbit-HRP antibodies, polyclonal anti-human-HRP antibodies. After secondary antibody incubation, membranes were washed three times with TBST and placed face down on a drop of ECL detection solution (consisting of 1ml ECL-A, 100 μ l ECL-B and 2 μ l H₂O₂) for 2 minutes.

After that time, membranes were placed in a light protected cassette and exposed on x-ray films in a dark room for 2-10 minutes (depending on the signal intensities) until the x-ray films were developed. Therefore the films were kept for 3 minutes in a developer solution

(Kodak), shortly washed in ion free water and placed in a fixation bath for one minute. After the fixation was completed, the films were washed under tap water to remove fixation solution. Once dried, the films were scanned and the signal intensities of the protein bands were analyzed using the image J software (Schneider et al., 2012).

2.2.10 Methods for gene expression analysis

2.2.10.1 Isolation of RNA from immune cells and HUVEC cells

5×10^6 immune cells and 2.5×10^6 HUVEC cells were seeded in 24 well plates in 1 ml RPMI-complete medium and either treated with 100 ng /ml recombinant GDF-15 (R&D Systems) or left untreated for six hours and 24 hours, respectively, at 37°C in the cell incubator. Then cells were detached using accutase and transferred to 1.5 ml caps, washed in 1 ml cold PBS (1x) and centrifuged at 2000 rpm in a table top centrifuge (Eppendorf). The pellet was resuspended in 1 ml Trifast® reagent (Peqlab) for 15 minutes at room temperature. 0.2 ml of chloroform was added to each sample and shaken vigorously for 15 seconds. Samples were kept for another 5 minutes at room temperature before centrifugation at 15,000 rpm at 4°C. The aqueous phase was carefully aspirated and transferred to a new 1.5 ml cap (~ 0.5 ml). 0.5 ml isopropanol was added to the RNA and incubated for 15 min at 4°C for RNA precipitation. The samples were then centrifuged for 10 minutes at 15,000 rpm at 4°C. The resulting RNA pellet was washed twice with 0.7 ml ethanol (100 % ethanol). To dry the RNA pellet, the caps were left open and placed under a lamina flow for 10 minutes. The RNA was then resuspended in 15 µl aqua ad injectabilia (Braun). To properly dissolve the RNA in water, the caps were placed on a heat block at 37° C for 5 minutes.

2.2.10.2 Determination of RNA concentration

The RNA concentration was determined by measuring the absorbance (OD = optical density) at 260nm, 280nm and 320nm using a photometer. The 260 nm/280 nm ratio indicated the RNA quality. RNA with a quality of less than 260nm/280nm = 1.6 was not further processed. The concentration of the RNA was calculated as follows:

$$C_{\text{RNA}} [\mu\text{g} / \text{ml}] = \text{OD}_{260 \text{ nm}} \times \text{dilution factor} \times 40.$$

2.2.10.3 Synthesis of cDNA from isolated RNA

In order to generate cDNA of polyadenylated transcripts from monoclonal antibody producing hybridoma cells, a reverse transcription was performed. Therefore the iScript kit (Biorad) was utilized according to the manufacturer protocol (Geiduschek et al., 1961). A maximum of 1 μg RNA was used in one reaction (see table 14). The oligo-dT primers, provided in the reaction mix of the kit, assured the reverse transcription of protein coding RNA with poly-A tails. The cDNA was used for quantitative real time PCR described in section 2.2.9.4.

Component	Volume	Final concentration
5x iScript reaction mix	4 μl	1x
iScript reverse transcriptase	1 μl	n.d.
RNA template	up to 1 μg	~ 20ng/ μl
Nuclease free water	x μl	
Total volume	20 μl	

Table 19 Volumes and amounts of components for one iScript cDNA synthesis reaction

cDNA synthesis reaction:

Duration	Temperature
5 minutes	25°C
30 minutes	42°C
5 minutes	85°C
∞	4°C

Table 20 cDNA synthesis program (according to the manufacturer recommendation)

2.2.11 Polymerase Chain Reaction (PCR)

The polymerase chain reaction method (PCR) enables the amplification of genomic DNA sequences of interest (Mullis, 1990). Therefore specific primer pairs are used to define the starting points of the DNA amplification in forward as well as reverse direction. In short, the method is subdivided into three steps: the separation of double stranded DNA (genomic DNA as well as primer DNA) at 94°C, the primer annealing at a certain annealing temperature (has to be tested for each primer pair), and the elongation step, where a heat stable DNA polymerase amplifies the DNA strand, starting with the annealed primer on the DNA. These three steps represent one PCR cycle and are repeated up to 40 times, with an exponential amplification of DNA.

2.2.11.1 Isolation of genomic DNA from mouse ear punches

In order to obtain genomic DNA from B16/57 GDF-15 knock out mice, a small piece of the ear was taken by an ear puncher. Genomic DNA was isolated from the tissue according to the E.Z.N.A tissue DNA isolation kit (Omega bio-tek).

2.2.11.2 Mouse GDF-15 genotyping

Due to breeding of animals being heterozygous for GDF-15-knock-out allele, the genotype had to be confirmed by PCR method. Two PCR-programs were run using different primer pairs (see table 11). Annealing as well as elongation temperature for the GDF-15 PCR-program is shown in table 22.

Component	Volume	Final concentration
5x Crimson long amp buffer	5µl	1x
10mM dNTPs	0,75µl	300µM
10 µM Forward Primer	1 µl	0.04 µM
10 µM Reverse Primer	1 µl	0.04 µM
Template DNA	Variable	< 1ng

Crimson LongAmp <i>Taq</i> DNA Polymerase	1 μ l	2.5 units/ 25 μ l PCR
Nuclease-free water	To 25 μ l	

Table 21 Reaction setup for standard PCR

STEP	Temperature	Time	Cycles
Initial Denaturation	94°C	30 seconds	
Strand separation	94°C	30 seconds	30x
Primer annealing	62°C	60 seconds	
Elongation	65°C	50 seconds/kb	
Final extension	65°C	10 minutes	
Hold	4°C	∞	

Table 22 PCR program for GDF-15 knock-out genotyping

2.2.11.3 DNA gel electrophoresis

DNA gel electrophoresis was performed to separate DNA fragments according to their nucleotide length (e.g. from PCR products). Therefore 1 % agarose gels were prepared in TAE buffer (1x). To visualize the DNA under UV light, 10 μ l of Gelred (FIRMA) was added to the warm gel. 10 μ l of the GDF-15 PCR-products were directly loaded on a DNA gel (Crimson long amp buffer contained the loading dye) and run at 75V in a 0.5 x TAE buffer for one hour. To determine the length of PCR products, a 100 bp DNA ladder (TrackIt™ 1 Kb Plus DNA Ladder (Invitrogen), see figure 2.2) was loaded on the gel as a reference standard.

2.2.11.4 Quantitative Realtime Polymerase Chain Reaction (qPCR)

To quantify the expression of selected mRNAs in PBMC or HUVEC cells, the quantitative realtime PCR (qRT-PCR) method with SYBR-Green incorporation was applied. It is based on

a standard PCR (described in 2.2.11). mRNA was reverse transcribed to cDNA (described in 2.2.10.3), which served as the template DNA in the qRT-PCR reaction mix. Individual primer pairs were used in the qRT-PCR run to amplify the respective cDNA. 18S RNA primers served as reference RNA expression (internal reference gene). 18S RNA is constitutively expressed in most cell types. During elongation of transcripts (with cDNA templates synthesized from mRNA) by DNA polymerase, the newly generated DNA double strands incorporate a fluorescent dye (SYBR Green), which is a component of the master mix (table 18). SYBR Green labelled dsDNA can be excited by a blue laser ($\lambda_{\max} = 488 \text{ nm}$) and emits green light ($\lambda_{\max} = 522 \text{ nm}$) which can be quantified using the ABI 7500 fast thermocycler (Applied Biosystems, Life Technologies). cDNA can thus be PCR-amplified and analyzed simultaneously. Quantification of relative mRNA expression was calculated according to the CT method described in the journal of molecular medicine (Scheffe et al., 2006).

Component	Volume	Final concentration
2x Absolute blue qPCR SYBR Green low Rox mix	7.5 μl	1x
1.1 μM Forward Primer	1 μl	0.07 μM
1.1 μM Reverse Primer	1 μl	0.07 μM
cDNA (diluted 1:10 in water)	5 μl	< 1ng
Nuclease-free water	to 15 μl total	

Table 23 qRT-PCR Mastermix

STEP	Temperature	Time	Cycles
Initial Denaturation	50°C	2 minutes	
	95°C	15 minutes	
Strand Separation	95°C	15 seconds	40x
Annealing & Elongation	60°C	60 seconds	
Final extension	65°C	10 minutes	

Hold	4°C	∞	

Table 24 qRT-PCR program on the ABI 7500 instrument

2.2.12 DNA-Microarray (Affymetrix) on human PBMCs and HUVECs

The GeneChip® Human Transcriptome Array 2.0 (Affymetrix) was performed in collaboration with the micro-array core unit at the University of Wuerzburg, to investigate the effect of GDF-15 on gene expression. Therefore, PBMC or HUVEC cells were treated with GDF-15 for six and 24 hours or left untreated. Then, RNA was isolated at each time point (see 2.2.8) and its quality was analyzed by measuring the OD-260/280-ratio on a NanoDrop spectrophotometer. The RNA integrity numbers (RIN) of all samples were validated with a bioanalyzer instrument (Agilent). RNA samples of high quality were further processed and hybridized on the GeneChip® Human Transcriptome Array 2.0 (HTA 2.0). A cluster analysis with PBMC and HUVEC including two kinetics of treatment was performed.

2.2.13 Cloning

In the underlying work, cloning was used to integrate the – at this particular time - unknown DNA sequences of the immunoglobulin B1-23 (heavy chain and light chain) into a pJET1.2 vector, which could subsequently be sequenced. This sequence information was indispensable for humanization of the antibody (described in detail in 2.2.24).

2.2.13.1 Ligation

In order to insert DNA fragments into the pJET1.2 vector (CloneJet PCR cloning Kit, Thermo Fisher Scientific), a ligation reaction was performed according to the CloneJet protocol. Since the PCR products were generated by using a DNA polymerase with proofreading activity, blunting reaction could be omitted. Furthermore, digestion of the pJET1.2 vector was not needed, as the kit contained an already linearized plasmid. After PCR products had been quantified photometrically and on DNA gel by comparison with DNA products of known concentration (50 bp, 100 bp, 150 bp, 200 bp), ligation reaction was performed at a 3:1 - (insert: vector) molar ratio as follows:

Component	Volume
2x Reaction Buffer	10 μ l
pJET1.2/blunt Cloning Vector (50 ng/ μ l)	1 μ l (0.05 pmol ends)
PCR product	1 μ l 0.15 pmol ends
T4 DNA-ligase	1 μ l
Nuclease free water	up to 19 μ l
Total volume	20 μ l

Table 25 Ligation reaction mix

STEP	Temperature	Time
Ligation	22°C	20 minutes
Hold	4°C	∞

Table 26 Ligation reaction - program

2.2.13.2 Transformation in C2988 bacteria

In order to amplify the pJet1.2 including the new DNA sequence, competent *E. coli* bacteria (C2988, New England Biolabs) were transformed according to standard procedures (Sambrook J., 2001). Therefore, the *E. coli* bacteria – kept as glycerol stock at -80°C- were thawed at room temperature for 5 minutes. 1 μ l ligation reaction mix (from 2.2.13.1) was added to 50 μ l of bacteria in a 1.5 ml cap and mixed gently. Cells were incubated in a heat block at 42°C for 45 seconds and rapidly put on ice to stop the transformation reaction. 1 ml of LB medium was added to the transformation mix and the 1.5 ml cap was placed in a bacterial shaker at 200 rpm at 37°C for one hour. Afterwards, cells were plated on LB-ampicillin dishes and incubated at 37°C overnight. Since the original pJET1.2/blunt vector expresses a lethal restriction enzyme, once recircularized during the ligation reaction, vectors without insert kill the *E. coli* hosts after transfection. Therefore, exclusively bacteria transfected with vectors containing an insert survive and were propagated after transformation.

2.2.13.3 Preparation of plasmids

Plasmid preparations were performed to obtain purified, concentrated and endotoxin free vectors for sequencing. Therefore, colonies grown out on LB agar were picked from ampicillin plates and transferred to 50 ml Falcon tubes containing 5 ml LB medium (+ ampicillin) for an overnight culture at 37°C in the shaker (Brunswick). A mini preparation (mini prep) was performed according to the manufacturer recommendation (Zyppy™ Plasmid Miniprep Kit). Purified Plasmid DNA was eluted in dH₂O and the concentration was determined by measuring the absorption at OD260 nm. Using the ZYMO Research mini prep kit, plasmid DNA concentration between 0.5 mg/ml and 1.5 mg/ml were obtained.

2.2.13.4 Restriction digest of pJET1.2/blunt (Fermentas)

Restriction digestion can be used to selectively cut a plasmid or other types of DNA and to analyze the fragments obtained thereby (Cohen et al., 1973). Here, restriction digestion was performed to proof that an insert has been ligated into the vector. FastDigest (Fermentas) enzymes cutting the vector at insert-flanking sequences were chosen in the following restriction fast digestion reaction:

Component	Volume
XbaI (FastDigest)	1 µl
EcoRI (FastDigest)	1 µl
Plasmid DNA	1 µg
10x FastDigest-buffer	2 µl
Water	up to 20 µl

Table 27 Restriction double digest reaction mix

The reaction was incubated for 10 min at 37°C on a heat block. The product of the restriction digest was loaded and run for 30 min on a DNA gel (0.8 % agarose in 1x TAE) to separate DNA inserts from linearized vector backbone.

2.2.13.5 Colony polymerase chain reaction (colony PCR)

A further method to assess proper insertion of DNA sequences in a vector after ligation is the colony PCR method. Thereby, single colonies from LB ampicillin plates were picked using a 1 µl pipette tip and transferred directly into a conventional PCR mastermix (described in

2.2.11). In this method, transformed bacteria were used as DNA template in the following reaction (adapted from pJET1.2 PCR-protocol):

Component	Volume
5x Crimson long amp buffer	5µl
10mM dNTPs	0,75µl
10 µM pJET1.2 Forward Sequencing Primer	1 µl
10 µM pJET1.2 Reverse Sequencing Primer	1 µl
Single colony from ampicillin plate	Variable
Crimson LongAmp <i>Taq</i> DNA Polymerase	1 µl
Nuclease-free water	To 25 µl

Table 28 Components for colony PCR

STEP	Temperature	Time	Cycles
Initial Denaturation	95°C	3 minutes	
Strand separation	94°C	30 seconds	25x
Primer annealing	60°C	30 seconds	
Elongation	72°C	60 seconds/kb	
Final extension	72°C	10 minutes	
Hold	4°C	∞	

Table 29 Colony PCR program, modified from the original pJet1.2 protocol (Fermentas)

2.2.13.6 Vector Sequencing (Geneart)

To obtain the sequence of a cloned DNA fragment, as in case of the variable light and heavy chains of the generated antibody B1-23, the according plasmids were sent to and sequenced by Geneart AG in Regensburg (Germany). The pJET1.2 forward sequencing primer supplied with the CloneJet kit (Fermentas) was used for sequencing. Geneart AG also performed sequence confirmation of the expression plasmids pcDNA-3.1-hGDF-15 and pIRESeGFP-GDF15 (see table 15 and supplements).

2.2.14 Transfection of cells

To produce the light and heavy variable chains of humanized H1L5 in a suitable expression system, chinese hamster ovary cells (CHO) were transiently transfected with two heavy and light chain (antibody-) coding vectors: the L5-construct encoding the light chain variable region and the H1 construct encoding the heavy chain variable region. To express the entire antibody, co-transfection with both constructs was performed. Transfection was carried out using the XtremeGene transfection kit (Promega). 24 hours post transfection, the antibody was harvested from CHO supernatants.

2.2.15 Generation of monoclonal antibodies against GDF-15

Monoclonal antibodies can be used as a tool for molecular biological applications, as clinical diagnostics and moreover administered as therapeutic drugs. In section 2.2.14, all methods described were necessary to generate monoclonal antibodies to human GDF-15, which are produced from a single hybridoma clone (Köhler and Milstein, 2005). The reason for the immunization of GDF-15 knock out mice was to increase the chance of obtaining antibodies to GDF-15, since mouse and human GDF-15 display 70 % sequence similarity (shown in table 26), a fact that might lower immunogenicity even for the human homologue.

2.2.15.1 Immunization of mice

Three female GDF-15 deficient Bl6/57 mice (provided by Dr. Jens Strelau, Heidelberg) were immunized subcutaneously with 165 µg native recombinant GDF-15 each (E.coli derived material, obtained from Professor Thomas Müller, Würzburg) using TiterMaxGOLD® adjuvant. Blood sera from all animals were isolated 3 weeks post immunization to determine an antibody titer against the immunogen. Mice received a boost with GDF15-TiterMax emulsion 5 weeks after first immunization and a final intravenous boost 3 weeks afterwards. 3 days after the final boost the animals were sacrificed and the spleens thereof were isolated and placed in HBSS at 4°C.

2.2.15.2 Hybridoma fusion, selection and expansion

Splenocytes were isolated from the fresh mouse spleens by straining the spleen through a 70 µm cell sieve. Cells were collected in RPMI medium and kept in 75 cm² flasks for two hours to allow the fibroblasts to adhere. After the fibroblast depletion, 120 Mio splenocytes from the supernatant were mixed with 25 Mio HAT- (hypoxanthine-aminopterin-thymidine) sensitive

P3-X63.Ag8.653 myeloma cells in 50 ml tubes (final volume) and centrifuged at 1200 rpm to receive a dry cell pellet. Fusion of the cells occurred by adding poly ethylene glycol (PEG) to the pellet, thereby gently stirring the cells. Subsequently 30 ml HAT medium were drop-by-drop added to the fused cells. Cells were then carefully transferred into u-bottom plates in a final volume of 100 μ l per well and cultured for 14 days. Cells were supplemented with 15 μ l of medium every five days. Since the X63.Ag8.653 cells are deficient for the enzyme hypoxanthine guanine phosphoribosyltransferase (HGPRT⁻), these cells are sensitive to and die in HAT medium (Szybalski, 1992). When HGPRT⁻ myeloma cells were successfully fused with splenocytic cells, which are HGPRT⁺, the hybridoma cells can now survive in HAT medium. The HAT selection process was done for 14 days until replacing it by HT-medium (omitting aminopterin).

2.2.15.3 Screening for GDF-15 positive clones

After 14 days of hybridoma cell culture, aliquots (10 μ l) of cell supernatants were transferred without diluting onto a GDF-15 pre-spotted nitrocellulose membrane using a 12-channel pipette and incubated for 10 seconds. At that point, membranes were processed analogous to the described immunoblot procedure (see 2.2.9.3). Hybridoma cells, of which supernatants were positive for GDF-15 antibodies, were subcloned and further expanded (see next section).

2.2.15.4 Cloning/Subcloning for monoclonal antibodies

Subcloning is a useful method to obtain monoclonal antibodies from a pool of hybridoma cells. During the generation of monoclonal antibodies, this method ensures to receive antibodies produced by a single cell clone (monoclonal).

Therefore, the limiting dilution method was performed (Staszewski, 1984). Herein, cells were seeded in 96 well u-bottom plates in 100 μ l medium at a concentration of 0.5 cells / 100 μ l, resulting in the majority of wells seeded with one single cell. Single cells can easily be seen using a microscope, since the u-bottom shaped wells force the cells to roll into the middle of each well. Once the hybridoma cells were outgrown to a visible population in the respective wells and the color of the hybridoma supernatant turned yellowish (indicating a metabolic turnover), screening for specific antibody production was repeated. This selection procedure was repeated twice with positive clones to ensure monoclonal antibodies. Antibody producing cell clones were then stored in nitrogen until further characterization or production of larger batches.

2.2.15.5 Production of mABs in CELLline Bioreactors / Antibody Expression

To generate monoclonal antibodies (of the selected clone – here B1-23) in larger amounts, the static CELLline bioreactor (Integra) was used (see figure 2-4). The reactor comprises two compartments. The medium compartment and the cell compartment with a 10 kDa semi-permeable, cellulose acetate membrane. This membrane allows small molecules to diffuse from one compartment to the other, whereas higher molecular weight molecules secreted by the proliferating hybridoma are retained within the cell compartment. This leads to a continuous flow of nutrients into the cell compartment and a concurrent removal of any inhibitory waste products, however the secreted antibodies remained in the cellular compartment. After equilibration of the semi-permeable membrane with 10 ml medium for five minutes, 8×10^6 viable hybridoma cells from a pre-culture in log growth phase were suspended in 5 ml fresh medium resulting in a minimal concentration of 1.5×10^6 viable cells/ml and cell compartment was inoculated with hybridoma cells. 340 ml Hybridoma-medium was added to the medium compartment and the CELLline reactor was placed in an incubator at 37°C. Hybridoma cells were harvested every five days by slowly aspirating the antibody-hybridoma mix from the cell compartment of the reactor. 1 ml (~ 20 %) cell suspension was diluted in 5 ml fresh Hybridoma medium and pipetted back into the cell compartment of the bioreactor. The other 4-5 ml were centrifuged at 1200 rpm for 10 minutes and supernatants were further affinity purified, described in the next section.

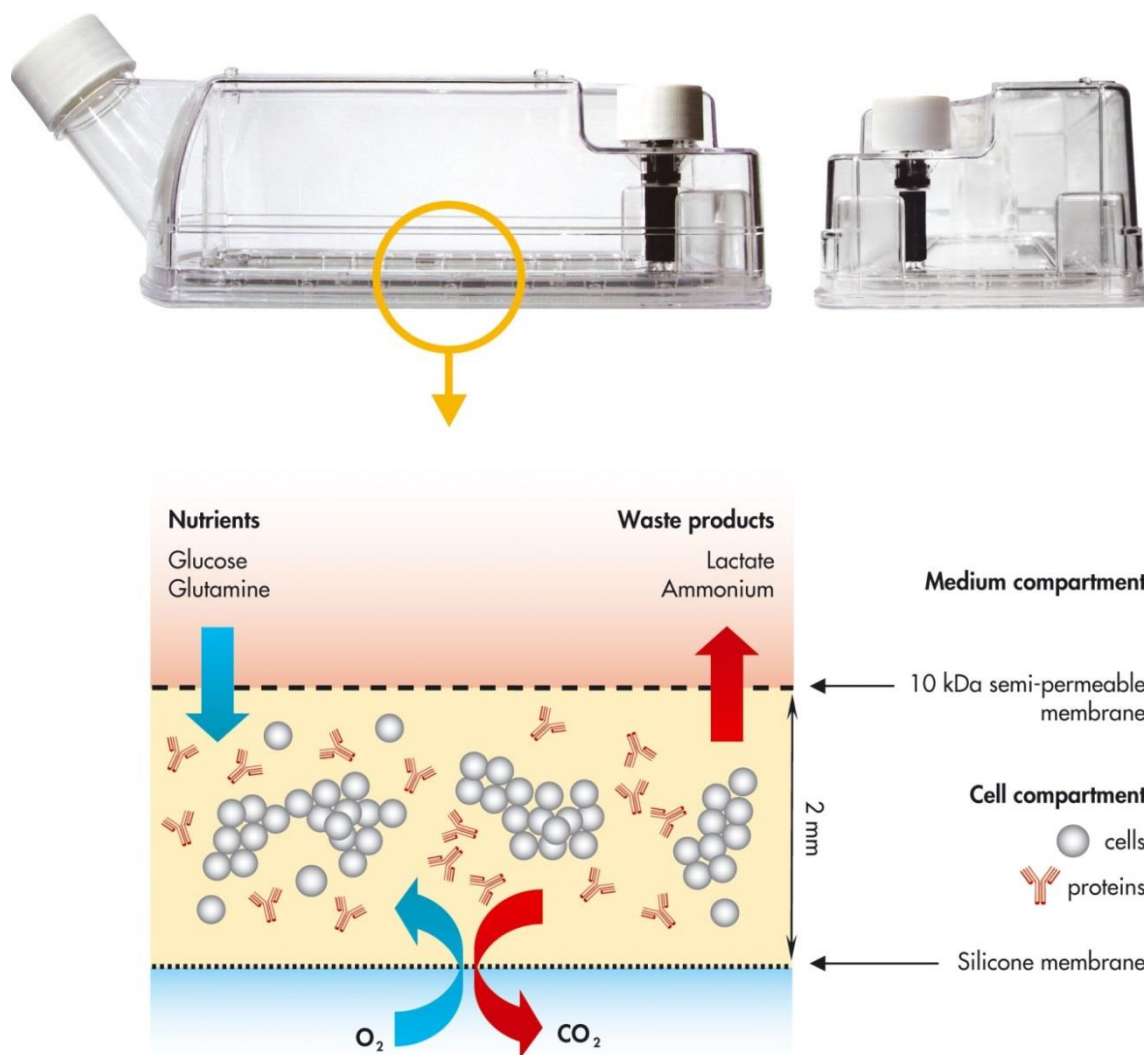


Figure 2-4 Illustration of the CELLline Bioreactor system for antibody production
(image kindly provided by INTEGRA-biosciences)

2.2.16 Purification of mABs using Proteus A columns

To purify the antibodies from the cell supernatant, Proteus A purification columns (AbD) were utilized. These columns contain recombinant protein A, derived from expression in *E. coli*, which has a high affinity to the Fc part of an antibody, enabling an affinity purification of antibodies from crude hybridoma supernatant. After pre-equilibration of the Proteus A columns with 2 ml binding buffer A pH 9 (see table 11), supernatants from CELLline reactor were clarified using a 70 μm nylon mesh and diluted 1:1 in binding buffer A. 20 ml diluted antibody was transferred on the Proteus A column and centrifuged at 100x g for 30 minutes. Flow through was discarded and columns were washed twice with 10 ml of binding buffer.

Antibodies bound to protein A within the column were eluted by low pH using the elution buffer B2 pH 2.5. The eluate was then spun down into a tube containing 1.3 ml neutralization buffer C pH 9 for 3 min at 500x g. In this step, the pH of the sample reaches approximately 7.5. Depending on the yield, the affinity purified antibody was either used for in vitro applications directly after the neutralization step or further concentrated using MWCO-spin columns (Sartorius).

2.2.17 Isotyping of GDF-15 positive monoclonal antibodies

Depending on its application, knowledge about the isotype of an antibody is unavoidable. To determine the isotype of mouse anti GDF-15 antibody B1-23, AbD serotec isotyping stripes were used. The assay principle is based on anti-mouse kappa and anti-mouse lambda antibodies coupled onto coloured micro particles and equally reactive to any mouse monoclonal antibody regardless of its isotype. The isotyping strip has immobilized bands of goat anti-mouse antibodies corresponding to each of the common mouse antibody isotypes (IgG1, IgG2a, IgG2b, IgG3, IgM, and IgA) and to the kappa and lambda light chains. Both sides of the strip bear a positive flow control band, which indicates that the antibody-coated coloured micro particles have migrated through the strip.

To start the isotyping reaction, the provided stripes were dipped into the diluted antibody sample. The results were visible in less than 10 minutes on the assigned stripe (figure 2-5).

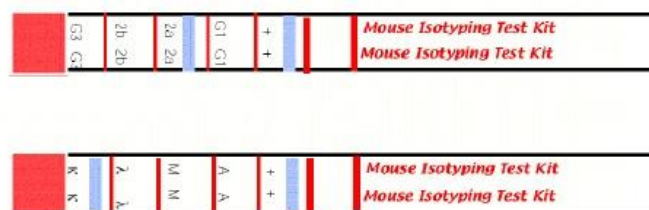


Figure 2-5 Mouse isotyping strip (AbD Serotec) for identification of the heavy chain isotype and light chain subtype

2.2.18 Epitope mapping

In order to identify the epitope of GDF-15 bound by the antibody B1-23, two different epitope mapping methods were applied. Mapping of linear epitopes and mapping of discontinuous three dimensional epitopes (Middeldorp and Meloen, 1988, Stefanescu et al., 2007).

2.2.18.1 Linear epitope mapping (pepperprint GmbH)

Mapping of linear epitopes was performed externally by pepperprint. Therefore, monoclonal mouse antibody GDF-15 (B1-23) was tested for binding linear peptides derived from GDF-15 on a single array.

Antigen: GDF-15

GSGSGSGMPGQELRTVNGSQMLLVLLVLSWLPHGALS LAEASRASFPGPSELHSED
SRFREL RKRYEDLLTRLRANQSWEDSNTDLVPAPAVRILTPEVRLGSGGHLHLRISRA
ALPEGLPEASRLHRALFRLSPTASRSWDVTRPLRRQLSLARPQAPALHLRLSPPPSQSD
QLLAESSARPQLELHLRPQAARGRRRARARNGDHCPLGPGRCCRLHTVRASLEDLG
WADWVLSPREVQVTMCIGACPSQFRAANMHAQIKTSLHRLKPDTVPAPCCVPASYN
PMVLIQKTDTGVSLQTYDDLLAKDCHCIGSGSGSG

(322 amino acids including linker)

The GDF15 protein sequence was translated into 13mer peptides with a shift of one amino acid. The C- and N-termini were elongated by a neutral GSGS linker to avoid truncated peptides (bold letters) and spotted on the peptide array. Flag (DYKDDDDKGG) and HA (YPYDVPDYAG) served as control peptides in form of 78 spots surrounding the array. Monoclonal mouse antibody GDF-15 (1 µg/µl) was stained on the array in incubation buffer for 16 h at 4°C at a dilution of 1:100 and shaken at 500 rpm. As secondary antibody, a goat anti-mouse IgG (H+L) IRDye680 diluted 1:5000 in incubation buffer, was stained for 30 min at room temperature (RT). Monoclonal anti-HA (12CA5)-LL-Atto 680 (1:1000), monoclonal anti-FLAG(M2)-FluoProbes752 (1:1000) served as control antibodies and were stained in incubation buffer for one hour at RT. The array was scanned using the Odyssey Imaging System, LI-COR Biosciences.

Standard buffer: PBS, pH 7.4 + 0.05 % Tween 20
Blocking buffer: Rockland blocking buffer MB-070
Incubation buffer: Standard buffer with 10 % Rockland blocking buffer MB-070

Table 30 Buffers used for linear epitope mapping on peptide array (performed by pepperprint GmbH)

2.2.18.2 Epitope mapping of 3-dimensional epitopes (epitope excision)

Epitope excision and epitope extraction method was externally performed at the Steinbeis Zentrum Konstanz together with the group of professor Przybilski according to their established and published protocols (Stefanescu, Iacob et al., 2007).

In short, the antibody B1-23 was covalently immobilized on a sepharose column. Subsequently, recombinant human GDF-15 was added on the columns. Bound GDF-15 was enzymatically digested by means of different proteases (trypsin). Cleaved peptides were harvested and analyzed by liquid chromatography–mass spectrometry (LC^{MS/MS}-) method. The antibody shielded peptide fragments were then eluted by trifluoroacetic acid (TFA), a very acidic solution, thereby liberating the epitope defining peptides from the monoclonal antibody. These peptides were further analyzed by mass spectrometry and LC^{MS/MS} method.

2.2.19 kD-values-determination of antibodies

Affinities of humanized GDF-15 antibodies were analyzed externally at the Steinbeis Zentrum Konstanz using the SAW Chips according to the manufacturer recommendation (SAW instruments).

2.2.20 CDR Cloning of B1-23 heavy and light chains using degenerate primers (mouse IgG2a)

The unknown complementarity determining regions (CDRs) of GDF-15 antibody B1-23 light and heavy chains were cloned according to the following procedure: RNA from hybridoma clone B1-23 was isolated (RNA isolation 2.2.10.1). Beside numerous transcripts generated by the hybridoma, mRNA of the light chain as well as the heavy chain of the antibody B1-23 were isolated, followed by reverse transcriptase reaction in order to generate cDNA (as described in 2.2.10.3). cDNA was subjected to a polymerase chain reaction using specific primer combinations enabling the amplification of unknown (but relatively conserved) sequences (Wang et al., 2000). So called degenerate primers were adapted in such way, that binding to certain mouse immunoglobulin sequences within the variable region of the antibody binding site was able.

PCR resulted in PCR products of a length of 300nts containing blunt ends, further cloned into sequencing vector (further described in 2.2.13.1)

2.2.21 Chimerization of B1-23

Chimerization of the murine GDF-15 binding antibody B1-23 was performed externally by evitria AG (using its proprietary technology). Hereby the antigen binding site of the mouse antibody (Fab) was grafted on a human IgG1 antibody backbone.

2.2.22 Humanization of B1-23

Prior to humanization of the monoclonal antibody B1-23, which was performed externally, evitria AG performed a codon optimization and offered 5 different light chain variable regions as well as 5 different heavy chain regions, which were transplanted on a human IgG1 antibody framework (evitria's proprietary technology). There are a number of methods describing the process of humanizing antibodies (Weissenhorn et al., 1991) (Kettleborough, Saldanha et al., 1991, Near, 1992). (LoRusso, Weiss et al., 2011) The exact procedure applied here underlies evitria's proprietary technology was protected by the company.

2.2.23 Animal Experiments

2.2.23.1 Glioma model

Glioma bearing animals, study was performed in collaboration with and details are described in the methods section of the publication in Clin Cancer Res. 2010 (Roth, Junker et al., 2010).

2.2.23.2 Melanoma Xenograft model

In order to assess an effect of GDF-15 antibodies in regard to tumor growth inhibition as well as prevention of cachexia, athymic female BALB/C^{Nu/Nu} (CAnN.Cg-Foxn1^{<nu>}/Crl) mice (obtained from Charles River) were inoculated with 10×10^6 UACC-257 melanoma cells. Prior inoculation, the melanoma cells were diluted 1:1 in matrigel, which was kept on ice until injecting the cell suspension. 200 μ l of matrigel cell suspension was injected subcutaneously in the flank of the animals. Each treatment group contained 10 animals. Antibodies and substances (apart from dacarbazine) were administered intraperitoneally twice a week. Dacarbazine treatment was performed on 5 consecutive days starting at day 0. All antibodies were administered at a concentration of 25 mg/kg body weight. All treatments started on day of tumor inoculation, defined day 0. Body weight measured every 3 and 4 days. Tumor growth was measured twice a week. Food consumption, body weight, tumor volume (measured using a caliper) was analyzed until the end of the study.

<u>Group nr. 1 - 7 (10 mice each group)</u>	<u>amount of substances (for 45 d)</u>
1. Dacarbazine* (Referenz, Lot.: C120522C)	80 mg
2. PBS (SIGMA, Lot.: RNBD0341).....	30 ml
3. B1-23 (murin, Lot.: 515980)	75 mg
4. ChimB1-23 (chim., Lot.: PR0057)	75 mg
5. H1L5 (humanis. B1-23, Lot.: PR3176)	75 mg
6. B12 (IsoAK, Lot.: ID3195)	75 mg
7. Fab (from ChimB1-23 Lot.: PR0057)	75 mg

*Detimedac 500 mg (exp.: 03.2015)

Table 31 Setup UACC-257 Xenograft Study (Substances & total amounts required)

Brief explanation in regard to the individual treatment groups (shown in Table 31):

1. Dacarbazine: Reference-/positive control for tumor growth inhibition (anti neoplastic chemotherapeutic drug for the treatment of malignant melanoma in human)
2. PBS: Growth-/Vehicle-control (all substances (1, 3-7) were dissolved in PBS)
3. B1-23 (murin): lead antibody, as reference group for comparison with the chimeric and humanized GDF-15 antibodies (ChimB1-23 and H1L5).
4. ChimB1-23: chimeric B1-23 (murine Fab-sequence grafted on human IgG-1 antibody [Trastuzumab-backbone])
5. H1L5: humanized B1-23 (see 3.4.10) [Trastuzumab-backbone]).
6. B12-Iso-antibody: the antibody served as isotype-control, to exclude unspecific effects due to IgG-1-type immunoglobulins. The iso antibody B12 (Lot.ID3195) was generated by Evitria AG. B12 binds HIV antigens and thus should not react with human GDF-15 and neither crossreact with murine antigens.
7. Fab: the Fab fragments were included to enable enhanced tumor penetration due to small molecular weight compared to full antibody size

2.2.24 Statistics

Experiments were performed at least three times independently with similar results. For *in vivo* studies a two-way ANOVA test was performed. The applied statistical tests for *in vitro* experiments are indicated in the results section.

3 Results

3.1 GDF-15 expression in solid tumors

3.1.1 GDF-15 is highly expressed in ovarian cancer

GDF-15 is overexpressed in many solid tumors (Corre, Labat et al., 2012). It has been reported by Staff and colleagues that high GDF-15 serum levels in patients with ovarian carcinoma correlate with a poor prognosis (Staff, Trovik et al., 2011). To visualize the GDF-15 protein expression and its distribution in the tumor, several ovarian cancer tissues were stained immunohistochemically using a commercial anti-GDF-15 antibody (Prestige Antibody, Sigma) suitable for paraffin embedded tissues. At least three specimens from each tumor type were stained. As a positive control placental tissue was stained, revealing a strong GDF-15 expression in the syncytiotrophoblasts, whereas the endothelial cells and stromal cells were GDF-15 negative. In ovarian cancer tissue, GDF-15 shows a high expression in transformed cells and endothelial cells while stromal cells seemed to be predominantly GDF-15 negative. Interestingly, the endothelial cells in placental tissue appeared to be GDF-15 negative (figure 3-1-1).

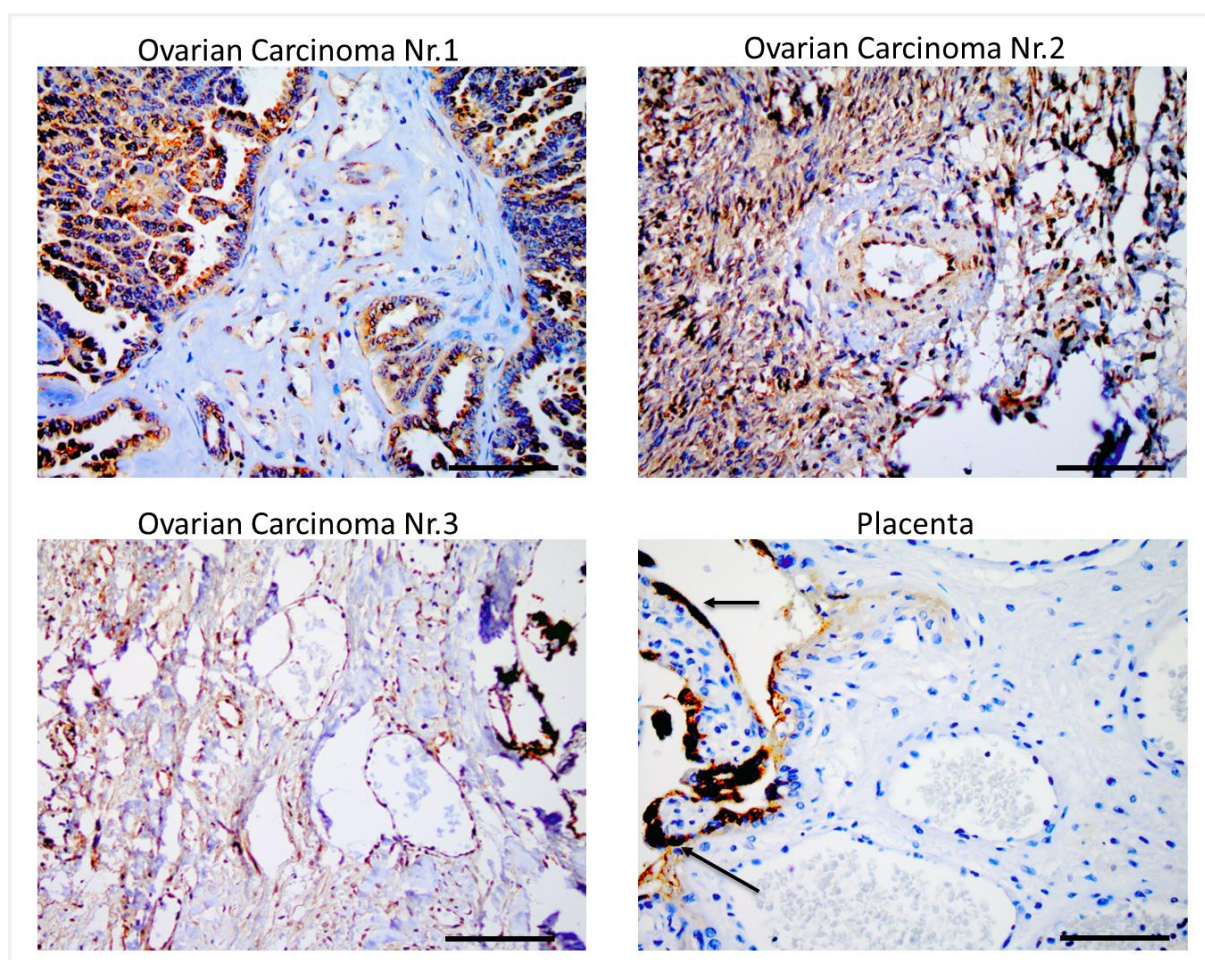


Figure 3-1-1 GDF-15 expression in human malignant ovarian cancer

Paraffin-embedded tissue sections of human ovarian carcinoma patients were assessed by immunohistochemistry (IHC) and stained for GDF-15 with the GDF-15-Atlas-antibody from Sigma-Aldrich. The presented tissues comprised a serous papillary ovarian carcinoma (Nr.1), a mucinous carcinoma (Nr.2) and a high grade endometrioid carcinoma (Nr.3). Human placenta served as positive control for GDF-15. Placental syncytiotrophoblasts, which are known to highly express GDF-15, are indicated by arrows. Representative images are shown (original magnification, $\times 200$ for all photomicrographs).

3.1.2 GDF-15 is overexpressed in brain tumors

GDF-15 is highly expressed in different brain tumors (Roth, Junker et al., 2010). It is known from literature, that high GDF-15 serum levels found in the cerebrospinal fluid (CSF) in glioma patients are associated with a poor prognosis (Shnaper, Desbaillets et al., 2009). For that reason we investigated the expression pattern and the intensity of GDF-15 in different types of brain tumors, WHO grade I to IV. We observed intensive GDF-15 staining in all glioma sections and very rare GDF-15 expression in normal brain tissue. Like seen in ovarian cancer, endothelial cells of the blood vessels appeared to be GDF-15 positive as well. Interestingly, high levels of GDF-15 did not correlate with the WHO grade (stages I- IV) of the malignant tumor. However, the protein expression in tumor tissue was increased compared to healthy brain tissue (figure 3-1-2).

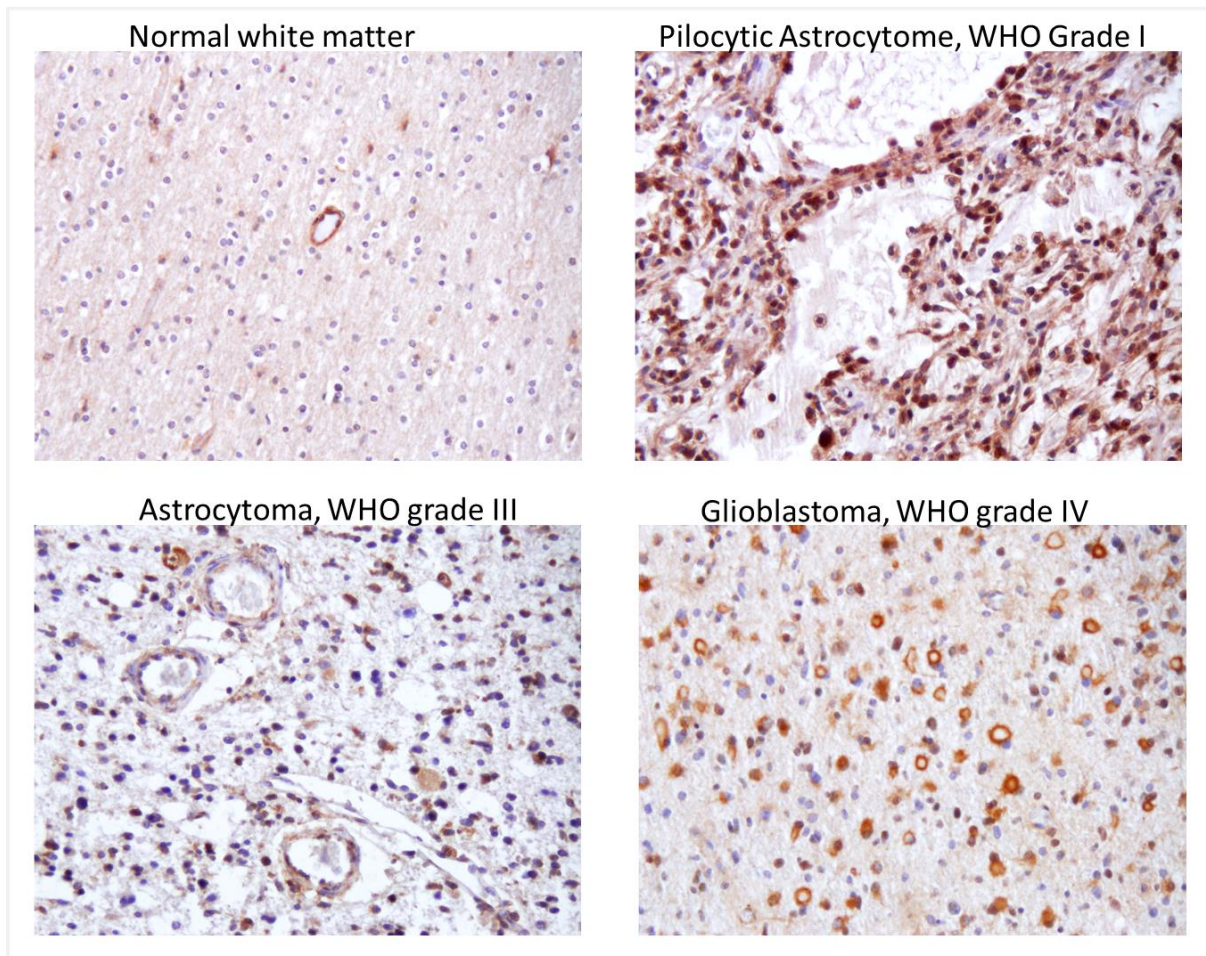


Figure 3-1-2 Human malignant gliomas express GDF-15 *in vivo*

Paraffin-embedded tissue sections of normal human white matter (top left), diffuse astrocytomas (WHO grade I, top right), anaplastic astrocytomas (WHO grade III, bottom left), and glioblastomas (WHO grade IV, bottom right) were assessed by immunohistochemistry. Five specimens from each entity were stained. Representative images are shown (original magnification, $\times 200$ for all photomicrographs). Pathological evaluation was performed and pictures were taken by Michel Mittelbronn.

3.2 The effects of GDF-15 *in vitro*

3.2.1 GDF-15 does not activate the canonical TGF- β signaling pathway in human PBMC

In 2007, it has been reported by Johnen and colleagues, that the TGF- β receptor type II is likely to be involved GDF-15 mediated effects on hypothalamic neurons in mice, leading to anorexia (Johnen, Lin et al., 2007). Furthermore, Tan and colleagues suggested that GDF-15 inhibits the proliferation of different tumor cell lines through the TGF- β signaling pathway (Tan et al., 2000). Assuming that GDF-15 signal transduction is a result of the TGF-beta receptor activation, we expected an enhanced Smad2/3 phosphorylation in TGF- β sensitive cells. Human peripheral blood mononuclear cells (PBMC) express the TGF- β receptor and respond (highly sensitive) to TGF- β by activating the canonical TGF- β signaling pathway. Thus, we investigated the phosphorylation of Smad2/3 protein of human PBMC in response to recombinant GDF-15 by Western Blot analysis. First, peripheral blood lymphocytes from four different donors were treated with 100 ng /ml recombinant GDF-15 and 5 ng /ml TGF-beta for 10 minutes. Recombinant TGF- β was used as a positive control. SD208, a TGF- β receptor tyrosine kinase-I inhibitor, was used as an indicator for autocrine TGF- β signaling, when compared to the untreated control (Sun et al., 2014). TGF- β induced the phosphorylation of Smad2/3, whereas GDF-15 did not activate the canonical TGF- β pathway in lymphocytes from four different healthy donors (figure 3-2-1a). Furthermore, different GDF-15 batches were used to exclude batch to batch variations or impurities with other growth factors and cytokines as for instance TGF- β itself. None of the commercially acquired recombinant GDF-15 batches led to an increased phosphorylation of Smad2/3, compared to recombinant TGF- β (figure 3-2-1), confirming the results obtained in figure 3.2-1a. These data suggest that recombinant human mature GDF-15 does not activate the canonical TGF-beta signaling pathway in human peripheral blood mononuclear cells.

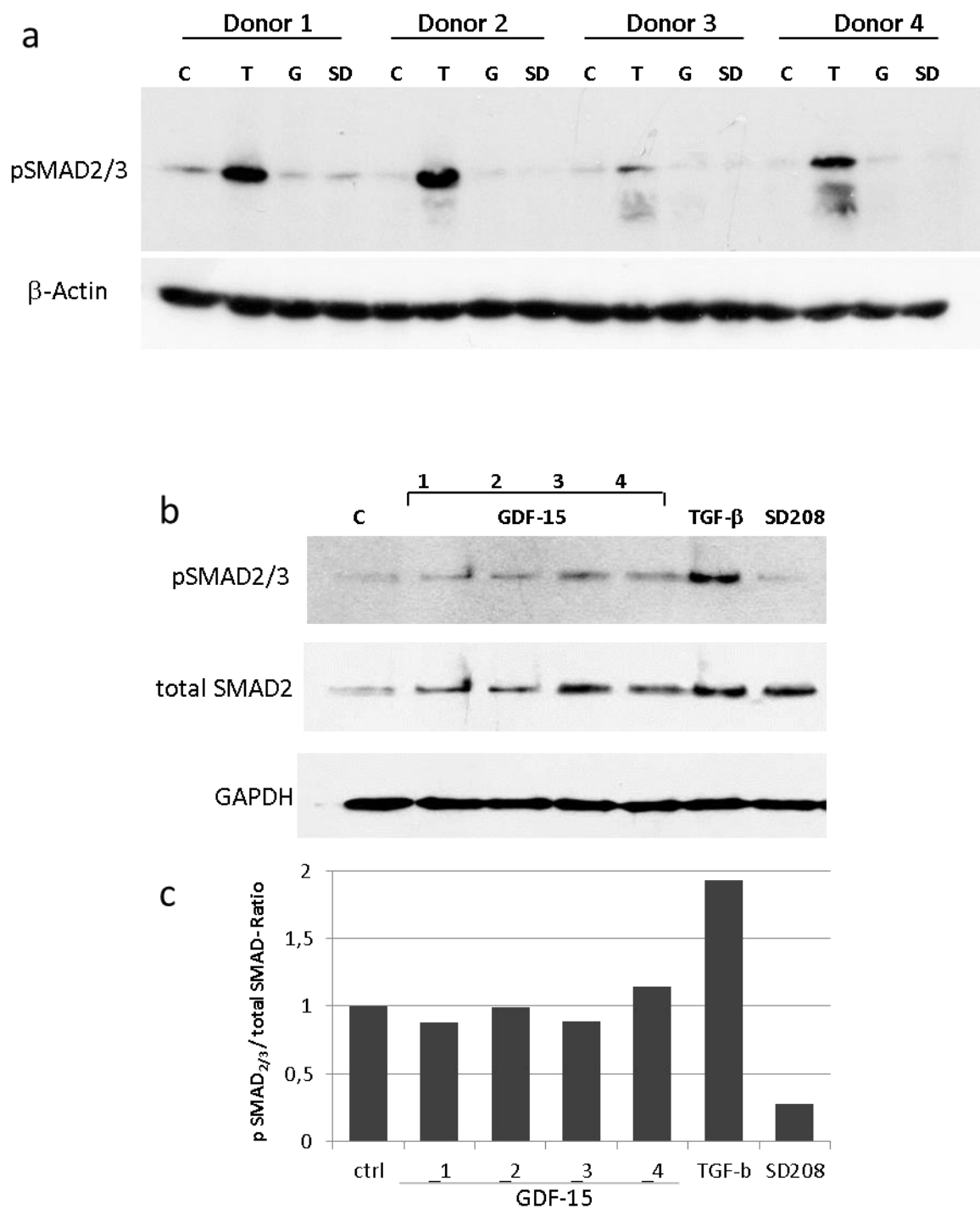
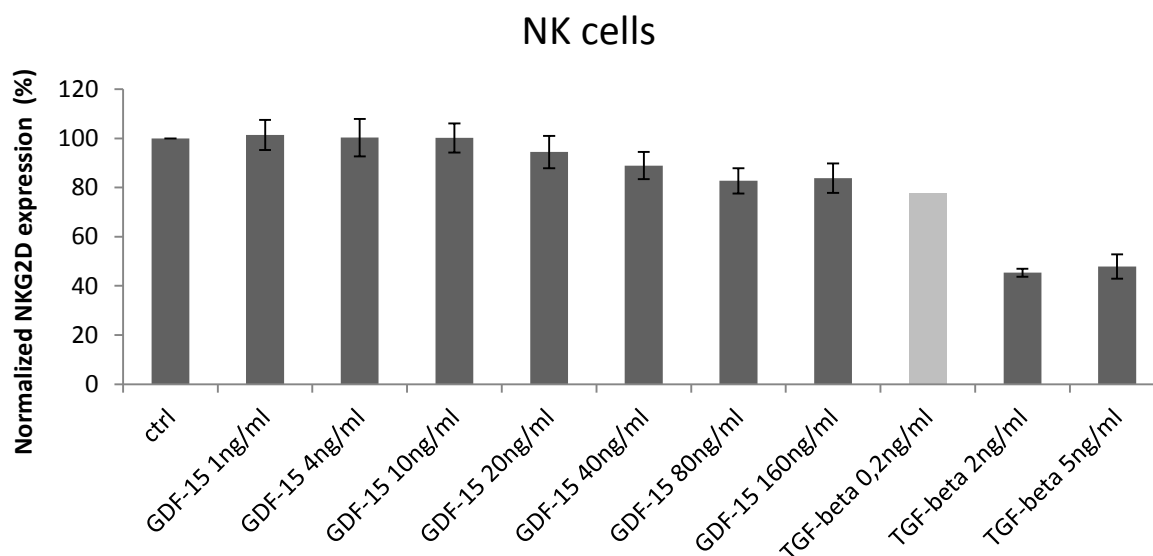


Figure 3-2-1: Effects of TGF beta and GDF-15 on the phosphorylation of Smad2/3 in PBMC

Western Blot analysis using lysates of human PBMCs. Lymphocytes were treated with 100 ng/ml recombinant GDF-15 or 5 ng/ml TGF-beta-1 for 10 minutes. Furthermore, PBMCs were treated with 1 μM SD208 for 30 minutes. SD208 was utilized as an inhibitor of the TGF-beta receptor tyrosine kinase 1, disclosing basal TGF-β signaling in the untreated control. (a) PBMC of four different healthy blood donors responded to TGF-β with a Smad2/3 phosphorylation (C: control, T: TGF-β, G: GDF-15 (Peprtech), SD: SD208). β-Actin served as positive control.(b) Four commercially acquired batches of GDF-15 (1:R&D, 2:Peprtech;3:Invigate;4:Peprtech) were tested for their ability to activate the TGF-beta signaling pathway. Total SMAD2 as well as GAPDH served as a loading control. This figure represents 3 individual Western Blots with a similar result. (c) Densitometrically quantified pSMAD2/3 using the image J software. The ratio of pSMAD2/3 to total SMAD protein was calculated and normalized to the untreated control.

3.2.2 The effect of GDF-15 on the NKG2D receptor on NK cells and CD8⁺ T cells

One of its various effects of TGF beta is the downregulation of the activating killing receptor NKG2D on NK cells and CD8⁺ T cells (Lee et al., 2004, Crane, Han et al., 2010). As a divergent member of the TGF- β superfamily, we raised the question, whether GDF-15 shows similar effects on the NKG2D surface expression on immune cells. Therefore, PBMCs were treated with recombinant GDF-15 and the downregulation of the surface NKG2D receptor on immune cells was assessed by fluorescence activated flow cytometry. We could observe a dose dependent reduction of NKG2D receptor expression on NK cells and CD8⁺ T cells with increasing GDF-15 concentrations (figure 3-2-2): The strongest effect of GDF-15 on NK cells could be observed at a concentration of 80 ng /ml and higher. Compared with the untreated control (100 %), GDF-15 treatment revealed a reduction in the surface NKG2D receptor expression of about 18 % \pm 5.1 with 80ng /ml and 17 % \pm 6.0 with 160ng /ml (figure 3-2-2a). 2ng /ml and 5ng /ml recombinant TGF- β lead to a reduction of the surface NKG2D receptor of 54.7 % \pm 1.2 and 52.2 % \pm 4.9, respectively. On CD8⁺ T cells, GDF-15 treatment resulted in a reduction of the NKG2D receptor of about 21.6 % \pm 10.5 with 40 ng /ml and 21.3 % \pm 12.9 with 80 ng /ml (figure 3-2-2b). 2 ng /ml and 5 ng /ml recombinant TGF- β lead to a reduction of the surface NKG2D receptor of 45.9 % \pm 8.6 and 43.2 % \pm 8.1, respectively. On NK cells a concentration of 80 ng /ml recombinant GDF-15 reached its maximum effect. On CD8⁺ T cells GDF-15 reached a saturated plateau at 40 ng /ml GDF-15, indicating that T cells are more responsive to GDF-15 than NK cells. Recombinant TGF- β was used as a positive control, showing a far stronger reduction of NKG2D surface expression compared to GDF-15.



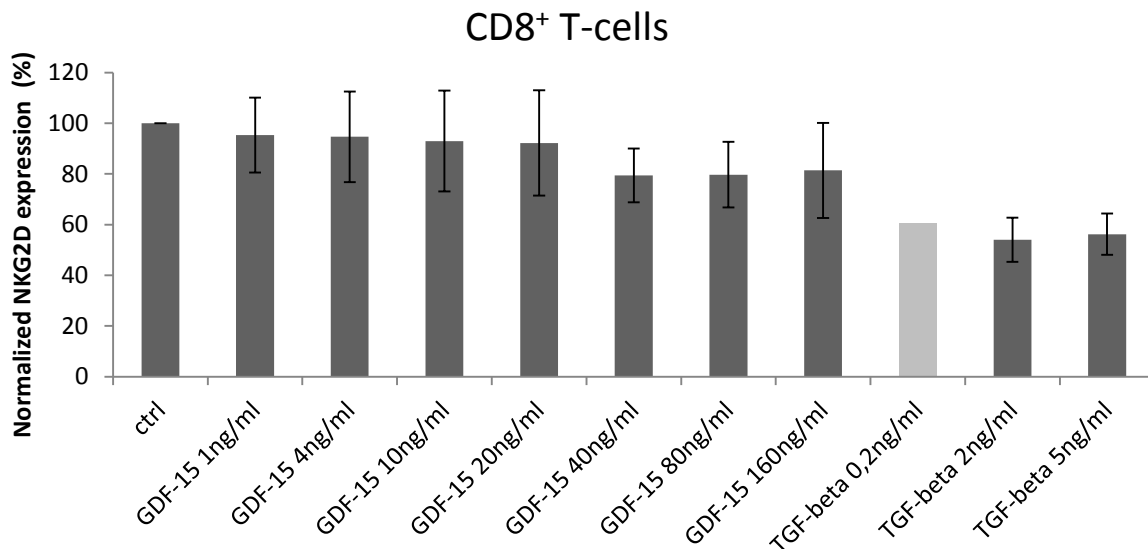


Figure 3-2-2: NKG2D receptor surface expression on natural killer cells and CD8⁺ T cells

Human PBMCs were isolated from a blood donor and treated with recombinant GDF-15 (SF9 derived, provided by Professor Müller) (6 concentrations) and TGF- β -1 (3 different concentrations) for 24 hrs. SD208 was used in a concentration of 1 μ M to inhibit autocrine TGF- β signaling within the immune cells. The figure displays the specific fluorescence intensities (SFI) of the NKG2D surface expression on CD3⁻ CD56⁺ NK cells, measured by flow cytometry. The NKG2D specific intensities were quantified relative to an unspecific isotype-control antibody, labelled with the same fluorochrome as the specific antibody. In this experiment TGF-beta-1 served as a positive control for the downregulation of NKG2D receptor on NK cells. Only one measurement has been performed for the TGF-beta concentration at 0.2 ng /ml (light gray bar). Each bar represents 3 individual experiments from different blood donors. The control represents 100 % NKG2D expression.

3.2.3 GDF-15 reduces T-cell-adherence on endothelial cells

Kempf and colleagues reported in 2011 that GDF-15 influences the adherence of mouse polymorphonuclear lymphocytes (PMNs) *in vitro* (Kempf, Zarbock et al., 2011). The authors demonstrated that the treatment of mouse immune cells with GDF-15 leads to the inactivation of β -integrins on the surface of immune cells, suggesting a decreased ability to adhere to the blood vessel endothelium. To investigate the effect of GDF-15 on human immune cell adherence, human PBMC were treated with recombinant GDF-15 and adherence on HUVEC cells was investigated. Prior treatment of GDF-15, the endothelial cells were pre-treated with TNF alpha in order to induce the surface exposure of specific adhesion molecules on HUVEC. Pre-treatment of PBMC with phytohemagglutinin (PHA) served as control, which mediated global adherence of leukocytes on endothelial cells. TNF α induced adherence could be slightly lowered by the treatment of CD4⁺ T cells and CD8⁺ T cells with 100 ng /ml of recombinant GDF-15 (figure 3-2-3). Macrophages (CD14⁺ cells) did not lose their potential to adhere to endothelial cells when treated with GDF-15. These data indicate that GDF-15 influences the leukocyte-endothelial interaction either by suppression of the TNF α induced

induction of surface molecules on the HUVEC (e.g. LFA-1/ICAMs, CD44, etc.) or reduction/inactivation of adhesion molecules on the immune cell surface.

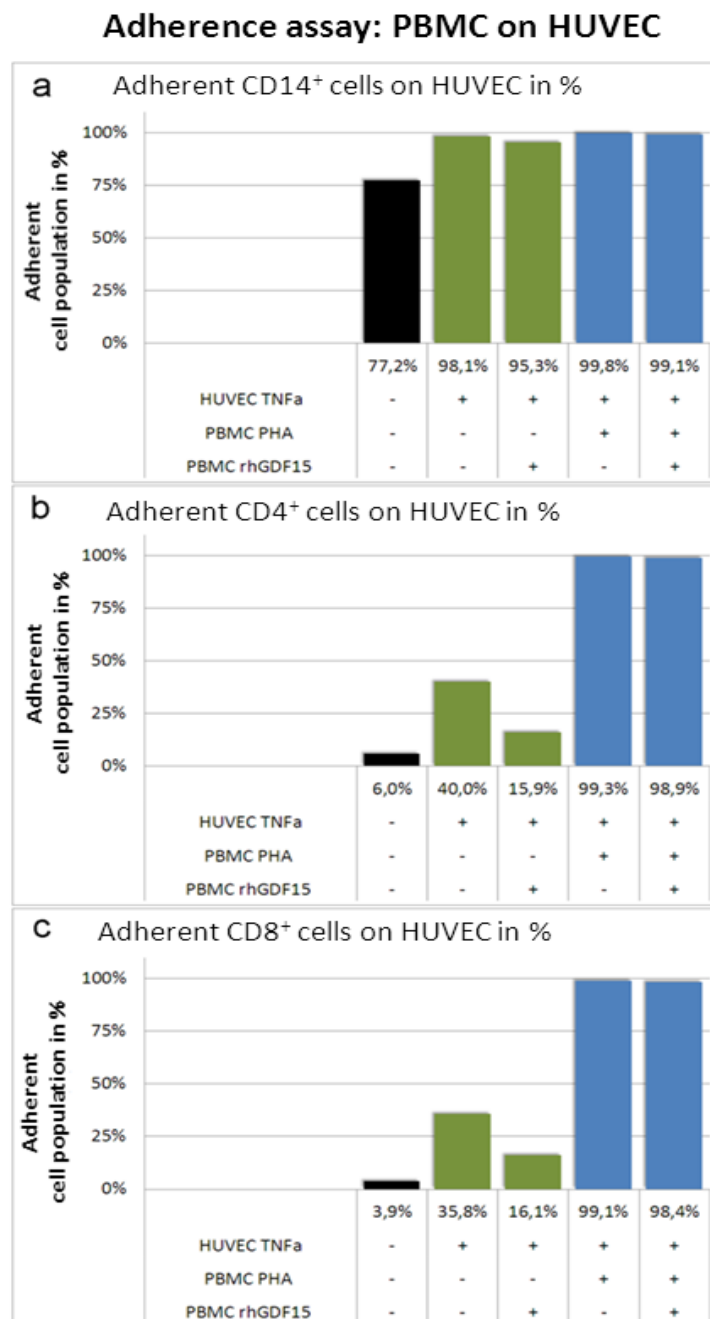


Fig 3-2-3 *In vitro* adherence of PBMC on HUVEC under the influence of GDF-15

Human PBMC were co-cultured on a monolayer of the HUVEC cell line for 1 hour. The adherent fraction as well as cells in suspension were stained for CD14 (monocytes), CD4 (T_H-cells) and CD8 (CTLs) -positive cells and quantified using fluorescent activated flow cytometry. In order to induce adhesion molecule expression, HUVEC cells were stimulated with TNF- α or phytohemagglutinin (PHA). The TNF α induced adhesion could be partially suppressed by the simultaneous treatment with recombinant GDF-15 (R&D Systems). CD14 positive monocytes were not affected in regard to their adherence on endothelial cells, when treated with GDF-15. (n=3) (This experiment was kindly provided by Dr. Dirk Pühringer)

3.2.4 Microarray Analysis – the influence of GDF-15 on PBMC and HUVEC cells

Numerous cytokines and growth factors lead to transcriptional deregulations in cells. For example, TGF- β -1 activates the transcription of mammalian genes important for cell cycle regulation, for extracellular matrix formation and which are known to promote immunosuppressive functions (Docagne et al., 2001). TGF- β -1 induces the expression of PAI-1 in different human tissues (Kutz et al., 2001). We speculated that GDF-15, similar to TGF- β , leads to an alteration in gene expression in different cell types. To test this hypothesis, a DNA Microarray (GeneChip® Human Transcriptome Array 2.0 from Affymetrix) was performed in collaboration with the micro-array core facility at the University Wuerzburg, analyzing transcriptional regulations in human umbilical vein endothelial cells (HUVEC) as well as human PBMC upon GDF-15 treatment. Peripheral human immune cells were chosen because of their asserted responsiveness to GDF-15, which has been reported by Kempf and colleagues (Kempf, Zarbock et al., 2011). Furthermore, the slight effects shown in section 3.2.2 and 3.2.3 allowed to hypothesize a transcriptional response of human lymphocytes upon GDF-15 treatment. HUVEC seemed to be an appropriate cell type, since Whitson and colleagues could demonstrate a suppressive effect of GDF-15 on endothelial growth and thus transcriptional alterations might play a role in mediating this effect (Whitson et al., 2013). Different treatment conditions were applied on PBMC before analyzing the gene expression pattern: Both cell types were treated with recombinant human GDF-15 (R&D Systems) or left untreated for six hours and 24 hours. PBMCs were additionally treated with supernatants of HEK293-T cells overexpressing human GDF-15 and with supernatants of empty vector transfected HEK293-T-cells for six hours and 24 hours. A cluster analysis with all the samples being integrated was performed and illustrated in form of a heat map (figure 3-2-4). As a result, the transcriptional profile of the HUVEC cells appeared as a separate cluster when compared to their gene expression pattern of the PBMC. However, the clustering within the different PBMC treatment groups appeared unexpectedly scattered. In regard to the whole gene expression array, the effect of GDF-15 seemed to be too weak to lead to an appropriate clustering of the different treatment groups.

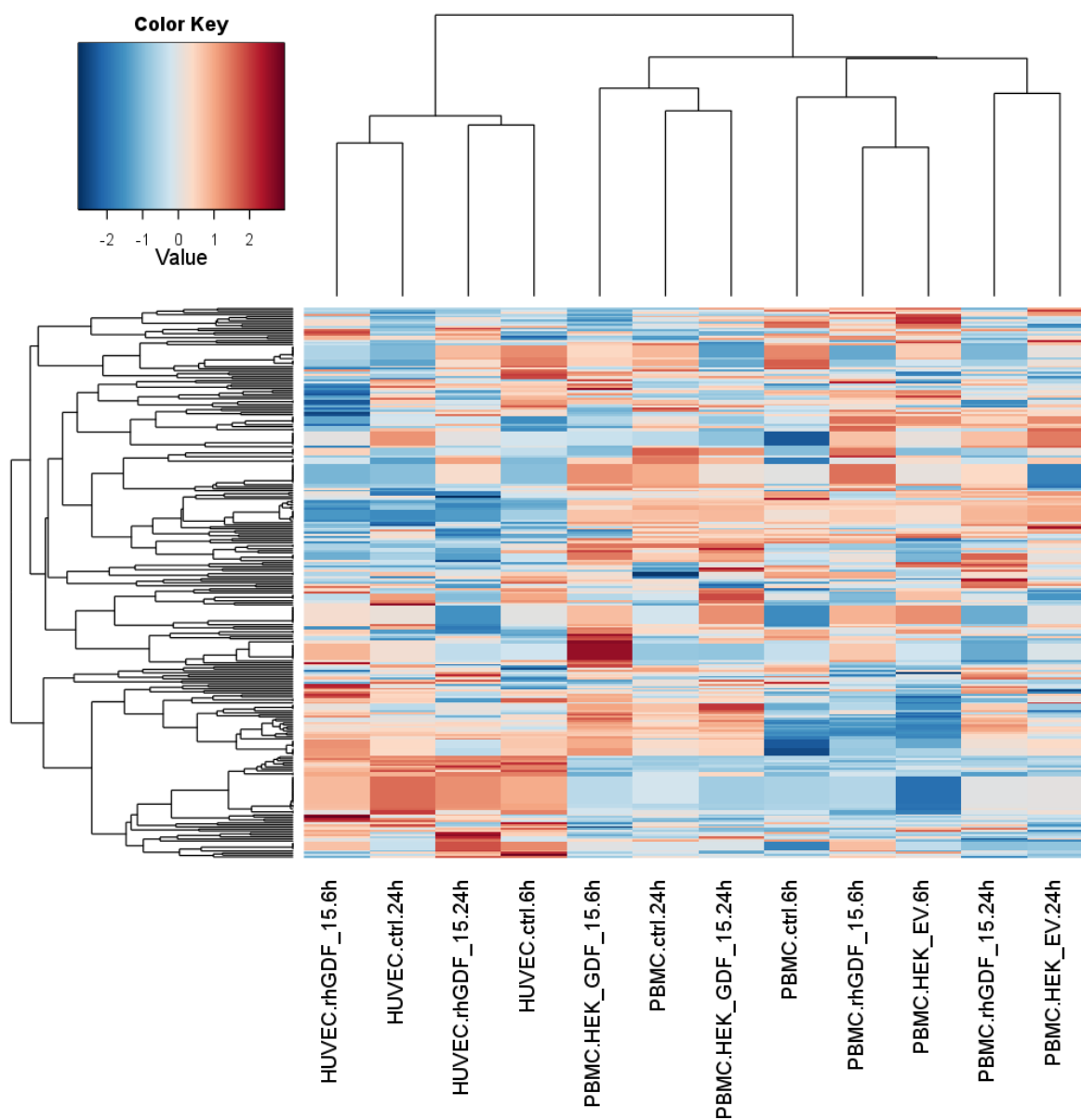


Figure 3-2-4 Heat map for hierarchical clustering of gene expression pattern in HUVEC and PBMC

The signal intensities (indicating the gene expression level) obtained from the affymetrix microarray of the HUVEC cells and PBMC, which were treated for different points of time, were represented in a cluster analysis (using the software R). The intensities received from arrays with the GDF-15 treated cells were normalized to the intensities of genes resulting from the untreated controls. High gene expression level is indicated in the heat map by red. Low gene expression is presented by blue (see colour key, top left). The hierarchical cluster trees on top of the heat map indicate the coherence of different samples. The cluster trees on the left side represent the coherent genes on the array. The cluster analysis was performed with the help of Dr. Claus Scholz, from the microarray core unit of the University of Wuerzburg.

Since the array covered 245.000 transcripts, including ~ 40.000 non-coding ones, a stringent pre-selection has been performed (tables 32-37). Either protein coding genes or nucleic acids with potential regulatory functions were selected for further analysis.

Exclusion criteria for the selection of either “up regulated or down regulated” transcripts were determined as follows: Transcripts with a \log_2 -fold change (log FC) above 0.5 or below -0.5 compared to the untreated control cells were selected. The statistical significance (FDR) was set to a p-value of less than 0.05. As a result, very few and slight deregulations could be observed in PBMCs as well as HUVEC cells (tables 32-43). Human PBMCs as well as HUVEC responded to recombinant GDF-15 with a slight up regulation of different olfactory receptors. While in HUVEC five different olfactory receptor transcripts are up regulated upon GDF-15 treatment after six hours and 24 hours, in PBMC two olfactory receptors genes (OR104A, OR2M7) are up regulated at the early point of time (six hours) and down regulated after 24 hours (OR104A, OR7G2). In HUVEC, BLID, SPINT-3 and CD44 transcripts were slightly down regulated after 6 hours of GDF-15 treatment compared to the control HUVEC (figure 3-2-4). CD44 has been described to be involved in adherence of immune cells on endothelial cells, and is thus an interesting target in the context of the proposed immunomodulatory function of GDF-15. This decrease of CD44 in endothelial cells could be confirmed by a further quantitative approach using realtime PCR techniques (qRT-PCR, data not shown). Interferon gamma, a potent proinflammatory cytokine, was downregulated in PMBCs after 6 hours of recombinant GDF-15 treatment (\log_2 -fold change = - 0.69 ; ***p < 0.00054). Since the values of induction were quite low, an altered protein expression level is rather unexpected for the respective genes.

Table 32: Upregulated transcripts of PBMCs treated for six hours with recombinant GDF-15 (R&D Systems)

PBMC 6h rhGDF-15_ctrl Upregulated transcripts								
log FC	FDR	Symbol	Gene	mRNA	Chromosome	Start	Stop	
0,91	7,2421E-08	IGHD2-2	ENST00000390591	ENST00000390591 // ENSEMBL // cdna:known chromosome:GRCh3	chr14	106382685	106382715	
0,76	2,7834E-05	MIR320C1	NR_031565	NR_031565 // RefSeq // Homo sapiens microRNA 320c-1 (MIR320C1)	chr18	19263471	19263558	
0,54		MIR99A	NR_029514	NR_029514 // RefSeq // Homo sapiens microRNA 99a (MIR99A), mi	chr21	17911409	17911489	
0,64	0,00417265	MCCD1	NM_001011700	NM_001011700 // RefSeq // Homo sapiens mitochondrial coiled-coil	chr6	31496494	31498009	
0,64	0,00429144	MCCD1	NM_001011700	NM_001011700 // RefSeq // Homo sapiens mitochondrial coiled-coil	chr6_apd_hap1	2811182	2812697	
0,64	0,00440906	MCCD1	NM_001011700	NM_001011700 // RefSeq // Homo sapiens mitochondrial coiled-coil	chr6_ssto_hap1	2827299	2828814	
0,66	0,00231314	OR2M7	NM_001004691	NM_001004691 // RefSeq // Homo sapiens olfactory receptor, fami	chr1	248486894	248487899	
0,55	0,01033198	OR10A4	ENST00000379829	ENST00000379829 // ENSEMBL // cdna:known chromosome:GRCh3	chr11	6897856	6898850	
0,62	0,01408666	BPESC1	NR_026783	NR_026783 // RefSeq // Homo sapiens blepharophimosis, epicant	chr3	138823027	138844009	

Table 33: Downregulated transcripts of PBMCs treated for six hours with recombinant GDF-15(R&D-Systems)

PBMC 6h rhGDF-15_ctrl							
Downregulated transcripts							
log FC	FDR	Symbol	Gene	mRNA	Chromosome	Start	Stop
-0,82	3,5968E-06	SCARNA4	NR_003005	NR_003005 // RefSeq // Homo sapiens small Cajal body-specific RNA 4	chr1	155895749	155895877
-0,62	0,00774903	IGKV1D-43	ENST00000468879	ENST00000468879 // ENSEMBL // cdna:known chromosome:GRCh38	chr2	90248739	90249395
-0,57	0,04022937	MIR3189	NR_036156	NR_036156 // RefSeq // Homo sapiens microRNA 3189 (MIR3189), r	chr19	18497372	18497444
-0,71	0,00020609	MIR4308	NR_036194	NR_036194 // RefSeq // Homo sapiens microRNA 4308 (MIR4308), r	chr14	55344831	55344911
-0,66	0,00278387	MIR4443	NR_039645	NR_039645 // RefSeq // Homo sapiens microRNA 4443 (MIR4443), r	chr3	48238054	48238106
-0,66	0,00155982	MIR188	NR_029708	NR_029708 // RefSeq // Homo sapiens microRNA 188 (MIR188), mi	chrX	49768109	49768194
-0,77	2,0037E-05	FAM218A	NM_153027	NM_153027 // RefSeq // Homo sapiens family with sequence simil	chr4	165878100	165880274
-0,59	0,03153807	PSORS1C3	NR_026816	NR_026816 // RefSeq // Homo sapiens psoriasis susceptibility 1 car	chr6	31141512	31145676
-0,62	0,00944506	IFIT2	NM_001547	NM_001547 // RefSeq // Homo sapiens interferon-induced protein	chr10	91061706	91069033
-0,69	0,00054761	IFNG	NM_000619	NM_000619 // RefSeq // Homo sapiens interferon, gamma (IFNG),	chr12	68548548	68553527
-1,45	1,0084E-22	IGHD3-16	ENST00000390577	ENST00000390577 // ENSEMBL // cdna:known chromosome:GRCh38	chr14	106361492	106361528

Table 34: Upregulated transcripts of PBMCs treated for 24 hours with recombinant GDF-15 (R&D-Systems)

PBMC 24h rhGDF-15_ctrl							
Upregulated transcripts							
log FC	FDR	Symbol	Gene	mRNA	Chromosome	Start	Stop
1,72	1,4546E-31	IGHD3-10	ENST00000390583	ENST00000390583 // ENSEMBL // cdna:known chromosome:GRCh38	chr14	106370355	106370385
0,63	0,01046782	LRR3C	NM_001195545	NM_001195545 // RefSeq // Homo sapiens leucine rich repeat cont	chr17	38097727	38100987
0,86	2,8797E-05	RNU1-12P	ENST00000365194	ENST00000365194 // ENSEMBL // ncna:snRNA chromosome:GRCh38	chr1	147860642	147860803
0,86	2,6122E-05	RNU1-13P	ENST00000384499	ENST00000384499 // ENSEMBL // ncna:snRNA chromosome:GRCh38	chr1	143673129	143673290
0,59	0,04845273	RN5549	ENST00000516450	ENST00000516450 // ENSEMBL // ncna:rRNA chromosome:GRCh37	chr1	63652007	63652121
0,61	0,01929214	RN55329	ENST00000365277	ENST00000365277 // ENSEMBL // ncna:rRNA chromosome:GRCh37	chr11	6038226	6038344
0,62	0,01344175	TP1P3	NR_027338	NR_027338 // RefSeq // Homo sapiens triosephosphate isomerase	chr6	116359894	116361107
0,73	0,00022538	RN55438	ENST00000516561	ENST00000516561 // ENSEMBL // ncna:rRNA chromosome:GRCh37	chr17	32447075	32447186
0,61	0,01736291	MIR668	NR_030408	NR_030408 // RefSeq // Homo sapiens microRNA 668 (MIR668), mi	chr14	101521595	101521660
0,7	0,00081981	LOC1720	NR_033423	NR_033423 // RefSeq // Homo sapiens dihydrofolate reductase pse	chr2	83083927	83084893

Table 35: Downregulated transcripts of PBMCs treated for 24hours with recombinant GDF-15 (R&D-Systems)

PBMC 24h rhGDF-15_ctrl							
Downregulated transcripts							
log FC	FDR	Symbol	Gene	mRNA	Chromosome	Start	Stop
-1,25	5,267E-16	SCARNA3	NR_002998	NR_002998 // RefSeq // Homo sapiens small Cajal body-specific RN	chr1	175937533	175937676
-2,35	2,5759E-59	SNORA2A	NR_002950	NR_002950 // RefSeq // Homo sapiens small nucleolar RNA, H/ACA	chr12	49050431	49050565
-0,63	0,00976311	NRARP	NM_001004354	NM_001004354 // RefSeq // Homo sapiens NOTCH-regulated ankyr	chr9	140194083	140196703
-0,6	0,02103293	MIR4456	NR_039661	NR_039661 // RefSeq // Homo sapiens microRNA 4456 (MIR4456), r	chr5	535955	535997
-0,6	0,03255464	MIR3662	NR_037435	NR_037435 // RefSeq // Homo sapiens microRNA 3662 (MIR3662), r	chr6	135300476	135300570
-0,7	0,00062106	MIR3666	NR_037439	NR_037439 // RefSeq // Homo sapiens microRNA 3666 (MIR3666), r	chr7	114293400	114293510
-0,6	0,02146283	MIR124-2	NR_029669	NR_029669 // RefSeq // Homo sapiens microRNA 124-2 (MIR124-2)	chr8	65291706	65291814
-0,65	0,00395116	KANSL1-AS1	NR_034172	NR_034172 // RefSeq // Homo sapiens KANSL1 antisense RNA 1 (nchr17_ctg5_hap	chr17	592236	595386
-0,59	0,04606536	SIDT1-AS1	ENST00000462180	ENST00000462180 // ENSEMBL // cdna:putative chromosome:GRCh38	chr3	113307595	113309036
-0,76	0,00010524	OR10A4	ENST00000379829	ENST00000379829 // ENSEMBL // cdna:known chromosome:GRCh38	chr11	6897856	6898850
-0,64	0,00772518	OR7G2	NM_001005193	NM_001005193 // RefSeq // Homo sapiens olfactory receptor, fami	chr19	9212945	9213982
-0,66	0,00620013	OPCML-IT2	ENST00000533260	ENST00000533260 // ENSEMBL // havana:sense_intronic chromoso	chr11	132729140	132729972

Table 36: Upregulated transcripts of HUVECs treated for six hours with recombinant GDF-15 (R&D-Systems)

HUVEC 6h rhGDF-15_ctrl							
Upregulated transcripts							
log FC	FDR	Symbol	Gene	mRNA	Chromosome	Start	Stop
0,87	7,5707E-07	SPINT3	NM_006652	NM_006652 // RefSeq // Homo sapiens serine peptidase inhibitor,	chr20	44141101	44144264
0,58	0,05566055	SLITRK1	NM_052910	NM_052910 // RefSeq // Homo sapiens SLIT and NTRK-like family,	chr13	84451340	84456528
0,58	0,04799373	OR2G3	NM_00100191	NM_00100191 // RefSeq // Homo sapiens olfactory receptor, fami	chr1	247768856	247769847
0,63	0,01061762	IGLV3-27	ENST00000390304	// ENSEMBL // cdna:known chromosome:GRCh3	chr22	23010758	23011276
0,65	0,00760766	OR52N5	ENST00000317093	// ENSEMBL // cdna:known chromosome:GRCh3	chr11	5798864	5799897
0,61	0,02591484	OR56A5	NM_001146033	// RefSeq // Homo sapiens olfactory receptor, fami	chr11	5988783	5989724
0,6	0,02719129	C6orf47	NM_021184	// RefSeq // Homo sapiens chromosome 6 open reading fr	chr6_qbl_hap6	2919712	2922186
0,6	0,02761223	C6orf47	NM_021184	// RefSeq // Homo sapiens chromosome 6 open reading fr	chr6_ssto_hap7	2956873	2959347
0,94	2,1539E-08	RNY4	NR_004393	// RefSeq // Homo sapiens RNA, Ro-associated Y4 (RNY	chr6	80451636	80451669
0,62	0,02550134	LINC00545	ENST00000440633	// ENSEMBL // havana:lincRNA chromosome:GR	chr13	31456688	31457532
0,68	0,00308428	SNAP47-IT1	ENST00000413347	// ENSEMBL // havana:sense intronic chromoso	chr1	227931532	227934892
0,61	0,02328954	FLJ42102	NR_038862	// RefSeq // Homo sapiens uncharacterized LOC399923	chr11	71116792	71134400
0,72	0,00042525	FLJ33065	NR_033965	// RefSeq // Homo sapiens uncharacterized LOC440952	chr3	40214638	40351189

Table 37: Downregulated transcripts of HUVECs treated for six hours with recombinant GDF-15 (R&D-Systems)

HUVEC 6h rhGDF-15_ctrl							
Downregulated transcripts							
log FC	FDR	Symbol	Gene	mRNA	Chromosome	Start	Stop
-0,92	1,677E-07	BLID	NM_001001786	// RefSeq // Homo sapiens BH3-like motif containi	chr11	121986062	121986923
-0,75	0,00016235	HCG4B	NR_001317	// RefSeq // Homo sapiens HLA complex group 4B (non	chr6_mann_hap	1186623	1187678
-0,73	0,00045054	HCG4B	NR_001317	// RefSeq // Homo sapiens HLA complex group 4B (non	chr6_ssto_hap7	1223623	1224684
-0,73	0,00296169	CD44	ENST00000528922	// ENSEMBL // cdna:putative chromosome:GRCh	chr11	35218709	35220102
-0,68	5,4548E-05	MIR765	NR_030527	// RefSeq // Homo sapiens microRNA 765 (MIR765), mi	chr1	156905923	156906036
-0,65	0,00852196	RN55465	ENST00000391195	// ENSEMBL // ncrna:rRNA chromosome:GRCh37	chr19	12138728	12138836
-0,6	0,03956776	RN55165	ENST00000517142	// ENSEMBL // ncrna:rRNA chromosome:GRCh37	chr4	148666454	148666568
-0,81	1,2567E-05	SNORD114-2	NR_003222	// RefSeq // Homo sapiens small nucleolar RNA, C/D bc	chr14	101456428	101456497
-0,63	0,01131375	SNORD18B	NR_002442	// RefSeq // Homo sapiens small nucleolar RNA, C/D bc	chr15	66794358	66794429

Table 38: Upregulated transcripts of HUVECs treated for 24 hours with rhGDF-15 (R&D-Systems)

HUVEC 24h rhGDF-15_ctrl							
Upregulated transcripts							
log FC	FDR	Symbol	Gene	mRNA	Chromosome	Start	Stop
0,61	0,04464764	SLITRK1	NM_052910	// RefSeq // Homo sapiens SLIT and NTRK-like family,	chr13	84451340	84456528
0,63	0,03439017	OR5V1	NM_030876	// RefSeq // Homo sapiens olfactory receptor, family 5	chr6_mcf_hap5	626641	627688
0,63	0,02748337	OR8B12	NM_001005195	// RefSeq // Homo sapiens olfactory receptor, fami	chr11	124412578	124413575
0,68	0,00962336	TAS2R8	BC096701	// GenBank // Homo sapiens taste receptor, type 2, men	chr12	10958650	10959892
0,8	8,8763E-05	MIR99A	NR_029514	// RefSeq // Homo sapiens microRNA 99a (MIR99A), mi	chr21	17911409	17911489
0,63	0,02441537	SNORA72	NR_002581	// RefSeq // Homo sapiens small nucleolar RNA, H/ACA	chr8	99054314	99054445
0,62	0,03637279	HCP5	NR_040662	// RefSeq // Homo sapiens HLA complex P5 (non-prote	chr6_mcf_hap5	2811904	2813367
0,66	0,01796958	FLJ33065	ENST00000363973	// ENSEMBL // ncrna:misc_RNA chromosome:GR	chr3	136307051	136307153
0,69	0,00388722	RN55105	ENST00000391123	// ENSEMBL // ncrna:rRNA chromosome:GRCh37	chr2	138269668	138269780
0,63	0,02541741	RN55505	ENST00000364748	// ENSEMBL // ncrna:rRNA chromosome:GRCh37	chrX	53935488	53935595

Table 39: Downregulated transcripts of HUVECs treated for 24hours with rhGDF-15 (R&D-Systems)

HUVEC 24h rhGDF-15_ctrl							
Downregulated transcripts							
log FC	FDR	Symbol	Gene	mRNA	Chromosome	Start	Stop
-0,61	0,0407614	OR1K1	NM_080859	// RefSeq // Homo sapiens olfactory receptor, family 1	chr9	125562370	125563395
-0,84	1,3763E-05	SNORD56B	NR_001276	// RefSeq // Homo sapiens small nucleolar RNA, C/D bc	chr14	71865054	71865124
-0,66	0,00934067	IGLV3-27	ENST00000390304	// ENSEMBL // cdna:known chromosome:GRCh3	chr22	23010758	23011276
-0,7	0,00266864	MIR493	NR_030172	// RefSeq // Homo sapiens microRNA 493 (MIR493), mi	chr14	101335397	101335485
-0,68	0,02302805	MIR548W	NR_036146	// RefSeq // Homo sapiens microRNA 548w (MIR548W), mi	chr17	60798858	61268734
-0,66	0,0158322	MIR548AA2	ENST00000384955	// ENSEMBL // ncrna:miRNA chromosome:GRCh3	chr17	65467605	65467701
-0,65	0,01870367	RNU7-3P	ENST00000516435	// ENSEMBL // ncrna:snRNA chromosome:GRCh3	chr6	149838092	149838153
-0,65	0,01090682	LINC00420	ENST00000443554	// ENSEMBL // havana:lincRNA chromosome:GR	chr13	19982182	19983669
-0,64	0,02342578	DKFZP586I14	NR_002186	// RefSeq // Homo sapiens uncharacterized protein DK	chr7	30409666	30412410
-0,65	0,01161706	CN5H6.4	NR_024009	// RefSeq // Homo sapiens uncharacterized LOC150384	chr22	46691040	46692557

Table 40: Upregulated transcripts of HUVECs treated for six hours with HEK-GDF-15

PBMC 6h HEK-GDF-15_HEK-SN							
Upregulated transcripts							
log FC	FDR	Symbol	Gene	mRNA	Chromosome	Start	Stop
0,79	0,00264608	OR7G3	NM_001001958	NM_001001958 // RefSeq // Homo sapiens olfactory receptor, fam	chr19	9236688	9237626
0,76	0,00372418	HIST3H3	NM_003493	NM_003493 // RefSeq // Homo sapiens histone cluster 3, H3 (HIST3	chr1	228612539	228613074
1,29	1,3633E-11	SCARNA3	NR_002998	NR_002998 // RefSeq // Homo sapiens small Cajal body-specific RN	chr1	175937533	175937676
0,84	0,00060882	MIR4740	NR_039894	NR_039894 // RefSeq // Homo sapiens microRNA 4740 (MIR4740), r	chr17	79374516	79374578
0,73	0,0212929	MIR197	NR_029583	NR_029583 // RefSeq // Homo sapiens microRNA 197 (MIR197), mi	chr1	110141513	110141593
0,75	0,0080074	MIR3945	NR_037510	NR_037510 // RefSeq // Homo sapiens microRNA 3945 (MIR3945), r	chr4	185772167	185772264
0,71	0,01828178	MIR182	NR_029614	NR_029614 // RefSeq // Homo sapiens microRNA 182 (MIR182), mi	chr7	129410223	129410332
1,4	1,3137E-14	MIR1208	NR_031613	NR_031613 // RefSeq // Homo sapiens microRNA 1208 (MIR1208), r	chr8	129162362	129162434
0,86	0,00010776	MIR3074	NR_036109	NR_036109 // RefSeq // Homo sapiens microRNA 3074 (MIR3074), r	chr9	97848296	97848376
2,61	9,8956E-53	SNORA2A	NR_002950	NR_002950 // RefSeq // Homo sapiens small nucleolar RNA, H/ACA	chr12	49050431	49050565
0,68	0,03375834	LOC401557	NR_046107	NR_046107 // RefSeq // Homo sapiens uncharacterized LOC401557	chr9	138073455	138079152
0,82	0,00065104	FRBV25OR9-2	ENST0000043817	ENST0000043817 // ENSEMBL // cdna:known chromosome:GRCh3	chr9	33662188	33662660
0,82	0,00054808	RNS5162	ENST00000516014	ENST00000516014 // ENSEMBL // ncrna:rRNA chromosome:GRCh37	chr4	57197343	57197383
1,3	7,9866E-13	LINC00501	ENST00000425388	ENST00000425388 // ENSEMBL // havana:lincRNA chromosome:GR	chr3	177012230	177041206

Table 41: Downregulated transcripts of HUVECs treated for six hours with HEK-GDF-15

PBMC 6h HEK-GDF-15_HEK-SN							
Downregulated transcripts							
log FC	FDR	Symbol	Gene	mRNA	Chromosome	Start	Stop
-0,69	0,03536784	OR2B3	NM_001005226	NM_001005226 // RefSeq // Homo sapiens olfactory receptor, fam	chr6_qbl_hap6	357384	358489
-0,77	0,00937977	MIR320E	NR_036157	NR_036157 // RefSeq // Homo sapiens microRNA 320e (MIR320E), r	chr19	47212541	47212607
-0,78	0,02756574	MIR4449	NR_039651	NR_039651 // RefSeq // Homo sapiens microRNA 4449 (MIR4449), r	chr4	53578849	53578914
-0,68	0,03754775	MIR105-1	NR_029521	NR_029521 // RefSeq // Homo sapiens microRNA 105-1 (MIR105-1)	chrX	151560691	151560771
-0,76	0,00335663	MIR4733	NR_039886	NR_039886 // RefSeq // Homo sapiens microRNA 4733 (MIR4733), r	chr17	29421368	29421443
-0,74	0,01883533	RNY5	NR_001571	NR_001571 // RefSeq // Homo sapiens RNA, Ro-associated Y5 (RNY	chr12	45580874	45581252

Table 42: Upregulated transcripts of HUVECs treated for six hours with HEK-GDF-15

PBMC 24h HEK-GDF-15_HEK-SN							
Upregulated transcripts							
log FC	FDR	Symbol	Gene	mRNA	Chromosome	Start	Stop
0,8	0,00098935	MIR4287	NR_036249	NR_036249 // RefSeq // Homo sapiens microRNA 4287 (MIR4287), r	chr8	27743556	27743633
0,75	0,00452943	MIR1827	ENST00000408549	ENST00000408549 // ENSEMBL // ncrna:miRNA chromosome:GRCh	chr15	78330872	78330937
1,12	5,3636E-09	MIR4434	NR_039633	NR_039633 // RefSeq // Homo sapiens microRNA 4434 (MIR4434), r	chr2	64752647	64752699
0,69	0,03064097	IMMP2L-IT1	ENST00000451832	ENST00000451832 // ENSEMBL // havana:sense_intronic chromoso	chr7	110364215	110365881

Table 43: Downregulated transcripts of HUVECs treated for six hours with HEK-GDF-15

PBMC 24h HEK-GDF-15_HEK-SN							
Downregulated transcripts							
log FC	FDR	Symbol	Gene	mRNA	Chromosome	Start	Stop
-0,8	0,00318969	MIR548W	NR_036146	NR_036146 // RefSeq // Homo sapiens microRNA 548w (MIR548W)	chr17	60798858	61268734
-0,83	0,00028172	MIR4774	NR_039933	NR_039933 // RefSeq // Homo sapiens microRNA 4774 (MIR4774), r	chr2	169439453	169439528
-0,73	0,01500178	MIR561	NR_030287	NR_030287 // RefSeq // Homo sapiens microRNA 561 (MIR561), mi	chr2	189162219	189162315
-0,76	0,00258041	MIR576	ENST00000385253	ENST00000385253 // ENSEMBL // ncrna:miRNA chromosome:GRCh	chr4	110409854	110409951
-0,89	4,0844E-05	MIR548E	ENST00000408287	ENST00000408287 // ENSEMBL // ncrna:miRNA chromosome:GRCh	chr10	112748684	112748771
-0,75	0,00982347	RNY4	NR_004393	NR_004393 // RefSeq // Homo sapiens RNA, Ro-associated Y4 (RNY	chr6	80451636	80451669
-0,69	0,02056594	RNU1-24P	ENST00000364285	ENST00000364285 // ENSEMBL // ncrna:snRNA chromosome:GRCh	chr13	102431234	102431398
-1,25	5,644E-12	IGHD3-16	ENST00000390577	ENST00000390577 // ENSEMBL // cdna:known chromosome:GRCh3	chr14	106361492	106361528
-0,71	0,01200196	EEF1B2P1	ENST00000443885	ENST00000443885 // ENSEMBL // cdna:known chromosome:GRCh3	chr15	52797386	52798060

To summarize these preselected microarray data, a comparative analysis has been performed in order to see overlapping gene expression patterns within the different samples. This should reveal a conserved pathway initiated by GDF-15. Surprisingly, very little overlap could be observed, except of transcripts of the olfactory receptor gene family.

3.2.5 In vitro scratch assay

Today, in several publications GDF-15 is described as a cancer promoting factor. Staff et al. reported that GDF-15 correlates with metastasis in endometrial cancer (Staff, Trovik et al., 2011). Furthermore, Bruzzese and colleagues could demonstrate that an overexpression of GDF-15 in fibroblasts drives forth proliferation and migration of prostate cancer cells (Bruzzese et al., 2014). In order to study effects of GDF-15 on the migration of tumor cells *in vitro*, an in vitro scratch assay, also known as “*wound healing assay*” was performed according to a published nature protocol (Liang, Park et al., 2007). A MCF-7 breast cancer cell line was utilized due to their low endogenous GDF-15 expression. These cells were stably transfected with a vector encoding human GDF-15 (pIRES-full-length-GDF-15-eGFP-reporter construct) as well as a control reporter construct (pIRES-empty-eGFP-reporter construct). Stable transfection of the vector was monitored by eGFP-expression using flow cytometry (figure 3-2-5a). Since the partially disabled IRES sequence leads to a reduced eGFP expression compared to the transcripts of the cloned gene of interest (according to the manufacturer protocol), the expression of the target protein GDF-15 was assessed indirectly by the GFP positive MCF-7 cells. The scratch size was measured daily for a period of 4 days after pictures had been taken using of a microscope compatible camera. We observed a similar wound closure pattern when comparing MCF-7 cells transfected with the empty pIRES-eGFP-vector with the MCF-7 cells overexpressing GDF-15. This observation indicates that GDF-15 has no tumor proliferating effect on this particular cell line *in vitro*. The antagonization of GDF-15 with a neutralizing GDF-15 antibody (B1-23, further described in section 3.4) had no effect on the migration of tumor cells, when compared to untreated MCF-7 cells (figure 3-2-5). The difference in wound healing was less than 2 % when using 2 µg /ml of the GDF-15 binding antibody B1-23 compared to untreated MCF-7 cells (ctrl: 12.11 % +/- 1.04, B1-23: 12.76 % +/- 1.63 after 24 hours. ctrl: 28.68 % +/- 1.63, B1-23: 29.28 % +/- 2.67 after 96 hours).

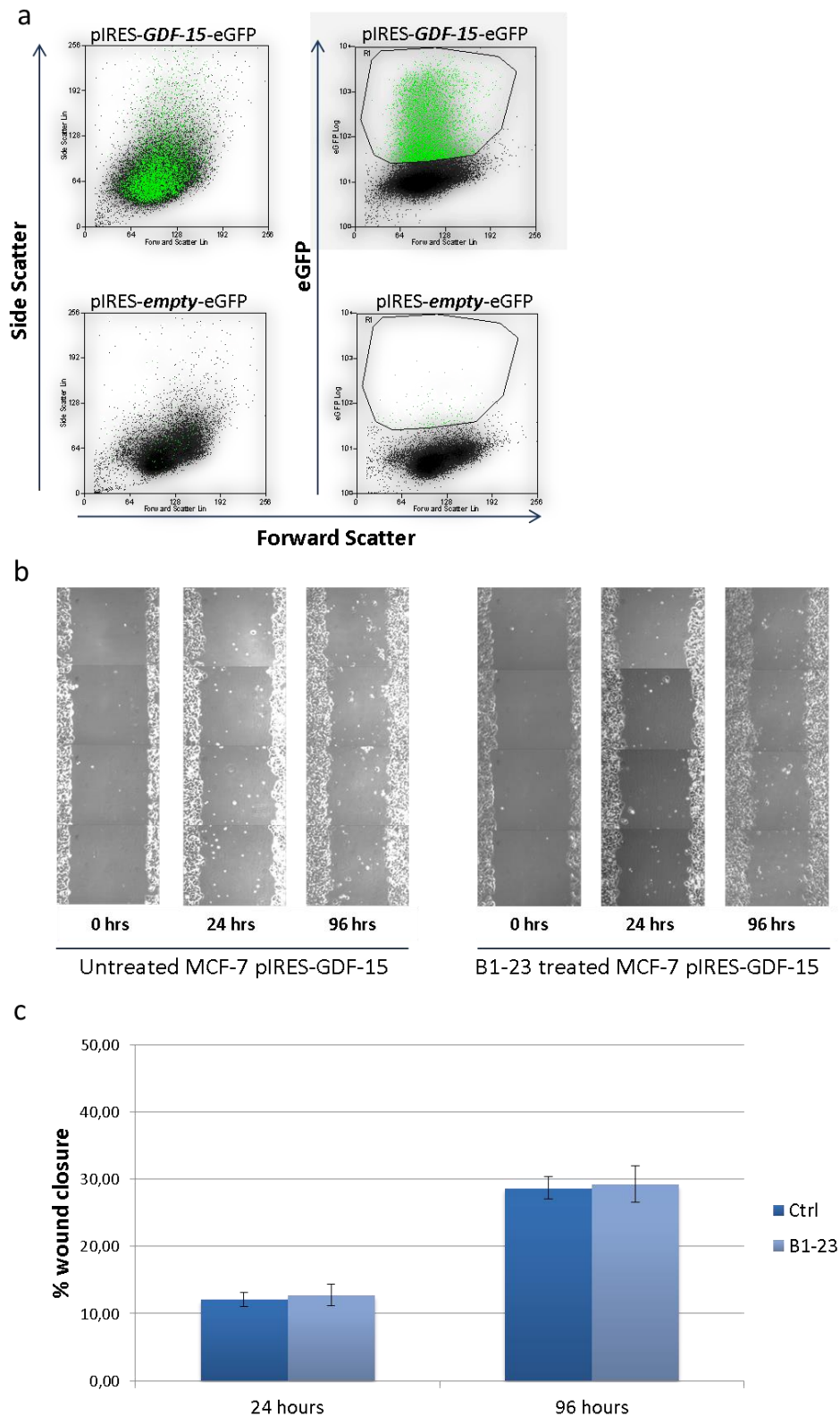


Figure 3-2-5: *In vitro* scratch assay with a GDF-15 overexpressing MCF-7 breast cancer cell line

a) GDF-15 expression was measured indirectly by eGFP positive MCF-7 breast cancer cells using flow cytometry. Green fluorescence positive cells (pool) were used for the wound healing assay. Empty vector transfected MCF-7 cells served as an internal control for transfection efficacy. b) Wound healing of GDF-15 expressing MCF-7 cells, treated with 2 $\mu\text{g/ml}$ B1-23 or left untreated, was observed for 96 hours. Snapshots were taken on day 0, 1 and 4 and analyzed using the image J software. c) % Wound closure represents the % change of the scratch area to the starting point at 0 hrs. The scratches were quantified for each snapshot (four snapshots were taken for each well and point of time, according edges were realigned using Adobe photoshop).

3.3 GDF-15 knock down leads to prolonged survival in mice bearing glioma

[The following section shows one data set published by Roth, Junker,...Wischhusen (Clin.Canc.Res 2010). The *in vivo* experiment shown here has been performed by Dr. Patrick Roth. It is necessary to show this key experiment at this point of my thesis, since it illustrates the relevance of the target protein GDF-15 and explains why the main focus of the underlying thesis was the generation of a monoclonal anti-GDF-15 antibody, followed by its *in vitro*-, *in vivo* validation, characterization and preclinical development].

The question, whether GDF-15 is just a biomarker or mediates tumor progression should be answered in an *in vivo* approach using the following syngenic glioma mouse model. The SMA-560 astroglioma cell line was stably transfected with a short hairpin RNA construct, directed against mouse GDF-15. The control SMA-560 cells as well as the GDF-15 knockdown cells were injected intracerebrally into mice of the same genetic background (VM/Dk-mice) and survival of the animals was observed. Mice bearing the pSUPER-GDF-15 mediated knock-down cells survived about 40 % longer than the mice injected with the pSUPER-control cells (figure 3-3-1a). To confirm the knock down of GDF-15 prior to tumor inoculation, a Western Blot was performed, revealing the efficient knock down of mouse GDF-15 in the respective shGDF-15 glioma cell line. The prolonged survival of animals carrying the GDF-15 deficient tumor cells led to the conclusion that GDF-15 has a malignant effect on tumor progression in brain cancers.

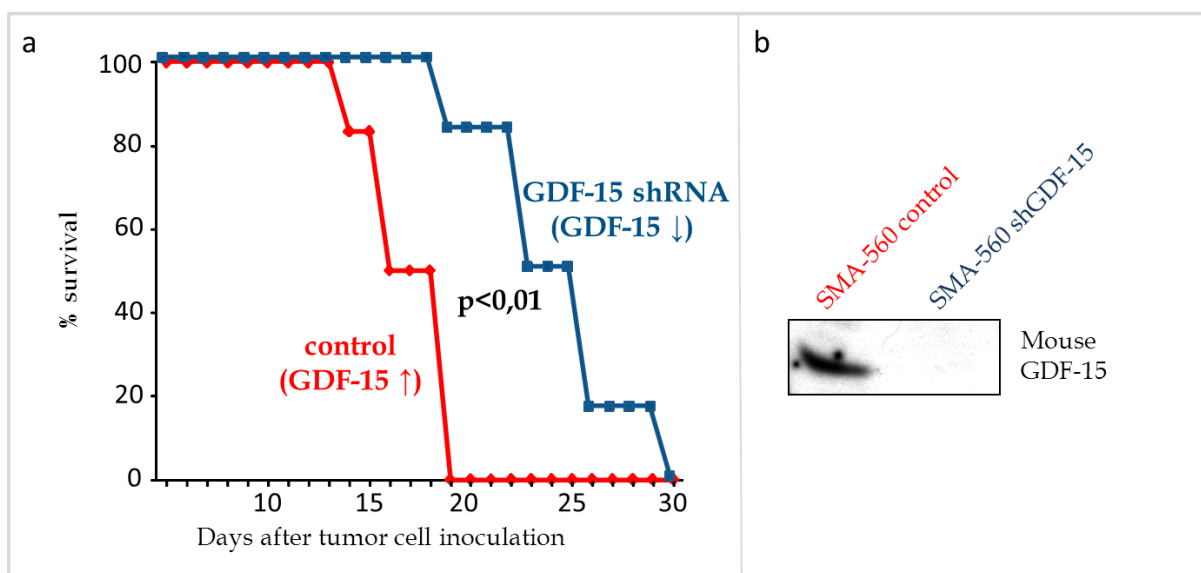


Figure 3-3-1: Kaplan Meier plot of tumor cell bearing mice with pSUPER-control and pSUPER-GDF-15 knock down construct

a) SMA-560 control or shGDF-15 transfected cells were inoculated intracerebrally in syngenic VM/Dk mice. Survival data for six animals per group were presented as Kaplan-Meier plot. b) Mouse GDF-15 protein amount in SMA-560 control cells and shGDF-15 cells were analyzed by Western Blotting. The graphically depicted *in vivo* results were adapted from figure 4 published in Clin Cancer Res. (Roth, Junker et al., 2010). The

experiment was performed and kindly provided by Dr. Patrick Roth, USZ Zürich. The Knock-down cells (SMA-560shGDF-15) were a kind gift of Dr. Jörg Wischhusen.

When comparing the presence of T cells and macrophages in the glioma tissues of the sacrificed animals, GDF-15 knock down tumors could be shown to be infiltrated by T cells, whereas the GDF-15 expressing control tumors were lacking these immune effector cells (figure 3-3-2). Macrophages were also observed within the GDF-15 deficient tumors, even if to a far lesser degree than the T cells.

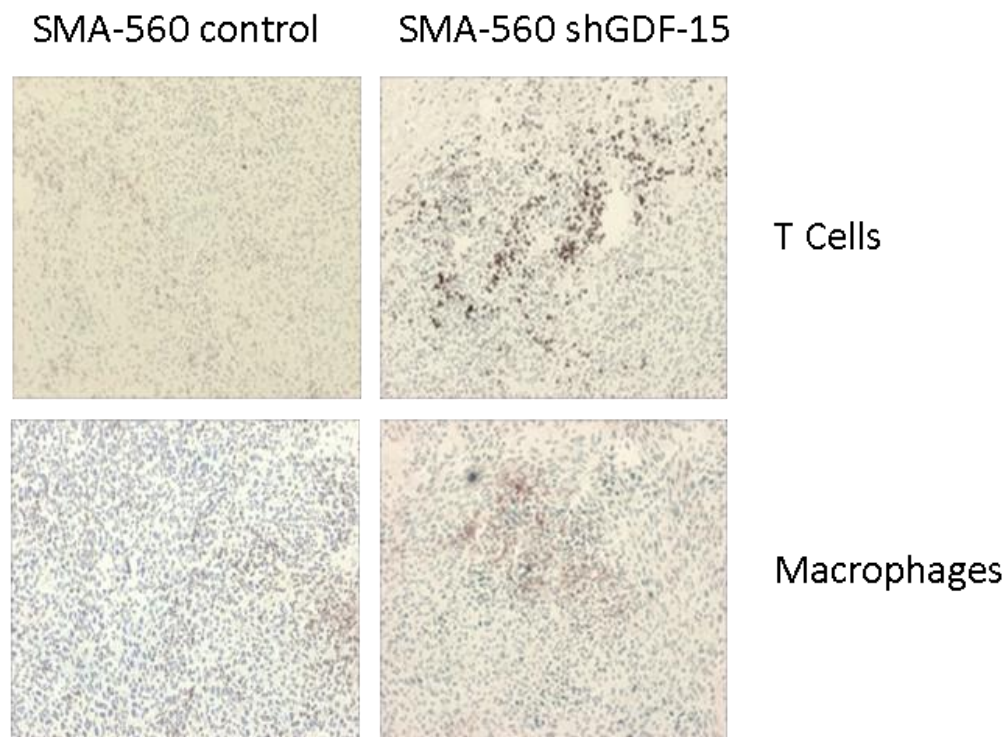


Figure 3-3-2: Immune cell infiltration in mouse glioma tissue sections FFPE sections

Mice bearing GDF-15 knock-down tumors were analyzed immunohistochemically for immune cell infiltration. T cells were highly infiltrated in the microenvironment of GDF-15 deficient tumors. Macrophage infiltration was also enhanced compared the GDF-15 expressing glioma tissue. (Figure adapted from Roth, Junker, et al. Clinical Cancer Research, 2010). (Roth, Junker et al., 2010) The experiment was performed and kindly provided by Dr. Patrick Roth, USZ Zürich.

3.4 Generation and characterization of monoclonal anti-GDF-15 antibodies

There are several reasons why GDF-15 represents a valuable cancer target rationalizing the development of a neutralizing antibody for a possible clinical application:

- 1) The amount of GDF-15 in tumor patients correlates with tumorigenicity (Boyle, Pedley et al., 2009) [gastric-cancer] and a poor prognosis (Brown, Ward et al., 2003, Staff, Trovik et al., 2011) [endometrial cancer, colorectal cancer]
- 2) GDF-15 has been described as a marker for metastasis in uveal melanoma (Suesskind et al., 2012), prostate as well as colon carcinoma (Aw Yong et al., 2014) [skin cancer, prostate cancer, colorectal cancer]
- 3) Own published *in vivo* data (Roth, Junker, Wischhusen, 2010), demonstrating prolonged survival of mice bearing GDF-15 knock down tumor cells [glioma] (see figure 3-3)
- 4) GDF-15 is a soluble factor, which is found in elevated levels in the serum of cancer patients. A GDF-15 binding antibody could possibly block the tumorigenic effects of GDF-15. As a consequence, an anti GDF-15 monoclonal antibody was generated for *in vitro* and *in vivo* application during my PhD thesis.

3.4.1 Confirmation of GDF-15 knock-out animals by PCR

Prior to immunization of GDF-15 knock out mice with recombinant human GDF-15, the genotype of the animals was confirmed by two individual polymerase chain reactions, using specific primer pairs. A typical mouse GDF-15 PCR, which is further described in the material and method section, is represented in figure 3-4-1. Genotyping was performed according to Strelau and colleagues, who generated the GDF-15 deficient animals by insertion of a LacZ cassette, resulting in the deletion of the murine GDF-15 locus (Strelau et al., 2009). Even though the term GDF-15 knock-out mouse is used here, the correct term for a GDF-15 deficient animal would be lacZ / knockin mouse.

Lane 9 and 10 show the verified genotype of a GDF-15 knock-out mouse from the homozygous knock-out breeding. The 690bp PCR product represents the partially amplified lacZ gene, whereas the 320 bp product embodies the wildtype mouse GDF-15 amplicon (figure 3-4-1).

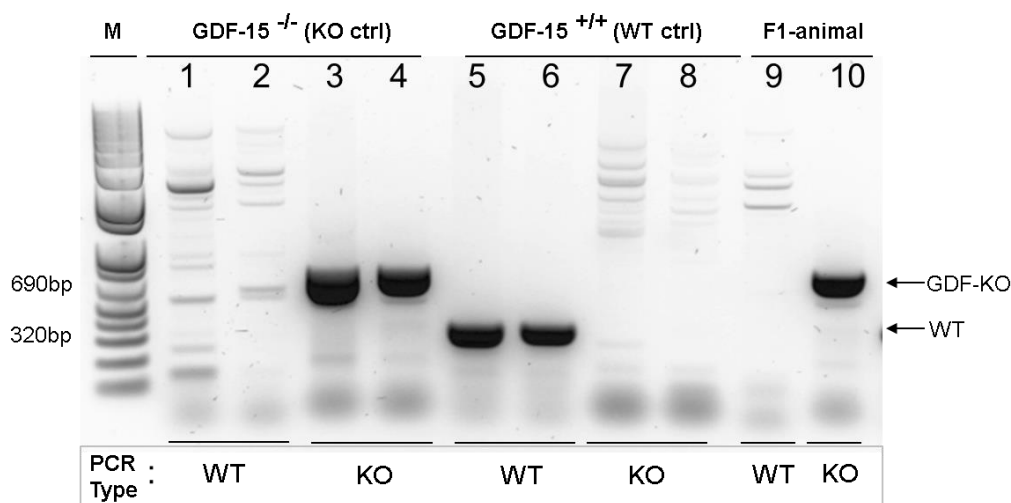


Figure 3-4-1: Genotyping of GDF-15 knock-out animals

The presence or deficiency of wild type genomic mouse GDF-15 was confirmed by PCR with all animals/progenies from the GDF-15-knock-out breeding. PCR products were run on a 1 % TAE DNA gel and visualized by Gelred™ using a gel-illumination device. As positive control for the wild type GDF-15 PCR, genomic DNA from kidney and heart tissue from GDF-15^{+/+} mice were used (lanes 1, 2 and 5, 6). The positive control for the GDF-15 knock-out PCR has been performed with genomic DNA from kidney and heart tissue from GDF-15^{-/-} animals and underwent a different PCR program (shown in the methods section). PCR products on lanes 1, 3, 5, 7 are from genomic DNA derived from kidney, 2, 4, 6, 8 from heart tissue, respectively). Lane 9 and 10 represent the PCR products of genomic DNA obtained from ear clips from an offspring of the GDF-15 knock-out breeding.

3.4.2 Immunization of GDF-15 knock out mice with human GDF-15 resulted in several GDF-15 Abs for further characterization and development

For the generation of monoclonal antibodies to human GDF-15, the standard hybridoma fusion technology described by Milstein and Köhler in 1975 was applied (Köhler and Milstein, 2005). 2000 hybridoma supernatants were screened for GDF-15 positive clones. Screening was performed on a nitrocellulose membrane, which was spotted with recombinant mature GDF-15 (described in detail in methods section). Out of these 2000 clones most of the supernatants gave no or very low signal. A few supernatants appeared with low to moderate signal intensity and less than 10 supernatants emerged as strong GDF-15 binders (figure 3-4-2). Four hybridoma clones (X5H, X7D, X8C and X8G) displaying the highest signal intensities were picked for further subcloning and characterization. The antibodies were named according to their plate letter and well position (e.g. X7D). Initially, X5H showed the strongest GDF-15 signal and consequently served as a positive control on each screening membrane. After the first round of subcloning, the production or the specificity of the antibodies for GDF-15 were lost for the X8 clones (X8C and X8G). The subcloned X7D4 appeared to be a high producing hybridoma clone, binding recombinant mature GDF-15 with

high affinity. X5H2-Hybridoma could be expanded, but after further rounds in culture the antibodies lost its binding capacity to GDF-15 (figure 3-4-2b). The low percentage of monoclonal anti-GDF-15 antibodies from two immunized GDF-15 knock out animals could be explained by the applied conditions of the antibody-“screening procedure”: the incubation of the supernatants was kept very short due to technical limitations (less than 10 seconds). Very stringent washing conditions were applied for the first round of screening. This could have resulted in the appearance of mostly high affinity antibodies. Low affinity binding anti-GDF-15 antibodies could have existed, but have been lost during the screening process.

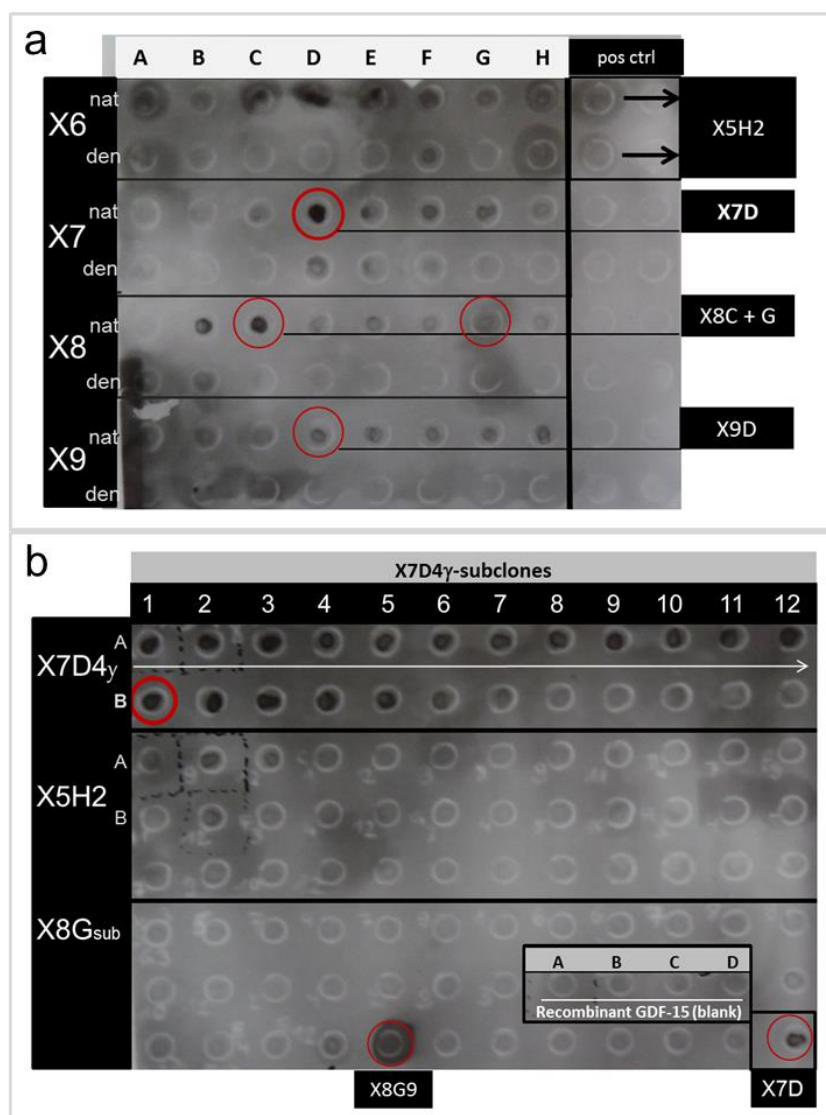


Figure 3-4-2: Screening of GDF-15 antibody producing hybridoma clones

Recombinant human GDF-15 (SF9, provided by Professor Müller) was spotted on a nitrocellulose membrane in its native (nat) and denatured form (den) (each spot contained 20 ng of protein) a) Supernatants of 2000 hybridomas were harvested after 10 days of culture and transferred from a 96 well plate onto the nitrocellulose membrane using a multichannel (12x) pipette. (b) One representative out of 40 second round screening membranes, showing mostly GDF-15 negative or low affinity binding hybridoma supernatants (b). The first and second row shows the binding of subcloned X7D antibodies. The candidate for further preclinical development B1-23 is demarcated with a red circle.

A cloning of X7D4 by the limited dilution method and a further subcloning of X7D4 γ (figure 3-4-2b) finally resulted in the hybridoma clone X7D4 γ -B1-23, which received the short name **B1-23**. This nomenclature is of great importance, since the preclinical development of the anti GDF-15 antibody, which is ongoing in the department of gynecology and obstetrics of the university hospital of wuerzburg is exclusively based on the clone B1-23 and a substantial part of that thesis. The hybridoma cell line B1-23 was deposited at the DSMZ, the 'German Collection of Microorganisms and Cell cultures' under the accession no. *DSM ACC3142* in agreement of the Budapest treaty, followed by a subsequent patent application [PCT/EP2013/070127]: WO2014049087A1.

3.4.3 Antibody production of hybridoma clones

In order to assess the productivity of the antibody expression, supernatants of the selected hybridomas X8G9, X5H2 and B1-23 were analyzed by SDS-PAGE using Coomassie stain (not shown here) and Western Blot analysis (figure 3-4-3). To visualize murine immunoglobulins, an anti-mouse-IgG-(H+L)-HRP-coupled antibody, was used as a secondary antibody. To rule out immunoglobulin background from fetal calf serum, two different culture conditions were applied on the monoclonal hybridoma cultures: 10 % FCS containing RPMI complete (+) and Ig-stripped serum, which is supposed to lack calf immunoglobulins according to the manufacturer protocol (-). The clones X8G9, X5H2 and B1-23 from hybridoma supernatants were compared to supernatants of the myeloma cell line X63AG8.653, which served as an immunoglobulin background control (figure 3-4-3). B1-23 appeared under reducing conditions as two bands, 25 kDa and 50 kDa, representing the light and the heavy chain of the antibody, respectively. We observed one single 25 kDa band using supernatants of the clone X5H2, leading to the conclusion that only the light chain of this type of antibody cross reacted with the secondary anti-mouse IgG antibody, but not the heavy chain. For the clone X8G9 no immunoglobulin signal could be detected, indicating that the respective hybridoma clone stopped producing antibodies in general.

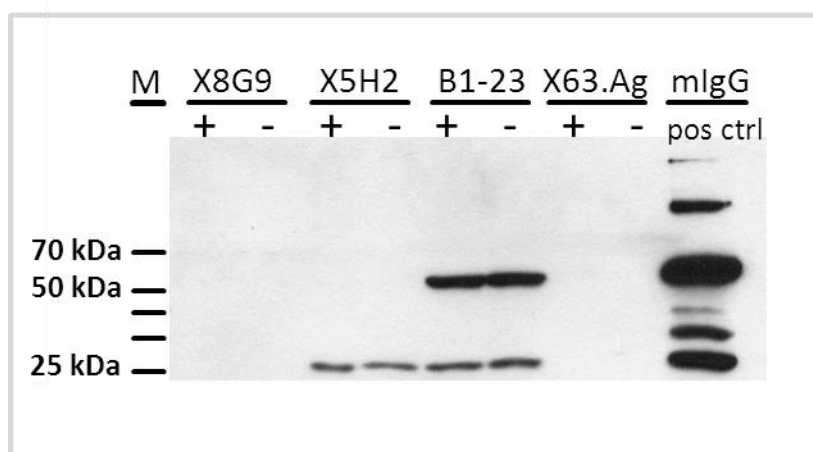


Figure 3-4-3: Heavy and light chains of hybridoma cell derived antibodies

To assess the antibody production of hybridoma cells, a Western Blot analysis has been performed with 10 μ l of hybridoma cell supernatants, cultured for 5 days. The clones X8G9, X5H2, B1-23 were compared to the X63AG8.653 myeloma cell supernatants (X63.Ag). Culture conditions of hybridoma cells: (+) normal fetal calf serum, (-) Ig-stripped fetal calf serum. A mouse IgG antibody was used as positive control (right lane). An anti-mouse IgG (H+L)-HRP conjugated antibody was used for detection of the immunoglobulins.

3.4.4 B1-23 detects GDF-15 under semi-native conditions on Western Blots

Preclinical drug development requires an extensive characterization of a lead candidate as well as the target molecule. Since a variety of different GDF-15 protein forms can be found in supernatants of tumor cells (3-4-3b), we wanted to elucidate, which of these GDF-15 forms were engaged by the antibody B1-23. Consequently, B1-23 was used as a “detection” antibody for human GDF-15 in a Western Blot under semi-native conditions. B1-23 detected recombinant mature GDF-15 dimer at a size of 25 kDa. The calculated molecular weight of the mature GDF-15 monomer is about 12.5 kDa. Moreover, the antibody B1-23 was able to detect several GDF-15 forms in supernatants of HEK293-T cells overexpressing full length GDF-15 (figure 3-4-3a), appearing at the following molecular weights: 25 kDa, 40 kDa and 70 kDa. These protein bands are likely to represent the mature dimeric GDF-15 (25 kDa), the hemi-dimer (40 kDa) and the full length homodimer of GDF-15 (70 kDa) (described in detail in section 1.2). The antibody did not detect recombinant GDF-15 under reducing conditions together with heat-denaturation at 90°C for 10 minutes (not shown). Instead, B1-23 detected all known forms of GDF-15 under non reducing conditions. Since B1-23 was able to recognize recombinant GDF-15 in a semi native SDS-PAGE, the antibody was likely to bind a discontinuous epitope of GDF-15 rather than a linear epitope.

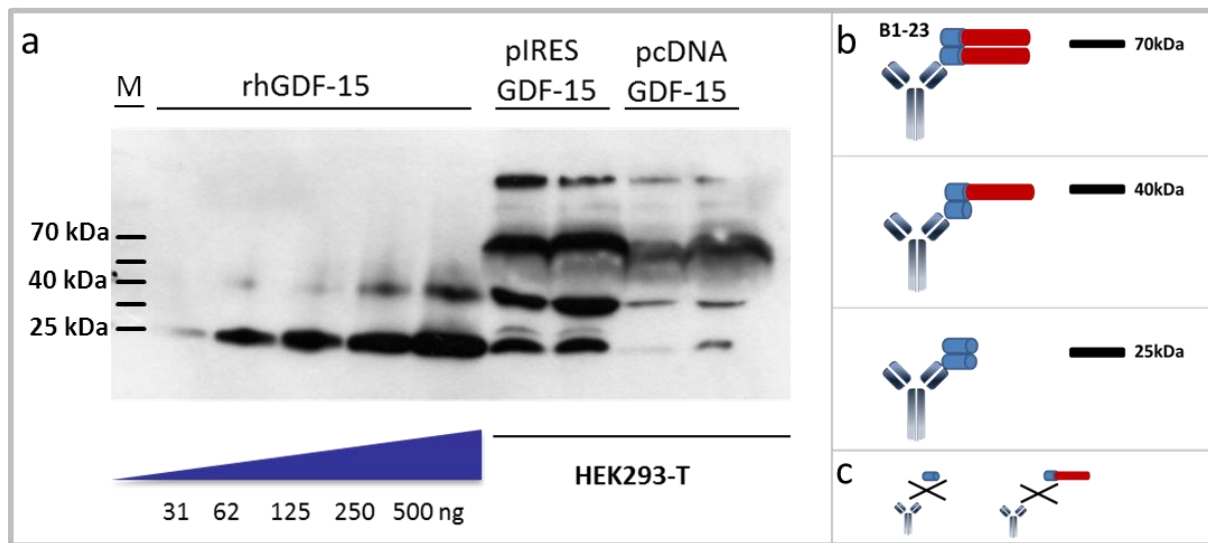


Figure 3-4-4: B1-23 is suitable for WB-detection of recombinant and overexpressed full length GDF-15

a) Western Blot for the detection of human GDF-15 was performed under non reducing conditions. Accordingly, B1-23 detected the increasing amounts of recombinant human GDF-15 (R&D Systems) in lane 1-5 (31ng – 500ng). Moreover, B1-23 recognizes full length human GDF-15 transiently overexpressed in HEK293 T cells using the expression vectors pIRES-hGDF-15-eGFP (lane 6+7) and pcDNA3.1-hGDF-15 (lane 8+9). (b) Schematic: GDF-15 forms and B1-23 detection pattern thereof: B1-23 detects mature dimeric GDF-15 at 25 kDa (blue dimer), the GDF-15 ‘hemi-dimer’ at 40 kDa (blue dimer containing one red precursor protein) and the full length homodimer at about 70 kDa. (c) B1-23 does not detect the monomeric mature GDF-15 or the monomeric full length protein.

3.4.5 Isotyping of B1-23

Human and mouse immunoglobulins exist in different forms of isotypes (IgA, D, G (1,2a, 2b, 3, 4), E, M). Every isotype behaves differently from each other. Large scale production of an antibody requires the information of its isoform, since every isoform requires special purification conditions. For example: an IgM cannot be purified using protein A columns compared to an IgG1 or an IgG2a. It is also crucial to know the isotype of an antibody used for Western Blot staining, since some secondary antibodies specifically bind a sequence of the primary antibody in an isotype specific manner. Isotyping stripes from AbDSerotec and Roche (IsoStrip, mouse monoclonals) were used to identify the B1-23 as a murine IgG2a antibody consisting of the kappa light chain type.

The isotype of two further supernatants of hybridoma cells producing GDF-15 reactive antibodies were tested as well. The candidate X5H2 could be detected as an IgM isotype, which matched the immunoglobulin Western Blot in figure 3-4-2. Whereas the light chains of the pentameric IgM antibody could be detected on a Western Blot, the secondary anti mouse HRP (raised against heavy and light chain) did not cross react with a heavy IgM chain. The isotype of the hybridoma clone X8G9 was also tested. No isotype could be determined, since

the production of antibodies from that specific clone had come to an end and could be confirmed by SDS-PAGE, shown in 3-4-2.

3.4.6 Epitope mapping of B1-23

- *mapping of linear epitopes [Pepperprint GmbH]*

To investigate whether B1-23 binds a continuous epitope within the GDF-15 protein, an epitope mapping for linear epitopes was performed externally by the company Pepperprint GmbH (Heidelberg, Germany). Therefore, a customized chip with spotted peptides of the full length human GDF-15 protein sequence was generated. The 324 linear GDF-15 peptides comprised a length of 13 amino acids, with an overlap of one amino acid. The secondary goat-anti-mouse IgG (H+L) IRDye680 was applied separately as a background control. B1-23 was applied on the peptide array over night at 4°C, followed by the secondary antibody incubation. The arrays were subsequently analyzed using the Odyssey Imaging System. A weak interaction of the arginine-rich peptides (ELHLRPQAARGRR, LHLRPQAARGRRR, HLRPQAARGRRRA, LRPQAARGRRRAR, RPQAARGRRRARA, PQAARGRRRARAR and QAARGRRRARARN) could be observed using the secondary anti-mouse antibody alone. According to the report provided by the company, these sequences and the basic peptide MHAQIKTSLHRLK are known to be frequent binders due to ionic interactions with the charged antibody dye (figure 3-4-5, a). None of the linear 13mer peptides derived from human full length GDF-15 interacted with the monoclonal GDF-15 antibody B1-23, even at overregulated intensities (figure 3-4-5, b). A positive control staining of Flag and HA control peptides that frame the array, resulted in clear and homogeneous spot intensities, demonstrating that no technical problems occurred while the experimental setup and performance.

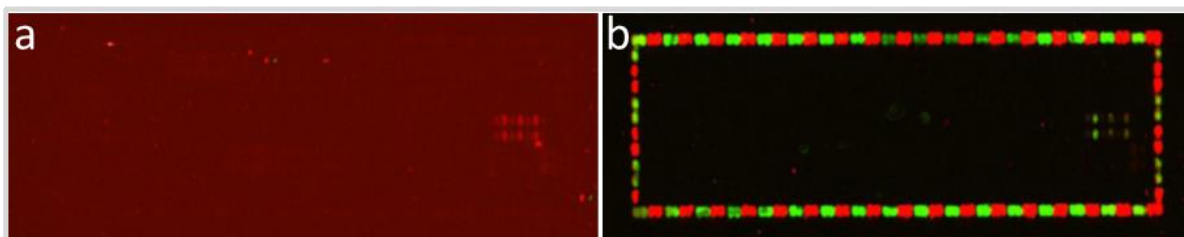


Figure 3-4-5: Linear epitope mapping of full length GDF-15 with anti GDF-15 antibody B1-23

324 linear peptides (13mers) of human GDF-15 were spotted on a microarray. As a blank subtraction, background intensities were analyzed using the secondary goat anti-mouse IgG(H+L) IRDye680 antibody separately (a); B1-23 was subjected to the microarray, followed by staining with the anti-mouse (H+L)-IRDye680 antibody, resulting in no specific signal to the spotted GDF-15 peptides. The green and red spots framing the array comprised HA and Flag control peptides. (The linear epitope mapping data were performed and kindly provided by Pepperprint GmbH, Heidelberg).

The mapping of monoclonal mouse GDF-15 antibody against the human full length GDF-15 did not reveal a single linear epitope with the 13mer peptides derived from the antigen. According to this finding it is likely that B1-23 recognizes a three-dimensional or discontinuous epitope with low or no affinity to linear stretches of the protein.

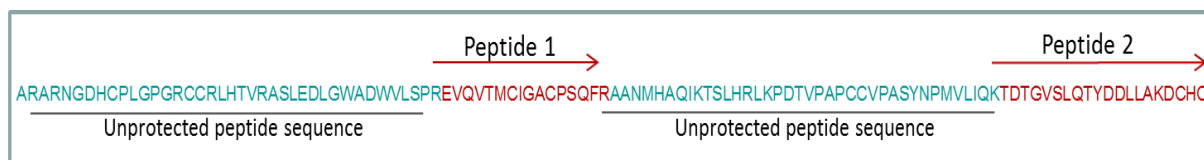
- *mapping of discontinuous epitopes by epitope excision [Steinbeis-Zentrum]*

B1-23 did not bind a continuous linear epitope within the GDF-15 amino acid sequence, as shown in figure 3-4-5. We hypothesized that the interaction between GDF-15 and B1-23 occurred exclusively when GDF-15 maintained its three-dimensional protein conformation. In order to reveal a discontinuous epitope of B1-23 on its target molecule, an epitope excision method was performed externally in collaboration with the Steinbeis-Zentrum Konstanz. Therefore, the immobilized antibody-antigen-complex B1-23-rhGDF-15 was digested with trypsin followed by the elution of the resulting antibody shielded peptides under acidic conditions. Eluates were analyzed using a high resolution spectrometer LC/MS-MS. (Professor Przybilski, Steinbeis-Zentrum Konstanz, for detailed information see methods section, chapter 2). By this method, two peptide stretches of mature human GDF-15 were identified being protected by B1-23, representing the epitope engaged by the antibody:

Peptide sequence 1: **evqvtmcigacpsqfr**

Peptide sequence 2: **tdtgvslqtyddllakdchci**

Table 44 B1-23 interacting peptides 1 and 2 located in the mature GDF-15 sequence



Peptide 1 and peptide 2 (in red) are linked by a peptide sequence, which could not be shielded by B1-23 during tryptic digestion (blue letters). This result demonstrated that the monoclonal antibody B1-23 detects a discontinuous epitope comprising the peptides 1 and 2 listed above and confirmed the missing reactivity of B1-23 to shorter linear epitopes, covering a length of only 13 amino acids (figure 3-4-5).

For further characterization of B1-23, the antibody was produced in a larger scale, culturing the hybridoma cell clone in a CELL-LINE bioreactor (Integra). The resulting antibody titer revealed concentrations between 0.5 mg/ml and 2 mg/ml. These hybridoma cell supernatants, received from the static bioreactor, were harvested in an interval of 5-7 days of culture and affinity purified on protein A columns.

Using the purified and specifically formulated antibody B1-23, functional assays and cytotoxicity tests were performed as shown in the following sections.

3.4.7 Sequence identification of the hypervariable regions of B1-23

To receive the nucleotide sequence of the murine anti GDF-15 antibody B1-23, a proprietary PCR based method described by Wang and colleagues was applied (Wang, Raifu et al., 2000). Thereby, the hypervariable regions and thus the antigen binding site of the antibody B1-23 could be amplified using degenerate primers. These primers had been validated to bind the variable regions of many different mouse IgG2a isotype antibodies. The light chain and heavy chain sequences of the antibody were amplified in individual polymerase chain reactions using cDNA templates from the B1-23-hybridoma RNA (the procedure was described in detail in chapter 2). The resulting PCR products (figure 3-4-6), comprising the complementarity determining regions (CDRs) of the light and heavy chain of the B1-23

antibody were cloned into the clone JET vector (pJET1.2/blunt, Life Technologies), which was then successfully sequenced by GENEART AG (table 45).

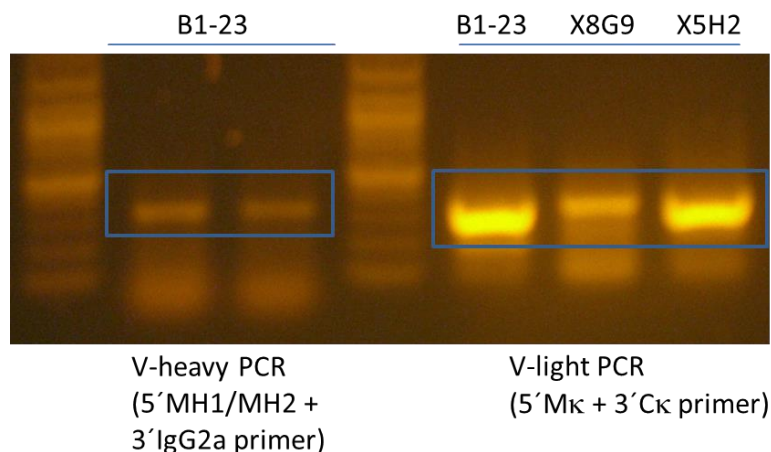


Figure 3-4-6: Amplification of heavy and light chain DNA of hybridoma antibodies

In order to receive the unknown Fab sequences, cDNA of the monoclonal hybridoma cell clones B1-23, X8G9 and X5H2 were PCR-amplified for further cloning into the pJET1.2 vector for sequencing. Therefore, degenerate primers were used for either the light chain (5' M κ + 3' C κ primers) or the heavy chain (5' MH1 + 5' MH2 + 3' IgG2a primers) of murine antigen binding sequences. After the first PCR, the amplified sequences were hardly visible on the DNA gel. Following the protocol for degenerated primers, the PCR product was used for a second PCR, revealing the visible bands, representing the amplified CDRs of the according chains. The heavy chain PCR failed for the hybridoma cell clones X8G9 and X5H2.

Sequence of the **light** chain variable region of B1-23:

```

ATTGGGCTGACACCATATCCATCCGGCGTAATACGACTCACTATAGGGAGAGCGGCCGC
CAGATCTTCCGGATGGCTCGAGTTTTTCAGCAAGATGG-GAG-CTC-GAC-ATT-GTG-CTC-
ACCCAGTCTCCA AAATTCATGTCCACATCAGTAGGAGACAGGGTCAGCGTCACCTGCAAG
GCCAGTCAGAATGTGGGTAATAATGTGGCCTGGTTTCTACAGAAACCAGGGCAATCTCCT
AAAGCACTTATTTACTCGGCATCTACCGGTACAGTGGAGTCCTGATCGCTTCACAGGC
AGTGGATCTGGGACAGATTTCACTCTACCATCAGCAACGTGCAGTCTGAAGACTTGGCA
GAGTATTTCTGTCAGCAATATAACAACCTTTCCGTACACGTTCCGAGGGGGGACCAAGCTG
GAAATAAACCGGGCTGATGCTGCACCAACTGTATCCGCATGCAATCTTTCAATCTTTCTAG
AAGATCTCCTACAATATTCTCAGCTGCCATGGAAAATCGATGTTCTTCTTTTATTCTCTCAAG
ATTTTCAGGCTGTATATTAATAAATTATATTAAGAACTATGCTAACCACTCATCAGGAACCG
TTGTAG

```

Sequence of the **heavy** chain variable region: of B1-23:

```

ATTGTGCTGAACACCATATCCATCCGGCGTAATACGACTCACTATAGGGAGAGCGGCCGC
CAGATCTTCCGGATGGCTCGAGTTTTTCAGCAAGATCTTCCGGAA-TTC-CAA-GTG-AAG-
CTG-CAG-CAG-TCAGGCCCTGGGATATTGCAGTCTCCAGACCCCTAGTCTGACTTGTTTC
TTTCTCTGGGTTTTCACTGAGTACTTCTGGTATGGGTGTGAGCTGGATTCGTCAGCCTTCA
GGAAAGGGTCTGGAGTGGCTGGCACACATTTACTGGGATGATGACAAGCGCTATAACCC
AACCTGAAGAGCCGGCTCACAATCTCCAAGGATCCCTCCAGAAACCAGGTATTCTCAA
GATCACCAGTGTGGACACTGCAGATACTGCCACATACTACTGTGCTCGAAGTTCCTACGG
GGCAATGGACTACTGGGGTCAAGGAACCTCAGTACCCGTCTCTCAGCCAAAAACAACAGC
CCCATCGGTCTATCCACTGGCCCCTGTGTGTGGAGGTACAACTGGCTCTCGGTGACTCTA
GGATGCCTGGTCTAAGAGATCTCCATCTTTCTAGAAGATCTCTACAATATTCTCAGCTGCC
ATGGAAAATCGATGTTCTTCTTTATTCTCTCAAGATTTTCAGGCTGTATATTAAACTTATA
TTATGAACTATGCTAACACCTCATCAGGAACCGTTGTAGGTG

```

Table 45: Sequence of the Fab region of B1-23 after amplification with degenerate primers

(Green) forward primer sequence, (Red) Fab-sequence including 3 complementarity determining regions, comprising CDR1, CDR2, CDR3, which are interconnected with 3 framework sequences (FR1, FR2, FR3). (Black) Framework 1-reverse primer. For the heavy chain variable region the priming sequence is demarcated as a short sequence, since 2 different primer pairs are used (MH1 + MH2).

3.4.8 Chimerization of B1-23

The development of the chimeric anti GDF-15 antibody was an intermediate step prior the humanization of B1-23. The “grafting” of the B1-23-Fab-site on a human IgG1 backbone, done externally by evitria’s proprietary technology, was performed to confirm the cloned hypervariable regions in the antigen binding site of B1-23 as the correct sequence. The functionality of the designated ChimB1-23 was still given, the Fabs of B1-23 (CDRs) were properly integrated into a human IgG1 antibody framework. The resulting chimeric antibody was transiently expressed by evitria and supernatants thereof were tested in regard to their quality and specificity to GDF-15. Three different recombinant GDF-15 batches (B41 [E. coli], SF9B [eukaryotic], R+D-Systems [eukaryotic]) could be detected by the chimeric antibody ChimB1-23, indicating the correct sequence of the antigen binding site of B1-23 (figure 3-4-7). Using the chimeric immunoglobulin resulted in the same staining pattern compared to the origin B1-23, which was used as a positive control. Interestingly, the E. Coli derived GDF-15 (B41) appeared on the SDS-Gel as two distinct bands, one of them representing the expected 25 kDa dimeric GDF-15 and the other band at about 40 kDa. We assume that the higher band, which is also slightly visible in the eukaryotic derived GDF-15 (SF9, R&D), embodies multimers of GDF-15 molecules.

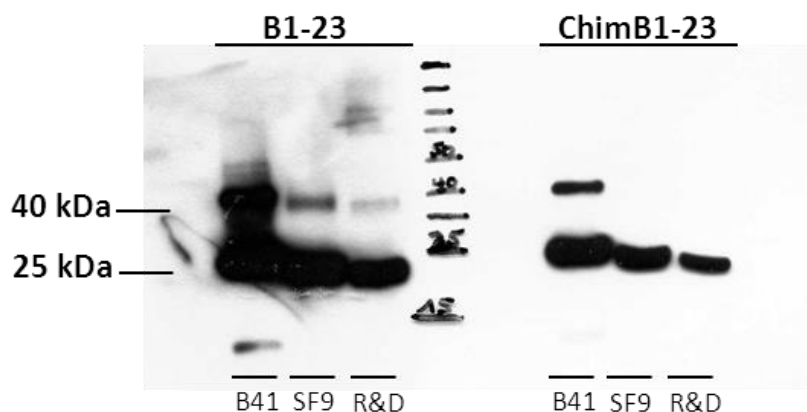


Figure 3-4-7 Detection of mature human GDF-15 by the chimeric antibody ChimB1-23

Chimeric B1-23 was compared to the murine B1-23 in regard to its GDF-15 binding ability. 100 ng of recombinant human GDF-15 was added on each lane on the SDS-PAG (B41, SF9, R&D are different GDF-15 batches). A Western Blot was performed under non reducing (semi native) conditions to retain the 3 dimensional structure of GDF-15. Whereas B41 is an *E. coli* derived protein, the SF9 and R&D-GDF-15 proteins were produced in eukaryotic cells.

3.4.9 Humanization of B1-23 and characterization of the humanized variants

Based on the CDR sequence shown in section 3.4.7, the expression constructs encoding the heavy and light chains of the humanized B1-23 were generated externally by evitria AG. Five different heavy chain variants and five light chain variants of the original antigen binding site of B1-23 were generated (table 46). Amino acids were altered exclusively within the framework sequence of the immunoglobulin, but not in the CDRs of the respective antibody chains. The *in silico* generated derivatives of the hypervariable regions of B1-23 were synthesized and cloned into a proprietary expression vector of evitria. All 25 combinations of the heavy and light chains of the antibody (H1L1-//H5L5, table 46) were transiently co-expressed in CHO cells and tested for their binding specificity to GDF-15. The humanized antibody H1L5, comprising the humanized heavy chain H1 and light chain L5, was selected as the candidate for further preclinical development due to its highest affinity to GDF-15.

The K_D -value of H1L5 was 5.6 nM (list of humanized K_D values in table 47).

H1L5 consisted of the following amino acid sequences:

Heavy chain 1:

QITLKQITLKESGPTLVKPTQTLTLTCTFSGFSLSTSGMGVSWIRQPPGKGLEWLAHIY
 WDDDKRYNPTLKSRLTITKDPSKNQVVLTMNMDPVDATYYCARSSYGAMDYWG
 QGTLVTVSS

Light chain 5:

DIVLTQSPSFLSASVGDRTITCKASQNVGTNVAWFQQKPGKSPKALIYSASYRYSYSGV
 PDRFTGSGSGTEFTLTISLQPEDFAAYFCQQYNNFPYTFGGGKLEIKR

Table 46: Sequences of the humanized light and heavy chains (performed by evitria AG)

	10	20	30	40	50	60
LC chimera	DIVLTQSP	EKENSS	SGDRVSV	TKASQNV	GTNVAWF	QKPGKSP
LC1	DIVLTQSP	ESSISS	SGDRVTI	TKASQNV	GTNVAWF	QKPGKSP
LC2	DIVLTQSP	SEFSSS	SGDRVTI	TKASQNV	GTNVAWF	QKPGKSP
LC3	DIVLTQSP	EATISS	SGDRVTS	TKASQNV	GTNVAWF	QKPGKSP
LC4	DIVLTQSP	EKENSS	SGDRVSI	TKASQNV	GTNVAWF	QKPGKSP
LC5	DIVLTQSP	SEFSSS	SGDRVTI	TKASQNV	GTNVAWF	QKPGKSP
	70	80	90	100		
LC chimera	RFTGSGSG	TEFTLTIS	LVQSEDL	AYFCQQY	NNFPYTF	GGGKLEIKR
LC1	RFTGSGSG	TEFTLTIS	LVQSEDL	AYFCQQY	NNFPYTF	GGGKLEIKR
LC2	RFTGSGSG	TEFTLTIS	LVQSEDL	AYFCQQY	NNFPYTF	GGGKLEIKR
LC3	RFTGSGSG	TEFTLTIS	LVQSEDL	AYFCQQY	NNFPYTF	GGGKLEIKR
LC4	RFTGSGSG	TEFTLTIS	LVQSEDL	AYFCQQY	NNFPYTF	GGGKLEIKR
LC5	RFTGSGSG	TEFTLTIS	LVQSEDL	AYFCQQY	NNFPYTF	GGGKLEIKR
	10	20	30	40	50	60
HC chimeric	QVQLTQ	SGPGILQ	SSQTL	SLTCS	FSGFSL	STSGMGV
HC1	QVQLTQ	SGPGLVQ	SSQTL	SLTCS	FSGFSL	STSGMGV
HC2	QVQLTQ	SGPGLVQ	SSQTL	SLTCS	FSGFSL	STSGMGV
HC3	QVQLTQ	SGPGLVQ	SSQTL	SLTCS	FSGFSL	STSGMGV
HC4	QVQLTQ	SGPGLVQ	SSQTL	SLTCS	FSGFSL	STSGMGV
HC5	QVQLTQ	SGPGLVQ	SSQTL	SLTCS	FSGFSL	STSGMGV
	70	80	90	100	110	
HC chimeric	YNPTLKS	RITISKD	PSNVE	LKITSV	DTADTA	YYCARSS
HC1	YNPTLKS	RITISKD	PSNVE	LKITSV	DTADTA	YYCARSS
HC2	YNPTLKS	RITISKD	PSNVE	LKITSV	DTADTA	YYCARSS
HC3	YNPTLKS	RITISKD	PSNVE	LKITSV	DTADTA	YYCARSS
HC4	YNPTLKS	RITISKD	PSNVE	LKITSV	DTADTA	YYCARSS
HC5	YNPTLKS	RITISKD	PSNVE	LKITSV	DTADTA	YYCARSS

Table 47: K_D value determination of 13 pre-selected humanized antibodies derived from B1-23 (performed by Steinbeis Zentrum Konstanz)

Antibody	KD value (nM)	Antibody	KD value (nM)
Murine ab	28,8	Lysate F - H3L2	6,42
Chimeric ab	14	Lysate G - H3L4	14,14
Rituximab	1116	Lysate H – H4L3	47,78
Herceptin	No binding	Lysate I – H4L4	17,19
Lysate A – H1L3	13,62	Lysate J - H4L5	9,69
Lysate B - H1L5	5,62	Lysate K - H5L1	10,17
Lysate C - H2L3	6,66	Lysate L - H5L2	24,21
Lysate D - H4L3	18,79	Lysate M - H5L4	21,56
Lysate E – H3L1	90,83		

The expression vectors for H1 and L5 were obtained from evitra AG and tested for their “in-house” expression in CHO cells.

Transient co-expression of both vectors (pHC1 +pLC5) in CHO cells resulted in specific anti-GDF-15 antibody expression (figure 3-4-8). We observed no binding to GDF-15, when CHO cells were transfected exclusively with either the light chain expression vector pLC5, or the heavy chain expression vector pHC1. This result led to the conclusion, that the variable regions of both the light and heavy chain of the humanized antibody H1L5 are necessary for proper antigen binding. This information is useful for prospective construction of modified GDF-15 binding proteins derived from the B1-23 sequence, such as single chain variable fragments (scFv), diabodies and many other Fc-lacking proteins with preserved neutralizing potential.

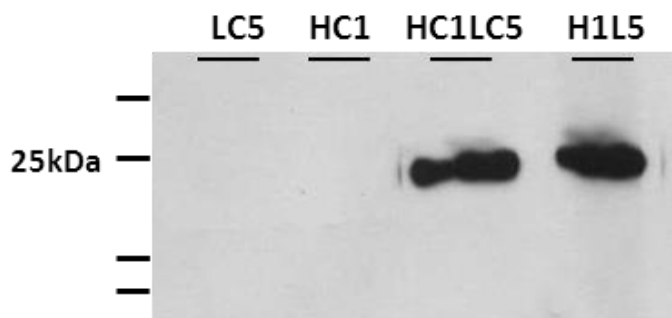


Figure 3-4-8 GDF-15 is detected by co-expression of light and heavy chain constructs of H1L5

Semi native Western Blot was performed with 100ng recombinant GDF-15 (Invigate) on all 4 lanes. After the transfer the PVDF membranes were cut in four stripes and incubated (according to the Western Blotting procedure described in the methods section) with supernatants from CHO cells, transiently transfected with the light chain pLC5, heavy chain pHC1 and co-expression of light and heavy chain pHC1 + pLC5 constructs (lane 1,2,3, respectively). The expression vectors containing the humanized light and heavy chain sequence (table13) were designed by and obtained from evitria AG). Binding of the recombinant human GDF-15 was observed only when both chains of H1L5, light and heavy, were overexpressed and thus assembled. As a positive control, the purified and Western Blot validated H1L5 was used on lane 4 (number of lanes from left to right).

As shown in figure 3-4-8, only in the presence of both light and heavy chain of B1-23/H1L5 the antigen GDF-15 could be targeted by the antibody. Using the IMGT database, an alignment of B1-23 variable regions with existing IgG2a mouse immunoglobulins resulted in antibodies with 97 % and 96% sequence homology for the heavy chain and light chain, respectively (table 48). The CDR1 and CDR2 of both the light and the heavy chain of our drug candidate revealed a sequence similarity of 100 % with one antibody from that database. The CDR3 appeared as the most altered sequence when compared to the even most similar immunoglobulin from the IMGT library. Because of the unique CDR3 sequence of B1-23, we assumed that this particular hypervariable region is necessary for the antigen binding. To test the hypothesis that the CDR3 is required for proper binding of the antigen, the CDR3 sequence of B1-23 was exchanged by a CDR3 sequence of an antibody engaging an HIV epitope (performed by evitria AG). The replacement of the CDR3 within the anti-GDF-15 antibody B1-23 resulted in a complete loss of binding to recombinant GDF-15 (figure 3-4-9). As an additional proof that the antigen binding to B1-23 is mediated by its CDRs and not by the interaction of the framework sequences of the antibody, all 3 CDR sequences have been replaced by 3 hypervariable regions of an HIV specific antibody, without changing the framework amino acids. As an expected consequence, the antibody completely lost its ability to bind GDF-15 (figure 3-4-9).

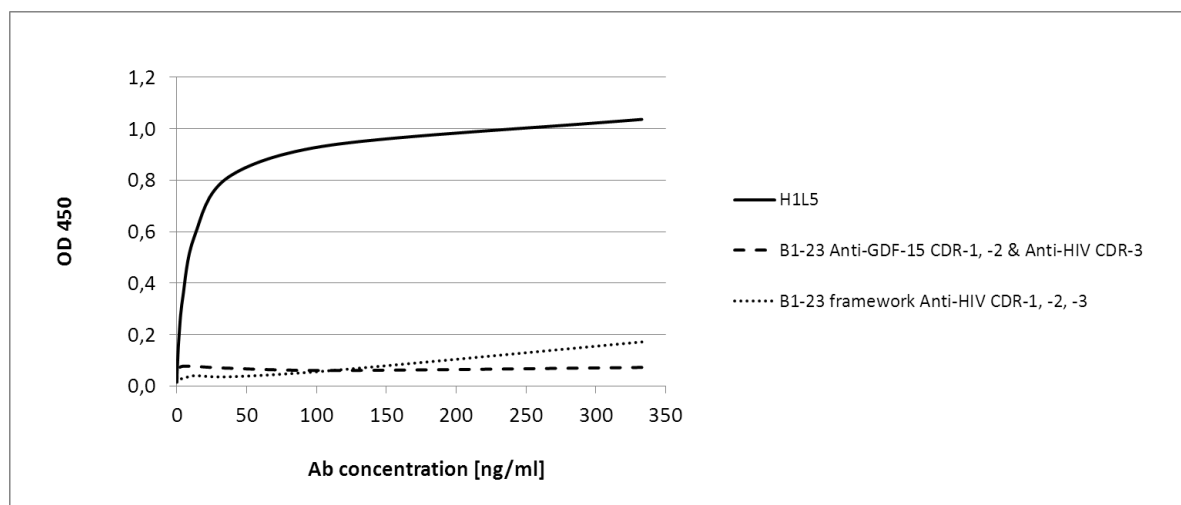


Figure 3-4-9 Replacement of the CDR3 of B1-23 leads to the loss of antigen binding

Antibody binding was tested in a colorimetric assay. Recombinant GDF-15 was coated on Maxisorp™ 96 well plates. Antibodies were incubated at six different concentrations ranging from low to high concentrations. H1L5 served as a positive control for GDF-15 binding. The modified antibodies designated “B1-23 Anti-GDF-15 CDR-1,-2& Anti-HIV CDR-3” and “B1-23 framework Anti-HIV CDR-1,-2,-3” were grafted on a human IgG1 antibody, the reason why the humanized H1L5 had to be used in this experiment. As a secondary antibody, an anti-human-HRP conjugated antibody was used. Antibody binding was assayed by conventional ELISA measurement determining the optical densities at 450 nm.

Table 48: IMGT database: Sequence alignment of B1-23 hypervariable regions including framework sequence

Variable **heavy** chain:

V-GENE and allele	Musmus IGHV8-12*01 F	score = 1327	identity = 97.49% (272/279 nt)
J-GENE and allele	Musmus IGHJ4*01 F	score = 216	identity = 88.89% (48/54 nt)
D-GENE and allele by IMGT/JunctionAnalysis	Musmus IGHD1-1*01 F	D-REGION is in reading frame 3	
FR-IMGT lengths, CDR-IMGT lengths and AA JUNCTION	[21.17.38.11]	[10.7.10]	CARSSYGAMDYW

Variable **light** chain:

V-GENE and allele	Musmus IGKV6-15*01 F	score = 1309	identity = 96.77% (270/279 nt)
J-GENE and allele	Musmus IGKJ2*01 F	score = 190	identity = 100.00% (38/38 nt)
FR-IMGT lengths, CDR-IMGT lengths and AA JUNCTION	[26.17.36.10]	[6.3.9]	CQQYNNFPYTF

3.4.10 In vitro effects of the developed anti GDF-15 antibodies

Preclinical development of a drug substance requires a very intensive characterization of the therapeutic biological. This is one reason, why my thesis has a substantial focus on the antibody development and characterization. Whereas externally performed proliferation assays with LnCap cells seemed to reveal a moderate antitumor effect *in vitro* when using 100 µg /ml B1-23 for 72 hrs (not shown here), own experiments could not significantly confirm such a result. Neither the addition of recombinant GDF-15 on tumor cell lines nor the antagonization of mature GDF-15 led to an altered proliferation *in vitro* (data not shown).

As GDF-15 is a soluble protein being elevated in the serum of a variety of cancer patients, we hypothesized that B1-23 should complex this growth factor *in vitro*. As a first step we monitored the secretion of GDF-15 into supernatants of the melanoma cell line UACC-257 over a period of six days by Western Blot analysis (figure 3-4-10, a). 20 µl of UACC-257 supernatants were taken from the same well every 24 hours. The mature GDF-15 hemidimer (40 kDa) as well as the GDF-15 homodimer (~70 kDa) accumulated over time reaching a saturated protein level between day 4 and day 5.

To answer the question of how much antibody is necessary to antagonize the tumor cell produced GDF-15, B1-23 was given in different concentrations to UACC-257 melanoma cells cultured for 48 hours. 10 µg /ml B1-23 and higher concentrations thereof resulted in a complete loss of signals representing the mature GDF-15 dimer as well as all isoforms containing the mature dimer (figure 3-4-10, b). A concentration of 1 µg /ml anti-GDF-15 antibody resulted in a decrease of GDF-15 related signals in the cell culture supernatant, but is not enough to remove the molecule from supernatant completely (figure 3-4-10, b).

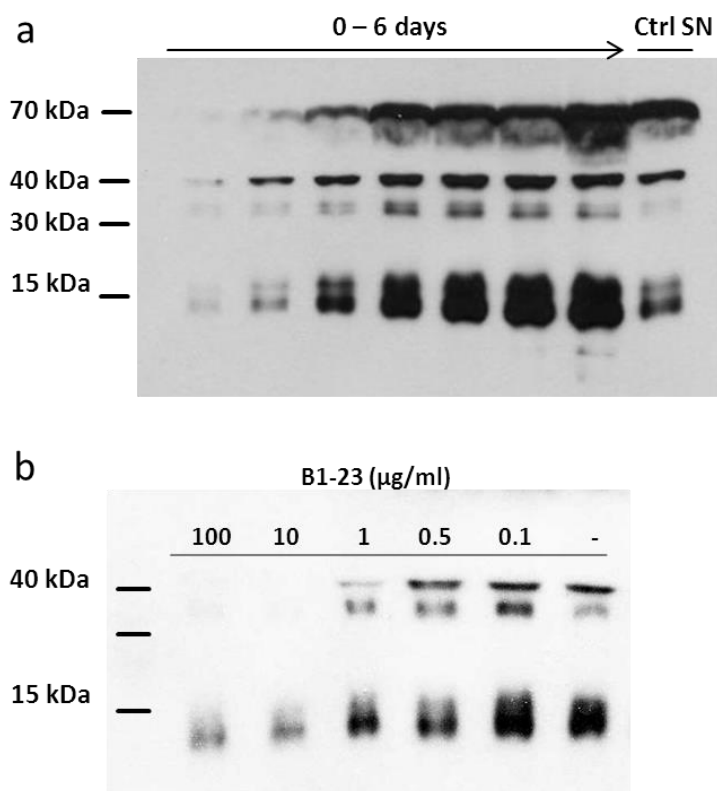


Figure 3-4-10: GDF-15 accumulation in supernatants of UACC-257 cells and its depletion by B1-23

(a, b) Western Blot analysis was performed with 20 µl of supernatants from each sample of UACC-257 melanoma cells. The anti-pro-GDF-15 antibody (Sigma) was used for the detection of the GDF-15 protein. (a) 50 µl of supernatants of UACC-257 cells was harvested daily, starting at day 0 (2 hours after seeding the melanoma cells), ending on day six. On the last lane a control supernatant was utilized as a technical control. (b) UACC-257 melanoma cells were cultured and treated for 48 hours with different concentrations of the anti-GDF-15 antibody B1-23 (from left to right lane: 100, 10, 1, 0.5, 0.1 µg/ml; last lane: untreated supernatant).

Knowing that 10 µg/ml of B1-23 sufficiently depletes tumor cell derived GDF-15 *in vitro*, we investigated the derivatives of B1-23 in the same “antagonization-assay” described in 3.4.10. All applied substances, comprising GDF-15 blocking antibodies and control antibodies, were administered at a concentration of 10 µg/ml. Beside B1-23, the antibodies ChimB1-23, H1L5, B12 (isotype-antibody), Rituximab as well as Fab fragments of ChimB1-23 were tested on UACC-257 melanoma cells for 48 hours. All GDF-15 antibodies were capable to efficiently clear the cell derived GDF-15 from the supernatant (figure 3-4-11). This effect could also be observed with the Fab fragments of B1-23, indicating that the antigen binding site of the antibody is sufficient for the clearance of GDF-15 *in vitro*. As expected, Rituximab and the isotype antibody B12 did not lead to a decrease of GDF-15 in the respective cell culture supernatants.

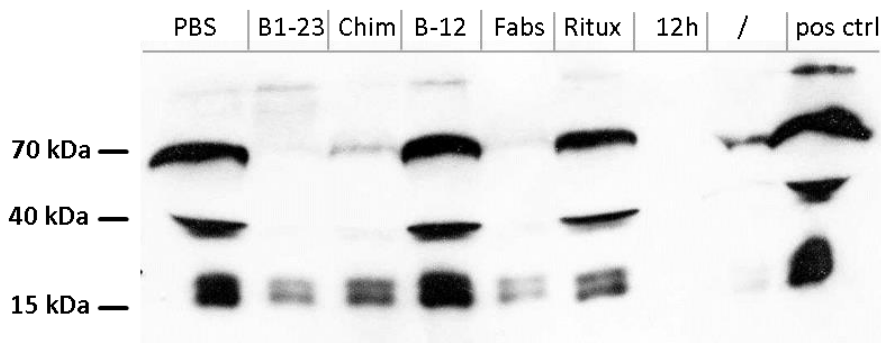


Figure 3-4-11: Antagonization of tumor cell derived GDF-15 with B1-23

Western Blot analysis with supernatants from UACC-257 cells. The melanoma cells were seeded in 24 well plates and incubated for 24 hours. Subsequently, these cells were treated with the anti-GDF-15 antibodies B1-23 and ChimB1-23 (Chim), an Iso-antibody (B12), Rituximab (Ritux), antibody fragments of the chimeric B1-23 (Fabs) and PBS for 48 hours. Rituximab and the Iso-antibody B12 served as negative controls, PBS represents the vehicle control.

3.4.11 Assessment of cytotoxic effects of B1-23

Preclinical development of a drug substance requires a very intensive characterization of the therapeutic biological in regard to its toxicity profile. Many side effects of antibodies have to be examined pre-cautious, before entering clinical trials in humans.

As a first approach, we tested the drug candidate B1-23 *in vitro* on human blood cells. B1-23 had no toxic effect on human peripheral lymphocytes, when compared to small molecule inhibitors, which are frequently dissolved in DMSO due to solubility issues (figure 3-4-12). Compared to the untreated control, we observed an equal turnover of WST-1 substrate, when treating peripheral blood lymphocytes with 10 µg /ml B1-23/H1L5 for a period of 24 hours. In addition, B12, an unspecific isotype, and the FDA approved antibodies Ipilimumab and Bevacizumab were tested. These antibodies were applied at a concentration of 10 µg /ml and did not reveal a negative effect on the viability compared to the untreated control. Treatment of 5 % DMSO, which served as a control condition, resulted in a viability of 40 %, compared to the untreated control PBMC. Similarly, Paclitaxel, which was applied on PBMC at its IC₅₀ of 5nM (Liebmann et al., 1993), which negatively affected the leukocyte viability, resulting in 60 % decreased WST-1 turnover. Dacarbazine, which is a FDA approved substance for the treatment of metastatic melanoma, was further applied to assess its toxicity on leukocytes (Hill et al., 1984). Dacarbazine was dissolved in PBS and added to the lymphocytes at a

concentration of 50 μM (Samulitis et al., 2011). Dacarbazine had no effect on human immune cells when compared to the control group (figure 3-4-12).

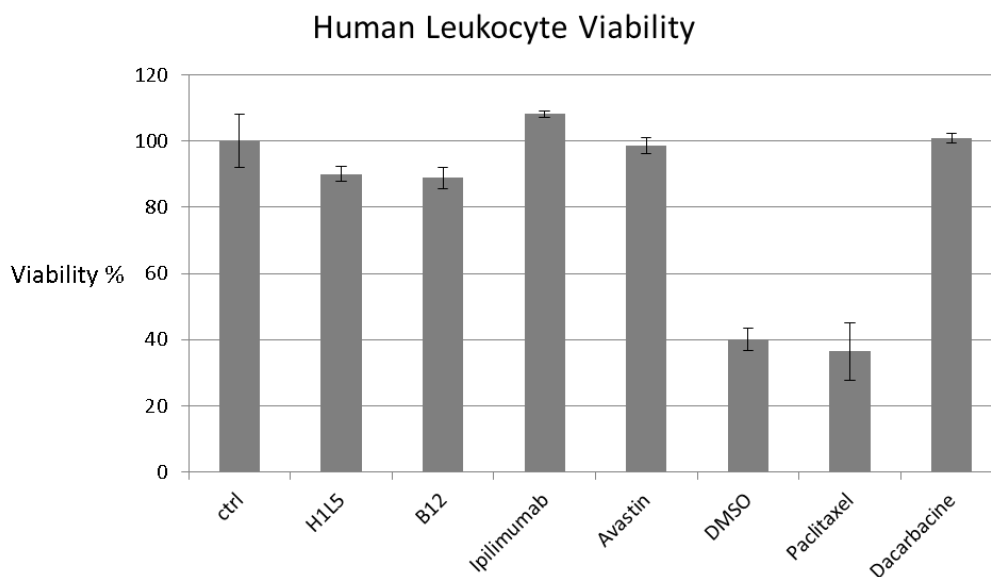


Figure 3-4-12 Toxicity test of B1-23 on blood lymphocytes

2×10^6 PBMC from different blood donors were seeded in 24 well plates (in triplicates) and treated with B1-23/H1L5, B12, Ipilimumab, Bevacizumab (Avastin), 5 % DMSO, Paclitaxel, Dacarbazine or left untreated for 24 hours. Then WST-1 substrate was added to the cells for a period of two hours. The measurement of the absorbance was performed using the Tecan Sunrise Reader (OD450nm). This figure represents 3 individual experiments with similar results.

Furthermore, we did not observe any adverse events in mice - related to direct or indirect toxic effects - after B1-23 had been administered intraperitoneally. The antibody was found in high concentrations (> 2 mg/ml) in the blood of the animals at the time of necropsy, suggesting a systemic distribution of the immunoglobulin, “reaching” all organs of the animal. The nude mice treated with the anti GDF-15 monoclonal antibodies resembled the PBS treated control mice, which did not show any symptoms. Parameters to investigate the physiological condition of the treated animals were body weight, activity, social interactions, alertness, perception, moving and reaction to stimuli.

3.5 B1-23 prevents tumor associated cachexia in BalbC^{nu/nu} mice

Johnen and colleagues reported in 2007 that tumor derived GDF-15 leads to anorexia resulting in body weight loss in mice (Johnen, Lin et al., 2007). In this publication it could be demonstrated that anti-GDF-15 antibodies are able to reverse the cachectic effect of GDF-15 in nude mice xenografted with GDF-15-transgenic prostate cancer cells. To investigate whether B1-23 and the chimeric and humanized forms thereof are able to revert the effect of body weight loss, we used an own melanoma tumor model, in which we observed a tumor mediated cachectic effect in Balb/c^{nu/nu} mice. In this model, 1.0×10^7 UACC-257 melanoma cells, which produce high endogenous GDF-15 levels (shown in figure 3-4-10a), were subcutaneously inoculated into the immunocompromised animals (details in section 2). The antibodies were administered twice a week starting at day 0 (day of tumor inoculation). Body weight as well as food uptake was measured twice a week until day 38. At day 38, we observed a decline of body weight to 85 % of the initial body weight (set to 100 %) for the PBS treated group (figure 3-5). The administration of the iso-antibody B12 resulted in a decline of body weight to 82 %. Conversely, the application of B1-23, ChimB1-23 and H1L5-B1-23 led to a total increase in body weight on day 38. Compared to the initial body weight of each treatment group on day 0, mice treated with the GDF-15 antibodies reached the following body weights at the end of the experiment (day 38): 102 % for the administration of the murine antibody B1-23, 105 % with ChimB1-23 treatment and 107 % when animals were treated with the humanized H1L5 (figure-3-5). The effect was significant for all of the groups treated with anti-GDF-15 antibodies (two-way ANOVA; $p < 0.05$). Interestingly, the Fab fragments of ChimB1-23 could not prevent the loss of body weight in the animals, but even led to a decline of the initial body weight to 78 %.

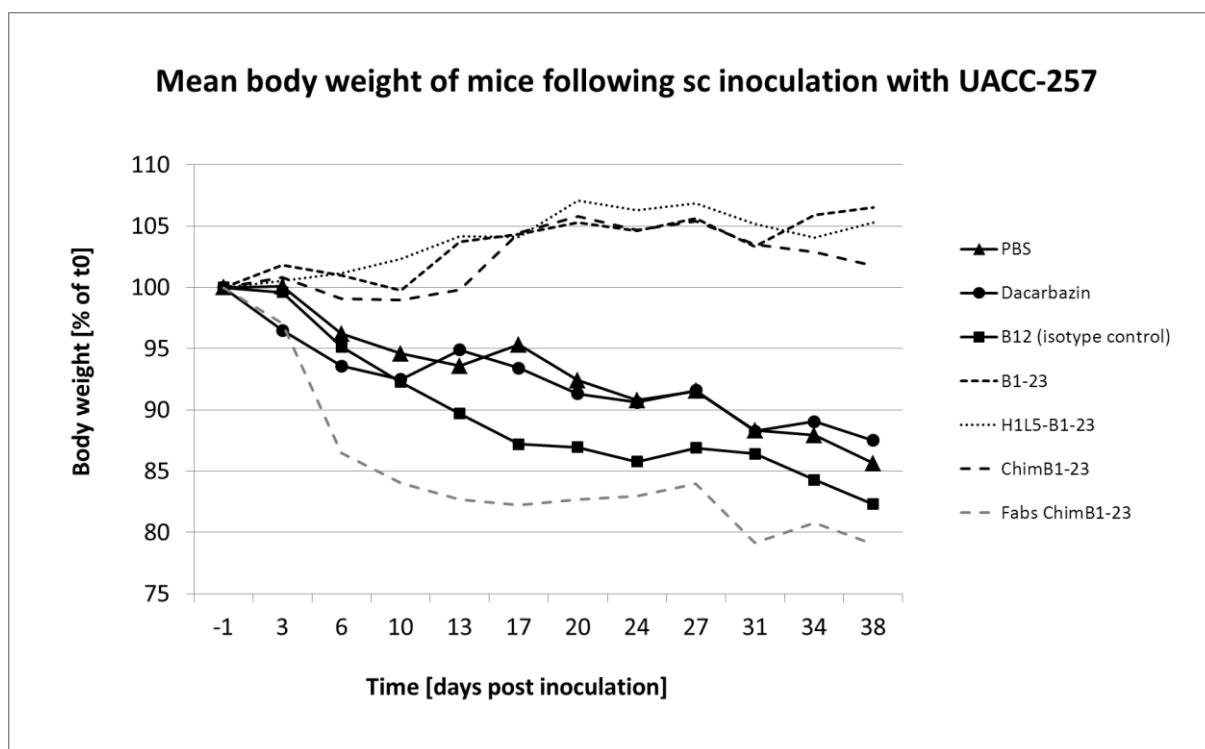


Figure 3-5 B1-23 prevents GDF-15 mediated cachexia *in vivo*

Treatment of mice with anti GDF-15 antibodies B1-23, ChimB1-23, H1L5-B1-23 prevented tumor induced body weight loss in mice. The antibodies were given on the day of tumor cell inoculation. As a control antibody B12 was used. Beside the exchanged CDRs (anti-HIV epitope CDRs) the iso-antibody B12 is almost identical to the humanized antibody H1L5-B1-23. Dacarbazine was used as a positive control for tumor growth reduction (data not shown in this thesis). This experiment was performed together with Dr. Tina Schäfer and Dr. Dirk Pühringer.*

At this point of the thesis it has to be mentioned that the melanoma xenograft experiments were initially performed to investigate antitumor effects of the generated GDF-15 antibodies and variants thereof. Even though external data from independent contract research organizations demonstrated tumor growth reduction using B1-23, we did not observe significant tumor inhibiting effects using the GDF-15 antibodies B1-23, ChimB1-23 as well as H1L5. However, cachexia could be completely prevented in this model.

* Dr. Tina Schäfer subcutaneously inoculated the tumor cells in the animals. Dr. Dirk Pühringer and I labelled the tails of the animals, measured the body weight and food intake. Intraperitoneal injection of antibodies and drug substances were performed by myself, Dr. Dirk Pühringer and Dr. Tina Schäfer. Mice were sacrificed using CO₂.

4 Discussion

Tumors are facing an enormous challenge: they need to protect themselves from immune cell destruction by host cytotoxic effector cells. Therefore, malignant tumors develop certain strategies to escape anti-tumor immunity (see section 1.2) (Hanahan and Weinberg, 2011, Vinay et al., 2015). The expression of immunosuppressive cytokines, which are essential in healthy humans to prevent autoimmunity, can be “*abused*” by tumors, leading to a microenvironment which favors the recruitment of and polarization towards tolerized immune effector cells, sparing the transformed cells from immune attack, and allowing an unrestricted tumor growth (Bommireddy and Doetschman, 2004, Massague, 2008, Caja and Vannucci, 2015). TGF- β is one of the best studied molecules with such immune inhibitory effects (Wahl et al., 1988, Thomas and Massagué, 2005, Massague, 2008, Caja and Vannucci, 2015). GDF-15, as a member of the TGF- β superfamily, is far less understood, even though many publications arose in the last years with regard to its pro-tumorigenic and anti-inflammatory functions and the conclusion that GDF-15 is a promising target in the field of cancer therapy. GDF-15 is, like TGF- β , a self-tolerated antigen, which is “temporally” required during pregnancy – conceivably to avoid immune mediated fetal abortion (Tong, Marjono et al., 2004). Except during human pregnancy, GDF-15 has not been reported to exceed physiological levels in healthy humans. Of note, non-steroidal-anti-inflammatory drugs (NSAID) lead to an increase in GDF-15/NAG-1 expression, thus reflecting a non-physiological condition (Baek et al., 2002). Under pathological conditions, GDF-15 can be found in high amounts in different tissue and blood sera, where several “*pleiotropic roles*”, in particular in “*cancer, obesity and inflammation*” were attributed to GDF-15 (Breit et al., 2011). Interestingly, GDF-15 was reported to promote angiogenesis in tumors via hypoxia induced factor-1 alpha (HIF-1 α). This transcription factor induces vascular endothelial growth factor (VEGF) expression, the primary growth factor related to angiogenesis (Lin et al., 2004, Song et al., 2012) Of note, Krieg and colleagues could demonstrate that HIF-1 α itself mediated the expression of GDF-15 in the HCT116 colorectal cancer cell line under hypoxic conditions (Krieg et al., 2010). Since the GDF-15 promoter contains a HIF-1 recognition sequence, this underlines the strong interrelation of these two molecules (Krieg, Rankin et al., 2010). When combining the models of Song et al. and Krieg et al., hypoxia would lead to HIF-1 α mediated GDF-15 expression, which in turn promotes angiogenesis and further enhances HIF-1 α expression ending in a positive feedback loop (Krieg, Rankin et al., 2010, Song, Yin et al., 2012). In fast growing solid tumors, which develop a hypoxic

environment, the expression of GDF-15 seems to be essential in order to activate angiogenesis-promoting pathways. This represents an elegant strategy for tumors to achieve a growth advantage – to express a multimodal factor, which on the one hand promotes the new formation of blood vessels in the tumor (oxygen and nutrients supply) and on the other hand exerts an immunosuppressive function (protection of the tumor). Evidence that GDF-15 is involved in immunological processes became clear when it was first described as macrophage inhibitory cytokine 1 (MIC-1) (Bootcov, Bauskin et al., 1997). Under pathological conditions, a variety of influences of GDF-15 on immune cells have been described, including decreased macrophage adherence under diagnosed atherosclerosis and prevention of PMN infiltration in heart tissue upon myocardial infarction in mice (de Jager et al., 2011, Kempf, Zarbock et al., 2011, Bonaterra et al., 2012). Most importantly, GDF-15 was shown to contribute to tumor progression and immune escape in glioma bearing mice, by keeping T cell and macrophages out of the tumor microenvironment (further discussed in 4.3) (Roth, Junker et al., 2010). These data were giving rise to investigate the role of GDF-15 in cancer and to develop antibodies against the human growth factor.

4.1 GDF-15 expression and physiological relevance

To identify a biological factor for a prospective therapeutic intervention in cancer, the target needs to be substantially analyzed in regard to its tissue expression and distribution, as well as its association between expression and grade of malignancy. Further, its physiological and pathophysiological function must be elucidated *ex vivo* as well as *in vivo*. From the present knowledge, the target's function can be turned off e.g. by direct blockade of the target protein (as for instance by use of a monoclonal antibody), by complete knock down of the protein, and eventually by inhibiting its receptor. Peer reviewed reports in the literature, online databases (Sigma Atlas database) as well as own tissue staining confirmed the elevated expression of GDF-15 in many cancer types, compared to the respective healthy tissue. Comparability between own findings and the published data was given, since GDF-15 expression was analyzed with the Atlas-GDF-15-antibody HPA1109 suitable for formalin fixed paraffin embedded tissue, and being the basis for the Atlas Database (<http://www.proteinatlas.org/>) (Uhlen et al., 2010). In accordance to a publication by Staff, our data confirmed that ovarian carcinoma tissues were highly positive for GDF-15, whereas in contrast to the malignant tissue, GDF-15 protein is not detected in female reproductive system, including ovaries, cervix, fallopian tube and endometrium (human tissue information is provided in the human protein atlas) (Staff, Bock et al., 2010). Most intense GDF-15

staining could be observed in own studies in a serous papillary type of ovarian carcinomas (section 3.1). Our data demonstrate that GDF-15 expression is not restricted to the tumor cells itself, but also expressed in endothelial cells. Similarly to the ovarian carcinoma, we could show that GDF-15 expression is increased in human brain tumors, which is in accordance with the literature, where several correlations between GDF-15 expression and grade of malignancy have been reported (Staff, Trovik et al., 2011, Mehta et al., 2015). However, in these sections, endothelial cells were also GDF-15 positive within normal white matter. It was further reported, that high cerebrospinal fluid GDF-15 level correlate with shorter survival in glioma patients (Shnaper, Desbaillets et al., 2009). Interestingly, Shnaper and colleagues did not observe a correlation between the high GDF-15 values measured in human CSF and the according plasma levels (Shnaper, Desbaillets et al., 2009). These observations are not in line with our findings, where GDF-15 tissue expression correlates with the GDF-15 serum level (Roth, Junker et al., 2010).

Despite all these findings, the question of whether GDF-15 is concomitantly apparent in progressed malignancies, or whether it plays a functional tumor promoting role, still remains unclear (Mehta, Chong et al., 2015).

The strongest GDF-15 protein expression described so far can be seen in placental syncytiotrophoblasts (section 3.1 and *atlas database*). Under physiological conditions, GDF-15 was shown to exert a life-saving function during embryonic and fetal development (Tong, Marjono et al., 2004). Here, low GDF-15 serum levels during pregnancy were reported to correlate with fetal abortion. This allowed Tong and colleagues the suggestion, that GDF-15 - as an immunomodulatory molecule, which “*favours fetal viability*”- possesses not only predictive but also causative role during pregnancy (Tong, Marjono et al., 2004).

But still, the function of GDF-15 under pathological conditions remains unclear. Since the synthesis of GDF-15 in cells requires a lot of energy, its overexpression by several solid tumors needs to yield an advantage for the neoplastic tissue, otherwise it would be an implausible waste of energy. The function of GDF-15 as an immunomodulatory molecule, contributing to immune evasion, might be a plausible reason for tumor cells to produce it in high amounts. Still, the mode of action in this respect is unknown so far.

Johnen and co-workers could elucidate one mechanism of action of human GDF-15 on murine neurons: Here, GDF-15 mediates cancer associated cachexia (Johnen, Lin et al., 2007). GDF-15 was shown to induce anorexia in animals, which is followed by loss of body weight, revealing symptoms of cancer related anorexia-cachexia. Accordingly, our own xenograft studies confirmed this function of GDF-15 on body weight loss of tumor

transplanted animals (further discussed in 4.5). However, the influence of GDF-15 on weight loss due to neuronal induced anorexia rather seems to be an adverse reaction and cannot explain the findings of us and others, namely direct tumor-promoting effects and an immunomodulatory influence of GDF-15 (Kim, Lee et al., 2008, Roth, Junker et al., 2010, de Jager, Bermudez et al., 2011, Kempf, Zarbock et al., 2011, Bonaterra, Zugel et al., 2012). Therefore, further approaches were undertaken, to elucidate the mode of action, confirming a pathological function in regard to tumor immunity.

4.2 GDF-15: Growth Factor and Ligand - without a yet known receptor?

Growth factors and cytokines play an important role in physiological processes, e.g. tissue development, homeostasis as well as the coordination of organ- and cellular function (Dinarello, 2007). The impact of cytokines on human health can be observed best, when the respective protein is deregulated (Orzechowski et al., 2014). This can occur, when a cytokine is lacking, mutated and thus dysfunctional or even overexpressed (for instance by cancer cells). At that time, the cytokines can contribute to life threatening pathological conditions.

In the tumor-immunological context, TGF- β reveals a variety of different functions. On one hand, TGF- β suppresses immune cells by modulating lymphocytes upon ligation of the TGF- β receptor complex (Thomas and Massagué, 2005). On the other hand, TGF- β was described to promote tumor growth directly by autocrine signals on cancer cells (Massague, 2008). However, at earlier stages of cancer development, TGF- β exerts tumor inhibiting functions (Massague, 2008). The functional complexity of that molecule impedes to dissect singular effects *in vitro*.

As a member of the TGF- β super-family, GDF-15 is far less characterized compared to the other family members and little is known about its mode of action on cellular level. Therefore, characterization of GDF-15 and its role in cancer is the object of my thesis. To elucidate its biological function, several experimental *in vitro* and *in vivo* approaches were performed, allowing for the first time not only to identify the tissue distribution and influence on signaling pathways, but also to demonstrate effects on tumor growth and immune reaction *in vivo* (Roth, Junker et al., 2010).

GDF-15 was demonstrated by Johnen and colleagues to activate hypothalamic neurons via the TGF- β receptor I in mice (Johnen, Lin et al., 2007). These *in vivo* results would be very attractive to be translated into an *in vitro* model. Tsai and colleagues dissected certain brain

regions in regard to their anorexic area (Tsai et al., 2014). They were able to demonstrate that laser depletion of neurons located within the area postrema, results in animals being unresponsive to GDF-15 induced anorexia. The isolation of certain neuronal cell types represent an enormous obstacle for *in vitro* investigations not only because of technical issues but also because of the enormous amount of animals required for a sufficient number of primary cells (Strelau J., personal communication).

Since my work predominantly focused on the function of human GDF-15 on human cells, signaling pathway analysis had to be performed in cell types differing from the above mentioned murine cells in terms of species and anatomic location. It is known, that TGF- β is able to activate the canonical TGF- β pathway in various different benign and malign cell types. This ends in the same pattern of kinase activity, ending in a phosphorylated Smad2/3 protein level (Santibanez, Quintanilla et al., 2011). In case, a GDF-15 induced signaling pathway was conserved throughout different cellular populations, even other than neuronal cell types should respond to the “ligand”. Since the literature described GDF-15 to be involved in anti-inflammatory processes, human immune cells seemed to be an optimal “cellular target” to confirm the observations of Johnen and colleagues *in vitro* (de Jager, Bermudez et al., 2011, Kempf, Zarbock et al., 2011, Li et al., 2013). Unexpectedly, recombinant GDF-15 was not able to activate the canonical TGF- β signaling pathway in human peripheral blood lymphocytes in our experiments. Whereas TGF- β potently activated Smad signaling pathway, four commercially acquired GDF-15 batches left the Smad2/3 proteins de-phosphorylated, indicating that immune cells do not respond to recombinant human GDF-15 in regard to canonical TGF- β signaling pathway in human PBMC. One could speculate that immune cells lack a GDF-15 receptor, which could unfortunately not be verified due to the yet unknown nature of this presumable receptor. Human GDF-15 evoked TGF- β signaling in mouse neurons *in vivo* (Johnen, Lin et al., 2007). However, the human GDF-15 may not activate a respective receptor expressed on immune cells, which could be due to tissue specific receptor polymorphisms. Furthermore, one cannot exclude that human GDF-15 only specifically - more or less non-physiologically- evokes a response on murine cells in regard to TGF- β receptor activation. The latter suggestion would complicate to further elucidate the role of GDF-15 in human pathogenesis, particularly in cancer.

Even though the signaling pathway of TGF- β and GDF-15 did not resemble in human lymphocytes, we wanted to see whether a temporally later effect of TGF- β , the downregulation of NKG2D receptor on NK cells and CTLs, converges between the two family members (Crane, Han et al., 2010). Therefore, we compared direct effects of both

recombinant GDF-15 and TGF- β on NK cells and CTLs, respectively, by analysis of the NKG2D receptor surface expression using flow cytometry. Whereas TGF- β revealed more than 50 % NKG2D receptor downregulation, GDF-15 could only slightly downregulate NKG2D (section 3.2). The fact, that GDF-15 was capable to diminish NKG2D at least at high cytokine concentrations, could be explained by a signaling event on lymphocytes, which follows a new pathway. Importantly, NKG2D reduction on NK cells, which were treated with GDF-15, seemed to occur in a dose dependent manner, further consolidating a direct effect of the ligand GDF-15 on immune cells.

Since GDF-15 was further reported to reduce adherence of polymorphonuclear leukocytes (PMNs) to the endothelium after myocardial infarction, a next step was to investigate the influence of GDF-15 on the adherence of immune cells on endothelial cells (Kempf, Zarbock et al., 2011). Mechanistically, GDF-15 is essential to prevent the arrest of PMNs on the endothelium by inactivation of β -integrins on immune cells (Kempf, Zarbock et al., 2011). This effect described by Kempf, represents a potent approach to investigate GDF-15 mediated effects *in vitro* and would support the finding that GDF-15 lowers the number of infiltrating T cells and macrophages in glioma bearing mice (see section 3.3) (Roth, Junker et al., 2010). In accordance to Johnen and co-workers, immune cell adherence on endothelial cells was slightly reduced by GDF-15 *in vitro*. However, our experiments revealed effects of GDF-15 rather on lymphoid immune cells than myeloid cells, as shown by Kempf and colleagues. In our own study, macrophages hardly showed a loss of adherence after GDF-15 treatment, whereas for CD4⁺ T cells a reduction of adherence of ~24 % and of ~20 % for CD8⁺ T cells was observed upon GDF-15 pre-incubation. We could not recognize a change from the active state of β_2 integrin towards the inactive one on immune cells, as observed by Johnen and colleagues (data not shown in my thesis, part of a running project). However, the group examined the effect on mouse PMN whereas human PBMC were used here.

Taken these GDF-15 mediated effects on both NKG2D receptor expression as well as immune cell adherence on endothelial monolayers, we suggested that GDF-15 might ligate a yet unknown receptor on either immune or endothelial cells, possibly leading to transcriptional activation in the respective cell. Therefore, a micro array was performed, after human PBMC and HUVEC cells were treated with GDF-15 or left untreated. Unexpectedly, the changes in gene expression upon recombinant GDF-15 treatment were only marginal. Therefore, further investigation of those genes “seemingly” being deregulated, was not of

highest priority. Surprisingly, the most notable group of genes deregulated upon GDF-15 stimulation of both HUVEC and PBMC were the olfactory receptors. Interestingly, olfactory receptor activation was reported to promote cancer cell invasiveness and metastasis (Sanz et al., 2014), a possible hint for tumor-promoting effects of GDF-15. Expecting genes involved in cancer, the clarification of the causal relationship between GDF-15 and olfactory receptors should be further investigated, however, this was not part of this thesis).

A last step of my thesis was to investigate the influence of GDF-15 on migration and thus indirectly on metastasis: GDF-15 was reported to significantly increase invasiveness when overexpressed in gastric cancer cell line SNU-216 (Lee, Yang et al., 2003). Furthermore, Senapati demonstrated that GDF-15 overexpression leads to metastasis of human prostate cancer cells by promoting cellular motility (Senapati et al., 2010). In contrast to those data, we could not observe enhanced migration of GDF-15 overexpressing breast cancer cell line MCF-7, compared to low GDF-15 expressing cells (see 3.2.5). Neither could we observe an effect when blocking GDF-15 with an antibody, drawing the conclusion that MCF-7 breast cancer cell line cannot be influenced by GDF-15 in regard to motility. The MCF-7 cells were chosen because of their low GDF-15 expression, expected to be even more responsive to GDF-15. Probably cells, which are not dependent on GDF-15, lack its potential receptor, which could otherwise be activated in an autocrine signaling manner.

4.3 GDF-15 and its function *in vivo*

To unmask the function of GDF-15 *in vivo*, mouse GDF-15 was silenced in the SMA-560 glioma cell line and compared to the GDF-15 expressing wild-type SMA-560 cells by our group. Here, GDF-15 deficient animals showed prolonged survival (section 3.3) (Roth, Junker et al., 2010). From these studies one could conclude that GDF-15 negatively influences survival of brain tumor bearing animals and promotes tumor growth *in vivo*. However, studies with MIC-1/GDF-15 overexpressing animals revealed no tumor growth promoting effects of GDF-15, but high metastatic potential in the TRAMP transgenic prostate cancer model (Husaini, Qiu et al., 2012). As discussed in our publication (Roth et al.), overexpression of GDF-15, which reaches concentrations far beyond the physiological amount of GDF-15 in tumors, might exert unexpected effects (Roth, Junker et al., 2010). This implicates that GDF-15 overexpression could change its function compared to the pathophysiological tumor-produced GDF-15 and thus cannot mimic the “behaviour” of tumors in patients. As an

example, the group around Hegi published two opposing functions of GDF-15 in human glioma: An ectopic expression of GDF-15 in the glioblastoma cell line LN-Z308 led to the complete loss of tumorigenicity in nude mice and thus GDF-15 was described to act as an anti-tumorigenic protein (Albertoni et al., 2002). However, the same group demonstrated that glioblastoma patients with elevated GDF-15 levels in the cerebrospinal fluid have a shorter survival, which allowed Shnaper and colleagues the conclusion, that GDF-15 may serve as a prognostic factor in humans suffering from intracranial tumors (Shnaper, Desbaillets et al., 2009). These findings demonstrate, that investigations based on ectopic overexpression of certain molecules, have to be interpreted very carefully and eventually lead scientists on the wrong track, regarding the function of a protein.

Since GDF-15 has been associated with inflammation and was reported as macrophage inhibitory cytokine 1 (MIC-1), the focus was further placed on immune cell infiltrates within the SMA-560 glioma tissue, which was known to have an enormous impact on a patients prognosis (Pages et al., 2009, Kmiecik et al., 2013). Therefore, T cells and macrophages were stained immunohistochemically on SMA-560 glioma sections. Surprisingly, GDF-15 deficient animals revealed a strong infiltration of intratumoral T cells, whereas in GDF-15 producing glioma tissue T cell infiltrates could hardly be observed (section 3.3). Unexpectedly, macrophage infiltration in GDF-15 deficient tumors was lower than T cell infiltrates, even though the presence of macrophages within the GDF-15 knock-down glioma sections were enhanced, when compared to the wild-type tumors. However, we speculated that GDF-15, in its role as the macrophage inhibitory molecule, would rather influence the macrophages and not the T cells. Still, these findings from mouse models are in line with our results on the adherence assay (see 4.2) and implicate that GDF-15 not only acts on myeloid derived immune cells, but also on T cells, which belong to the lymphoid lineage.

Summing up the information about GDF-15 in the cancer context this molecule can be attributed to...

- I) tumor promoting effect in glioma bearing mice with shorter survival,
- II) correlations of serum levels and poor prognosis in cancer patients
- III) its pathological function of tumor associated cachexia.

Therefore, the blockade of GDF-15 was postulated to be a potent therapeutic approach to cope with the above mentioned unwanted effects of GDF-15 in cancer. As a consequence, the next step was to develop an antibody against GDF-15, which was a major part of the experimental

setting of this thesis and finally resulted inter alia in two patent applications of the monoclonal GDF-15 antibody suitable for cancer- as well as cancer associated cachexia treatment.

4.4 Generation of GDF-15 antibodies and preclinical testing thereof

Preceding *in vivo* data demonstrated the therapeutic potential of targeting GDF-15 and reinforced the intention to generate neutralizing immunoglobulins against that protein. Therefore, a monoclonal antibody was strategically generated in GDF-15 knock-out animals. The GDF-15 deficient mouse was utilized, since human and mouse GDF-15 exhibit 70 % DNA-sequence homology (see supplements, table 42), probably decreasing the immunogenicity of human recombinant GDF-15. The monoclonal antibody B1-23, which was developed during my thesis, was deposited under the Budapest treaty at the DSMZ (Accession number: DSM_ACC_3142). The immunoglobulin revealed a high affinity to GDF-15, with a dissociation constant (K_D -value) of less than 1 nM (WO2014049087A1), which could be explained by the specific immunization protocol in GDF-15 knock out mice and resulted in a mouse monoclonal IgG2a isotype. For comparison, the K_D -value of the Rituximab (Rituxan®), a FDA approved monoclonal anti-CD20 specific antibody, is at ~ 8nM (<http://www.rxlist.com/rituxan-drug.htm>). We thus concluded that B1-23, which had a more than eight times higher affinity to its target antigen compared to the clinically applied antibody Rituximab, might represent an optimal preclinical drug candidate with neutralizing potential. With the focus on clinical applicability of the antibody in humans, further considerations regarding regulatory demands, such as knowledge about target expression and antibody cross reactivity, were inevitable. According to the literature and open access databases (see section 4.1), GDF-15 could be shown to be overexpressed in several types of cancer (see section 1, table 1), but hardly in healthy tissue (Uhlen, Oksvold et al., 2010). Consequently, as GDF-15 is highly upregulated in the human placenta and required during pregnancy, pregnant women would represent a contra-indication for a clinical application of GDF-15 antibodies in humans (Tong, Marjono et al., 2004). Once a monoclonal antibody represents a suitable drug candidate, a tissue cross reactivity panel (as for example FDA/EMA panels of normal tissue) is an inevitable part of the preclinical development. This will, apart from the underlying thesis, be further performed for the anti-GDF-15 antibody B1-23/H1L5. In order to prevent human anti mouse antibody (HAMA) generation, which in some cases can be followed by an uncontrollable immune response in humans, the immunoglobulin

B1-23 has been humanized as part of my thesis (Brennan et al., 2010, Nelson, Dhimolea et al., 2010).

Taken together the utility of the antibody B1-23 *in vitro*, the antibody is applicable for the detection of native GDF-15 in a semi native Western Blot system (3.4.4). This enabled to intensively characterize GDF-15 and its various forms. Importantly, B1-23 revealed to bind a conformational epitope of GDF-15 (3.4.6), which is preferred for a clinical application as a neutralizing antibody (Forsstrom et al., 2015). B1-23 can further be used as detection antibody in a colorimetric assay, e.g. when maxisorb plates are coated with recombinant GDF-15. Moreover, B1-23 or the humanized variant thereof is able to serve as a capture antibody in a sandwich enzyme linked immunosorbent assay (ELISA), which allows for the measurement of patients GDF-15 serum level, which could then be stratified according to defined GDF-15 thresholds of the individual cancer type. Most importantly, B1-23 reveals antagonizing effects *in vitro* (3.10). Here, B1-23 was capable to deplete tumor cell derived soluble GDF-15 in cell culture, an effect which is desired to occur in tumor patients.

4.5 Therapeutic potential of B1-23 / H1L5

GDF-15 was shown to induce cancer associated cachexia when expressed in prostate cancer cells inoculated in mice (Johnen, Lin et al., 2007). Here, anti GDF-15 antibodies were able to reverse the effect of body weight loss. However, the model used by Johnen and colleagues was based on a transgenic prostate carcinoma cell line. Here, GDF-15 was ectopically overexpressed in DU145 cells, which were transfected with a pIRES2-EGFP overexpression vector containing the human GDF-15 sequence. As discussed in the previous section, artificially overexpressed GDF-15 might act contrarious to from tumors physiologically secreted GDF-15. Therefore, we used the human melanoma cell line UACC-257, which highly expresses endogenous levels of GDF-15, representing a more clinically relevant model. Furthermore, we administered purified and toxicity tested monoclonal antibodies, which reduced the risk of undesired side effects due to cross reactivity with other molecules. The murine (B1-23), chimeric (ChimB1-23) as well as the humanized (H1L5) version of the developed GDF-15 antibodies were administered to the mice at day of tumor inoculation, which resembles a prevention model. In accordance with Johnen and colleagues, the application of all of our monoclonal antibodies could prevent the tumor associated loss of body weight of the animals (section 3.5). Surprisingly, only the intact antibodies were effective while GDF-15 specific Fab fragments could not counteract the GDF-15 mediated

weight loss in mice. It could be speculated, that B1-23-Fab fragments, which have a molecular weight of only ~ 110 kDa were cleared earlier from the blood than the 150 kDa IgG full antibodies. In this respect, Covell and colleagues reported that Fab fragments are cleared from the body 35 times faster than full IgG molecules, whereas the F(ab)₂ clearance is situated in between the full length IgG and Fab molecules (Covell et al., 1986). In line with Covell's reported pharmacokinetic of immunoglobulin clearance, the *in vitro* depletion of UACC-257 cell line secreted GDF-15 works efficiently, when using F(ab)₂, but no longer than four days. In contrast, all three GDF-15 antibodies (B1-23, ChimB1-23, H1L5) were able to deplete GDF-15 over a period of more than 7 days. With this study we could demonstrate that the human melanoma cell line UACC-257 induces GDF-15 mediated cachexia in nude mice which could be prevented with all monoclonal GDF-15 antibodies. This effect is GDF-15 specific, since PBS, the isotype IgG1 antibody, the F(ab)₂ fragments as well as dacarbazine could not halt the loss of body mass. We did not expect to observe anti cachectic effects of Dacarbazine. However, dacarbazine (DTIC) was supposed to serve as antineoplastic chemotherapeutic control group, leading to tumor growth arrest in melanoma studies (Zhang et al., 2013). Surprisingly, no tumor growth reduction could be observed in our model, when treating the animals for five consecutive days with 80 mg /kg dacarbazine. Since Dacarbazine is mainly used for the treatment of advanced metastatic melanoma (Zhang, Qiao et al., 2013), the missing efficacy could be explained by the UACC-257 cell line, which was reported to highly express GAS1, a suppressor of metastasis (Gobeil et al., 2008).

Summarizing the *in vivo* effects of anti-GDF-15 blocking antibodies in an immunocompromised melanoma model, B1-23, ChimB1-23 and H1L5 prevents the GDF-15 mediated cachexia, proofing the functionality of the antibodies. Antitumor effects could not be observed with these GDF-15 specific antibodies, whereas external CRO could demonstrate growth inhibition in an analogous melanoma model. Thus, we speculate that either athymic mouse strains, which at least contain NK cells and macrophages, might differ in their NK cell activity. This would mean that tumor growth inhibition caused by the GDF-15 antibody B1-23 would only take an effect, if NK cells are potent enough to be inhibited by GDF-15. Furthermore, one cannot exclude, that keeping of animal differs in different facilities in regard to certain pathogens, leading to NK cells of distinct potency.

Conclusion

In my thesis, it could be shown that different types of cancer overexpress and secrete GDF-15. This growth factor is mainly expressed under pathological conditions and to low extent in healthy tissue, which is – from a regulatory perspective- a prerequisite for a contemplable therapeutic target molecule. GDF-15 expression was not only described to correlate with poor prognosis in several types of cancer. Several reports even attributed an immunomodulatory function to GDF-15, which was in line with our observation, that GDF-15 repressed the expression of the surface NKG2D receptor on NK and CD8⁺ T cells. Furthermore, the adhesion of CD4⁺ and CD8⁺ T cells to primary human endothelial cells (HUVEC) was decreased. Accordingly, GDF-15 might negatively influence effector cells of the lymphoid lineage in regard to their killing capability as well as their ability to transmigrate into the tumor microenvironment. A proper antitumor response requires not only functional cytotoxic T cells but also the presence of these immune subsets at the site of malignancy in order to ensure the necessary effector to target cell contact. Our *in vitro* findings therefore led to the conclusion that GDF-15 might contribute to tumor immune evasion. The fact, that tumor growth inhibition as well as an enhanced immune cell infiltration within the tumor microenvironment could be observed in GDF-15 knock down glioma cell bearing mice, supported this conclusion.

We speculate, that GDF-15 bears different mode of actions which harm cancer patients: On one hand GDF-15 induces tumor associated cachexia, a syndrome caused by anorexia, which in turn leads to a reduced food uptake (Johnen, Lin et al., 2007). On the other hand, GDF-15 seems to keep away immune cells from the tumor microenvironment and weakens their killing ability by mediating inter alia a NKG2D downregulation. This might be an important mode of action, which could also occur during pregnancy, where GDF-15 is required to prevent fetal abortion. Interestingly, there are remarkable analogies in the immune regulation of the human conceptus and a growing tumor (Ridolfi et al., 2009). Both tissues are recognized by the “host” immune system as an (semi-) allogenic transplant. The embryo comprises of about 50% paternal antigens recognized as foreign. Tumors typically acquire many mutations, which inevitably leads to the recognition of tumor associated antigens by the human immune system. Tumors might abuse GDF-15 to evade immune destruction by detaining effector immune cells from infiltration into the allogenic microenvironment, a mechanism initially developed in evolution to ensure a successful pregnancy.

We suggest that GDF-15 is a key factor, which contributes to escape the attack by the human immune system and thus represents a valuable target for a potential cancer therapy using blocking antibodies.

5 References

- Abul K. Abbas, A. H. L., Shiv Pillai (2007). Cellular and molecular immunology 6th edition.
- Adorno, M., M. Cordenonsi, M. Montagner, S. Dupont, C. Wong, B. Hann, A. Solari, S. Bobisse, M. B. Rondina, V. Guzzardo, A. R. Parenti, A. Rosato, S. Bicciato, A. Balmain and S. Piccolo (2009). "A Mutant-p53/Smad complex opposes p63 to empower TGFbeta-induced metastasis." Cell **137**(1): 87-98.
- Al-Lazikani, B., A. M. Lesk and C. Chothia (1997). "Standard conformations for the canonical structures of immunoglobulins1." Journal of Molecular Biology **273**(4): 927-948.
- Albertoni, M., P. H. Shaw, M. Nozaki, S. Godard, M. Tenan, M. F. Hamou, D. W. Fairlie, S. N. Breit, V. M. Paralkar, N. de Tribolet, E. G. Van Meir and M. E. Hegi (2002). "Anoxia induces macrophage inhibitory cytokine-1 (MIC-1) in glioblastoma cells independently of p53 and HIF-1." Oncogene **21**(27): 4212-4219.
- Alberts B., J. A., Lewis J., et al. (2002). "Molecular Biology of the Cell. 4th edition." New York: Garland Science **4th**.
- Alderson, K. L. and P. M. Sondel (2011). "Clinical cancer therapy by NK cells via antibody-dependent cell-mediated cytotoxicity." J Biomed Biotechnol **2011**: 379123.
- Alderton, G. K. and Y. Bordon (2012). "Tumour immunotherapy — leukocytes take up the fight." Nature Reviews Immunology **12**(4): 237-237.
- An, Z. (2008). "Antibody Therapeutics - a mini review." TRENDS IN BIO/PHARMACEUTICAL INDUSTRY **2**.
- Arteaga, C. L. (2006). "Inhibition of TGFβ signaling in cancer therapy." Current Opinion in Genetics & Development **16**(1): 30-37.
- Aw Yong, K. M., Y. Zeng, D. Vindivich, J. M. Phillip, P. H. Wu, D. Wirtz and R. H. Getzenberg (2014). "Morphological effects on expression of growth differentiation factor 15 (GDF15), a marker of metastasis." J Cell Physiol **229**(3): 362-373.
- Baba AI., C. C. (2007). "Comparative Oncology. 2007. Chapter 3, TUMOR CELL MORPHOLOGY " Bucharest: The Publishing House of the Romanian Academy.
- Baek, K. E., S. R. Yoon, J. T. Kim, K. S. Kim, S. H. Kang, Y. Yang, J. S. Lim, I. Choi, M. S. Nam, M. Yoon and H. G. Lee (2009). "Upregulation and secretion of macrophage inhibitory cytokine-1 (MIC-1) in gastric cancers." Clin Chim Acta **401**(1-2): 128-133.
- Baek, S. J., K.-S. Kim, J. B. Nixon, L. C. Wilson and T. E. Eling (2001). "Cyclooxygenase Inhibitors Regulate the Expression of a TGF-β Superfamily Member That Has Proapoptotic and Antitumorigenic Activities." Molecular Pharmacology **59**(4): 901-908.
- Baek, S. J., L. C. Wilson, C.-H. Lee and T. E. Eling (2002). "Dual Function of Nonsteroidal Anti-Inflammatory Drugs (NSAIDs): Inhibition of Cyclooxygenase and Induction of NSAID-

- Activated Gene." Journal of Pharmacology and Experimental Therapeutics **301**(3): 1126-1131.
- Baert, F., M. Noman, S. Vermeire, G. Van Assche, D. H. G, A. Carbonez and P. Rutgeerts (2003). "Influence of immunogenicity on the long-term efficacy of infliximab in Crohn's disease." N Engl J Med **348**(7): 601-608.
- Bahram, S., M. Bresnahan, D. E. Geraghty and T. Spies (1994). "A second lineage of mammalian major histocompatibility complex class I genes." Proc Natl Acad Sci U S A **91**(14): 6259-6263.
- Bakema, J. and M. van Egmond (2014). Fc Receptor-Dependent Mechanisms of Monoclonal Antibody Therapy of Cancer. Fc Receptors. M. Daeron and F. Nimmerjahn, Springer International Publishing. **382**: 373-392.
- Bakema, J. E. and M. van Egmond (2014). "Fc receptor-dependent mechanisms of monoclonal antibody therapy of cancer." Curr Top Microbiol Immunol **382**: 373-392.
- Baselga, J. (2010). "Treatment of HER2-overexpressing breast cancer." Annals of Oncology **21**(suppl 7): vii36-vii40.
- Bauskin, A. R., D. A. Brown, T. Kuffner, H. Johnen, X. W. Luo, M. Hunter and S. N. Breit (2006). "Role of macrophage inhibitory cytokine-1 in tumorigenesis and diagnosis of cancer." Cancer Res **66**(10): 4983-4986.
- Bauskin, A. R., L. Jiang, X. W. Luo, L. Wu, D. A. Brown and S. N. Breit (2010). "The TGF-beta superfamily cytokine MIC-1/GDF15: secretory mechanisms facilitate creation of latent stromal stores." J Interferon Cytokine Res **30**(6): 389-397.
- Bauskin, A. R., H. P. Zhang, W. D. Fairlie, X. Y. He, P. K. Russell, A. G. Moore, D. A. Brown, K. K. Stanley and S. N. Breit (2000). "The propeptide of macrophage inhibitory cytokine (MIC-1), a TGF-beta superfamily member, acts as a quality control determinant for correctly folded MIC-1." Embo j **19**(10): 2212-2220.
- Bellone, M. and A. Calcinotto (2013). "Ways to Enhance Lymphocyte Trafficking into Tumors and Fitness of Tumor Infiltrating Lymphocytes." Frontiers in Oncology **3**: 231.
- Benjamin Anderson, T. B., Freddie Bray, Carol DeSantis (2011). Global Cancer Facts & Figures 3rd Edition. A. C. Society.
- Bernstein, C., A. R. Prasad, V. Nfonam and H. Bernstein (2013). DNA Damage, DNA Repair and Cancer.
- Biswas, S., M. Guix, C. Rinehart, T. C. Dugger, A. Chytil, H. L. Moses, M. L. Freeman and C. L. Arteaga (2007). "Inhibition of TGF- β with neutralizing antibodies prevents radiation-induced acceleration of metastatic cancer progression." Journal of Clinical Investigation **117**(5): 1305-1313.
- Blay, J. Y., A. Le Cesne, L. Alberti and I. Ray-Coquart (2005). "Targeted cancer therapies." Bull Cancer **92**(2): E13-18.

- Boise, L. H., A. J. Minn, P. J. Noel, C. H. June, M. A. Accavitti, T. Lindsten and C. B. Thompson (2010). "CD28 costimulation can promote T cell survival by enhancing the expression of Bcl-xL. *Immunity*. 1995. 3: 87-98." *J Immunol* **185**(7): 3788-3799.
- Bommireddy, R. and T. Doetschman (2004). "TGF-beta, T-cell tolerance and anti-CD3 therapy." *Trends Mol Med* **10**(1): 3-9.
- Bonaterrea, G. A., S. Zugel, J. Thogersen, S. A. Walter, U. Haberkorn, J. Strelau and R. Kinscherf (2012). "Growth differentiation factor-15 deficiency inhibits atherosclerosis progression by regulating interleukin-6-dependent inflammatory response to vascular injury." *J Am Heart Assoc* **1**(6): e002550.
- Boniol, M., P. Autier, P. Boyle and S. Gandini (2012). "Cutaneous melanoma attributable to sunbed use: systematic review and meta-analysis." *Bmj* **345**: e4757.
- Bootcov, M. R., A. R. Bauskin, S. M. Valenzuela, A. G. Moore, M. Bansal, X. Y. He, H. P. Zhang, M. Donnellan, S. Mahler, K. Pryor, B. J. Walsh, R. C. Nicholson, W. D. Fairlie, S. B. Por, J. M. Robbins and S. N. Breit (1997). "MIC-1, a novel macrophage inhibitory cytokine, is a divergent member of the TGF-beta superfamily." *Proc Natl Acad Sci U S A* **94**(21): 11514-11519.
- Bottino C, R. C., L Moretta, A Moretta (2005). "Cellular ligands of activating NK receptors." *Trends in Immunology* **26**: 221-226.
- Boyle, G. M., J. Pedley, A. C. Martyn, K. J. Banducci, G. M. Stratton, D. A. Brown, S. N. Breit and P. G. Parsons (2009). "Macrophage inhibitory cytokine-1 is overexpressed in malignant melanoma and is associated with tumorigenicity." *J Invest Dermatol* **129**(2): 383-391.
- Breit, S. N., H. Johnen, A. D. Cook, V. W. Tsai, M. G. Mohammad, T. Kuffner, H. P. Zhang, C. P. Marquis, L. Jiang, G. Lockwood, M. Lee-Ng, Y. Husaini, L. Wu, J. A. Hamilton and D. A. Brown (2011). "The TGF-beta superfamily cytokine, MIC-1/GDF15: a pleiotropic cytokine with roles in inflammation, cancer and metabolism." *Growth Factors* **29**(5): 187-195.
- Brennan, F. R., L. D. Morton, S. Spindeldreher, A. Kiessling, R. Allenspach, A. Hey, P. Y. Muller, W. Frings and J. Sims (2010). "Safety and immunotoxicity assessment of immunomodulatory monoclonal antibodies." *MAbs* **2**(3): 233-255.
- Brown, D. A., F. Lindmark, P. Stattin, K. Balter, H. O. Adami, S. L. Zheng, J. Xu, W. B. Isaacs, H. Gronberg, S. N. Breit and F. E. Wiklund (2009). "Macrophage inhibitory cytokine 1: a new prognostic marker in prostate cancer." *Clin Cancer Res* **15**(21): 6658-6664.
- Brown, D. A., R. L. Ward, P. Buckhaults, T. Liu, K. E. Romans, N. J. Hawkins, A. R. Bauskin, K. W. Kinzler, B. Vogelstein and S. N. Breit (2003). "MIC-1 Serum Level and Genotype: Associations with Progress and Prognosis of Colorectal Carcinoma." *Clinical Cancer Research* **9**(7): 2642-2650.
- Browne, K. A., E. Blink, V. R. Sutton, C. J. Froelich, D. A. Jans and J. A. Trapani (1999). "Cytosolic delivery of granzyme B by bacterial toxins: evidence that endosomal disruption, in addition to transmembrane pore formation, is an important function of perforin." *Mol Cell Biol* **19**(12): 8604-8615.

- Bruzzese, F., C. Hagglof, A. Leone, E. Sjoberg, M. S. Roca, S. Kiflemariam, T. Sjoblom, P. Hammarsten, L. Egevad, A. Bergh, A. Ostman, A. Budillon and M. Augsten (2014). "Local and systemic protumorigenic effects of cancer-associated fibroblast-derived GDF15." Cancer Res **74**(13): 3408-3417.
- Bubeník (2003). "Tumour MHC class I downregulation and immunotherapy (Review)." Oncology Reports **10**(6): 2005-2008.
- Buijs, J. T., K. R. Stayrook and T. A. Guise (2012). "The role of TGF-beta in bone metastasis: novel therapeutic perspectives." Bonekey Rep **1**: 96.
- Burd, E. M. (2003). "Human Papillomavirus and Cervical Cancer." Clinical Microbiology Reviews **16**(1): 1-17.
- Burke-Gaffney, A. and P. G. Hellewell (1996). "Tumour necrosis factor-alpha-induced ICAM-1 expression in human vascular endothelial and lung epithelial cells: modulation by tyrosine kinase inhibitors." British Journal of Pharmacology **119**(6): 1149-1158.
- Burnet (1957). "Cancer: a biological approach " Br Med J **1**: 779-786.
- Caja, F. and L. Vannucci (2015). "TGFbeta: A player on multiple fronts in the tumor microenvironment." J Immunotoxicol **12**(3): 300-307.
- Cerwenka, A. and L. L. Lanier (2001). "Natural killer cells, viruses and cancer." Nat Rev Immunol **1**(1): 41-49.
- Chames, P., M. Van Regenmortel, E. Weiss and D. Baty (2009). "Therapeutic antibodies: successes, limitations and hopes for the future." British Journal of Pharmacology **157**(2): 220-233.
- Chew, V., J. Chen, D. Lee, E. Loh, J. Lee, K. H. Lim, A. Weber, K. Slankamenac, R. T. P. Poon, H. Yang, L. L. P. J. Ooi, H. C. Toh, M. Heikenwalder, I. O. L. Ng, A. Nardin and J.-P. Abastado (2012). "Chemokine-driven lymphocyte infiltration: an early intratumoural event determining long-term survival in resectable hepatocellular carcinoma." Gut **61**(3): 427-438.
- Chowdhury, D. and J. Lieberman (2008). "Death by a Thousand Cuts: Granzyme Pathways of Programmed Cell Death." Annual review of immunology **26**: 389-420.
- Chua, H. L., Y. Serov and Z. Brahmi (2004). "Regulation of FasL expression in natural killer cells." Hum Immunol **65**(4): 317-327.
- Coder, B. D., H. Wang, L. Ruan and D. M. Su (2015). "Thymic involution perturbs negative selection leading to autoreactive T cells that induce chronic inflammation." J Immunol **194**(12): 5825-5837.
- Cohen, S. N., A. C. Chang, H. W. Boyer and R. B. Helling (1973). "Construction of biologically functional bacterial plasmids in vitro." Proc Natl Acad Sci U S A **70**(11): 3240-3244.

- Cooper, G. (2000). *The Cell: A Molecular Approach. Tumor Suppressor Genes*. Sunderland (MA), Sinauer Associates. **2nd edition**.
- Corre, J., E. Labat, N. Espagnolle, B. Hebraud, H. Avet-Loiseau, M. Roussel, A. Huynh, M. Gadelorge, P. Cordelier, B. Klein, P. Moreau, T. Facon, J. J. Fournie, M. Attal and P. Bourin (2012). "Bioactivity and prognostic significance of growth differentiation factor GDF15 secreted by bone marrow mesenchymal stem cells in multiple myeloma." *Cancer Res* **72**(6): 1395-1406.
- Cosman, D., J. Mullberg, C. L. Sutherland, W. Chin, R. Armitage, W. Fanslow, M. Kubin and N. J. Chalupny (2001). "ULBPs, novel MHC class I-related molecules, bind to CMV glycoprotein UL16 and stimulate NK cytotoxicity through the NKG2D receptor." *Immunity* **14**(2): 123-133.
- Coulie, P. G., B. J. Van den Eynde, P. van der Bruggen and T. Boon (2014). "Tumour antigens recognized by T lymphocytes: at the core of cancer immunotherapy." *Nat Rev Cancer* **14**(2): 135-146.
- Courtois, A., S. Gac-Breton, C. Berthou, J. Guézennec, A. Bordron and C. Boisset (2012). Complement dependent cytotoxicity activity of therapeutic antibody fragments is acquired by immunogenic glycan coupling.
- Covell, D. G., J. Barbet, O. D. Holton, C. D. Black, R. J. Parker and J. N. Weinstein (1986). "Pharmacokinetics of monoclonal immunoglobulin G1, F(ab')₂, and Fab' in mice." *Cancer Res* **46**(8): 3969-3978.
- Crane, C. A., S. J. Han, J. J. Barry, B. J. Ahn, L. L. Lanier and A. T. Parsa (2010). "TGF-beta downregulates the activating receptor NKG2D on NK cells and CD8+ T cells in glioma patients." *Neuro Oncol* **12**(1): 7-13.
- Cuenca, A., F. Cheng, H. Wang, J. Brayer, P. Horna, L. Gu, H. Bien, I. M. Borrello, H. I. Levitsky and E. M. Sotomayor (2003). "Extra-Lymphatic Solid Tumor Growth Is Not Immunologically Ignored and Results in Early Induction of Antigen-Specific T-Cell Anergy: Dominant Role of Cross-Tolerance to Tumor Antigens." *Cancer Res* **63**(24): 9007-9015.
- Dahlin, A. M., M. L. Henriksson, B. Van Guelpen, R. Stenling, A. Oberg, J. Rutegard and R. Palmqvist (2011). "Colorectal cancer prognosis depends on T-cell infiltration and molecular characteristics of the tumor." *Mod Pathol* **24**(5): 671-682.
- Davies, M. A. and Y. Samuels (2010). "Analysis of the genome to personalize therapy for melanoma." *Oncogene* **29**(41): 5545-5555.
- De Bont, R. and N. van Larebeke (2004). "Endogenous DNA damage in humans: a review of quantitative data." *Mutagenesis* **19**(3): 169-185.
- de Jager, S. C., B. Bermudez, I. Bot, R. R. Koenen, M. Bot, A. Kavelaars, V. de Waard, C. J. Heijnen, F. J. Muriana, C. Weber, T. J. van Berkel, J. Kuiper, S. J. Lee, R. Abia and E. A. Biessen (2011). "Growth differentiation factor 15 deficiency protects against atherosclerosis by attenuating CCR2-mediated macrophage chemotaxis." *J Exp Med* **208**(2): 217-225.

- De, P., M. Hasmann and B. Leyland-Jones (2013). "Molecular determinants of trastuzumab efficacy: What is their clinical relevance?" Cancer Treat Rev **39**(8): 925-934.
- Derynck, R. and Y. E. Zhang (2003). "Smad-dependent and Smad-independent pathways in TGF- β family signalling." Nature **425**(6958): 577-584.
- Descot, A. and T. Oskarsson (2013). "The molecular composition of the metastatic niche." Exp Cell Res **319**(11): 1679-1686.
- Devereux, T. R., J. I. Risinger and J. C. Barrett (1999). "Mutations and altered expression of the human cancer genes: what they tell us about causes." IARC Sci Publ(146): 19-42.
- Dewys, W. D., C. Begg, P. T. Lavin, P. R. Band, J. M. Bennett, J. R. Bertino, M. H. Cohen, H. O. Douglass, Jr., P. F. Engstrom, E. Z. Ezdinli, J. Horton, G. J. Johnson, C. G. Moertel, M. M. Oken, C. Perlia, C. Rosenbaum, M. N. Silverstein, R. T. Skeel, R. W. Sponzo and D. C. Tormey (1980). "Prognostic effect of weight loss prior to chemotherapy in cancer patients. Eastern Cooperative Oncology Group." Am J Med **69**(4): 491-497.
- Diefenbach, A. and D. H. Raulet (2002). "The innate immune response to tumors and its role in the induction of T-cell immunity." Immunol Rev **188**: 9-21.
- Dillman, R. O., J. C. Beauregard, S. E. Halpern and M. Clutter (1986). "Toxicities and side effects associated with intravenous infusions of murine monoclonal antibodies." J Biol Response Mod **5**(1): 73-84.
- Dillman, R. O., D. L. Shawler, T. J. McCallister and S. E. Halpern (1994). "Human anti-mouse antibody response in cancer patients following single low-dose injections of radiolabeled murine monoclonal antibodies." Cancer Biother **9**(1): 17-28.
- Dinarello, C. A. (2007). "Historical Review of Cytokines." European journal of immunology **37**(Suppl 1): S34-S45.
- Docagne, F., N. Colloc'h, V. Bougueret, M. Page, J. Paput, M. Tripier, P. Dutartre, E. T. MacKenzie, A. Buisson, S. Komesli and D. Vivien (2001). "A soluble transforming growth factor-beta (TGF-beta) type I receptor mimics TGF-beta responses." J Biol Chem **276**(49): 46243-46250.
- Eling, T. E., S. J. Baek, M. Shim and C. H. Lee (2006). "NSAID activated gene (NAG-1), a modulator of tumorigenesis." J Biochem Mol Biol **39**(6): 649-655.
- Elsamadicy, A. A., R. Babu, J. P. Kirkpatrick and D. C. Adamson (2015). "Radiation-Induced Malignant Gliomas: A Current Review." World Neurosurgery **83**(4): 530-542.
- Fearon, E. R. and B. Vogelstein (1990). "A genetic model for colorectal tumorigenesis." Cell **61**(5): 759-767.
- Ferrara, N., K. J. Hillan, H. P. Gerber and W. Novotny (2004). "Discovery and development of bevacizumab, an anti-VEGF antibody for treating cancer." Nat Rev Drug Discov **3**(5): 391-400.

- Finlay, G. J. (1993). "Genetics, molecular biology and colorectal cancer." Mutat Res **290**(1): 3-12.
- Fisher, O. M., A. J. Levert-Mignon, S. J. Lord, K. K. Lee-Ng, N. K. Botelho, D. Falkenback, M. L. Thomas, Y. V. Bobryshev, D. C. Whiteman, D. A. Brown, S. N. Breit and R. V. Lord (2015). "MIC-1/GDF15 in Barrett's oesophagus and oesophageal adenocarcinoma." Br J Cancer **112**(8): 1384-1391.
- Forsstrom, B., B. B. Axnas, J. Rockberg, H. Danielsson, A. Bohlin and M. Uhlen (2015). "Dissecting antibodies with regards to linear and conformational epitopes." PLoS One **10**(3): e0121673.
- Fridman, W. H., F. Pages, C. Sautes-Fridman and J. Galon (2012). "The immune contexture in human tumours: impact on clinical outcome." Nat Rev Cancer **12**(4): 298-306.
- Friese, M. A., J. Wischhusen, W. Wick, M. Weiler, G. Eisele, A. Steinle and M. Weller (2004). "RNA Interference Targeting Transforming Growth Factor- β Enhances NKG2D-Mediated Antiglioma Immune Response, Inhibits Glioma Cell Migration and Invasiveness, and Abrogates Tumorigenicity In vivo." Cancer Research **64**(20): 7596-7603.
- Fu, S., N. Zhang, A. C. Yopp, D. Chen, M. Mao, D. Chen, H. Zhang, Y. Ding and J. S. Bromberg (2004). "TGF-beta induces Foxp3 + T-regulatory cells from CD4 + CD25 - precursors." Am J Transplant **4**(10): 1614-1627.
- Gatenby, R. A. and R. J. Gillies (2004). "Why do cancers have high aerobic glycolysis?" Nat Rev Cancer **4**(11): 891-899.
- Geiduschek, E. P., T. Nakamoto and S. B. Weiss (1961). "The enzymatic synthesis of RNA: complementary interaction with DNA." Proc Natl Acad Sci U S A **47**: 1405-1415.
- Gobeil, S., X. Zhu, C. J. Doillon and M. R. Green (2008). "A genome-wide shRNA screen identifies GAS1 as a novel melanoma metastasis suppressor gene." Genes & Development **22**(21): 2932-2940.
- Golay, J., M. Manganini, A. Rambaldi and M. Introna (2004). "Effect of alemtuzumab on neoplastic B cells." Haematologica **89**(12): 1476-1483.
- Goldrath AW, M. B. (1999). "Selecting and maintaining a diverse T-cell repertoire." Nature **402**: 255-262.
- Guinan, E., J. Gribben, V. Boussiotis, G. Freeman and L. Nadler (1994). Pivotal role of the B7:CD28 pathway in transplantation tolerance and tumor immunity.
- Hall, E. J. and D. J. Brenner (2008). "Cancer risks from diagnostic radiology." The British Journal of Radiology **81**(965): 362-378.
- Hanahan, D. and R. A. Weinberg (2011). "Hallmarks of cancer: the next generation." Cell **144**(5): 646-674.

- Harding, F. A., M. M. Stickler, J. Razo and R. B. DuBridg (2010). "The immunogenicity of humanized and fully human antibodies: Residual immunogenicity resides in the CDR regions." mAbs **2**(3): 256-265.
- Hecht, S. S. (1999). "Tobacco Smoke Carcinogens and Lung Cancer." Journal of the National Cancer Institute **91**(14): 1194-1210.
- Heyman, B. (1996). "Complement and Fc-receptors in regulation of the antibody response." Immunol Lett **54**(2-3): 195-199.
- Hill, G. J., 2nd, E. T. Kremetz and H. Z. Hill (1984). "Dimethyl triazeno imidazole carboxamide and combination therapy for melanoma. IV. Late results after complete response to chemotherapy (Central Oncology Group protocols 7130, 7131, and 7131A)." Cancer **53**(6): 1299-1305.
- Höchst, B. and L. Diehl (2012). "Antigen shedding into the circulation contributes to tumor immune escape." Oncoimmunology **1**(9): 1620-1622.
- Honig, A., L. Rieger, M. Kapp, J. Dietl and U. Kammerer (2005). "Immunohistochemistry in human placental tissue--pitfalls of antigen detection." J Histochem Cytochem **53**(11): 1413-1420.
- Hromas, R., M. Hufford, J. Sutton, D. Xu, Y. Li and L. Lu (1997). "PLAB, a novel placental bone morphogenetic protein." Biochimica et Biophysica Acta (BBA) - Gene Structure and Expression **1354**(1): 40-44.
- Hudis, C. A. (2007). "Trastuzumab--mechanism of action and use in clinical practice." N Engl J Med **357**(1): 39-51.
- Huh, S. J., C. Y. Chung, A. Sharma and G. P. Robertson (2010). "Macrophage inhibitory cytokine-1 regulates melanoma vascular development." Am J Pathol **176**(6): 2948-2957.
- Husaini, Y., M. R. Qiu, G. P. Lockwood, X. W. Luo, P. Shang, T. Kuffner, V. W. Tsai, L. Jiang, P. J. Russell, D. A. Brown and S. N. Breit (2012). "Macrophage inhibitory cytokine-1 (MIC-1/GDF15) slows cancer development but increases metastases in TRAMP prostate cancer prone mice." PLoS One **7**(8): e43833.
- Hussein, M. R. (2005). "Ultraviolet radiation and skin cancer: molecular mechanisms." Journal of Cutaneous Pathology **32**(3): 191-205.
- Inui, A. (1999). "Cancer Anorexia-Cachexia Syndrome: Are Neuropeptides the Key?" Cancer Research **59**(18): 4493-4501.
- Janeway CA Jr, T. P., Walport M, et al. (2001). Immunobiology: The Immune System in Health and Disease. 5th edition.
- Johnen, H., S. Lin, T. Kuffner, D. A. Brown, V. W. Tsai, A. R. Bauskin, L. Wu, G. Pankhurst, L. Jiang, S. Junankar, M. Hunter, W. D. Fairlie, N. J. Lee, R. F. Enriquez, P. A. Baldock, E. Corey, F. S. Apple, M. M. Murakami, E. J. Lin, C. Wang, M. J. During, A. Sainsbury, H. Herzog and S. N. Breit (2007). "Tumor-induced anorexia and weight loss are mediated by the TGF-beta superfamily cytokine MIC-1." Nat Med **13**(11): 1333-1340.

- Kadara, H., C. P. Schroeder, D. Lotan, C. Pisano and R. Lotan (2006). "Induction of GDF-15/NAG-1/MIC-1 in human lung carcinoma cells by retinoid-related molecules and assessment of its role in apoptosis." Cancer Biol Ther **5**(5): 518-522.
- Kammerer, U., A. Germeyer, S. Stengel, M. Kapp and J. Denner (2011). "Human endogenous retrovirus K (HERV-K) is expressed in villous and extravillous cytotrophoblast cells of the human placenta." J Reprod Immunol **91**(1-2): 1-8.
- Kammerer, U., O. Gires, N. Pfetzer, A. Wiegner, R. J. Klement and C. Otto (2015). "TKTL1 expression in human malign and benign cell lines." BMC Cancer **15**: 2.
- Kastrinos, F. and S. Syngal (2011). "Inherited colorectal cancer syndromes." Cancer J **17**(6): 405-415.
- Kempf, T., A. Zarbock, C. Widera, S. Butz, A. Stadtmann, J. Rossaint, M. Bolomini-Vittori, M. Korf-Klingebiel, L. C. Napp, B. Hansen, A. Kanwischer, U. Bavendiek, G. Beutel, M. Hapke, M. G. Sauer, C. Laudanna, N. Hogg, D. Vestweber and K. C. Wollert (2011). "GDF-15 is an inhibitor of leukocyte integrin activation required for survival after myocardial infarction in mice." Nat Med **17**(5): 581-588.
- Kettleborough, C. A., J. Saldanha, V. J. Heath, C. J. Morrison and M. M. Bendig (1991). "Humanization of a mouse monoclonal antibody by CDR-grafting: the importance of framework residues on loop conformation." Protein Eng **4**(7): 773-783.
- Kim, K. K., J. J. Lee, Y. Yang, K. H. You and J. H. Lee (2008). "Macrophage inhibitory cytokine-1 activates AKT and ERK-1/2 via the transactivation of ErbB2 in human breast and gastric cancer cells." Carcinogenesis **29**(4): 704-712.
- Kim, R., M. Emi and K. Tanabe (2007). "Cancer immunoediting from immune surveillance to immune escape." Immunology **121**(1): 1-14.
- Kingsley, D. M. (1994). "The TGF-beta superfamily: new members, new receptors, and new genetic tests of function in different organisms." Genes & Development **8**(2): 133-146.
- Klee, G. G. (2000). "Human anti-mouse antibodies." Arch Pathol Lab Med **124**(6): 921-923.
- Kmiecik, J., A. Poli, N. H. C. Brons, A. Waha, G. E. Eide, P. Ø. Enger, J. Zimmer and M. Chekenya (2013). "Elevated CD3+ and CD8+ tumor-infiltrating immune cells correlate with prolonged survival in glioblastoma patients despite integrated immunosuppressive mechanisms in the tumor microenvironment and at the systemic level." Journal of Neuroimmunology **264**(1-2): 71-83.
- Köhler, G. and C. Milstein (2005). "Pillars Article: Continuous cultures of fused cells secreting antibody of predefined specificity. Nature, 1975, 256 (5517): 495-497." The Journal of Immunology **174**(5): 2453-2455.
- Koopmann, J., P. Buckhaults, D. A. Brown, M. L. Zahurak, N. Sato, N. Fukushima, L. J. Sokoll, D. W. Chan, C. J. Yeo, R. H. Hruban, S. N. Breit, K. W. Kinzler, B. Vogelstein and M. Goggins (2004). "Serum macrophage inhibitory cytokine 1 as a marker of pancreatic and other periampullary cancers." Clin Cancer Res **10**(7): 2386-2392.

- Krieg, A. J., E. B. Rankin, D. Chan, O. Razorenova, S. Fernandez and A. J. Giaccia (2010). "Regulation of the Histone Demethylase JMJD1A by Hypoxia-Inducible Factor 1 α Enhances Hypoxic Gene Expression and Tumor Growth." Molecular and Cellular Biology **30**(1): 344-353.
- Kucik, D. F. and C. Wu (2005). "Cell-adhesion assays." Methods Mol Biol **294**: 43-54.
- Kunkel EJ, E. B. (2002). "Chemokines and the tissue specific migration of lymphocytes." Immunity **16**: 1-4.
- Kutz, S. M., J. Hordines, P. J. McKeown-Longo and P. J. Higgins (2001). "TGF- β 1-induced PAI-1 gene expression requires MEK activity and cell-to-substrate adhesion." Journal of Cell Science **114**(21): 3905-3914.
- Kuus-Reichel, K., L. S. Grauer, L. M. Karavodin, C. Knott, M. Krusemeier and N. E. Kay (1994). "Will immunogenicity limit the use, efficacy, and future development of therapeutic monoclonal antibodies?" Clin Diagn Lab Immunol **1**(4): 365-372.
- Laemmli, U. K. (1970). "Cleavage of structural proteins during the assembly of the head of bacteriophage T4." Nature **227**(5259): 680-685.
- Lanier, L. L. (1998). "NK cell receptors." Annu Rev Immunol **16**: 359-393.
- Law, S. K. (1991). "Antigen shedding and metastasis of tumour cells." Clin Exp Immunol **85**(1): 1-2.
- Leal, M., P. Sapra, S. A. Hurvitz, P. Senter, A. Wahl, M. Schutten, D. K. Shah, N. Haddish-Berhane and O. Kabbarah (2014). "Antibody-drug conjugates: an emerging modality for the treatment of cancer." Ann N Y Acad Sci **1321**: 41-54.
- Lee, D. H., Y. Yang, S. J. Lee, K. Y. Kim, T. H. Koo, S. M. Shin, K. S. Song, Y. H. Lee, Y. J. Kim, J. J. Lee, I. Choi and J. H. Lee (2003). "Macrophage inhibitory cytokine-1 induces the invasiveness of gastric cancer cells by up-regulating the urokinase-type plasminogen activator system." Cancer Res **63**(15): 4648-4655.
- Lee, J. C., K. M. Lee, D. W. Kim and D. S. Heo (2004). "Elevated TGF- 1 Secretion and Down-Modulation of NKG2D Underlies Impaired NK Cytotoxicity in Cancer Patients." The Journal of Immunology **172**(12): 7335-7340.
- Ley, K., C. Laudanna, M. I. Cybulsky and S. Nourshargh (2007). "Getting to the site of inflammation: the leukocyte adhesion cascade updated." Nat Rev Immunol **7**(9): 678-689.
- Li, J., L. Yang, W. Qin, G. Zhang, J. Yuan and F. Wang (2013). "Adaptive induction of growth differentiation factor 15 attenuates endothelial cell apoptosis in response to high glucose stimulus." PLoS One **8**(6): e65549.
- Liang, C. C., A. Y. Park and J. L. Guan (2007). "In vitro scratch assay: a convenient and inexpensive method for analysis of cell migration in vitro." Nat Protoc **2**(2): 329-333.

- Liebmann, J. E., J. A. Cook, C. Lipschultz, D. Teague, J. Fisher and J. B. Mitchell (1993). "Cytotoxic studies of paclitaxel (Taxol) in human tumour cell lines." British Journal of Cancer **68**(6): 1104-1109.
- Lin, C., R. McGough, B. Aswad, J. A. Block and R. Terek (2004). "Hypoxia induces HIF-1alpha and VEGF expression in chondrosarcoma cells and chondrocytes." J Orthop Res **22**(6): 1175-1181.
- Liu, T., A. R. Bauskin, J. Zaunders, D. A. Brown, S. Pankhurst, P. J. Russell and S. N. Breit (2003). "Macrophage inhibitory cytokine 1 reduces cell adhesion and induces apoptosis in prostate cancer cells." Cancer Res **63**(16): 5034-5040.
- Lodish H, B. A., Zipursky SL, et al. (2000). Tumor Cells and the Onset of Cancer / Section 24.1, . Molecular Cell Biology. 4th edition. New York, W. H. Freeman.
- LoRusso, P. M., D. Weiss, E. Guardino, S. Girish and M. X. Sliwkowski (2011). "Trastuzumab Emtansine: A Unique Antibody-Drug Conjugate in Development for Human Epidermal Growth Factor Receptor 2-Positive Cancer." Clinical Cancer Research **17**(20): 6437-6447.
- Lu, B. and O. J. Finn (2008). "T-cell death and cancer immune tolerance." Cell Death Differ **15**(1): 70-79.
- Luther, U., S. Dichmann, A. Schlobe, W. Czech and J. Norgauer (2000). "[UV light and skin cancer]." Med Monatsschr Pharm **23**(8): 261-266.
- Malmqvist, M. (1993). "Surface plasmon resonance for detection and measurement of antibody-antigen affinity and kinetics." Curr Opin Immunol **5**(2): 282-286.
- Mapara, M. Y. and M. Sykes (2004). "Tolerance and cancer: mechanisms of tumor evasion and strategies for breaking tolerance." J Clin Oncol **22**(6): 1136-1151.
- Marcucci, F., M. Bellone, C. Rumio and A. Corti (2013). "Approaches to improve tumor accumulation and interactions between monoclonal antibodies and immune cells." MABs **5**(1): 34-46.
- Massague, J. (2008). "TGFbeta in Cancer." Cell **134**(2): 215-230.
- Mehta, R. S., D. Q. Chong, M. Song, J. A. Meyerhardt, K. Ng, R. Nishihara, Z. Qian, T. Morikawa, K. Wu, E. L. Giovannucci, C. S. Fuchs, S. Ogino and A. T. Chan (2015). "Association Between Plasma Levels of Macrophage Inhibitory Cytokine-1 Before Diagnosis of Colorectal Cancer and Mortality." Gastroenterology **149**(3): 614-622.
- Middeldorp, J. M. and R. H. Melen (1988). "Epitope-mapping on the Epstein-Barr virus major capsid protein using systematic synthesis of overlapping oligopeptides." J Virol Methods **21**(1-4): 147-159.
- Mimeault, M. and S. K. Batra (2010). "Divergent molecular mechanisms underlying the pleiotropic functions of macrophage inhibitory cytokine-1 in cancer." J Cell Physiol **224**(3): 626-635.

- Min, K. W., J. L. Liggett, G. Silva, W. W. Wu, R. Wang, R. F. Shen, T. E. Eling and S. J. Baek (2015). "NAG-1/GDF15 accumulates in the nucleus and modulates transcriptional regulation of the Smad pathway." Oncogene.
- Moore, A. G., D. A. Brown, W. D. Fairlie, A. R. Bauskin, P. K. Brown, M. L. Munier, P. K. Russell, L. A. Salamonsen, E. M. Wallace and S. N. Breit (2000). "The transforming growth factor- β superfamily cytokine macrophage inhibitory cytokine-1 is present in high concentrations in the serum of pregnant women." J Clin Endocrinol Metab **85**(12): 4781-4788.
- Morrison, S. L., M. J. Johnson, L. A. Herzenberg and V. T. Oi (1984). "Chimeric human antibody molecules: mouse antigen-binding domains with human constant region domains." Proc Natl Acad Sci U S A **81**(21): 6851-6855.
- Mullis, K. B. (1990). "Target amplification for DNA analysis by the polymerase chain reaction." Ann Biol Clin (Paris) **48**(8): 579-582.
- Nadler, L. M., P. Stashenko, R. Hardy, W. D. Kaplan, L. N. Button, D. W. Kufe, K. H. Antman and S. F. Schlossman (1980). "Serotherapy of a Patient with a Monoclonal Antibody Directed against a Human Lymphoma-associated Antigen." Cancer Research **40**(9): 3147-3154.
- Near, R. I. (1992). "Gene conversion of immunoglobulin variable regions in mutagenesis cassettes by replacement PCR mutagenesis." Biotechniques **12**(1): 88-97.
- Nelson, A. L., E. Dhimolea and J. M. Reichert (2010). "Development trends for human monoclonal antibody therapeutics." Nat Rev Drug Discov **9**(10): 767-774.
- Newton, P., G. O'Boyle, Y. Jenkins, S. Ali and J. A. Kirby (2009). "T cell extravasation: Demonstration of synergy between activation of CXCR3 and the T cell receptor." Molecular Immunology **47**(2-3): 485-492.
- Nimmerjahn, F., S. Gordan and A. Lux (2015). "Fc γ R dependent mechanisms of cytotoxic, agonistic, and neutralizing antibody activities." Trends in Immunology **36**(6): 325-336.
- Oelkrug, C. and J. M. Ramage (2014). "Enhancement of T cell recruitment and infiltration into tumours." Clinical & Experimental Immunology **178**(1): 1-8.
- Oldham, R. K. and R. O. Dillman (2008). "Monoclonal Antibodies in Cancer Therapy: 25 Years of Progress." Journal of Clinical Oncology **26**(11): 1774-1777.
- Orzechowski, A., A. A. Rostagno, S. Pucci and G. Chiochia (2014). "Cytokines and Disease." Mediators of Inflammation **2014**: 2.
- Pages, F., J. Galon, M. C. Dieu-Nosjean, E. Tartour, C. Sautès-Fridman and W. H. Fridman (2009). "Immune infiltration in human tumors: a prognostic factor that should not be ignored." Oncogene **29**(8): 1093-1102.
- Pahl, J. and A. Cerwenka "Tricking the balance: NK cells in anti-cancer immunity." Immunobiology.

- Palmer, E. (2003). "Negative selection [mdash] clearing out the bad apples from the T-cell repertoire." Nat Rev Immunol **3**(5): 383-391.
- Palucka, K. and J. Banchereau (2012). "Cancer immunotherapy via dendritic cells." Nat Rev Cancer **12**(4): 265-277.
- Pegram, H. J., D. M. Andrews, M. J. Smyth, P. K. Darcy and M. H. Kershaw (2011). "Activating and inhibitory receptors of natural killer cells." Immunol Cell Biol **89**(2): 216-224.
- Pende, D., C. Bottino, R. Castriconi, C. Cantoni, S. Marcenaro, P. Rivera, G. M. Spaggiari, A. Dondero, B. Carnemolla, N. Reymond, M. C. Mingari, M. Lopez, L. Moretta and A. Moretta (2005). "PVR (CD155) and Nectin-2 (CD112) as ligands of the human DNAM-1 (CD226) activating receptor: involvement in tumor cell lysis." Mol Immunol **42**(4): 463-469.
- Pereira, A. A., J. F. Rego, V. Morris, M. J. Overman, C. Eng, C. R. Garrett, A. T. Boutin, R. Ferrarotto, M. Lee, Z. Q. Jiang, P. M. Hoff, J. N. Vauthey, E. Vilar, D. Maru and S. Kopetz (2015). "Association between KRAS mutation and lung metastasis in advanced colorectal cancer." Br J Cancer **112**(3): 424-428.
- Pindjakova, J. and M. D. Griffin (2011). "Defective neutrophil rolling and transmigration in acute uremia." Kidney Int **80**(5): 447-450.
- Prendergast, G. C. (2008). "Immune escape as a fundamental trait of cancer: focus on IDO." Oncogene **27**(28): 3889-3900.
- Raulet, D. H. and R. E. Vance (2006). "Self-tolerance of natural killer cells." Nat Rev Immunol **6**(7): 520-531.
- Ravetch, J. V. and L. L. Lanier (2000). "Immune inhibitory receptors." Science **290**(5489): 84-89.
- Reff, M. E., K. Carner, K. S. Chambers, P. C. Chinn, J. E. Leonard, R. Raab, R. A. Newman, N. Hanna and D. R. Anderson (1994). "Depletion of B cells in vivo by a chimeric mouse human monoclonal antibody to CD20." Blood **83**(2): 435-445.
- Renart, J., J. Reiser and G. R. Stark (1979). "Transfer of proteins from gels to diazobenzyloxymethyl-paper and detection with antisera: a method for studying antibody specificity and antigen structure." Proceedings of the National Academy of Sciences of the United States of America **76**(7): 3116-3120.
- Ridolfi, L., M. Petrini, L. Fiammenghi, A. Riccobon and R. Ridolfi (2009). "Human embryo immune escape mechanisms rediscovered by the tumor." Immunobiology **214**(1): 61-76.
- Robinson, B. W. S., R. A. Lake, D. J. Nelson, B. A. Scott and A. L. Marzo (1999). "Cross-presentation of tumour antigens: Evaluation of threshold, duration, distribution and regulation." Immunol Cell Biol **77**(6): 552-558.
- Roth, P., M. Junker, I. Tritschler, M. Mittelbronn, Y. Dombrowski, S. N. Breit, G. Tabatabai, W. Wick, M. Weller and J. Wischhusen (2010). "GDF-15 contributes to proliferation and immune escape of malignant gliomas." Clin Cancer Res **16**(15): 3851-3859.

- Rothkamm, K. and M. Löbrich (2003). "Evidence for a lack of DNA double-strand break repair in human cells exposed to very low x-ray doses." Proceedings of the National Academy of Sciences of the United States of America **100**(9): 5057-5062.
- Rouas-Freiss, N., P. Moreau, S. Ferrone and E. D. Carosella (2005). "HLA-G proteins in cancer: do they provide tumor cells with an escape mechanism?" Cancer Res **65**(22): 10139-10144.
- Rybicki, B. A., D. Chitale, N. Gupta, L. Jackson, T. Wheeler, S. Trudeau, M. Jankowski, K. Bobbitt, A. Rundle and D. Tang (2015). "Abstract 849: The changing role of GDF15 (growth/differentiation factor 15) during prostate carcinogenesis." Cancer Research **75**(15 Supplement): 849.
- Sambrook J., M. T., Russel D.W. (2001). Molecular cloning: a laboratory manual 3rd edition.
- Samulitis, B. K., R. T. Dorr and H.-H. S. Chow (2011). "Interaction of Dacarbazine and Imexon, In Vitro and In Vivo, in Human A375 Melanoma Cells." Anticancer Research **31**(9): 2781-2785.
- Santibanez, J. F., M. Quintanilla and C. Bernabeu (2011). "TGF-beta/TGF-beta receptor system and its role in physiological and pathological conditions." Clin Sci (Lond) **121**(6): 233-251.
- Sanz, G., I. Leray, A. Dewaele, J. Sobilo, S. Lerondel, S. Bouet, D. Grebert, R. Monnerie, E. Pajot-Augy and L. M. Mir (2014). "Promotion of cancer cell invasiveness and metastasis emergence caused by olfactory receptor stimulation." PLoS One **9**(1): e85110.
- Scheffe, J. H., K. E. Lehmann, I. R. Buschmann, T. Unger and H. Funke-Kaiser (2006). "Quantitative real-time RT-PCR data analysis: current concepts and the novel "gene expression's CT difference" formula." J Mol Med (Berl) **84**(11): 901-910.
- Schneider, C. A., W. S. Rasband and K. W. Eliceiri (2012). "NIH Image to ImageJ: 25 years of image analysis." Nat Methods **9**(7): 671-675.
- Scott, A. M., J. D. Wolchok and L. J. Old (2012). "Antibody therapy of cancer." Nat Rev Cancer **12**(4): 278-287.
- Screpanti, V., R. P. Wallin, A. Grandien and H. G. Ljunggren (2005). "Impact of FASL-induced apoptosis in the elimination of tumor cells by NK cells." Mol Immunol **42**(4): 495-499.
- Senapati, S., S. Rachagani, K. Chaudhary, S. L. Johansson, R. K. Singh and S. K. Batra (2010). "Overexpression of macrophage inhibitory cytokine-1 induces metastasis of human prostate cancer cells through the FAK-RhoA signaling pathway." Oncogene **29**(9): 1293-1302.
- Shiao, S. L., A. P. Ganesan, H. S. Rugo and L. M. Coussens (2011). "Immune microenvironments in solid tumors: new targets for therapy." Genes & Development **25**(24): 2559-2572.

- Shnaper, S., I. Desbaillets, D. A. Brown, A. Murat, E. Migliavacca, M. Schluep, S. Ostermann, M. F. Hamou, R. Stupp, S. N. Breit, N. de Tribolet and M. E. Hegi (2009). "Elevated levels of MIC-1/GDF15 in the cerebrospinal fluid of patients are associated with glioblastoma and worse outcome." Int J Cancer **125**(11): 2624-2630.
- Smyth, M. J., E. Cretney, J. M. Kelly, J. A. Westwood, S. E. A. Street, H. Yagita, K. Takeda, S. L. H. v. Dommelen, M. A. Degli-Esposti and Y. Hayakawa (2005). "Activation of NK cell cytotoxicity." Molecular Immunology **42**(4): 501-510.
- Smyth, M. J., J. M. Kelly, V. R. Sutton, J. E. Davis, K. A. Browne, T. J. Sayers, and J. and A. Trapani (2001). "Unlocking the secrets of cytotoxic granule proteins." Journal of leukocyte biology **70**: 18-29.
- Song, H., D. Yin and Z. Liu (2012). "GDF-15 promotes angiogenesis through modulating p53/HIF-1 α signaling pathway in hypoxic human umbilical vein endothelial cells." Molecular Biology Reports **39**(4): 4017-4022.
- Staff, A. C., A. J. Bock, C. Becker, T. Kempf, K. C. Wollert and B. Davidson (2010). "Growth differentiation factor-15 as a prognostic biomarker in ovarian cancer." Gynecol Oncol **118**(3): 237-243.
- Staff, A. C., J. Trovik, A. G. Eriksson, E. Wik, K. C. Wollert, T. Kempf and H. B. Salvesen (2011). "Elevated plasma growth differentiation factor-15 correlates with lymph node metastases and poor survival in endometrial cancer." Clin Cancer Res **17**(14): 4825-4833.
- Staszewski, R. (1984). "Cloning by limiting dilution: an improved estimate that an interesting culture is monoclonal." The Yale Journal of Biology and Medicine **57**(6): 865-868.
- Stefanescu, R., R. E. Iacob, E. N. Damoc, A. Marquardt, E. Amstalden, M. Manea, I. Perdivara, M. Maftai, G. Paraschiv and M. Przybylski (2007). "Mass spectrometric approaches for elucidation of antigenantibody recognition structures in molecular immunology." Eur J Mass Spectrom (Chichester, Eng) **13**(1): 69-75.
- Stinchcombe, J. C., G. Bossi, S. Booth and G. M. Griffiths (2001). "The immunological synapse of CTL contains a secretory domain and membrane bridges." Immunity **15**(5): 751-761.
- Strelau, J., A. Schober, A. Sullivan, L. Schilling and K. Unsicker (2003). "Growth/differentiation factor-15 (GDF-15), a novel member of the TGF- β superfamily, promotes survival of lesioned mesencephalic dopaminergic neurons in vitro and in vivo and is induced in neurons following cortical lesioning." J Neural Transm Suppl(65): 197-203.
- Strelau, J., A. Strzelczyk, P. Rusu, G. Bendner, S. Wiese, F. Diella, A. L. Altick, C. S. von Bartheld, R. Klein, M. Sendtner and K. Unsicker (2009). "Progressive postnatal motoneuron loss in mice lacking GDF-15." J Neurosci **29**(43): 13640-13648.
- Strelau, J., A. Strzelczyk, P. Rusu, G. Bendner, S. Wiese, F. Diella, A. L. Altick, C. S. von Bartheld, R. Klein, M. Sendtner and K. Unsicker (2009). "Progressive postnatal motoneuron loss in mice lacking GDF-15." The Journal of Neuroscience **29**(43): 13640-13648.

- Strelau, J., A. Sullivan, M. Bottner, P. Lingor, E. Falkenstein, C. Suter-Crazzolara, D. Galter, J. Jaszai, K. Kriegelstein and K. Unsicker (2000). "Growth/differentiation factor-15/macrophage inhibitory cytokine-1 is a novel trophic factor for midbrain dopaminergic neurons in vivo." J Neurosci **20**(23): 8597-8603.
- Sudhakar, A. (2009). "History of Cancer, Ancient and Modern Treatment Methods." Journal of cancer science & therapy **1**(2): 1-4.
- Suesskind, D., A. Schatz, S. Schnichels, S. E. Coupland, S. L. Lake, B. Wissinger, K. U. Bartz-Schmidt and S. Henke-Fahle (2012). "GDF-15: a novel serum marker for metastases in uveal melanoma patients." Graefes Arch Clin Exp Ophthalmol **250**(6): 887-895.
- Sun, Y., P. Ye, J. Wu, Z. Liu, A. Zhang, L. Ren, C. Cheng, X. Huang, K. Wang, P. Deng, C. Wu, Z. Yue and J. Xia (2014). "Inhibition of intimal hyperplasia in murine aortic allografts by the oral administration of the transforming growth factor-beta receptor I kinase inhibitor SD-208." J Heart Lung Transplant **33**(6): 654-661.
- Szybalski, W. (1992). "Use of the HPRT gene and the HAT selection technique in DNA-mediated transformation of mammalian cells: first steps toward developing hybridoma techniques and gene therapy." Bioessays **14**(7): 495-500.
- Tan, M., Y. Wang, K. Guan and Y. Sun (2000). "PTGF- β , a type β transforming growth factor (TGF- β) superfamily member, is a p53 target gene that inhibits tumor cell growth via TGF- β signaling pathway." Proceedings of the National Academy of Sciences **97**(1): 109-114.
- Tarin, D. (2013). "Role of the host stroma in cancer and its therapeutic significance." Cancer Metastasis Rev **32**(3-4): 553-566.
- Teicher, B. A. (2007). "Transforming growth factor-beta and the immune response to malignant disease." Clin Cancer Res **13**(21): 6247-6251.
- Thomas, D. A. and J. Massagué (2005). "TGF- β directly targets cytotoxic T cell functions during tumor evasion of immune surveillance." Cancer Cell **8**(5): 369-380.
- Tisdale, M. J. (2002). "Cachexia in cancer patients." Nat Rev Cancer **2**(11): 862-871.
- Tisdale, M. J. (2009). Mechanisms of Cancer Cachexia.
- Tomasetti, C. and B. Vogelstein (2015). "Variation in cancer risk among tissues can be explained by the number of stem cell divisions." Science **347**(6217): 78-81.
- Tong, S., B. Marjono, D. A. Brown, S. Mulvey, S. N. Breit, U. Manuelpillai and E. M. Wallace (2004). "Serum concentrations of macrophage inhibitory cytokine 1 (MIC 1) as a predictor of miscarriage." Lancet **363**(9403): 129-130.
- Tsai, V. W., R. Manandhar, S. B. Jorgensen, K. K. Lee-Ng, H. P. Zhang, C. P. Marquis, L. Jiang, Y. Husaini, S. Lin, A. Sainsbury, P. E. Sawchenko, D. A. Brown and S. N. Breit (2014). "The anorectic actions of the TGFbeta cytokine MIC-1/GDF15 require an intact brainstem area postrema and nucleus of the solitary tract." PLoS One **9**(6): e100370.

- Tumeh, P. C., C. L. Harview, J. H. Yearley, I. P. Shintaku, E. J. Taylor, L. Robert, B. Chmielowski, M. Spasic, G. Henry, V. Ciobanu, A. N. West, M. Carmona, C. Kivork, E. Seja, G. Cherry, A. J. Gutierrez, T. R. Grogan, C. Mateus, G. Tomasic, J. A. Glaspy, R. O. Emerson, H. Robins, R. H. Pierce, D. A. Elashoff, C. Robert and A. Ribas (2014). "PD-1 blockade induces responses by inhibiting adaptive immune resistance." Nature **515**(7528): 568-571.
- Uhlen, M., P. Oksvold, L. Fagerberg, E. Lundberg, K. Jonasson, M. Forsberg, M. Zwahlen, C. Kampf, K. Wester, S. Hober, H. Wernerus, L. Bjorling and F. Ponten (2010). "Towards a knowledge-based Human Protein Atlas." Nat Biotech **28**(12): 1248-1250.
- van Domselaar, R., R. Quadir, A. M. van der Made, R. Broekhuizen and N. Bovenschen (2012). "All Human Granzymes Target hnRNP K That Is Essential for Tumor Cell Viability." The Journal of Biological Chemistry **287**(27): 22854-22864.
- Vasaturo, A., S. Di Blasio, D. G. A. Peeters, C. C. H. de Koning, J. M. de Vries, C. G. Figdor and S. V. Hato (2013). "Clinical Implications of Co-Inhibitory Molecule Expression in the Tumor Microenvironment for DC Vaccination: A Game of Stop and Go." Frontiers in Immunology **4**: 417.
- Vignali, D. A. A., L. W. Collison and C. J. Workman (2008). "How regulatory T cells work." Nat Rev Immunol **8**(7): 523-532.
- Vinay, D. S., E. P. Ryan, G. Pawelec, W. H. Talib, J. Stagg, E. Elkord, T. Lichtor, W. K. Decker, R. L. Whelan, H. M. Kumara, E. Signori, K. Honoki, A. G. Georgakilas, A. Amin, W. G. Helferich, C. S. Boosani, G. Guha, M. R. Ciriolo, S. Chen, S. I. Mohammed, A. S. Azmi, W. N. Keith, A. Bilsland, D. Bhakta, D. Halicka, H. Fujii, K. Aquilano, S. S. Ashraf, S. Nowsheen, X. Yang, B. K. Choi and B. S. Kwon (2015). "Immune evasion in cancer: Mechanistic basis and therapeutic strategies." Semin Cancer Biol.
- Vivier, E., S. Ugolini, D. Blaise, C. Chabannon and L. Brossay (2012). "Targeting natural killer cells and natural killer T cells in cancer." Nat Rev Immunol **12**(4): 239-252.
- Vogelstein, B. and K. W. Kinzler (1993). "The multistep nature of cancer." Trends in Genetics **9**(4): 138-141.
- Vogelstein, B. and K. W. Kinzler (2004). "Cancer genes and the pathways they control." Nat Med **10**(8): 789-799.
- Vogiannis, E. G. and D. Nikolopoulos (2014). "Radon sources and associated risk in terms of exposure and dose." Front Public Health **2**: 207.
- Wahl, S. M., D. A. Hunt, H. L. Wong, S. Dougherty, N. McCartney-Francis, L. M. Wahl, L. Ellingsworth, J. A. Schmidt, G. Hall and A. B. Roberts (1988). "Transforming growth factor-beta is a potent immunosuppressive agent that inhibits IL-1-dependent lymphocyte proliferation." The Journal of Immunology **140**(9): 3026-3032.
- Wahl, S. M., D. A. Hunt, H. L. Wong, S. Dougherty, N. McCartney-Francis, L. M. Wahl, L. Ellingsworth, J. A. Schmidt, G. Hall, A. B. Roberts and et al. (1988). "Transforming growth factor-beta is a potent immunosuppressive agent that inhibits IL-1-dependent lymphocyte proliferation." J Immunol **140**(9): 3026-3032.

- Wakefield, L. M. and C. S. Hill (2013). "Beyond TGF[beta]: roles of other TGF[beta] superfamily members in cancer." Nat Rev Cancer **13**(5): 328-341.
- Waldhauer, I. and A. Steinle (2008). "NK cells and cancer immunosurveillance." Oncogene **27**(45): 5932-5943.
- Wang, Z., M. Raifu, M. Howard, L. Smith, D. Hansen, R. Goldsby and D. Ratner (2000). "Universal PCR amplification of mouse immunoglobulin gene variable regions: the design of degenerate primers and an assessment of the effect of DNA polymerase 3' to 5' exonuclease activity." J Immunol Methods **233**(1-2): 167-177.
- Warren, S. (1932). "THE IMMEDIATE CAUSES OF DEATH IN CANCER." The American Journal of the Medical Sciences **184**(5): 610-615.
- Weigelin, B. and P. Friedl (2010). "A three-dimensional organotypic assay to measure target cell killing by cytotoxic T lymphocytes." Biochem Pharmacol **80**(12): 2087-2091.
- Weiner, G. J. (2007). "Monoclonal antibody mechanisms of action in cancer." Immunol Res **39**(1-3): 271-278.
- Weiner, L. M. and G. P. Adams (2000). "New approaches to antibody therapy." Oncogene **19**(53): 6144-6151.
- Weiss, A. and L. Attisano (2013). "The TGFbeta superfamily signaling pathway." Wiley Interdiscip Rev Dev Biol **2**(1): 47-63.
- Weissenhorn, W., E. Weiss, M. Schwirzke, B. Kaluza and U. H. Weidle (1991). "Chimerization of antibodies by isolation of rearranged genomic variable regions by the polymerase chain reaction." Gene **106**(2): 273-277.
- Whitson, R. J., M. S. Lucia and J. R. Lambert (2013). "Growth differentiation factor-15 (GDF-15) suppresses in vitro angiogenesis through a novel interaction with connective tissue growth factor (CCN2)." J Cell Biochem **114**(6): 1424-1433.
- Wiklund, F. E., A. M. Bennet, P. K. Magnusson, U. K. Eriksson, F. Lindmark, L. Wu, N. Yaghoutyfam, C. P. Marquis, P. Stattin, N. L. Pedersen, H. O. Adami, H. Gronberg, S. N. Breit and D. A. Brown (2010). "Macrophage inhibitory cytokine-1 (MIC-1/GDF15): a new marker of all-cause mortality." Aging Cell **9**(6): 1057-1064.
- Wittke, F., R. Hoffmann, J. Buer, I. Dallmann, K. Oevermann, S. Sel, T. Wandert, A. Ganser and J. Atzpodien (1999). "Interleukin 10 (IL-10): an immunosuppressive factor and independent predictor in patients with metastatic renal cell carcinoma." British Journal of Cancer **79**(7-8): 1182-1184.
- Woof, J. M. and D. R. Burton (2004). "Human antibody-Fc receptor interactions illuminated by crystal structures." Nat Rev Immunol **4**(2): 89-99.
- Wrzesinski, S. H., Y. Y. Wan and R. A. Flavell (2007). "Transforming growth factor-beta and the immune response: implications for anticancer therapy." Clin Cancer Res **13**(18 Pt 1): 5262-5270.

Young, J. D., C. C. Liu, L. G. Leong and Z. A. Cohn (1986). "The pore-forming protein (perforin) of cytolytic T lymphocytes is immunologically related to the components of membrane attack complex of complement through cysteine-rich domains." J Exp Med **164**(6): 2077-2082.

Zhang, L., X. Yang, H. Y. Pan, X. J. Zhou, J. Li, W. T. Chen, L. P. Zhong and Z. Y. Zhang (2009). "Expression of growth differentiation factor 15 is positively correlated with histopathological malignant grade and in vitro cell proliferation in oral squamous cell carcinoma." Oral Oncol **45**(7): 627-632.

Zhang, X.-H., E.-Q. Qiao, Z. Gao, H.-Q. Yuan, P.-F. Cai, X.-M. Li and Y.-H. Gu (2013). "Efficacy of combined axitinib with dacarbazine in a B16F1 melanoma xenograft model." Oncology Letters **6**(1): 69-74.

Patent citation:

WISCHHUSEN, J.; JUNKER, M.; Müller, T.; SAREMBA, S. (2014) „Monoclonal antibodies to growth and differentiation factor 15 (gdf-15); Google Patents; <http://www.google.com/patents/WO2014049087A1?cl=en>

List of Figures

Figure 1-1: Development of tumor cells by somatic mutations	15
Figure 1-2: Tumor immunity of NK cells	18
Figure 1-3: Activation of T cell by cross presentation of tumor antigens on APC	19
Figure 1-4: Cytotoxic T cell killing of a tumor cell presenting a specific peptide tumor antigen on MHC-class-I molecule	20
Figure 1-5: Rolling, adhesion and transmigration of leukocytes at the tumor site.....	21
Figure 1-6: Mechanisms of tumor immune evasion	23
Figure 1-7: The TGF- β superfamily, major groups and members	25
Figure 1-8: TGF- β signaling pathway and its components	26
Figure 1-9: Full length GDF-15 protein	28
Figure 1-10: Processed forms of GDF-15 protein	29
Figure 1-11: Schematic of GDF-15 forms expressed by tumor cells	29
Figure 1-12: Schematic of an antibody structure.....	37
Figure 1-13: Different forms of clinically applied antibodies	38
Figure 2-1: DNA and RNA ladders.....	52
Figure 2-2: Protein ladder: Spectra™ Multicolor Broad Range Protein Ladder	52
Figure 2-3: Schematic of human blood cells after centrifugation in density gradient.....	55
Figure 2-4: Illustration of the CELLline Bioreactor system for antibody production.....	73
Figure 2-5: Mouse isotyping strip (AbD Serotec).....	74
Figure 3-1-1: GDF-15 expression in human malignant ovarian cancer	80
Figure 3-1-2: Human malignant gliomas express GDF-15 in vivo	82
Figure 3-2-1: Effects of TGF beta and GDF-15 on the phosphorylation of Smad2/3 in PBMC.....	84
Figure 3-2-2: NKG2D receptor surface expression on natural killer cells and CD8 ⁺ T cells	85
Figure 3-2-3: In vitro adherence of PBMC on HUVEC under the influence of GDF-15	87
Figure 3-2-4: Heat map for hierarchical clustering of gene expression pattern in HUVEC and PBMC	89
Figure 3-2-5: In vitro scratch assay with a GDF-15 overexpressing MCF-7 breast cancer cell line.....	95
Figure 3-3-1: Kaplan Meier plot of tumor cell bearing mice with pSUPER-control and pSUPER-GDF-15 knock down construct.....	96
Figure 3-3-2: Immune cell infiltration in mouse glioma tissue sections FFPE sections	97
Figure 3-4-1: Genotyping of GDF-15 knock-out animals.....	99
Figure 3-4-2: Screening of GDF-15 antibody producing hybridoma clones.....	100
Figure 3-4-3: Heavy and light chains of hybridoma cell derived antibodies	102

Figure 3-4-4: B1-23 is suitable for WB-detection of recombinant and overexpressed full length GDF-15.....	103
Figure 3-4-5: Linear epitope mapping of full length GDF-15 with anti GDF-15 antibody B1-23	105
Figure 3-4-6: Amplification of heavy and light chain DNA of hybridoma antibodies	107
Figure 3-4-7: Detection of mature human GDF-15 by the chimeric antibody ChimB1-23	109
Figure 3-4-8: GDF-15 is detected by co-expression of light and heavy chain constructs of H1L5	112
Figure 3-4-9: Replacement of the CDR3 of B1-23 leads to the loss of antigen binding.....	113
Figure 3-4-10: GDF-15 accumulation in supernatants of UACC-257 cells and its neutralisation by B1-23.....	115
Figure 3-4-11: Antagonization of tumor cell derived GDF-15 with B1-23	116
Figure 3-4-12: Toxicity test of B1-23 on blood lymphocytes	117
Figure 3-5: B1-23 prevents GDF-15 mediated cachexia in vivo.....	119

List of Tables

Table 1: List of cancer types associated with elevated GDF-15 expression ...	30
Table 2: List of FDA approved monoclonal antibodies used for treatment of oncological indications	35
Table 3: Instruments and devices	42
Table 4: Material and reagents for immunohistochemical staining.....	43
Table 5: Buffers for SDS-PAGE	44
Table 6: Buffers used for Western Blotting	45
Table 7: Reagents and chemicals for molecular biology.....	45
Table 8: Overview of kits	46
Table 9: Components of plasmid isolation and purification kit (ZYPPY) for mini preparations	46
Table 10: Buffers and reagents for monoclonal antibody generation and production.....	47
Table 11: Buffers prepared for antibody purification with the proteus A kit.....	47
Table 12: Table of antibodies	48
Table 13: List of primers used for genotyping of mice or for realtime PCR.....	49
Table 14: Cell lines and primary cells used in vitro and in vivo	50
Table 15: List of plasmids	50
Table 16: List of FACS staining reagents and buffers	51
Table 17: Human cytokines.....	51
Table 18: Polyacrylamid gels for SDS PAG electrophoresis	60
Table 19: Volumes and amounts of components for one iScript cDNA synthesis reaction.....	62
Table 20: cDNA synthesis program	62
Table 21: Reaction setup for standard PCR	63
Table 22: PCR program for GDF-15 knock-out genotyping.....	64
Table 23: qRT-PCR Mastermix	65
Table 24: qRT-PCR program on the ABI 7500 instrument.....	65
Table 25: Ligation reaction mix	67
Table 26: Ligation reaction – program	67
Table 27: Restriction double digest reaction mix.....	68
Table 28: Components for colony PCR.....	69
Table 29: Colony PCR program	69
Table 30: Buffers used for linear epitope mapping on peptide array	75
Table 31: Setup UACC-257 Xenograft Study (Substances & total amounts required).....	78
Table 32: Upregulated transcripts of PBMCs treated for six hours with recombinant GDF-15.....	90
Table 33: Downregulated transcripts of PBMCs treated for six hours	

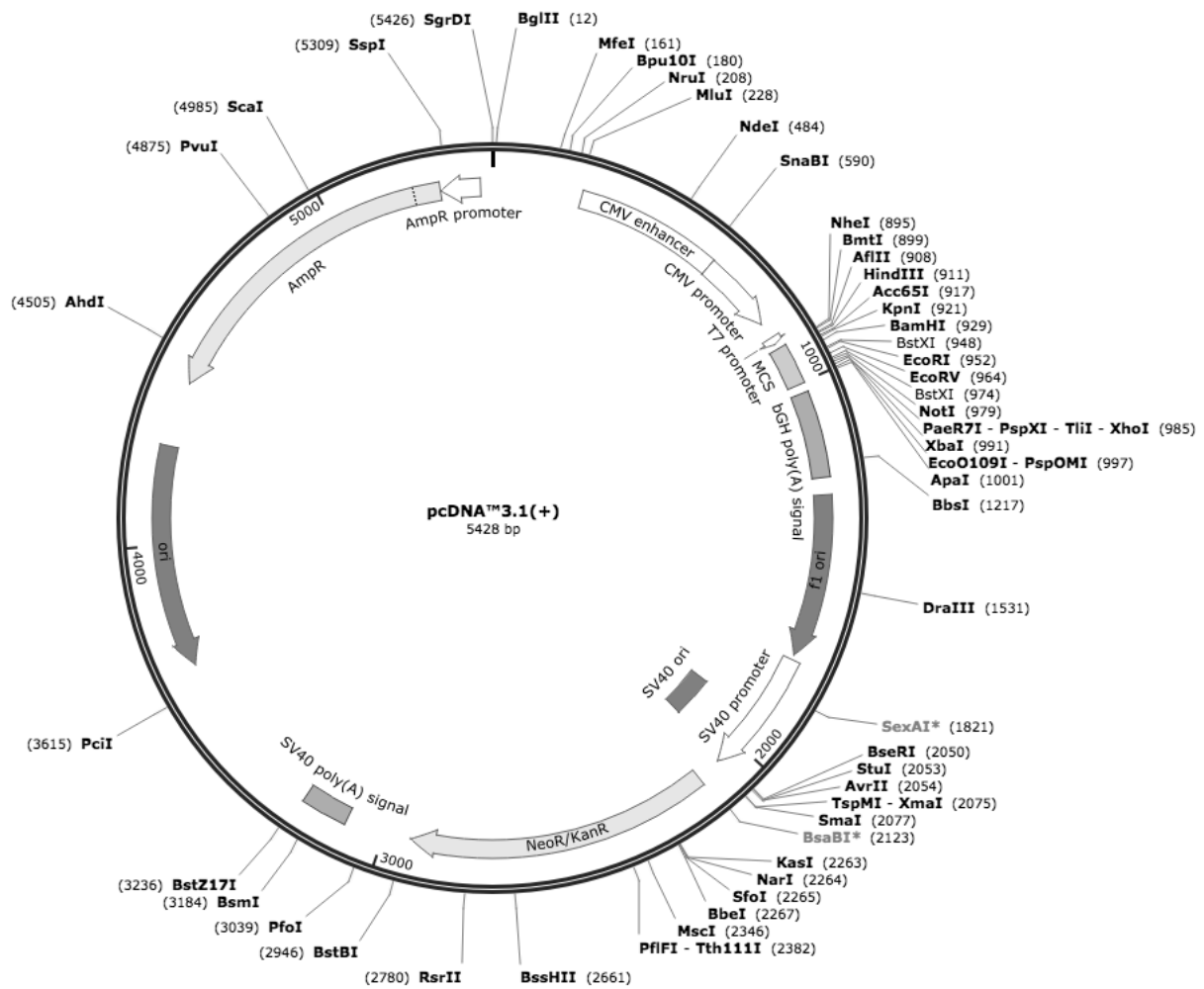
with recombinant GDF-15.....	91
Table 34: Upregulated transcripts of PBMCs treated for 24 hours with recombinant GDF-15.....	91
Table 35: Downregulated transcripts of PBMCs treated for 24hours with recombinant GDF-15.....	91
Table 36: Upregulated transcripts of HUVECs treated for six hours with recombinant GDF-15.....	92
Table 37: Downregulated transcripts of HUVECs treated for six hours with recombinant GDF-15.....	92
Table 38: Upregulated transcripts of HUVECs treated for 24 hours with rhGDF-15	92
Table 39: Downregulated transcripts of HUVECs treated for 24hours with rhGDF-15	92
Table 40: Upregulated transcripts of HUVECs treated for six hours with HEK-GDF-15	93
Table 41: Downregulated transcripts of HUVECs treated for six hours with HEK-GDF-15	93
Table 42: Upregulated transcripts of HUVECs treated for six hours with HEK-GDF-15	93
Table 43: Downregulated transcripts of HUVECs treated for six hours with HEK-GDF-15	93
Table 44: B1-23 interacting peptides 1 and 2 located in the mature GDF-15 sequence	106
Table 45: Sequence of the Fab region of B1-23 after amplification with degenerate primers	108
Table 46: Sequences of the humanized light and heavy chains (performed by evitria AG)	110
Table 47: KD value determination of 13 pre-selected humanized antibodies derived from B1-23	111
Table 48: IMGT database: Sequence alignment of B1-23 hypervariable regions including framework sequence.....	113
Table 49: Sequence Alignment of human and murine GDF-15 full length GDF-15	161

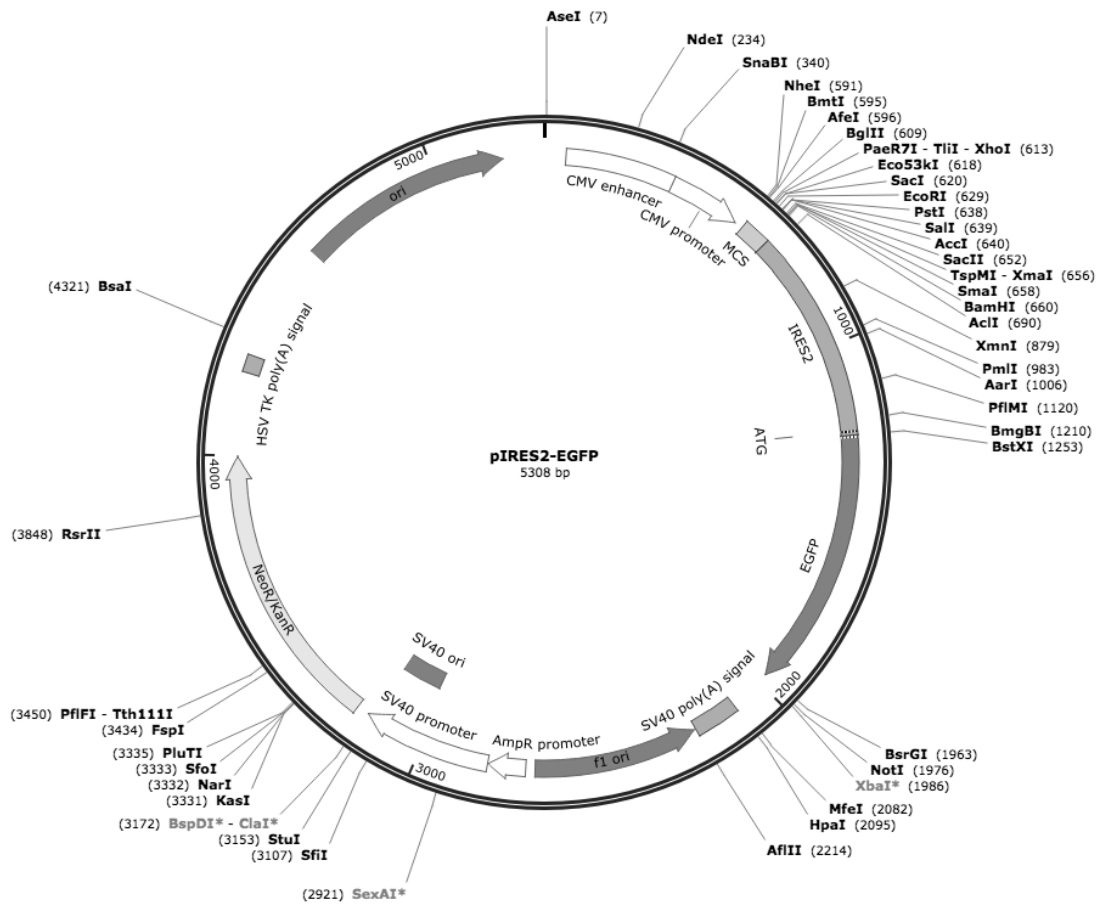
Supplements

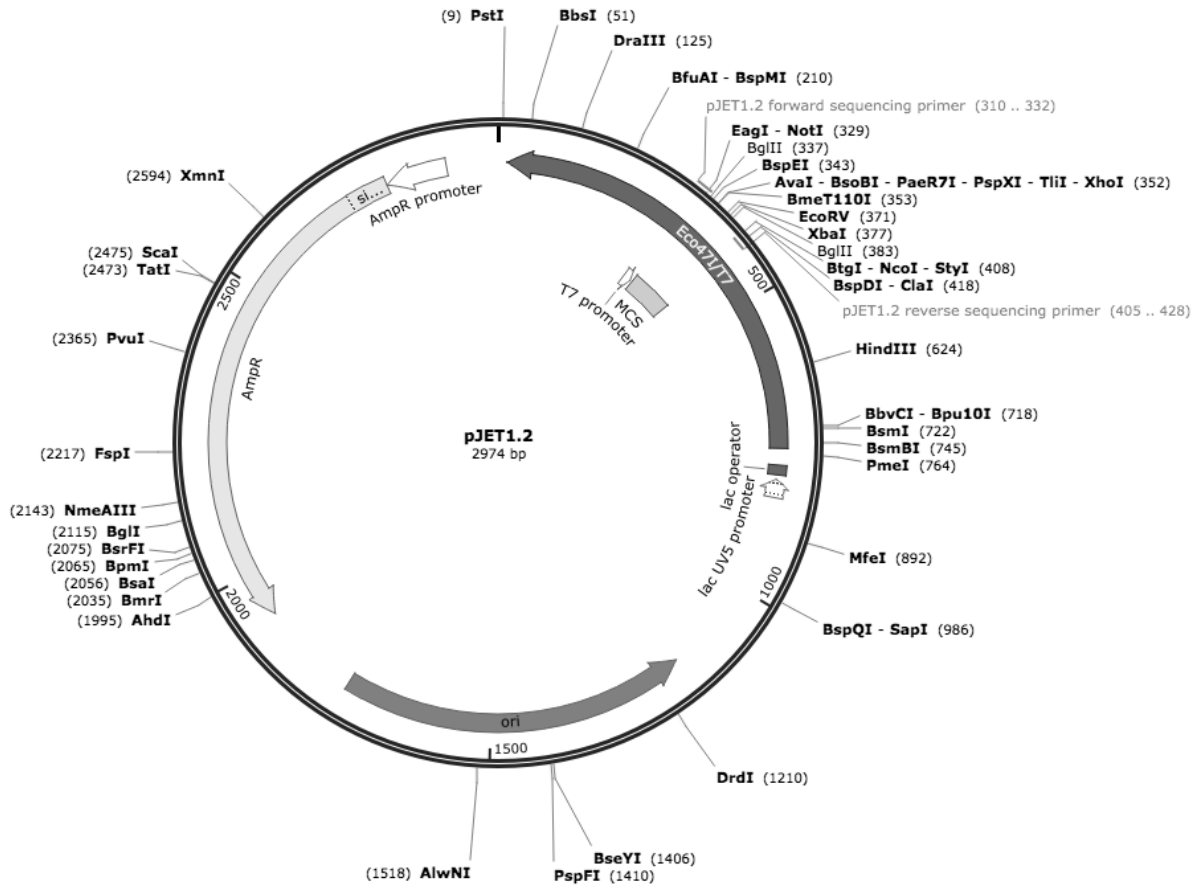
Vector maps:

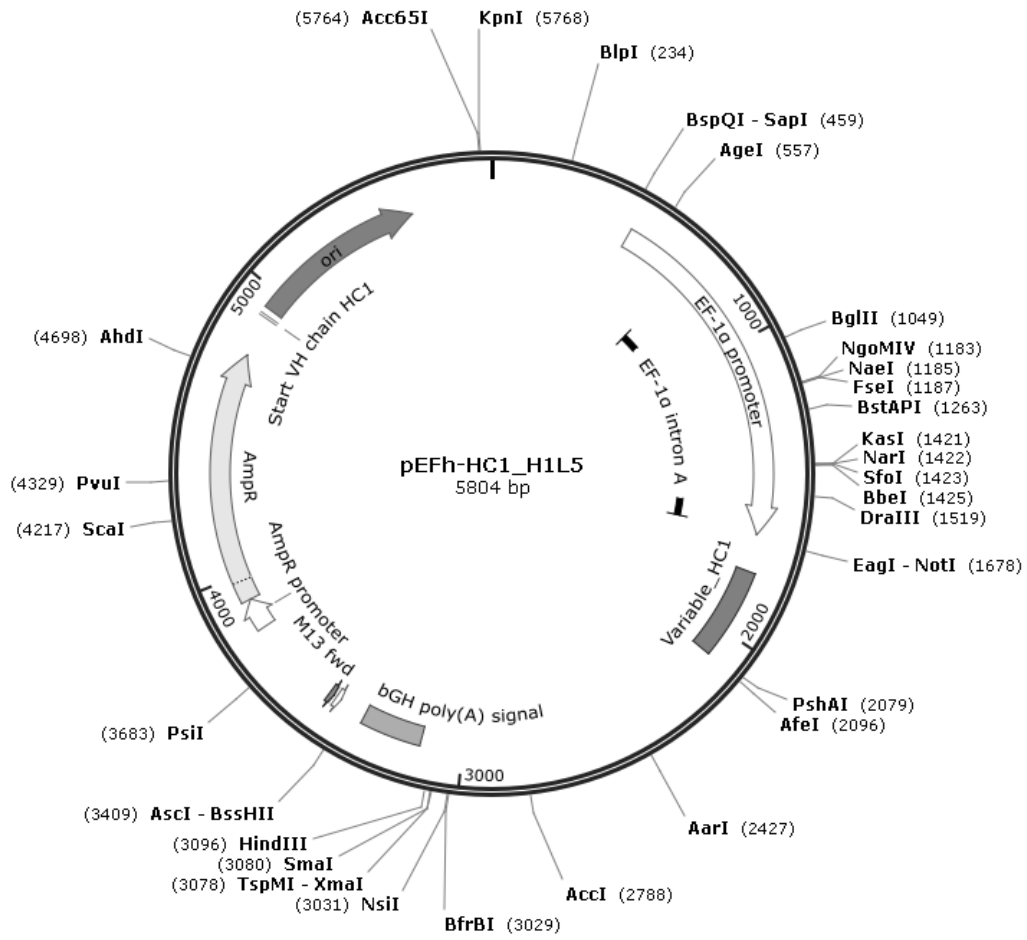
Designed with SnapGene viewer:

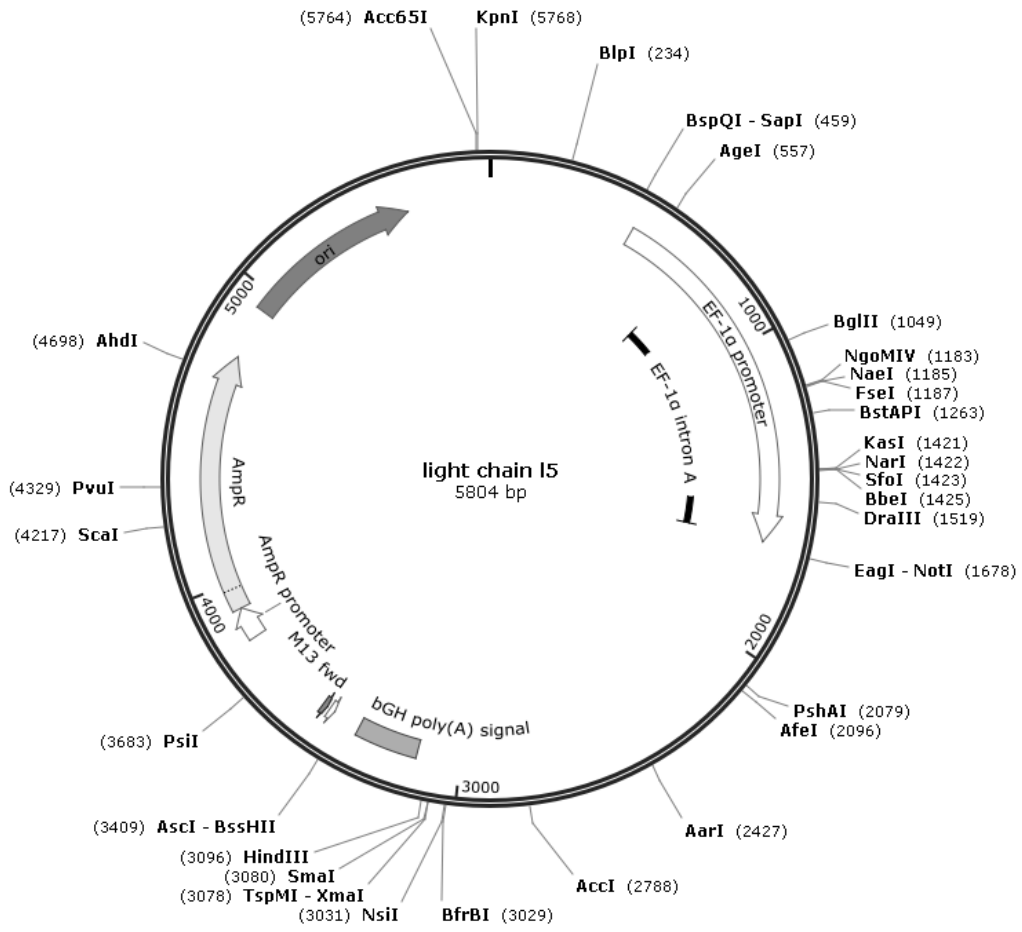
Created with SnapGene®











Sequence Alignment (NCBI-BLAST):

Sequence ID: lcl|Query_9107 Length: 1220 Number of Matches: 1

Range 1: 207 to 962 [Graphics](#)

▼ Next Match ▲ Previous Match

Score	Expect	Identities	Gaps	Strand
320 bits(354)	4e-91	528/757(70%)	20/757(2%)	Plus/Plus
Query 201	CGCTTCCAGGACCTGCTGAGCCGGCTGCATGCCAACCCAGAGCCGAGAGGACTCGAACTCA	260		
Sbjct 207	CGCTACGAGGACCTGCTAACCCAGGCTGCGGGCCAACCAGAGCTGGGAAGATTGAAACACC	266		
Query 261	GAACCAAGTCCTGACCCA-GCTGTCCGGATACTCAGTCCAGAGGTGAGATTGGGGTCCCA	319		
Sbjct 267	GA-CCTCGTCCCGGCCCTGCAGTCCGGATACTCACGCCAGAAGTCCGGCTGGGATCCGG	325		
Query 320	CGGCCAGCTGCTACTCCGCGTCAACCGGGCGTCCGCTGAGTCAGGGTCTCCCGAAGCCTA	379		
Sbjct 326	CGGCCACCTGCACCTGGTATCTCTCGGGCCGCCCTTCCCGAGGGGCTCCCGAGGGCCTC	385		
Query 380	CCGCGTGCACCGAGCGTGTCTCTGCTGACGCCGACGGCCC---GCCCTGGGACATCAC	436		
Sbjct 386	CCGCCCTTACCGGGCTCTGTTCCGGCTGTCCCGACGGCGTCAAGGTCGTGGGACGTGAC	445		
Query 437	TAGGCCCTGAAGCGTGCCTCAGCCTCCGGGGACCCCGTCTCCCGCATTACGCCTGCG	496		
Sbjct 446	ACGACCGCTGCGGGCTCAGCTCAGCCTTGCAAGACCCAGGGCGCCGCGCTGCACCTGCG	505		
Query 497	CCTGACGCCCGCTCCGGACCTGGCTA-----TGCTGCC---TCT--GGCGGCACG---	542		
Sbjct 506	ACTGTCCGCCCGCCGCTCGCAGTCGGACCAACTGCTGGCAGAATCTTCGTCCGCACGGCC	565		
Query 543	-CAGCTGGAAGTGCCTTACGGGTAGCCGCCGGCAGGGGGCGCCGAAGCGCGCATGCGCA	601		
Sbjct 566	CCAGCTGGAGTTGCACTTGCAGCCGCAAGCCGCCAGGGGGCGCCGAGAGCGGTGCGCG	625		
Query 602	CCCAAGAGACTCGTGCCCACTGGGTCCGGGGCGCTGCTGTCACTTGGAGACTGTGCAGGC	661		
Sbjct 626	CAACGGGGACCACTGTCCGCTCGGGCCCGGGCGTTGCTGCCGTCTGCACACGGTCCGCGC	685		
Query 662	AACTCTTGAAGACTTGGGCTGGAGCGACTGGGTGCTGTCCCGCGCCAGCTGCAGCTGAG	721		
Sbjct 686	GTCGCTGGAAGACTTGGGCTGGGCGGATTGGGTGCTGTGCCACGGGAGGTGCAAGTGAC	745		
Query 722	CAITGTGCGTGGGCGAGTGTCCCACTGTATCGCTCCGCGAACACGCATGCGCAGATCAA	781		
Sbjct 746	CAITGTGCAITCGGCGGTGCCGAGCCAGTTCGGGGCGCAAACATGCACGCGCAGATCAA	805		
Query 782	AGCACGCCCTGCATGGCCTGCAGCCTGACAAGGTGCCTGCCCGTGTGTGTCCCTCCAG	841		
Sbjct 806	GACGAGCCTGCACCGCCTGAAGCCGACACGGTGCCAGCGCCCTGCTGCGTGCCTCCAG	865		
Query 842	CTACACCCGGTGGTTCCTTATGCACAGGACAGACAGTGGTGTGCTACTGCAGACTTATGA	901		
Sbjct 866	CTACAATCCCATGGTGTCTATTCAAAGACCGACACCGGGGTGTCGCTCCAGACCTATGA	925		
Query 902	TGACCTGGTGGCCCGGGCTGCCACTGCGCTTGGCA 938			
Sbjct 926	TGACTTGTAGCCAAAGACTGCCACTGCATATGAGCA 962			

Table 49 Sequence Alignment of human and murine GDF-15 full length GDF-15 (NCBI Nucleotide BLAST was used for sequence alignment) [Query and Sbjct represent the murine and human GDF-15 sequence, respectively]

List of Abbreviations

AA	amino acid
ACD-A	acid citrate dextrose solution A
APC	antigen presenting cells
APC	allophycocyanin
APS	ammonium peroxodisulfate
Bp, kb	base pair(s); kilo base pairs
BSA	bovine serum albumin
CD	cluster of differentiation
cDNA	complementary DNA
CT	threshold cycle
CTL	cytotoxic T lymphocyte
Da, kDa	dalton, kilodalton
DAB	diaminobenzidine
DC	dendritic cells
ddH ₂ O	double distilled water
DMSO	dimethyl sulfoxide
DNA	deoxyribonucleic acid
DNAM-1	DNAX accessory molecule-1
dNTPs	deoxynucleotide triphosphates
ECL	enhanced chemiluminescence
EDTA	ethylenediaminetetraacetic acid
e.g.	exempli gratia
ELISA	enzyme-linked immunosorbent assay
FACS	fluorescence-activated cell sorting
Fc	fragment crystallizable
FCS	fetal calf serum
FFPE	formalin-fixed, paraffin-embedded
FITC	fluorescein isothiocyanate
HBSS	Hank's balanced salt solution
HER2	human epidermal growth factor receptor 2
HLA	human leukocyte antigen
HRP	horseradish peroxidase
HSA	human serum albumin
H&E	stain hematoxylin and eosin stain
IARC	international agency for research on cancer
IFN	interferon
IHC	immunohistochemistry
IL	interleukin
ILT	immunoglobulin-like transcript

KIR	killer cell immunoglobulin-like receptor
K-ras	kirsten rat sarcoma viral oncogene homolog protein
mAB	monoclonal antibody
MAPK	mitogen-activated protein kinase
mg	milligram
MHC	major histocompatibility complex
MIC-1	macrophage inhibitory cytokine-1
min	minute
ml	milliliters
mRNA	messenger RNA
NAG-1	nonsteroidal anti-inflammatory drug-activated gene-1
Ng	nanogram
NK	natural killer cells
NKG2D	natural killer group 2D
NP-40	nonyl phenoxypolyethoxylethanol
PBS	phosphate buffered Saline
PCR	polymerase chain reaction
PE	R-phycoerythrin
PFA	paraformaldehyde
PHA	phytohaemagglutinin
PMSF	phenylmethanesulfonylfluoride
PTEN	phosphatase and tensin homolog deleted on chromosome ten
PVDF	polyvinylidene Fluoride Membrane
RB	retinoblastoma protein
Rh	Recombinant human
RPM	revolutions per minute
RPMI	Roswell Park Memorial Institute
RT-PCR	reverse transcriptase PCR
TCR	t cell receptor
TGF- β	transforming growth factor-beta
TNF- α	tumor necrosis factor-alpha
Treg	regulatory T cells
ULBP	UL16 binding protein
UV	ultraviolet
V	volt
VEGF	vascular endothelial growth factor

Affidavit/Eidesstattliche Erklärung

Affidavit

I hereby confirm that my thesis entitled "**Development and characterization of monoclonal antibodies to GDF-15 for potential use in cancer therapy**" is the result of my own work. I did not receive any help or support from commercial consultants. All sources and / or materials applied are listed and specified in the thesis.

Furthermore, I confirm that this thesis has not yet been submitted as part of another examination process neither in identical nor in similar form.

Place, Date

Signature

Eidesstattliche Erklärung

Hiermit erkläre ich an Eides statt, die Dissertation mit dem Titel "**Die Entwicklung und Charakterisierung monoklonaler Antikörper gegen GDF-15 zur potenziellen Anwendung in der Krebstherapie**" eigenständig, d.h. insbesondere selbständig und ohne Hilfe eines kommerziellen Promotionsberaters, angefertigt und keine anderen als die von mir angegebenen Quellen und Hilfsmittel verwendet zu haben.

Ich erkläre außerdem, dass die Dissertation weder in gleicher noch in ähnlicher Form bereits in einem anderen Prüfungsverfahren vorgelegen hat.

Ort, Datum

Unterschrift

Danksagung

Zunächst möchte ich mich bei Herrn Professor Dr. Jörg Wischhusen für die Bereitstellung des Themas und die Finanzierung zur Durchführung meiner Arbeit bedanken.

Ich möchte mich ausdrücklich bei Herrn Professor Dr. Jürgen C. Becker bedanken, dass er so kurzfristig das Erstgutachten meiner Doktorarbeit übernimmt.

Ich möchte mich ganz herzlich bei Herrn Professor Dr. Roland Benz für die Betreuung und Unterstützung meiner Arbeit wie auch die Bereitschaft, das Zweitgutachten zu übernehmen, bedanken.

Mein Dank gilt auch Herrn Professor Dr. Thomas Hünig, der durch seine Erfahrung mit monoklonalen Antikörpern zur gelungenen Generierung des Antikörpers B1-23 und somit zur Entstehung eines großen Projektes beigetragen hat.

Ein ganz besonderer Dank gilt Frau Professor Dr. Ulrike Kämmerer für ihre großartige Unterstützung. Ich konnte jederzeit zu ihr kommen, wenn ich Fragen oder Probleme hatte. Vielen Dank, dass ich alle Räumlichkeiten nutzen konnte und ich derart willkommen im Turm aufgenommen wurde. Ohne diese Unterstützung wäre ich nicht, wo ich jetzt bin.

Außerdem möchte ich Michaela Kapp für die perfekten immunhistochemischen Färbungen zur Unterstützung unseres GO-Bio Projektes danken.

Ich möchte mich bei all meinen Laborkolleginnen und Kollegen der Sektion „experimentelle Tumormunologie“ für eine spannende Zeit bedanken.

Bei Frau Dr. Tina Schäfer möchte ich mich für die Generierung der Fab Fragmente des Antikörpers B1-23 danken, wie auch für die Durchführung des „Colorimetric Assay“ zur Testung der Bindungseigenschaften von B1-23 mit veränderten CDRs.

Mein Dank gilt auch Dr. Markus Hildinger, dem CEO der Firma Evitria AG in der Schweiz, für eine reibungslose Zusammenarbeit, blitzschnelle Antworten – ob bei Tag oder Nacht - konstruktive Planungen und Designs der Antikörper Konstrukte und natürlich eine gelungene Chimerisierung und Humanisierung unseres Entwicklungskandidaten B1-23.

Ich möchte mich ganz herzlich bei Dr. Dirk Pühringer für seine Mitarbeit und Unterstützung für das GO-Bio Projekt bedanken.

Curriculum Vitae

Personal Information

Name: Markus Junker
 Date of Birth: 02.07.1981
 Place of Birth: Ludwighshafen/Rhein
 Nationality: Germany

Grants

June 2013 - present BMBF grant: GO-Bio FKZ: 031A148
 „essentIGs - Therapeutische Antagonisierung von GDF-15 bei Tumorerkrankungen“
 February 2012 Winner business plan competition Northern Bavaria (Phase 1)
 September 2011 Winner BioEntrepreneur Boot Camp in Munich (Bio^M)

Patent applications

26th Sep. 2012 European patent application (EP2013/070127/PCT)
 Monoclonal antibodies to growth and differentiation factor 15
 Sep. 2013: PCT WO2014049087 A1
 25th March 2014 European patent application (EP2015/056654/PCT)
 Monoclonal antibodies to growth and differentiation factor 15
 (GDF-15), and uses thereof for treating cancer cachexia and cancer

Education

PhD

Nov 2008-present Graduate School of Life Sciences, Würzburg
Section Experimental Tumor Immunology
Department of Gynaecology and Obstetrics,
University Hospital Würzburg

Thesis: “Development and characterization of monoclonal antibodies to GDF-15 for potential use in cancer therapy”

Diploma Degree

September 2008 Diploma Degree at the University of Würzburg

Thesis: “The role of Notch during secondary neurogenesis in *Drosophila melanogaster*”

Department of Molecular, Cell, and Developmental Biology
at the University of California Los Angeles

2003-2008 Study of biology at the University of Würzburg, Germany

Diploma thesis at the University of California Los Angeles

2002-2003 Study of biotechnology at the University of Applied Sciences in
Gießen, Germany

High School

1991 – 2001: Karl-Theodor-v.-Dalberg-School in Aschaffenburg, Germany

Completed with: „Allgemeine Hochschulreife“

Training and Experiences

- 2013-present Project Leader of BMBF grant: FKZ: 031A148
„essentIGs - Therapeutische Antagonisierung von GDF-15 bei Tumorerkrankungen“ at the Department of Gynaecology and Obstetrics, University Hospital Würzburg
- Academic Associate member of GK 520 „Immunmodulation“

Associate member of the Graduate School of Life Science

Summer School “Gene regulation, cell differentiation and tolerance”, Goslar, 2010 (*Poster presentation*)

4th and 5th Network Meeting graduate schools GK1660, GK520 and GK794 Network Meeting of (DFG), Kloster Schöntal (*Poster presentation*)

5th International Symposium of GSLS “CHIASMA/on the cross roads of research”, Würzburg (*Poster presentation*)
- Conferences 19th Annual CRI Symposium, 2011, held in New York, NY, USA
20th Annual CRI Symposium, 2012, held in New York, NY, USA
Keystone Symposium: “Antibodies as drugs”, 2013, Vancouver
9th Annual European Antibody Congress 2013, Geneva

Publications

Peer-reviewed:

Characterization of myeloid derived suppressor cells (MDSC) in human decidua: key to immune tolerance in human pregnancy?

Bartmann C, **Junker M**, Segerer S, Häusler SF, Krockenberger M, Kämmerer U

Am J Reprod Immunol. - Revise and resubmit

The TGF- β -inducible miR-23a cluster attenuates IFN- γ levels and antigen-specific cytotoxicity in human CD8+T cells

Chandran PA, Keller A, Weinmann L, Seida AA, Braun M, Andreev K, Fischer B, Horn E, Schwinn S, **Junker M**, Houben R, Dombrowski Y, Dietl J, Finotto S, Wölfl M, Meister G, Wischhusen J

J Leukoc Biol, 2014, 96(4):633-45

Ectonucleotidases CD39 and CD73 on OvCA cells are potent adenosine-generating enzymes responsible for adenosine receptor 2A-dependent suppression of T cell function and NK cell cytotoxicity

Häusler SF, Montalbán Del Barrio I, Strohschein J, Chandran PA, Engel JB, Hönig A, Ossadnik M, Horn E, Fischer B, Krockenberger M, Heuer S, Seida AA, **Junker M**, Kneitz H, Kloor D, Klotz KN, Dietl J, Wischhusen J.

Cancer Immunol. Immunother., 2011, 60(10):1405-18

Transcriptional profiles of CD133+ and CD133- Glioblastoma-derived cancer stem cell lines suggest different cells of origin

Claudio Lottaz, Dagmar Beier, Katharina Meyer, Praveen Kumar, Andreas Hermann, Johannes Schwarz, **Markus Junker**, Peter J. Oefner, Ulrich Bogdahn, Jörg Wischhusen, Rainer Spang, Alexander Storch, Christoph P. Beier
Cancer Res., 2010, 70(5):2030-40

GDF-15 contributes to proliferation and immune escape of malignant gliomas

Roth P, **Junker M**, Tritschler I, Mittelbronn M, Dombrowski Y, Breit SN, Tabatabai G, Wick W, Weller M, Wischhusen J.
Clin Cancer Res., 2010, 16(15):3851-9

Concomitant requirement for Notch and Jak/Stat signaling during neuro-epithelial differentiation in the Drosophila optic lobe

Kathy T. Ngo, Jay Wang, **Markus Junker**, , Steve Kriz, Gloria Vo, Bobby Asem, John M. Olson, Utpal Banerjee, Volker Hartenstein
Developmental Biology, 2010, 60(10):1405-18
